ELECTROMAGNETIC SCATTERING BY SYSTEMS OF ARBITRARILY ORIENTED SPHEROIDS

BY

M. FRANCIS R. COORAY

A thesis
Submitted to the Faculty of Graduate Studies
in Partial Fulfillment of the Requirements
for the Degree of

DOCTOR OF PHILOSOPHY

Department of Electrical and Computer Engineering
University of Manitoba
Winnipeg, Manitoba

ISBN 0-315-63332-8

ELECTROMAGNETIC SCATTERING BY SYSTEMS OF ARBITRARILY ORIENTED SPHEROIDS

BY

M. FRANCIS R. COORAY

A thesis submitted to the Faculty of Graduate Studies of the University of Manitoba in partial fulfillment of the requirements of the degree of

DOCTOR OF PHILOSOPHY

ABSTRACT

The main objective of this thesis is to provide an exact solution to the problem of scattering of electromagnetic waves by spheroids of arbitrary orientation. The solution is obtained in general for the case of n dielectric spheroids of arbitrary orientation, by expanding the incident, scattered, and transmitted electromagnetic fields in terms of appropriate vector spheroidal eigenfunctions, the excitation being a monochromatic uniform plane electromagnetic wave of arbitrary polarization and angle of incidence. The boundary conditions at the surface of a given spheroid are imposed by using the rotational-translational addition theorems for vector spheroidal wave functions derived in this thesis, which transfer the outgoing waves from all the other spheroids, as incoming waves to the spheroid under consideration. Imposing the boundary conditions at the surfaces of each of the n spheroids leads to a set of algebraic equations, the solution of which can be expressed in matrix form such that the column matrix of the total transmitted and scattered field expansion coefficients is equal to the product of a system matrix, which is independent of the direction and polarization of the incident wave, and the column matrix of the known incident field expansion coefficients. This special feature of the system matrix makes it possible to evaluate the unknown transmitted and scattered field expansion coefficients for a new direction of incidence and for a different polarization, without repeatedly solving a new set of algebraic equations. The formulation for the special case of n perfectly conducting spheroids of arbitrary orientation is then deduced from that of the corresponding case of n dielectric spheroids. Numerical results are presented for the bistatic and backscattering cross sections for two prolate spheroids with various axial ratios, orientations, and a given

dielectric constant. An approximate method is described in this thesis too, for calculating the far field scattering cross sections for scattering by two coaxial spheroids at oblique incidence.

An analytic solution is also being obtained to the problem of electromagnetic coupling between two spheroidal dipole antennas in arbitrary configuration, each antenna being modeled by a very thin prolate spheroid which is centrally fed by a gap voltage. The problem is then solved by imposing the boundary conditions at the surface of each spheroidal antenna. Numerical results are presented for the mutual admittance of two center-fed thin spheroidal dipole antennas of arbitrary orientation, for various center displacements. Also given are the far field patterns for systems of two dipole antennas in various configurations, with one dipole being parasitic.

ACKNOWLEDGMENTS

I would like to express my gratitude to my advisor, Prof. I. R. Ciric for his valuable suggestions, continuing guidance, and specially for providing the necessary financial support to continue this research.

I am very grateful to the two members of my advisory committee, Prof. M. Hamid, and Prof. P. N. Shivakumar, for their interest and the constructive criticisms regarding this research.

I am greatly indebted to all my colleagues for all the support they provided me in numerous ways in carrying out this research.

Finally, I would like to thank the members of my family for the encouragement and moral support they provided me in pursuing this research.

TABLE OF CONTENTS

LIST OF FIGURES

LIST OF TABLES

CHAPTER 1

INTRODUCTION

1.1 Historical Survey and Applications

Solutions to problems in electromagnetic scattering have many important practical applications in the fields of applied physics, acoustics, and electrical engineering. During the past few decades, an extensive amount of research has been done on electromagnetic wave scattering by regular shaped bodies such as cylinders, spheres, and spheroids, as the effects due to scattering by real system objects can well be analyzed by modeling these objects using one of the aforementioned bodies. The important aspects of a scattering problem are the effects that arise due to the presence of a given object or a number of objects being in the path of a traveling wave. It is generally assumed that the field for the source in isolation is known. The requirement then is to find the redistribution of radiation arising from the presence of the objects. An exact solution to the problem can be presented only if it involves objects having a regular geometry. In this case, the method of solution is based on expanding the different associated electromagnetic fields in terms of an appropriate set of vector eigenfunctions. In this thesis, since we are interested only in scattering by spheroids, our concern will be on spheroidal wave functions.

The first investigation of the spheroidal wave functions was made by Niven [1] in 1880 in order to treat a problem on the conduction of heat in spheroidal bodies, by introducing series of Legendre functions for the spheroidal angle functions and series of spherical Bessel functions for the spheroidal radial functions. In 1898, Maclaurin [2] did a more extensive investigation with several applications, by introducing power

series solutions for the spheroidal wave functions. The free oscillations of a prolate spheroid was studied by Abraham [3] also in 1898, using integral representations of the spheroidal wave functions.

In 1941, Chu and Stratton [4] used the spheroidal wave functions they deduced to solve the boundary value problem of the forced electromagnetic oscillations of a conducting prolate spheroid which is fed by a gap of infinitesimal width across the central section of the spheroid. Ryder [5] also carried out a similar analysis for the same problem, using the earlier work of Page and Adams [6]. The model of a prolate spheroidal monopole antenna with a finite gap was treated by Flammer [7] by means of a variational approach. The radiation from a point electric dipole located at the tip of a prolate spheroid has been computed by Hatcher and Leitner [8]. The oblate spheroidal wave functions have also been used in antenna problems. Leitner and Spence [9] calculated the radiation from a quarter wavelength electric dipole situated axially over a conducting circular disk, and Kloepfer [10] calculated the radiation from a disk antenna with an infinitesimally narrow, circular gap. The classical boundary value problem of the diffraction of plane electromagnetic waves by a perfectly conducting circular disk and by the complementary circular aperture in a plane conducting screen was solved by Flammer [11] using oblate spheroidal wave functions. Wait [12] analyzed electromagnetic radiation from spheroidal structures, using both prolate and oblate spheroidal wave functions. The rapid development of computer facilities and numerical techniques during the recent past have become the foundations for many new approximate methods, which are based on integral equation formulation or on the volume integral and surface integral representations of the scattered fields obtained by using Green's theorem and are applicable in general, for the analysis of

electromagnetic scattering by arbitrary shaped bodies, including spheroids.

A well known method for solving problems in electromagnetics is the point matching technique, in which the electric and magnetic fields associated with the problem are expanded in terms of appropriate vector wave functions. The unknown coefficients in the field expansions are obtained from the boundary conditions for representative points on the surface of the scatterer. This method has been used by several authors to investigate scattering by spheroidal objects [13]–[15].

In 1965, Waterman [16] proposed a method for computing radar cross sections and other associated field quantities for scattering of electromagnetic waves by a smooth perfectly conducting obstacle. His method is essentially an integral equation formulation using Green's functions, and is known as the extended boundary condition method. Warner and Hizal [17] used this method to study the scattering and depolarization of microwaves by spheroidal raindrops. A modified form of this method was used by Barber and Yeh [18]–[19] in investigating the differential scattering characteristics of arbitrary shaped dielectric objects. The method proposed by Waterman which deals with one object was extended by Peterson and Strom [20], to be applicable for the case of several objects, and they used it in studying electromagnetic scattering by an arbitrary number of bodies, and from multilayered bodies [21].

For inhomogeneous and anisotropic media, the integral equation formulation is not very suitable, as Green's functions for this case become very complicated in comparison to the same for a homogeneous isotropic case. Since the finite difference or finite element equations are easily formulated, regardless of the complexity of the medium, they are more attractive than the integral equations in inhomogeneous media.

However, the large matrices obtained in this type of a formulation create a problem, making it difficult to perform matrix inversion using the general methods. The unimoment method introduced by Mei [22] presents a way of dealing with these matrices efficiently. The method was used by Mei et. al. [23], to treat electromagnetic scattering from two bodies of arbitrary shape. Finally, for the analysis of very large systems (consisting of say more than 100 scatterers), one can use the concepts of statistical ensemble averaging [24]–[26], or lattice sum techniques [27].

1.2 Exact Solutions for Scattering by Spheroids

In attempting exact solutions to the scattering problems, we find that solving problems associated with objects modeled by spheroids, is more difficult than solving those modeled by spheres or cylinders, due to the complex nature of the spheroidal wave functions, which also makes the numerical computation of these functions much more difficult. The very first attempt of obtaining a classical solution to the problem of electromagnetic scattering by a spheroid involved solving of the scalar Helmholtz equation

$$\nabla^2\psi + k^2\psi = 0 \tag{1.1}$$

in the spheroidal coordinate system. The solution results in the scalar spheroidal wave function, in terms of which the different vector spheroidal wave functions are defined [28]. In [28] and [29] we find tables of numerical values for different spheroidal wave functions, which are very useful for comparative purposes.

In reviewing the literature, we find that there are quite a few publications on the subject of obtaining an exact solution to the problem of scattering of electromagnetic waves by a single spheroid, by expanding each of the fields associated in terms of

appropriate vector spheroidal wave functions. Even though various applications of spheroidal wave functions have been there since 1880, it is the work of Schultz [30] in 1950 that gave for the first time a formulation for obtaining an exact solution to the problem of scattering of plane electromagnetic waves by a perfectly conducting prolate spheroid for axial incidence. Based on Schultz's technique, Siegel et. al. [31] carried out quantitative calculations of the backscattering from a prolate spheroid, and have given a curve which shows the variation of the backscattering cross section with the size of the spheroid for a prolate spheroid of axial ratio 10. Senior [32] compared these results with some experimental results obtained by him for the same case. Taylor [33] also obtained an exact solution to electromagnetic scattering by a prolate spheroid for broadside incidence and TM polarization of the incident wave, but has not presented any numerical results.

An exact solution for the more general case of scattering of plane electromagnetic waves by a conducting prolate spheroid for arbitrary polarization and angle of incidence was given by Reitilinger [34], but without any numerical results. There were two major drawbacks in this solution. One was the necessity to repeat the process of inverting matrices with changing direction of the incident wave. The other was the inability to use the same matrix to calculate the unknown coefficients in the series expansion of the scattered field for both TE and TM polarizations of the incident wave. These two problems were eliminated in the work of Sinha and MacPhie [35], who also presented numerical results in the form of plots of backscattering cross section versus angle of incidence for prolate spheroids of axial ratio 1, 2, 10, and 100. An exact solution to the same problem was also given by Dalmas [36]–[37], but using a different type of vector wave functions than in [35], for the expansion of the fields. Using the

latter type of vector wave functions Asano and Yamamoto [38] presented an exact solution to a similar problem involving a dielectric spheroid, and Sebak and Shafai [39] obtained an analytic solution for electromagnetic scattering by a single spheroid with impedance boundary conditions at axial incidence.

Research on electromagnetic scattering by two spheroids is not as extensive as in the case of a single spheroid due to the fact that the solution is now more complicated compared to that of scattering by a single spheroid, as the problem requires transferring of fields scattered by one of the spheroids as incoming fields to the other. For this purpose either the translational addition theorems or the rotational-translational addition theorems for vector spheroidal wave functions are used, depending on the orientation of one spheroid with respect to the other. The above mentioned theorems have been developed on the basis of the translational addition theorems for scalar spherical wave functions presented by Friedman and Russek [40], and the translational and rotational addition theorems for vector spherical wave functions presented by Stein [41] and Cruzan [42]. The translational addition theorems for the scalar spheroidal wave functions $\psi_{mn}^{(i)}(h;\xi,\eta,\phi)$ and vector spheroidal wave functions $\mathbf{M}_{mn}^{a(i)}(h;\xi,\eta,\phi) = \nabla\psi_{mn}^{(i)}(h;\xi,\eta,\phi)\times\boldsymbol{a}$, $\mathbf{N}_{mn}^{a(i)}(h;\xi,\eta,\phi) = k^{-1}\,\nabla\times\mathbf{M}_{mn}^{a(i)}(h;\xi,\eta,\phi)$ $(i=1,3,4)$, where $\boldsymbol{a}$ is any one of the Cartesian unit vectors $\hat{\mathbf{x}}, \hat{\mathbf{y}}$, or $\hat{\mathbf{z}}$, were deduced by Sinha and MacPhie, and these theorems have been used by them for the analysis of scattering of a plane electromagnetic wave by two spheroids with parallel major axes, and for deriving the mutual admittance characteristics of a pair of spheroidal dipole antennas with parallel major axes [43]–[45]. The same theorems were used by Cooray et. al. [46] for analyzing plane wave scattering by two parallel dielectric spheroids. Analogous theorems for

the vector wave functions in the case when $\boldsymbol{a}$ is the radial vector $\mathbf{r}$ were derived by Dalmas and Deleuil, and these have also been used in solving the problem of scattering of electromagnetic waves by two parallel perfectly conducting spheroids [47]–[50]. The rotational addition theorem and the rotational-translational addition theorems for scalar spheroidal wave functions were given by MacPhie et. al. [51].

In this thesis we use the addition theorems for scalar spheroidal wave functions [51] to derive the rotational-translational addition theorems for the vector spheroidal wave functions $\mathbf{M}_{mn}^{a(i)}(h;\xi,\eta,\phi)$ and $\mathbf{N}_{mn}^{a(i)}(h;\xi,\eta,\phi)$ with $a=x,y,z$; $i=1,2,3,4$, as well as for $\mathbf{M}_{e,omn}^{r(i)}(h;\xi,\eta,\phi)$ and $\mathbf{N}_{e,omn}^{r(i)}(h;\xi,\eta,\phi)$ ($i=1,2,3,4$) when $\boldsymbol{a}$ is the radial vector $\mathbf{r}$. We also derive the same theorems for the vector wave functions $\mathbf{M}_{mn}^{\pm(i)}(h;\xi,\eta,\phi)$ and $\mathbf{N}_{mn}^{\pm(i)}(h;\xi,\eta,\phi)$, which intervene in the solution of vector field problems in the presence of a system of two spheroids of arbitrary orientation. Then we use them to obtain exact solutions to the problems of scattering of electromagnetic waves by two spheroids of arbitrary orientation and electromagnetic coupling between two spheroidal dipole antennas in arbitrary configuration. The coordinates ξ,η,ϕ mentioned above are the spheroidal coordinates and $h=kF$, where k is the wavenumber of the time harmonic fields and F is the semi-interfocal distance of the spheroidal surfaces $\xi=\text{const.}$ The vector wave functions $\mathbf{M}_{mn}^{\pm(i)}(h;\xi,\eta,\phi)$ and $\mathbf{N}_{mn}^{\pm(i)}(h;\xi,\eta,\phi)$ are those defined in Appendix A, having a $e^{j(m\pm1)\phi}$ ϕ–dependence, with $j\equiv\sqrt{-1}$.

1.3 Synopsis

In Chapter 2 we derive the rotational-translational addition theorems for vector spheroidal wave functions $\mathbf{X}_{mn}^{a(i)}(h;\xi,\eta,\phi)$, $\mathbf{X}_{mn}^{\pm(i)}(h;\xi,\eta,\phi)$, $\mathbf{X}_{e,omn}^{r(i)}(h;\xi,\eta,\phi)$, where $\mathbf{X}$ is either of the vector spheroidal wave function $\mathbf{M}$ or $\mathbf{N}$, and also for vector spherical

wave functions $\mathbf{m}_{mn}^{r(i)}$ and $\mathbf{n}_{mn}^{r(i)}$. Sample results of some numerical experiments performed on the equations describing the rotational-translational addition theorems for vector spheroidal wave functions are given at the end of the chapter. Next, using the appropriate rotational-translational addition theorems for vector spheroidal wave functions, we present in Chapter 3 the formulation and analysis for the general problem of scattering of electromagnetic waves by n dielectric spheroids of arbitrary orientation. The transformation of the electromagnetic fields scattered by one spheroid as incoming to another, the imposing of the boundary conditions, and the derivation of the system matrix are discussed in detail. The solution of the problem of scattering by n perfectly conducting spheroids is then deduced from the above solution for n dielectric spheroids. The solutions for the special case $n=2$ are also given separately.

The numerical results that have been obtained by solving the problems of scattering by two perfectly conducting and by two dielectric spheroids of arbitrary orientation are presented in Chapter 4. Since all the matrices associated with the solutions are of infinite dimensions, the criteria used for truncating these matrices are described in this chapter, and the numerical results obtained in the form of plots of normalized bistatic and backscattering cross sections for various axial ratios, orientations, and center-to-center distances of the two spheroids are discussed. In Chapter 5, we describe an approximate method for solving the problem of scattering of electromagnetic waves by two coaxial spheroids at oblique incidence, based on the exact solution to scattering by a single spheroid, and present numerical results for the far field scattering cross sections.

An exact solution to the problem of electromagnetic coupling between two spheroidal dipole antennas in arbitrary configuration is obtained in Chapter 6, the formulation being done on the basis of the equivalence principle and the rotational-translational addition theorems for vector spheroidal wave functions. Numerical results are given in the form of plots of mutual admittance versus the separation between the two dipole antennas and plots of $E-$ and $H-$ plane patterns for different orientations of the two antennas, when one of them is parasitic. Finally, in Chapter 7 we present the general conclusions and make some recommendations for future research.

CHAPTER 2

ROTATIONAL-TRANSLATIONAL ADDITION THEOREMS FOR VECTOR SPHEROIDAL WAVE FUNCTIONS

In order to solve the problem of scattering of electromagnetic waves by $n(\geq 2)$ spheroids of arbitrary orientation, we require that the outgoing waves due to the fields scattered by one spheroid, which are functions of the coordinate system attached to that spheroid, be expressed as incoming waves to another spheroid in the coordinate system attached to it. Since the scattered field is expressed as a series expansion in terms of vector spheroidal wave functions, this requires rotational-translational addition theorems which express vector spheroidal wave functions of the third or fourth kind (depending on whether the time dependence of the field quantities is $e^{-j\omega t}$ or $e^{j\omega t}$, respectively,) in the outgoing system in terms of vector spheroidal wave functions of the first kind in the incoming system. As the problem can be formulated by using either vector spheroidal wave functions $\mathbf{X}_{mn}^{\pm(i)}$ and $\mathbf{X}_{mn}^{z(i)}$ or $\mathbf{X}_{e,omn}^{r(i)}$, (where $\mathbf{X}$ is either $\mathbf{M}$ or $\mathbf{N}$), we first derive in Section 2.1 the rotational-translational addition theorems for both types of vector spheroidal wave functions, even though we use only the former type in our formulation. Next we deduce in Section 2.2 the translational addition theorems for these vector spheroidal wave functions, as a special case, and finally obtain the rotational-translational addition theorems for vector spherical wave functions as another special case.

2.1 Derivation of the Rotational-translational Addition Theorems

In order to simplify the notation, without any loss of generality, consider only two Cartesian reference frames (x,y,z) and (x',y',z') as shown in Fig. 2.1. A point P

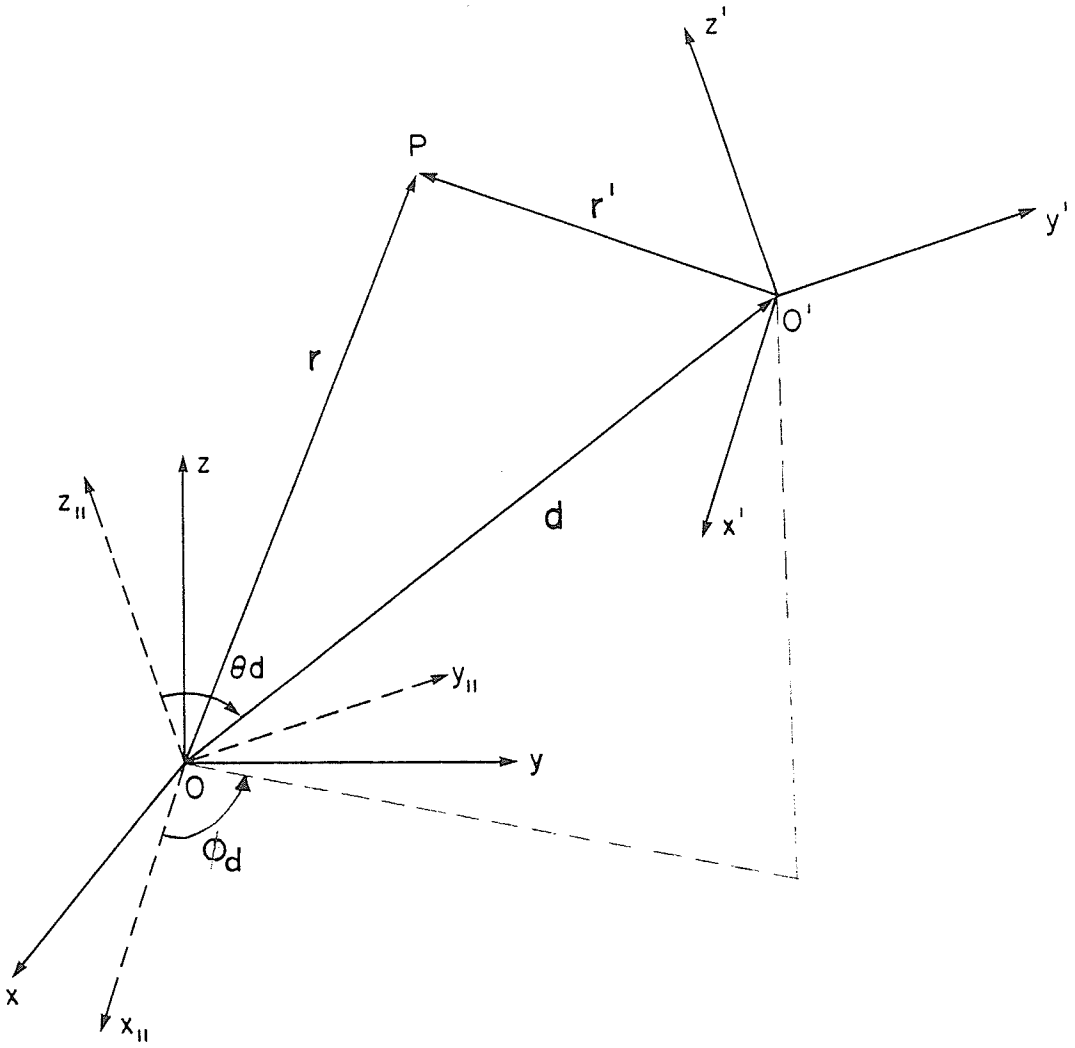

Fig. 2.1 Rotation and translation of the Cartesian system (x,y,z) to (x',y',z').

has spheroidal coordinates ξ,η,ϕ and ξ',η',ϕ' associated with these two reference frames, respectively. The system (x',y',z') is obtained from (x,y,z) by rotating the latter to $(x_{\parallel},y_{\parallel},z_{\parallel})$ which is parallel to (x',y',z') and then by a translation. The origin O' of (x',y',z') has spherical coordinates d,θ_d,ϕ_d with respect to the Cartesian system $(x_{\parallel},y_{\parallel},z_{\parallel})$.

By using the rotational-translational addition theorems for scalar spheroidal wave functions given in [51], the scalar spheroidal wave functions $\psi_{mn}^{(i)}(h;\xi,\eta,\phi)$ in the unprimed system can be expressed as series expansions in terms of scalar spheroidal wave functions in the primed system as,

$$\psi_{mn}^{(i)}(h;\xi,\eta,\phi)=\sum_{\nu=0}^{\infty}\sum_{\mu=-\nu}^{\nu}{}^{(i)}Q_{\mu\nu}^{mn}(\alpha,\beta,\gamma;\mathbf{d})\,\psi_{\mu\nu}^{(1)}(h';\xi',\eta',\phi'),\qquad r'\le d\ ;\ i=1,2,3,4 \tag{2.1}$$

$$\psi_{mn}^{(i)}(h;\xi,\eta,\phi)=\sum_{\nu=0}^{\infty}\sum_{\mu=-\nu}^{\nu}P_{\mu\nu}^{mn}(\alpha,\beta,\gamma;\mathbf{d})\,\psi_{\mu\nu}^{(i)}(h';\xi',\eta',\phi'),\qquad r'\ge d\ ;\ i=1,2,3,4 \tag{2.2}$$

in which α,β,γ are the Euler angles [52] that specify the rotation of the primed system with respect to the unprimed one, and ${}^{(i)}Q_{\mu\nu}^{mn}(\alpha,\beta,\gamma;\mathbf{d})$ and $P_{\mu\nu}^{mn}(\alpha,\beta,\gamma;\mathbf{d})$ are the rotational-translational expansion coefficients with ${}^{(1)}Q_{\mu\nu}^{mn}(\alpha,\beta,\gamma;\mathbf{d})\equiv P_{\mu\nu}^{mn}(\alpha,\beta,\gamma;\mathbf{d})$, defined in Appendix B. The unit vectors $\hat{\mathbf{x}},\hat{\mathbf{y}},\hat{\mathbf{z}}$ and $\hat{\mathbf{x}}',\hat{\mathbf{y}}',\hat{\mathbf{z}}'$ are related by

$$\boldsymbol{a}=c_{ax'}\hat{\mathbf{x}}'+c_{ay'}\hat{\mathbf{y}}'+c_{az'}\hat{\mathbf{z}}',\qquad \boldsymbol{a}=\hat{\mathbf{x}},\hat{\mathbf{y}},\hat{\mathbf{z}} \tag{2.3}$$

where the coefficients $c_{ax'},c_{ay'},c_{az'}$ are expressed in terms of the Euler angles,

$$\begin{aligned}
c_{xx'}&=\cos\alpha\cos\beta\cos\gamma-\sin\alpha\sin\gamma\\
c_{xy'}&=-(\cos\alpha\cos\beta\sin\gamma+\sin\alpha\cos\gamma)\\
c_{xz'}&=\cos\alpha\sin\beta\\
c_{yx'}&=\sin\alpha\cos\beta\cos\gamma+\cos\alpha\sin\gamma\\
c_{yy'}&=\cos\alpha\cos\gamma-\sin\alpha\cos\beta\sin\gamma\\
c_{yz'}&=\sin\alpha\sin\beta
\end{aligned} \tag{2.4}$$

$$c_{zx'} = -\sin\beta\cos\gamma$$
$$c_{zy'} = \sin\beta\sin\gamma$$
$$c_{zz'} = \cos\beta$$

The independent elementary solutions of the vector Helmholtz equation in the spheroidal coordinate system give the vector spheroidal wave functions [53],

$$\mathbf{M}_{mn}^{a(i)}(h;\xi,\eta,\phi) = \nabla\psi_{mn}^{(i)}(h;\xi,\eta,\phi)\times\boldsymbol{a} \tag{2.5}$$

$$\mathbf{N}_{mn}^{a(i)}(h;\xi,\eta,\phi) = k^{-1}\nabla\times\mathbf{M}_{mn}^{a(i)}(h;\xi,\eta,\phi) \tag{2.6}$$

where $\boldsymbol{a}$ is a constant vector or the radial vector. In this thesis we consider the vector wave functions given in (2.5) and (2.6) with $\boldsymbol{a}$ being one of the Cartesian unit vectors $\hat{\mathbf{x}},\hat{\mathbf{y}},\hat{\mathbf{z}}$, and their linear combinations which are particularly useful in the analysis of field problems involving spheroids [44]–[46]. Also considered are the vector wave functions with $\boldsymbol{a}$ being the radial vector $\mathbf{r}$.

2.1.1 Theorems for Vector Wave Functions Defined with $\hat{\mathbf{x}}$, $\hat{\mathbf{y}}$, or $\hat{\mathbf{z}}$

In the following, we will be denoting the coordinate triads (ξ,η,ϕ) and (ξ',η',ϕ') by $\mathbf{r}$ and $\mathbf{r}'$, respectively, and will be omitting the arguments of ${}^{(i)}Q_{\mu\nu}^{mn}(\alpha,\beta,\gamma;\mathbf{d})$ and $P_{\mu\nu}^{mn}(\alpha,\beta,\gamma;\mathbf{d})$. If we substitute (2.1) and (2.2) in (2.5) and then (2.5) in (2.6), for $a = x, y, z$, we obtain

$$\mathbf{X}_{mn}^{a(i)}(h;\mathbf{r}) = \sum_{\nu=0}^{\infty}\sum_{\mu=-\nu}^{\nu} {}^{(i)}Q_{\mu\nu}^{mn}\,[c_{ax'}\mathbf{X}_{\mu\nu}^{x'(1)}(h';\mathbf{r}') + c_{ay'}\mathbf{X}_{\mu\nu}^{y'(1)}(h';\mathbf{r}') + c_{az'}\mathbf{X}_{\mu\nu}^{z'(1)}(h';\mathbf{r}')], \quad r' \le d\,;\ i=1,2,3,4 \tag{2.7}$$

$$\mathbf{X}_{mn}^{a(i)}(h;\mathbf{r}) = \sum_{\nu=0}^{\infty}\sum_{\mu=-\nu}^{\nu} P_{\mu\nu}^{mn}\,[c_{ax'}\mathbf{X}_{\mu\nu}^{x'(i)}(h';\mathbf{r}') + c_{ay'}\mathbf{X}_{\mu\nu}^{y'(i)}(h';\mathbf{r}') + c_{az'}\mathbf{X}_{\mu\nu}^{z'(i)}(h';\mathbf{r}')], \quad r' \ge d\,;\ i=1,2,3,4 \tag{2.8}$$

where $\mathbf{X}$ is either of the vector spheroidal wave functions $\mathbf{M}$ or $\mathbf{N}$. These expressions

give the functions $\mathbf{M}$ and $\mathbf{N}$ in one system of spheroidal coordinates in terms of the same type of functions in another system of spheroidal coordinates, rotated and translated with respect to the first one. In the analysis of field problems, the following linear combinations [44] are used:

$$\mathbf{X}_{mn}^{\pm(i)}(h;\mathbf{r}) = \frac{1}{2}\,[\mathbf{X}_{mn}^{x(i)}(h;\mathbf{r}) \pm j\,\mathbf{X}_{mn}^{y(i)}(h;\mathbf{r})], \qquad i=1,2,3,4 \tag{2.9}$$

From (2.7), (2.8), and (2.9), the following expressions are derived finally [54], [55]:

$$\mathbf{X}_{mn}^{+(i)}(h;\mathbf{r}) = \sum_{\nu=0}^{\infty}\sum_{\mu=-\nu}^{\nu} {}^{(i)}Q_{\mu\nu}^{mn}\,[C_1\,\mathbf{X}_{\mu\nu}^{+(1)'}(h';\mathbf{r}') + C_2\,\mathbf{X}_{\mu\nu}^{-(1)'}(h';\mathbf{r}') + C_3\,\mathbf{X}_{\mu\nu}^{z'(1)}(h';\mathbf{r}')], \quad r' \le d\,;\ i=1,2,3,4 \tag{2.10}$$

$$\mathbf{X}_{mn}^{+(i)}(h;\mathbf{r}) = \sum_{\nu=0}^{\infty}\sum_{\mu=-\nu}^{\nu} P_{\mu\nu}^{mn}\,[C_1\,\mathbf{X}_{\mu\nu}^{+(i)'}(h';\mathbf{r}') + C_2\,\mathbf{X}_{\mu\nu}^{-(i)'}(h';\mathbf{r}') + C_3\,\mathbf{X}_{\mu\nu}^{z'(i)}(h';\mathbf{r}')], \quad r' \ge d\,;\ i=1,2,3,4 \tag{2.11}$$

$$\mathbf{X}_{mn}^{-(i)}(h;\mathbf{r}) = \sum_{\nu=0}^{\infty}\sum_{\mu=-\nu}^{\nu} {}^{(i)}Q_{\mu\nu}^{mn}\,[C_2^*\,\mathbf{X}_{\mu\nu}^{+(1)'}(h';\mathbf{r}') + C_1^*\,\mathbf{X}_{\mu\nu}^{-(1)'}(h';\mathbf{r}') + C_3^*\,\mathbf{X}_{\mu\nu}^{z'(1)}(h';\mathbf{r}')], \quad r' \le d\,;\ i=1,2,3,4 \tag{2.12}$$

$$\mathbf{X}_{mn}^{-(i)}(h;\mathbf{r}) = \sum_{\nu=0}^{\infty}\sum_{\mu=-\nu}^{\nu} P_{\mu\nu}^{mn}\,[C_2^*\,\mathbf{X}_{\mu\nu}^{+(i)'}(h';\mathbf{r}') + C_1^*\,\mathbf{X}_{\mu\nu}^{-(i)'}(h';\mathbf{r}') + C_3^*\,\mathbf{X}_{\mu\nu}^{z'(i)}(h';\mathbf{r}')], \quad r' \ge d\,;\ i=1,2,3,4 \tag{2.13}$$

$$\mathbf{X}_{mn}^{z(i)}(h;\mathbf{r}) = \sum_{\nu=0}^{\infty}\sum_{\mu=-\nu}^{\nu} {}^{(i)}Q_{\mu\nu}^{mn}\,[C_4\,\mathbf{X}_{\mu\nu}^{+(1)'}(h';\mathbf{r}') + C_4^*\,\mathbf{X}_{\mu\nu}^{-(1)'}(h';\mathbf{r}') + C_5\,\mathbf{X}_{\mu\nu}^{z'(1)}(h';\mathbf{r}')], \quad r' \le d\,;\ i=1,2,3,4 \tag{2.14}$$

$$\mathbf{X}_{mn}^{z(i)}(h;\mathbf{r}) = \sum_{\nu=0}^{\infty}\sum_{\mu=-\nu}^{\nu} P_{\mu\nu}^{mn}\,[C_4\,\mathbf{X}_{\mu\nu}^{+(i)'}(h';\mathbf{r}') + C_4^*\,\mathbf{X}_{\mu\nu}^{-(i)'}(h';\mathbf{r}') + C_5\,\mathbf{X}_{\mu\nu}^{z'(i)}(h';\mathbf{r}')], \quad r' \ge d\,;\ i=1,2,3,4 \tag{2.15}$$

where the asterisk denotes the complex conjugate, and

$$
\begin{aligned}
C_1 &= \frac{1}{2}\left[(c_{xx'}+c_{yy'})-j\,(c_{xy'}-c_{yx'})\right] \\
C_2 &= \frac{1}{2}\left[(c_{xx'}-c_{yy'})+j\,(c_{xy'}+c_{yx'})\right] \\
C_3 &= \frac{1}{2}\,(c_{xz'}+jc_{yz'}) \\
C_4 &= c_{zx'}-jc_{zy'} \\
C_5 &= c_{zz'}
\end{aligned}
\tag{2.16}
$$

The expressions in (2.7)–(2.8) and (2.10)–(2.15) constitute the rotational-translational addition theorems for the vector spheroidal wave functions $\mathbf{M}_{mn}^{a(i)}$, $\mathbf{M}_{mn}^{\pm(i)}$, $\mathbf{N}_{mn}^{a(i)}$, and $\mathbf{N}_{mn}^{\pm(i)}$.

2.1.2 Theorems for Vector Wave Functions Defined with the Radial Vector r

Using eq. (B.1) in the Appendix B and (2.1), the even and odd spheroidal scalar wave functions in the unprimed system can be expressed in the form of a series expansion in terms of both even and odd spheroidal scalar wave functions in the primed system, for $r' \le d$ and i=1,2,3,4, as

$$
\begin{aligned}
\psi_{e,omn}^{(i)}(h;\mathbf{r}) = \sum_{q=0,1}^{\infty}{}' \sum_{\bar{\mu}=-(|m|+q)}^{|m|+q} F_{\bar{\mu}q}^{mn} \sum_{\nu=0}^{\infty} \sum_{\mu=0}^{\nu} \sum_{l=\mu,\mu+1}^{\infty}{}' \Gamma_{\mu\nu l} \\
\cdot \left[{}_{c}^{e,o}B_{\mu\nu\bar{\mu}q}^{mn}\, \psi_{e,o\mu l}^{(1)'}(h';\mathbf{r}') \mp {}_{s}^{o,e}B_{\mu\nu\bar{\mu}q}^{mn}\, \psi_{o,e\mu l}^{(1)'}(h';\mathbf{r}') \right]
\end{aligned}
\tag{2.17}
$$

where

$$
\begin{aligned}
{}_{c}^{e,o}B_{\mu\nu\bar{\mu}q}^{mn} = j^{\,|m|+q-n}\, e^{-j\bar{\mu}\phi_d} \{ {}^{(i)}a_{\mu\nu}^{\bar{\mu},|m|+q}(\mathbf{d})\, e^{j\mu\phi_d} \cos\left[(\bar{\mu}-\mu)\phi_d + \bar{\mu}\gamma + m\alpha\right] \\
\pm (-1)^{\mu} \frac{(\nu-\mu)!}{(\nu+\mu)!}\, {}^{(i)}a_{-\mu\nu}^{\bar{\mu},|m|+q}(\mathbf{d})\, e^{-j\mu\phi_d} \cos\left[(\bar{\mu}+\mu)\phi_d + \bar{\mu}\gamma + m\alpha\right] \}
\end{aligned}
\tag{2.18}
$$

$$
\begin{aligned}
{}_{s}^{o,e}B_{\mu\nu\bar{\mu}q}^{mn} = j^{\,|m|+q-n}\, e^{-j\bar{\mu}\phi_d} \{ {}^{(i)}a_{\mu\nu}^{\bar{\mu},|m|+q}(\mathbf{d})\, e^{j\mu\phi_d} \sin\left[(\bar{\mu}-\mu)\phi_d + \bar{\mu}\gamma + m\alpha\right] \\
\mp (-1)^{\mu} \frac{(\nu-\mu)!}{(\nu+\mu)!}\, {}^{(i)}a_{-\mu\nu}^{\bar{\mu},|m|+q}(\mathbf{d})\, e^{-j\mu\phi_d} \sin\left[(\bar{\mu}+\mu)\phi_d + \bar{\mu}\gamma + m\alpha\right] \}
\end{aligned}
\tag{2.19}
$$

for μ>0,

$$ {}_{c}^{e}B_{0\nu\bar{\mu}q}^{mn} = j^{|m|+q-n}\, e^{-j\bar{\mu}\phi_d}\, {}^{(i)}a_{0\nu}^{\bar{\mu},|m|+q}(\mathbf{d}) \cos(\bar{\mu}\phi_d + \bar{\mu}\gamma + m\alpha) \tag{2.20} $$

$$ {}_{s}^{e}B_{0\nu\bar{\mu}q}^{mn} = j^{|m|+q-n}\, e^{-j\bar{\mu}\phi_d}\, {}^{(i)}a_{0\nu}^{\bar{\mu},|m|+q}(\mathbf{d}) \sin(\bar{\mu}\phi_d + \bar{\mu}\gamma + m\alpha) \tag{2.21} $$

for $\mu=0$,

$$ F_{\bar{\mu}q}^{mn} = d_q^{mn}(h)\,(-1)^{\bar{\mu}-m} \left[\frac{N_{m,|m|+q}}{N_{\bar{\mu},|m|+q}} \right]^{1/2} d_{\bar{\mu}m}^{(|m|+q)}(\beta) \tag{2.22} $$

and

$$ \Gamma_{\mu\nu l} = \frac{N_{\mu\nu}\, j^{l-\nu}}{N_{\mu l}(h')}\, d_{\nu-\mu}^{\mu l}(h') \tag{2.23} $$

Equation (2.17) gives the rotational-translational addition theorems for the scalar spheroidal wave functions $\psi_{e,omn}^{(i)}$ (i=1,2,3,4), for $r' \le d$. Using the relationship between the spheroidal and spherical scalar wave functions [28], we get for $r' \le d$

$$ \psi_{e,omn}^{(i)}(h;\mathbf{r}) = \sum_{q=0,1}^{\infty}{}' \sum_{\bar{\mu}=-(|m|+q)}^{|m|+q} F_{\bar{\mu}q}^{mn} \sum_{\nu=0}^{\infty} \sum_{\mu=0}^{\nu} [\, {}_{c}^{e,o}B_{\mu\nu\bar{\mu}q}^{mn}\, \psi_{e,o\,\mu\nu}^{(1)'}(r',\theta',\phi') \mp {}_{s}^{o,e}B_{\mu\nu\bar{\mu}q}^{mn}\, \psi_{o,e\,\mu\nu}^{(1)'}(r',\theta',\phi')\,] \tag{2.24} $$

where

$$ \psi_{e,o\,\mu\nu}^{(1)'} = j_\nu(kr')\, P_\nu^\mu(\cos\theta') \begin{matrix}\cos \\ \sin\end{matrix} \mu\phi' \tag{2.25} $$

The notation in (2.17)–(2.25) is explained in Appendix B.

Taking the gradient on both sides of (2.24) and then the cross product with $\mathbf{r}$ gives

$$ \begin{aligned} \mathbf{M}_{e,omn}^{r(i)}(h;\mathbf{r}) = \sum_{q=0,1}^{\infty}{}' \sum_{\bar{\mu}=-(|m|+q)}^{|m|+q} F_{\bar{\mu}q}^{mn} \sum_{\nu=0}^{\infty} \sum_{\mu=0}^{\nu} [\, & {}_{c}^{e,o}B_{\mu\nu\bar{\mu}q}^{mn}\, \nabla\psi_{e,o\,\mu\nu}^{(1)'}(r',\theta',\phi') \\ & \mp {}_{s}^{o,e}B_{\mu\nu\bar{\mu}q}^{mn}\, \nabla\psi_{o,e\,\mu\nu}^{(1)'}(r',\theta',\phi')\,] \times \mathbf{r} \end{aligned} \tag{2.26} $$

Since the gradient of a scalar function is invariant to a transformation of the coordinate system, denoting the vector spherical wave function $\nabla\psi_{e,o\,\mu\nu}^{(1)'}(r',\theta',\phi') \times \boldsymbol{a}'$ by $\mathbf{m}_{e,o\,\mu\nu}^{a'(1)}$ ($a'=x',y',z',r'$), and omitting the argument of $\mathbf{M}_{e,omn}^{r(i)}(h;\mathbf{r})$, we get

$$\mathbf{M}_{e,omn}^{r(i)} = \sum_{q=0,1}^{\infty}{}' \sum_{\bar{\mu}=-(|m|+q)}^{|m|+q} F_{\bar{\mu}q}^{mn} \sum_{\nu=0}^{\infty} \sum_{\mu=0}^{\nu} \{ {}_{c}^{e,o}B_{\mu\nu\bar{\mu}q}^{mn} (\mathbf{m}_{e,o\,\mu\nu}^{r'(1)} + d\sin\theta_d \cos\phi_d \mathbf{m}_{e,o\,\mu\nu}^{x'(1)}$$
$$+ d\sin\theta_d \sin\phi_d \mathbf{m}_{e,o\,\mu\nu}^{y'(1)} + d\cos\theta_d \mathbf{m}_{e,o\,\mu\nu}^{z'(1)}) \mp {}_{s}^{o,e}B_{\mu\nu\bar{\mu}q}^{mn} (\mathbf{m}_{o,e\,\mu\nu}^{r'(1)}$$
$$+ d\sin\theta_d \cos\phi_d \mathbf{m}_{o,e\,\mu\nu}^{x'(1)} + d\sin\theta_d \sin\phi_d \mathbf{m}_{o,e\,\mu\nu}^{y'(1)} + d\cos\theta_d \mathbf{m}_{o,e\,\mu\nu}^{z'(1)}) \} \tag{2.27}$$

where the following relations are used;

$$\mathbf{r} = \mathbf{r}' + \mathbf{d} \; ; \qquad \mathbf{d} = d\sin\theta_d \cos\phi_d \, \hat{\mathbf{x}}' + d\sin\theta_d \sin\phi_d \, \hat{\mathbf{y}}' + d\cos\theta_d \, \hat{\mathbf{z}}' \tag{2.28}$$

Now we express the vector spherical wave functions $\mathbf{m}_{e,o\,\mu\nu}^{a'(1)}$ $(a'=x',y',z')$ in terms of the vector spherical wave functions $\mathbf{m}_{e,o\,\mu\nu}^{r'(1)}$ and $\mathbf{n}_{e,o\,\mu\nu}^{r'(1)}$ in the following form, which is valid for any of ${}_{c}^{e,o}B_{\mu\nu\bar{\mu}q}^{mn}$ and ${}_{s}^{o,e}B_{\mu\nu\bar{\mu}q}^{mn}$ [47]:

$$\sum_{\nu=0}^{\infty} \sum_{\mu=0}^{\nu} B_{\mu\nu\bar{\mu}q}^{mn} \mathbf{m}_{e,o\,\mu\nu}^{x'(1)} = \sum_{\nu=1}^{\infty} \sum_{\mu=0}^{\nu} (a'_{\mu\nu\bar{\mu}q} \mathbf{m}_{e,o\,\mu\nu}^{r'(1)} + b'_{\mu\nu\bar{\mu}q} \mathbf{n}_{o,e\,\mu\nu}^{r'(1)})$$
$$\sum_{\nu=0}^{\infty} \sum_{\mu=0}^{\nu} B_{\mu\nu\bar{\mu}q}^{mn} \mathbf{m}_{e,o\,\mu\nu}^{y'(1)} = \sum_{\nu=1}^{\infty} \sum_{\mu=0}^{\nu} (a''_{\mu\nu\bar{\mu}q} \mathbf{m}_{o,e\,\mu\nu}^{r'(1)} + b''_{\mu\nu\bar{\mu}q} \mathbf{n}_{e,o\,\mu\nu}^{r'(1)}) \tag{2.29}$$
$$\sum_{\nu=0}^{\infty} \sum_{\mu=0}^{\nu} B_{\mu\nu\bar{\mu}q}^{mn} \mathbf{m}_{e,o\,\mu\nu}^{z'(1)} = \sum_{\nu=1}^{\infty} \sum_{\mu=0}^{\nu} (a'''_{\mu\nu\bar{\mu}q} \mathbf{m}_{e,o\,\mu\nu}^{r'(1)} + b'''_{\mu\nu\bar{\mu}q} \mathbf{n}_{o,e\,\mu\nu}^{r'(1)})$$

where $a'_{\mu\nu\bar{\mu}q}$, $b'_{\mu\nu\bar{\mu}q}$, $a''_{\mu\nu\bar{\mu}q}$, $b''_{\mu\nu\bar{\mu}q}$, $a'''_{\mu\nu\bar{\mu}q}$, and $b'''_{\mu\nu\bar{\mu}q}$ are given correspondingly by

$$a'_{\mu\nu\bar{\mu}q} = \frac{k}{2\nu(\nu+1)} \left\{ \frac{\nu}{(2\nu+3)} [(\nu+\mu+1)(\nu+\mu+2) B_{\mu+1,\nu+1,\bar{\mu}q}^{mn} - B_{\mu-1,\nu+1,\bar{\mu}q}^{mn}] \right.$$
$$\left. + \frac{(\nu+1)}{(2\nu-1)} [-(\nu-\mu-1)(\nu-\mu) B_{\mu+1,\nu-1,\bar{\mu}q}^{mn} + B_{\mu-1,\nu-1,\bar{\mu}q}^{mn}] \right\}$$

$$a''_{\mu\nu\bar{\mu}q} = \frac{\pm k}{2\nu(\nu+1)} \left\{ \frac{-\nu}{(2\nu+3)} [(\nu+\mu+1)(\nu+\mu+2) B_{\mu+1,\nu+1,\bar{\mu}q}^{mn} + B_{\mu-1,\nu+1,\bar{\mu}q}^{mn}] \right. \tag{2.30}$$
$$\left. + \frac{(\nu+1)}{(2\nu-1)} [(\nu-\mu-1)(\nu-\mu) B_{\mu+1,\nu-1,\bar{\mu}q}^{mn} + B_{\mu-1,\nu-1,\bar{\mu}q}^{mn}] \right\}$$

$$a'''_{\mu\nu\bar{\mu}q} = \frac{k}{\nu(\nu+1)} \left[\frac{(\nu+1)(\nu-\mu)}{2\nu-1} B_{\mu,\nu-1,\bar{\mu}q}^{mn} + \frac{\nu(\nu+\mu+1)}{2\nu+3} B_{\mu,\nu+1,\bar{\mu}q}^{mn} \right]$$

$$b'_{\mu\nu\bar{\mu}q} = \frac{\pm k}{2\nu(\nu+1)}\left[(\nu-\mu)(\nu+\mu+1)B^{mn}_{\mu+1,\nu\bar{\mu}q} + B^{mn}_{\mu-1,\nu\bar{\mu}q}\right]$$

$$b''_{\mu\nu\bar{\mu}q} = \frac{k}{2\nu(\nu+1)}\left[(\nu-\mu)(\nu+\mu+1)B^{mn}_{\mu+1,\nu\bar{\mu}q} - B^{mn}_{\mu-1,\nu\bar{\mu}q}\right] \tag{2.31}$$

$$b'''_{\mu\nu\bar{\mu}q} = \frac{\mp k\mu}{\nu(\nu+1)}B^{mn}_{\mu\nu\bar{\mu}q}$$

Substituting (2.29) in (2.27), and taking into account the cancellation of the three components of $\mathbf{m}^{r'(1)}_{e,o\,\mu\nu}$ and $\mathbf{n}^{r'(1)}_{e,o\,\mu\nu}$ for $\nu=\mu=0$, yields

$$\mathbf{M}^{r(i)}_{e,omn} = \sum_{q=0,1}^{\infty\prime}\sum_{\bar{\mu}=-(|m|+q)}^{|m|+q} F^{mn}_{\bar{\mu}q}\sum_{\nu=1}^{\infty}\sum_{\mu=0}^{\nu}\{{}^{e,o}x^{mn}_{\mu\nu\bar{\mu}q}\,\mathbf{m}^{r'(1)}_{e,o\,\mu\nu} + {}^{e,o}y^{mn}_{\mu\nu\bar{\mu}q}\,\mathbf{n}^{r'(1)}_{e,o\,\mu\nu} + {}^{o,e}z^{mn}_{\mu\nu\bar{\mu}q}\,\mathbf{m}^{r'(1)}_{o,e\,\mu\nu} + {}^{o,e}t^{mn}_{\mu\nu\bar{\mu}q}\,\mathbf{n}^{r'(1)}_{o,e\,\mu\nu}\} \tag{2.32}$$

where

$$\begin{aligned}
{}^{e,o}x^{mn}_{\mu\nu\bar{\mu}q} &= {}^{e,o}_{c}B^{mn}_{\mu\nu\bar{\mu}q} + d\sin\theta_d\cos\phi_d\ {}^{e,o}_{c}a'_{\mu\nu\bar{\mu}q} + d\cos\theta_d\ {}^{e,o}_{c}a'''_{\mu\nu\bar{\mu}q} \mp d\sin\theta_d\sin\phi_d\ {}^{o,e}_{s}a''_{\mu\nu\bar{\mu}q}\\
{}^{e,o}y^{mn}_{\mu\nu\bar{\mu}q} &= d\sin\theta_d\sin\phi_d\ {}^{e,o}_{c}b''_{\mu\nu\bar{\mu}q} \mp (d\sin\theta_d\cos\phi_d\ {}^{o,e}_{s}b'_{\mu\nu\bar{\mu}q} + d\cos\theta_d\ {}^{o,e}_{s}b'''_{\mu\nu\bar{\mu}q})\\
{}^{o,e}z^{mn}_{\mu\nu\bar{\mu}q} &= d\sin\theta_d\sin\phi_d\ {}^{e,o}_{c}a''_{\mu\nu\bar{\mu}q} \mp ({}^{o,e}_{s}B^{mn}_{\mu\nu\bar{\mu}q} + d\sin\theta_d\cos\phi_d\ {}^{o,e}_{s}a'_{\mu\nu\bar{\mu}q} + d\cos\theta_d\ {}^{o,e}_{s}a'''_{\mu\nu\bar{\mu}q})\\
{}^{o,e}t^{mn}_{\mu\nu\bar{\mu}q} &= d\sin\theta_d\cos\phi_d\ {}^{e,o}_{c}b'_{\mu\nu\bar{\mu}q} + d\cos\theta_d\ {}^{e,o}_{c}b'''_{\mu\nu\bar{\mu}q} \mp d\sin\theta_d\sin\phi_d\ {}^{o,e}_{s}b''_{\mu\nu\bar{\mu}q}
\end{aligned} \tag{2.33}$$

in which the coefficients ${}^{e,o}_{c}a'_{\mu\nu\bar{\mu}q}$, ${}^{e,o}_{c}b'_{\mu\nu\bar{\mu}q}$, . . . , are evaluated by replacing $B^{mn}_{\mu\nu\bar{\mu}q}$ in (2.30) and (2.31) by ${}^{e,o}_{c}B^{mn}_{\mu\nu\bar{\mu}q}$ and ${}^{o,e}_{s}B^{mn}_{\mu\nu\bar{\mu}q}$, appropriately.

Taking the curl of both sides of (2.32) and then multiplying by k^{-1} gives

$$\mathbf{N}^{r(i)}_{e,omn} = \sum_{q=0,1}^{\infty\prime}\sum_{\bar{\mu}=-(|m|+q)}^{|m|+q} F^{mn}_{\bar{\mu}q}\sum_{\nu=1}^{\infty}\sum_{\mu=0}^{\nu}\{{}^{e,o}x^{mn}_{\mu\nu\bar{\mu}q}\,\mathbf{n}^{r'(1)}_{e,o\,\mu\nu} + {}^{e,o}y^{mn}_{\mu\nu\bar{\mu}q}\,\mathbf{m}^{r'(1)}_{e,o\,\mu\nu} + {}^{o,e}z^{mn}_{\mu\nu\bar{\mu}q}\,\mathbf{n}^{r'(1)}_{o,e\,\mu\nu} + {}^{o,e}t^{mn}_{\mu\nu\bar{\mu}q}\,\mathbf{m}^{r'(1)}_{o,e\,\mu\nu}\} \tag{2.34}$$

where the invariance of the curl operator to a transformation of the coordinate system has been considered. Using the relations [28], [47]

$$\mathbf{m}^{r'(1)}_{e,o\,\mu\nu}(r',\theta',\phi') = \sum_{l=\mu,\mu+1}^{\infty}{}' \Gamma_{\mu\nu l}\, \mathbf{M}^{r'(1)}_{e,o\,\mu l}(h';\mathbf{r}') \tag{2.35}$$

$$\mathbf{n}^{r'(1)}_{e,o\,\mu\nu}(r',\theta',\phi') = \sum_{l=\mu,\mu+1}^{\infty}{}' \Gamma_{\mu\nu l}\, \mathbf{N}^{r'(1)}_{e,o\,\mu l}(h';\mathbf{r}') \tag{2.36}$$

in (2.32) and (2.34), gives [55]

$$\begin{aligned}\mathbf{M}^{r(i)}_{e,omn} = \sum_{q=0,1}^{\infty}{}' \sum_{\bar{\mu}=-(|m|+q)}^{|m|+q} \sum_{\nu=1}^{\infty} \sum_{\mu=0}^{\nu} \sum_{l=\mu,\mu+1}^{\infty}{}' (&A^{mn}_{\mu\nu\bar{\mu}ql}\, \mathbf{M}^{r'(1)}_{e,o\,\mu l} + B^{mn}_{\mu\nu\bar{\mu}ql}\, \mathbf{N}^{r'(1)}_{o,e\,\mu l} \\ &+ C^{mn}_{\mu\nu\bar{\mu}ql}\, \mathbf{M}^{r'(1)}_{o,e\,\mu l} + D^{mn}_{\mu\nu\bar{\mu}ql}\, \mathbf{N}^{r'(1)}_{e,o\,\mu l})\end{aligned} \tag{2.37}$$

$$\begin{aligned}\mathbf{N}^{r(i)}_{e,omn} = \sum_{q=0,1}^{\infty}{}' \sum_{\bar{\mu}=-(|m|+q)}^{|m|+q} \sum_{\nu=1}^{\infty} \sum_{\mu=0}^{\nu} \sum_{l=\mu,\mu+1}^{\infty}{}' (&A^{mn}_{\mu\nu\bar{\mu}ql}\, \mathbf{N}^{r'(1)}_{e,o\,\mu l} + B^{mn}_{\mu\nu\bar{\mu}ql}\, \mathbf{M}^{r'(1)}_{o,e\,\mu l} \\ &+ C^{mn}_{\mu\nu\bar{\mu}ql}\, \mathbf{N}^{r'(1)}_{o,e\,\mu l} + D^{mn}_{\mu\nu\bar{\mu}ql}\, \mathbf{M}^{r'(1)}_{e,o\,\mu l})\end{aligned} \tag{2.38}$$

The rotational-translational addition theorems for vector spheroidal wave functions were also obtained independently in [56]. The explicit form of the coefficients in the above two equations are obtained in this thesis as

$$\begin{aligned} A^{mn}_{\mu\nu\bar{\mu}ql} &= {}^{e,o}X^{mn}_{\mu\nu\bar{\mu}q}(\alpha,\beta,\gamma;\mathbf{d})\,\Gamma_{\mu\nu l}\,, \qquad C^{mn}_{\mu\nu\bar{\mu}ql} = {}^{o,e}Z^{mn}_{\mu\nu\bar{\mu}q}(\alpha,\beta,\gamma;\mathbf{d})\,\Gamma_{\mu\nu l} \\ D^{mn}_{\mu\nu\bar{\mu}ql} &= {}^{e,o}Y^{mn}_{\mu\nu\bar{\mu}q}(\alpha,\beta,\gamma;\mathbf{d})\,\Gamma_{\mu\nu l}\,, \qquad B^{mn}_{\mu\nu\bar{\mu}ql} = {}^{o,e}T^{mn}_{\mu\nu\bar{\mu}q}(\alpha,\beta,\gamma;\mathbf{d})\,\Gamma_{\mu\nu l} \end{aligned} \tag{2.39}$$

with

$$\begin{aligned} {}^{e,o}X^{mn}_{\mu\nu\bar{\mu}q}(\alpha,\beta,\gamma;\mathbf{d}) &= {}^{e,o}x^{mn}_{\mu\nu\bar{\mu}q}\,F^{mn}_{\bar{\mu}q}\,, \qquad {}^{o,e}Z^{mn}_{\mu\nu\bar{\mu}q}(\alpha,\beta,\gamma;\mathbf{d}) = {}^{o,e}z^{mn}_{\mu\nu\bar{\mu}q}\,F^{mn}_{\bar{\mu}q} \\ {}^{e,o}Y^{mn}_{\mu\nu\bar{\mu}q}(\alpha,\beta,\gamma;\mathbf{d}) &= {}^{e,o}y^{mn}_{\mu\nu\bar{\mu}q}\,F^{mn}_{\bar{\mu}q}\,, \qquad {}^{o,e}T^{mn}_{\mu\nu\bar{\mu}q}(\alpha,\beta,\gamma;\mathbf{d}) = {}^{o,e}t^{mn}_{\mu\nu\bar{\mu}q}\,F^{mn}_{\bar{\mu}q} \end{aligned} \tag{2.40}$$

Expressions in (2.37) and (2.38) give the rotational-translational addition theorems for vector spheroidal wave functions $\mathbf{M}^{r(i)}_{e,omn}$ and $\mathbf{N}^{r(i)}_{e,omn}$ for i=1,2,3,4 and $r' \le d$, which are necessary in the study of multiple scattering of electromagnetic waves by two spheroids of arbitrary orientation.

2.2 Special Cases

2.2.1 Translational Addition Theorems

This special case is obtained when $\alpha \to 0$, $\beta \to 0$, and $\gamma \to 0$. Referring to (B.3), (B.4), and (B.5) (see the Appendix B), we can write

$$R_{\bar{\mu}s}^{ms}(0,0,0) = \delta_{m\bar{\mu}} \tag{2.41}$$

where δ is the Kronecker delta function. By setting $s = |m|+q$, $l = |\mu|+r$ in (B.1) and (B.2), and then substituting ${}^{(i)}a_{\mu,|\mu|+r}^{m,|m|+q}(\mathbf{d})$ in (B.1) from (B.6), and $b_{\mu p}^{m,|m|+q}(\mathbf{d})$ in (B.2) from (B.8) and (B.9), (B.1) and (B.2) can be rewritten as

$$\begin{aligned} {}^{(i)}Q_{\mu\nu}^{mn} = \frac{2(-1)^{\mu}}{N_{\mu\nu}(h')} \sum_{q=0,1}^{\infty\prime} \sum_{r=0,1}^{\infty\prime} \sum_{p_0,p_0+1}^{|m|+q+|\mu|+r\prime} j^{p+\nu-n} \frac{(|\mu|+\mu+r)!}{(|\mu|-\mu+r)!} d_q^{mn}(h)\, d_r^{\mu\nu}(h') \\ \cdot a(m,|m|+q|-\mu,|\mu|+r|p)\, z_p^{(i)}(kd)\, P_p^{m-\mu}(\cos\theta_d)\, e^{j(m-\mu)\phi_d} \end{aligned} \tag{2.42}$$

$$\begin{aligned} P_{\mu\nu}^{mn} = \frac{2(-1)^{m-\mu}}{N_{\mu\nu}(h')} \sum_{q=0,1}^{\infty\prime} \sum_{p=|\mu|,|\mu|+1}^{\infty\prime} \sum_{l=l_0,l_0+1}^{p+|m|+q\prime} d_q^{mn}(h)\, a(m,|m|+q|\mu-m,l|p) \\ \cdot j^{l+\nu-n}(2l+1) \frac{d_{p-|\mu|}^{\mu\nu}(h')}{(2p+1)} \frac{(p+\mu)!}{(p-\mu)!} z_l^{(1)}(kd)\, P_l^{m-\mu}(\cos\theta_d)\, e^{j(m-\mu)\phi_d} \end{aligned} \tag{2.43}$$

When $\alpha \to 0, \beta \to 0, \gamma \to 0$, the coefficients $c_{ax'}, c_{ay'}, c_{az'}$ $(a = x,y,z)$ defined in (2.4) are all zero except $c_{xx'}, c_{yy'}$, and $c_{zz'}$ which are equal to unity. Substitution of these in (2.7)–(2.8) gives for $a = x,y,z$ and $a' = x',y',z'$

$$\mathbf{X}_{mn}^{a(i)}(h;\mathbf{r}) = \sum_{\nu=0}^{\infty} \sum_{\mu=-\nu}^{\nu} {}^{(i)}Q_{\mu\nu}^{mn}\, \mathbf{X}_{\mu\nu}^{a'(1)}(h';\mathbf{r}'), \quad r' \le d\ ;\ i = 1,2,3,4 \tag{2.44}$$

$$\mathbf{X}_{mn}^{a(i)}(h;\mathbf{r}) = \sum_{\nu=0}^{\infty} \sum_{\mu=-\nu}^{\nu} P_{\mu\nu}^{mn}\, \mathbf{X}_{\mu\nu}^{a'(i)}(h';\mathbf{r}'), \quad r' \ge d\ ;\ i = 1,2,3,4 \tag{2.45}$$

where $\mathbf{X}$ is either of the vector spheroidal wave functions $\mathbf{M}$ or $\mathbf{N}$.

Equation (2.44) for $\mathbf{X}=\mathbf{M}$ and $\mathbf{X}=\mathbf{N}$ is exactly the same as eqs. (2.42) and (2.44) in [43]. However eq. (2.45) for $\mathbf{X}=\mathbf{M}$ and $\mathbf{X}=\mathbf{N}$ is not the same as eqs. (2.43) and (2.45)

in [43], but can be brought to the same form by the following rearrangement and change of notation. After substituting $P_{\mu\nu}^{mn}$ from (2.43), (2.45) becomes

$$\mathbf{X}_{mn}^{a(i)}(h;\mathbf{r}) = \sum_{\nu=0}^{\infty} \sum_{\mu=-\nu}^{\nu} \frac{2(-1)^{m-\mu}}{N_{\mu\nu}(h')} \sum_{q=0,1}^{\infty}{}' \sum_{p=|\mu|,|\mu|+1}^{\infty}{}' \sum_{l=l_0,l_0+1}^{p+|m|+q}{}' d_q^{mn}(h)$$
$$\cdot j^{l+\nu-n}(2l+1)\, a(m,|m|+q|\mu-m,l|p)\, \frac{d_{p-|\mu|}^{\mu\nu}(h')}{(2p+1)}$$
$$\cdot \frac{(p+\mu)!}{(p-\mu)!}\, z_l^{(1)}(kd)\, P_l^{m-\mu}(\cos\theta_d)\, e^{j(m-\mu)\phi_d}\, \mathbf{X}_{\mu\nu}^{a'(i)}(h';\mathbf{r}') \qquad (2.46)$$

By replacing μ by $m-\mu$, ν by t, l by ν, and rearranging, we obtain

$$\mathbf{X}_{mn}^{a(i)}(h;\mathbf{r}) = \sum_{\nu=0}^{\infty} \sum_{\mu=-\nu}^{\nu} \sum_{t=|m-\mu|,|m-\mu|+1}^{\infty}{}' \frac{2(-1)^{\mu}}{N_{m-\mu,t}(h')}(2\nu+1)\, z_\nu^{(1)}(kd)$$
$$\cdot P_\nu^{\mu}(\cos\theta_d)\, e^{j\mu\phi_d} \sum_{q=0,1}^{\infty}{}' \sum_{p_0,p_0+1}^{|m|+q+\nu}{}' \frac{j^{\nu+t-n}}{(2p+1)} \frac{(p+m-\mu)!}{(p-m+\mu)!}$$
$$\cdot d_q^{mn}(h)\, d_{p-|m-\mu|}^{m-\mu,t}(h')\, a(m,|m|+q|-\mu,\nu|p)\, \mathbf{X}_{m-\mu,t}^{a'(i)}(h';\mathbf{r}') \qquad (2.47)$$

Equation (2.47) for **X**=**M** and **X**=**N** gives the translational addition theorems for the case $r' \geq d$. Also in the limit $\alpha \to 0$, $\beta \to 0$, $\gamma \to 0$, (2.37) and (2.38) give the translational addition theorems for the vector spheroidal wave functions $\mathbf{M}_{e,omn}^{r(i)}$ and $\mathbf{N}_{e,omn}^{r(i)}$, for $r' \leq d$. When i=3, their expressions are identical to those in [47].

2.2.2 Rotational-translational Addition Theorems for Vector Spherical Wave Functions

In this section we particularize the rotational-translational addition theorems for vector spheroidal wave functions to obtain the theorems for vector spherical wave functions. These theorems are necessary for solving problems involving spheres which do not have homogeneous material properties; e.g. spheres whose material properties vary with the spherical coordinate θ. Even though translational addition theorems and

rotational addition theorems for vector spherical wave functions are available separately, they cannot be combined in a straightforward manner to obtain the rotational-translational addition theorems for vector spherical wave functions.

In the limit $h \to 0$ and $h' \to 0$, the spheroidal coordinate systems (ξ,η,ϕ) and (ξ',η',ϕ') reduce to the spherical systems (r,θ,ϕ) and (r',θ',ϕ'), respectively, with the spheroidal angle functions and the spheroidal radial functions becoming the associated Legendre functions and spherical Bessel functions, respectively,

$$\begin{aligned} S_{mn}(h,\eta) &\to P_n^m(\cos\theta) \\ S_{\mu\nu}(h',\eta') &\to P_\nu^\mu(\cos\theta') \\ N_{\mu\nu}(h) &\to \frac{2}{2\nu+1}\frac{(\nu+\mu)!}{(\nu-\mu)!} \end{aligned} \tag{2.48}$$

$$\{R_{mn}^{(1)}(h,\xi), R_{mn}^{(3)}(h,\xi), R_{mn}^{(4)}(h,\xi)\} \to \{j_n(kr), h_n^{(1)}(kr), h_n^{(2)}(kr)\}$$

$$\{R_{\mu\nu}^{(1)}(h',\xi'), R_{\mu\nu}^{(3)}(h',\xi'), R_{\mu\nu}^{(4)}(h',\xi')\} \to \{j_\nu(kr'), h_\nu^{(1)}(kr'), h_\nu^{(2)}(kr')\}$$

Substituting (2.18)–(2.22) in (2.24), and rearranging, we get in the limit $h \to 0$, $h' \to 0$,

$$\cdot\psi_{mn}^{(i)}(r,\theta,\phi) = \sum_{\nu=0}^{\infty} \sum_{\mu=-\nu}^{\nu} {}^{(i)}G_{\mu\nu}^{mn} \cdot\psi_{\mu\nu}^{(1)'}(r',\theta',\phi') \tag{2.49}$$

where

$${}^{(i)}G_{\mu\nu}^{mn} = (-1)^\mu (2\nu+1)\, j^{\nu-n} \sum_{q=0,1}^{\infty}{}' d_q^{mn}(h) \sum_{\overline{\mu}=-(|m|+q)}^{|m|+q} R_{\overline{\mu},|m|+q}^{m,|m|+q}(\alpha,\beta,\gamma)$$
$$\cdot \sum_{p_0,p_0+1}^{|m|+q+\nu}{}' j^p\, a(\overline{\mu},|m|+q|-\mu,\nu|p)\, \cdot\psi_{\overline{\mu}-\mu,p}^{(i)}(\mathbf{d}) \tag{2.50}$$

By expanding $\cdot\psi_{\overline{\mu}-\mu,p}^{(i)}(\mathbf{d})$ in double integrals [40], [53], (2.50) becomes

$$
{}^{(i)}G_{\mu\nu}^{mn} = (-1)^{\mu}(2\nu+1)\, j^{\nu-n} \sum_{q=0,1}^{\infty}{}' \sum_{\bar{\mu}=-(|m|+q)}^{|m|+q} \sum_{p_0,p_0+1}^{|m|+q+\nu}{}' j^{p}\, d_q^{mn}(h)
$$

$$
\cdot R_{\bar{\mu},|m|+q}^{m,|m|+q}(\alpha,\beta,\gamma)\; a(\bar{\mu},|m|+q|-\mu,\nu|p)\,(4\pi j^{p})^{-1}
$$

$$
\cdot \int_0^{2\pi}\int_c \exp(jkd\cos\gamma_{kd})\, P_p^{\bar{\mu}-\mu}(\cos\theta_k')\, e^{j(\bar{\mu}-\mu)\phi_k'} \sin\theta_k'\, d\theta_k'\, d\phi_k' \tag{2.51}
$$

where

$$
\cos\gamma_{kd} = \sin\theta_k' \sin\theta_d \cos(\phi_d - \phi_k') + \cos\theta_k' \cos\theta_d \tag{2.52}
$$

with $\int_c$ being $\int_0^{\pi}$ for $i=1$, $2\int_0^{\pi/2-j\infty}$ for $i=3$, and $2\int_{\pi/2-j\infty}^{\pi}$ for $i=4$. Taking into account the linearization expansion [40], [41] of the product $P_{|m|+q}^{\bar{\mu}}(\cos\theta_k')\, P_{\nu}^{-\mu}(\cos\theta_k')$, (2.51) can be written in the limit $h' \to 0$ as

$$
{}^{(i)}G_{\mu\nu}^{mn} = (-1)^{\mu}(2\nu+1)\, j^{\nu-n}(4\pi)^{-1} \sum_{q=0,1}^{\infty}{}' \sum_{\bar{\mu}=-(|m|+q)}^{|m|+q} R_{\bar{\mu},|m|+q}^{m,|m|+q}(\alpha,\beta,\gamma)\, d_q^{mn}(h)
$$

$$
\cdot \int_0^{2\pi}\int_c \exp(jkd\cos\gamma_{kd})\, P_{|m|+q}^{\bar{\mu}}(\cos\theta_k')\, P_{\nu}^{-\mu}(\cos\theta_k')\, e^{j(\bar{\mu}-\mu)\phi_k'}
$$

$$
\cdot \sin\theta_k'\, d\theta_k'\, d\phi_k' \tag{2.53}
$$

Using the expansion [51],

$$
P_{|m|+q}^{m}(\cos\theta_k)\, e^{jm\phi_k} = \sum_{\bar{\mu}=-(|m|+q)}^{|m|+q} R_{\bar{\mu},|m|+q}^{m,|m|+q}(\alpha,\beta,\gamma)\, P_{|m|+q}^{\bar{\mu}}(\cos\theta_k')\, e^{j\bar{\mu}\phi_k'} \tag{2.54}
$$

yields, in the limit $h \to 0$,

$$
{}^{(i)}G_{\mu\nu}^{mn} = (-1)^{\mu}(2\nu+1)\, j^{\nu-n}(4\pi)^{-1} \int_0^{2\pi}\int_c \exp(jkd\cos\gamma_{kd})\, P_n^{m}(\cos\theta_k)
$$

$$
\cdot P_{\nu}^{-\mu}(\cos\theta_k')\, e^{jm\phi_k}\, e^{-j\mu\phi_k'} \sin\theta_k'\, d\theta_k'\, d\phi_k' \tag{2.55}
$$

Applying again the expansion of $P_n^{m}(\cos\theta_k)\, e^{jm\phi_k}$ as shown in (2.54) gives

$$ {}^{(i)}G_{\mu\nu}^{mn} = (-1)^{\mu}(2\nu+1)\, j^{\nu-n} \sum_{\bar{\mu}=-n}^{n} R_{\bar{\mu}n}^{mn}(\alpha,\beta,\gamma)\,(4\pi)^{-1} \int_0^{2\pi}\int_c \exp(jkd\cos\gamma_{kd}) $$

$$ \cdot\, P_n^{\bar{\mu}}(\cos\theta'_k)\, P_\nu^{-\mu}(\cos\theta'_k)\, e^{j(\bar{\mu}-\mu)\phi'_k} \sin\theta'_k\, d\theta'_k\, d\phi'_k \tag{2.56} $$

and with the linearization expansion of $P_n^{\bar{\mu}}(\cos\theta'_k)\,P_\nu^{-\mu}(\cos\theta'_k)$ and the expansion of $\psi_{\bar{\mu}-\mu,p}^{(i)}(\mathbf{d})$ in double integrals, we obtain finally

$$ {}^{(i)}G_{\mu\nu}^{mn} = (-1)^{\mu}(2\nu+1)\, j^{\nu-n} \sum_{\bar{\mu}=-n}^{n} R_{\bar{\mu}n}^{mn}(\alpha,\beta,\gamma) \sum_{p_0,p_0+1}^{n+\nu\,\prime} j^{p}\, a(\bar{\mu},n|-\mu,\nu|p) $$

$$ \cdot\, z_p^{(i)}(kd)\, P_p^{\bar{\mu}-\mu}(\cos\theta_d)\, e^{j(\bar{\mu}-\mu)\phi_d} \tag{2.57} $$

Equation (2.57) gives the rotational-translational coefficients for scalar spherical wave functions, when $r' \le d$.

From Fig. 2.1 we have

$$ \mathbf{r} = \mathbf{r}' + \mathbf{d} \tag{2.58} $$

Taking the cross product of $\nabla\psi_{mn}^{(i)}$ with each side of (2.58) gives

$$ \mathbf{m}_{mn}^{r(i)} = \nabla\psi_{mn}^{(i)} \times \mathbf{r}' + \nabla\psi_{mn}^{(i)} \times \mathbf{d} \tag{2.59} $$

Since the gradient of a scalar function is invariant to a transformation of the coordinate system, we use (2.49) to write

$$ \nabla\psi_{mn}^{(i)} \times \mathbf{r}' = \sum_{\nu=0}^{\infty} \sum_{\mu=-\nu}^{\nu} {}^{(i)}G_{\mu\nu}^{mn}\, \mathbf{m}_{\mu\nu}^{r'(1)} \tag{2.60} $$

Also

$$ \nabla\psi_{mn}^{(i)} \times \mathbf{d} = d_x\, \mathbf{m}_{mn}^{x(i)} + d_y\, \mathbf{m}_{mn}^{y(i)} + d_z\, \mathbf{m}_{mn}^{z(i)} \tag{2.61} $$

As given in [42], the vector spherical wave functions $\mathbf{m}_{mn}^{a(i)}$ $(a = x, y, z)$ can be expressed in terms of the vector spherical wave functions $\mathbf{m}_{mn}^{r'(1)}$ and $\mathbf{n}_{mn}^{r'(1)}$ in the form

$$\begin{aligned}
\mathbf{m}_{mn}^{x(i)} &= \sum_{\nu=0}^{\infty} \sum_{\mu=-\nu}^{\nu} (e'_{\mu\nu}\mathbf{m}_{\mu\nu}^{r'(1)} + g'_{\mu\nu}\mathbf{n}_{\mu\nu}^{r'(1)}) \\
\mathbf{m}_{mn}^{y(i)} &= \sum_{\nu=0}^{\infty} \sum_{\mu=-\nu}^{\nu} (e''_{\mu\nu}\mathbf{m}_{\mu\nu}^{r'(1)} + g''_{\mu\nu}\mathbf{n}_{\mu\nu}^{r'(1)}) \\
\mathbf{m}_{mn}^{z(i)} &= \sum_{\nu=0}^{\infty} \sum_{\mu=-\nu}^{\nu} (e'''_{\mu\nu}\mathbf{m}_{\mu\nu}^{r'(1)} + g'''_{\mu\nu}\mathbf{n}_{\mu\nu}^{r'(1)})
\end{aligned} \tag{2.62}$$

$e'_{\mu\nu}$, $g'_{\mu\nu}$, . . . have the same form as those of $a'_{\mu\nu\bar{\mu}q}$, $b'_{\mu\nu\bar{\mu}q}$, . . . , respectively, with $B^{mn}_{\mu\nu\bar{\mu}q}$ replaced by ${}^{(i)}G^{mn}_{\mu\nu}$, and $\pm$ in $a''_{\mu\nu\bar{\mu}q}$ and $b'_{\mu\nu\bar{\mu}q}$ and $\mp$ in $b'''_{\mu\nu\bar{\mu}q}$ by $-j$ and $+j$, respectively.

Finally (2.59) can be expressed in the form

$$\mathbf{m}_{mn}^{r(i)} = \sum_{\nu=0}^{\infty} \sum_{\mu=-\nu}^{\nu} (A^{mn}_{\mu\nu}\mathbf{m}_{\mu\nu}^{r'(1)} + B^{mn}_{\mu\nu}\mathbf{n}_{\mu\nu}^{r'(1)}), \quad r' \le d\,; i=1,2,3,4 \tag{2.63}$$

in which

$$A^{mn}_{\mu\nu} = \dot{A}_{\mu\nu} + {}^{(i)}G^{mn}_{\mu\nu} \tag{2.64}$$

where

$$\dot{A}_{\mu\nu} = d_x e'_{\mu\nu} + d_y e''_{\mu\nu} + d_z e'''_{\mu\nu} \tag{2.65}$$

$$B^{mn}_{\mu\nu} = d_x g'_{\mu\nu} + d_y g''_{\mu\nu} + d_z g'''_{\mu\nu} \tag{2.66}$$

with the x, y, and z components of $\mathbf{d}$ given by

$$\begin{aligned}
d_x &= d(\sin\theta_d \cos\phi_d c_{xx'} + \sin\theta_d \sin\phi_d c_{xy'} + \cos\theta_d c_{xz'}) \\
d_y &= d(\sin\theta_d \cos\phi_d c_{yx'} + \sin\theta_d \sin\phi_d c_{yy'} + \cos\theta_d c_{yz'}) \\
d_z &= d(\sin\theta_d \cos\phi_d c_{zx'} + \sin\theta_d \sin\phi_d c_{zy'} + \cos\theta_d c_{zz'})
\end{aligned} \tag{2.67}$$

Equation (2.63) gives the rotational-translational addition theorems for the vector spherical wave functions $\mathbf{m}_{mn}^{r(i)}$, when $r' \le d$. The expressions corresponding to the vector spherical wave functions $\mathbf{n}_{mn}^{r(i)}$ [41], [42] have the same form, with $\mathbf{m}_{\mu\nu}^{r'(1)}$ and $\mathbf{n}_{\mu\nu}^{r'(1)}$ in (2.63) replaced by $\mathbf{n}_{\mu\nu}^{r'(1)}$ and $\mathbf{m}_{\mu\nu}^{r'(1)}$, respectively. It is also possible to obtain these theorems starting directly from the corresponding theorems for vector spheroidal wave functions, given in (2.37) and (2.38). However this derivation is more elaborate than

that presented above.

The translational addition theorems for vector spherical wave functions $\mathbf{m}_{mn}^{r(i)}$ are obtained from (2.63) as a special case, when $\alpha \to 0, \beta \to 0, \gamma \to 0$. Now $c_{ax'}, c_{ay'}, c_{az'}$ $(a = x, y, z)$ are all zero except $c_{xx'}, c_{yy'}$, and $c_{zz'}$ which are equal to unity. In this case (2.57) reduces to

$$^{(i)}G_{\mu\nu}^{mn} = (-1)^{\mu}(2\nu+1)\, j^{\nu-n} \sum_{p_0, p_0+1}^{n+\nu}{}' j^{p}\, a(m, n|-\mu, \nu|p)\, z_p^{(i)}(kd)\, P_p^{m-\mu}(\cos\theta_d)\, e^{j(m-\mu)\phi_d} \quad (2.68)$$

and (2.63) becomes identical to Theorem I, given in [42]. Similarly, for the vector spherical wave functions $\mathbf{n}_{mn}^{r(i)}$ we obtain Theorem II given in [42].

2.3 Numerical Experiments

Some numerical experiments have been performed on the equations describing the rotational-translational addition theorems for vector spheroidal wave functions (equations (2.10), (2.12), (2.14)). The objective of these experiments was to determine how many values for μ and ν are required in the double summations on the right hand sides of each equation in order to obtain a two significant digit accuracy when compared with the corresponding left hand sides, for various values of m and n. Numerical results corresponding to a sample calculation are given below.

In performing the following calculations, we have taken the points P and O' in Fig. 2.1 to have coordinates $(-1.0, 4.0, 2.0)$ and $(15.0, 20.0, 25.0)$, respectively, with respect to $Oxyz$, and have considered the system $O'x'y'z'$ as being rotated by the Euler angles $\alpha = \pi/5$, $\beta = \pi/8$, $\gamma = \pi/3$, relative to $Oxyz$. The spheroidal systems associated with the unprimed and primed Cartesian systems are assumed to have semi-interfocal distances of 6 and 7 units, respectively. With these parameters, the η

component of the vector wave functions ${}_{\eta}\mathbf{M}_{mn}^{+(4)}$, ${}_{\eta}\mathbf{M}_{mn}^{-(4)}$, and ${}_{\eta}\mathbf{M}_{mn}^{z(4)}$ calculated directly using the unprimed spheroidal coordinates ξ,η,ϕ have the values $0.010178,-j0.011765$, $-0.007669,-j0.012229$, and $0.003172,-j0.011274$, respectively, for $m=1$, $n=2$. The same values calculated with respect to the primed spheroidal coordinates ξ',η',ϕ', but using the double summations in μ and ν on the right hand sides of eqs. (2.10), (2.12), and (2.14), are tabulated below for different values of μ and ν.

Table 2.1 Calculated values of ${}_{\eta}\mathbf{M}_{mn}^{+(4)}$, ${}_{\eta}\mathbf{M}_{mn}^{-(4)}$, and ${}_{\eta}\mathbf{M}_{mn}^{z(4)}$, using the summation on the right hand side of the addition theorem equations, for different values of μ and ν

		$-1\le\mu\le1$	
$\nu\le$	${}_{\eta}\mathbf{M}_{mn}^{+(4)}$	${}_{\eta}\mathbf{M}_{mn}^{-(4)}$	${}_{\eta}\mathbf{M}_{mn}^{z(4)}$
$\lvert\mu\rvert$	$0.035681,-j0.006774$	$-0.020981,-j0.006537$	$0.001523,-j0.001847$
$\lvert\mu\rvert+1$	$0.01046,-j0.018574$	$-0.016272,-j0.001801$	$0.000762,-j0.005542$
$\lvert\mu\rvert+2$	$0.005694,-j0.015367$	$-0.017525,-j0.001556$	$0.001431,-j0.000278$
$\lvert\mu\rvert+3$	$0.004164,-j0.020236$	$-0.012547,-j0.005426$	$0.002018,-j0.009143$
$\lvert\mu\rvert+4$	$0.006245,-j0.017337$	$-0.011620,-j0.008074$	$0.002535,-j0.007355$
$\lvert\mu\rvert+5$	$0.006581,-j0.021546$	$-0.010233,-j0.007068$	$0.002727,-j0.008434$
		$-2\le\mu\le2$	
$\lvert\mu\rvert+1$	(0.018461,–0.032574)	(–0.022781,–0.018271)	(0.005225,–0.018761)
$\lvert\mu\rvert+2$	(0.016123,–0.012316)	(–0.011562,–0.014357)	(0.003762,–0.020028)
$\lvert\mu\rvert+3$	(0.011593,–0.011660)	(–0.009525,–0.012425)	(0.003551,–0.013402)
$\lvert\mu\rvert+4$	(0.010246,–0.012028)	(–0.007533,–0.012243)	(0.003273,–0.011332)
$\lvert\mu\rvert+5$	(0.010316,–0.011243)	(–0.007692,–0.012374)	(0.003157,–0.011408)

$\lvert\mu\rvert+6$	(0.010320,–0.011238)	(–0.007686,–0.012383)	(0.003165,–0.011415)
		$-3\le\mu\le 3$	
$\lvert\mu\rvert+2$	(0.021069,–0.038446)	(–0.020720,–0.023278)	(0.004125,–0.029761)
$\lvert\mu\rvert+3$	(0.014233,–0.023564)	(–0.015476,–0.019342)	(0.003841,–0.014335)
$\lvert\mu\rvert+4$	(0.011934,–0.013721)	(–0.009632,–0.014563)	(0.003322,–0.012211)
$\lvert\mu\rvert+5$	(0.010566,–0.011411)	(–0.007602,–0.012553)	(0.003188,–0.011589)
$\lvert\mu\rvert+6$	(0.010432,–0.011326)	(–0.007658,–0.012099)	(0.003124,–0.011356)
$\lvert\mu\rvert+7$	(0.010428,–0.011313)	(–0.007633,–0.012087)	(0.003127,–0.011344)
		$-4\le\mu\le 4$	
$\nu\le$	${}_{\eta}\mathbf{M}_{mn}^{+(4)}$	${}_{\eta}\mathbf{M}_{mn}^{-(4)}$	${}_{\eta}\mathbf{M}_{mn}^{z(4)}$
$\lvert\mu\rvert+3$	(0.017832,–0.019578)	(–0.018533,–0.017265)	(0.003564,–0.021644)
$\lvert\mu\rvert+4$	(0.012103,–0.012377)	(–0.008724,–0.013521)	(0.003214,–0.012537)
$\lvert\mu\rvert+5$	(0.010421,–0.011233)	(–0.007681,–0.012199)	(0.003168,–0.011461)
$\lvert\mu\rvert+6$	(0.010398,–0.011203)	(–0.007653,–0.012078)	(0.003153,–0.011378)
$\lvert\mu\rvert+7$	(0.010381,–0.011215)	(–0.007643,–0.012067)	(0.003142,–0.011364)
$\lvert\mu\rvert+8$	(0.010428,–0.011313)	(–0.007638,–0.012059)	(0.003136,–0.011362)

The values on the column under $\nu\le$ indicate the maximum value of ν, with the starting value always being $\lvert\mu\rvert$. The results for ${}_{\phi}\mathbf{M}_{mn}^{+(4)}$, ${}_{\phi}\mathbf{M}_{mn}^{-(4)}$, and ${}_{\phi}\mathbf{M}_{mn}^{z(4)}$, have similar convergence. From these experiments it is obvious that it is sufficient to consider only $-2\le\mu\le 2$ and $\nu=\lvert\mu\rvert, \lvert\mu\rvert+1, \ldots \lvert\mu\rvert+5$ in the summations in μ and ν in order to obtain a two significant digit accuracy for the calculated vector spheroidal wave functions, for major axes of the spheroids in the range of magnitude considered.

CHAPTER 3

SCATTERING OF PLANE ELECTROMAGNETIC WAVES BY SPHEROIDS OF ARBITRARY ORIENTATION

By expanding the incident, scattered, and transmitted electromagnetic fields in terms of appropriate vector spheroidal eigenfunctions, an exact solution is obtained in this chapter to the more general problem of scattering of a plane electromagnetic wave by n dielectric prolate spheroids of arbitrary orientation. The boundary conditions at the surface of a given spheroid are imposed by expressing the electromagnetic fields scattered by all the other $n-1$ spheroids, in terms of the spheroidal coordinates attached to the spheroid considered, using the rotational-translational addition theorems for vector spheroidal wave functions. The solution of the associated set of algebraic equations yields the column matrix of the unknown scattered and transmitted field expansion coefficients, being expressed as the product of a system matrix and the column matrix of the known incident field expansion coefficients. In Section 3.1 we discuss the formulation and analysis of the problem and in Section 3.2, the imposing of the boundary conditions and the derivation of the system matrix $[G_d]$. Next, as a special case, the derivation of the system matrix $[G_c]$ associated with the solution to the problem of scattering by n perfectly conducting spheroids of arbitrary orientation is presented in Section 3.3, and finally in Section 3.4 we give the special form of the solution for the case of two spheroids of arbitrary orientation.

3.1 Formulation and Analysis of the General Problem

Let us consider in general n prolate spheroids of arbitrary orientation, with their centers located at the origins O_g of the Cartesian coordinate systems $O_g x_g y_g z_g$ $(g = 1, 2, \ldots, n)$, respectively, and the g th coordinate system attached to the g th spheroid. The major axes of the spheroids are along the z axes of the respective Cartesian systems. Each of the origins O_g has spherical coordinates $d_g, \theta_{0_g}, \phi_{0_g}$ with respect to the global Cartesian system $Oxyz$, and each system $O_g x_g y_g z_g$ is rotated with respect to $Oxyz$ through the Euler angles $\alpha_g, \beta_g, \gamma_g$. The positions and orientations of the q th and r th spheroids, which are two members of the above mentioned system of n spheroids, and the Cartesian systems attached to them are shown in Fig. 3.1. Let a linearly polarized, monochromatic uniform plane electromagnetic wave with an electric field of unit amplitude be incident at an angle θ_i with respect to the z axis of the system $Oxyz$, the plane of incidence being chosen as the $x-z$ plane $(\phi_i = 0)$, as shown in Fig. 3.1. The polarization angle γ_k is the angle between the direction of the incident electric field intensity vector and the direction of the normal to the plane of incidence. For transverse electric (TE) polarization γ_k is zero and for transverse magnetic (TM) polarization it is $\pi/2$. It is assumed that the medium in which the spheroids are embedded is isotropic and nonconducting, and further that both the medium and the spheroids are nonmagnetic. If we consider the r th spheroid to which the Cartesian system $O_r x_r y_r z_r$ is attached, then the incident electric field can be expanded in terms of vector spheroidal wave functions in the r th coordinate system as shown below. A time dependence of $e^{j\omega t}$ is assumed throughout, but suppressed for convenience.

Since the direction of the incident wave vector $\mathbf{k}$ with respect to the system $Oxyz$

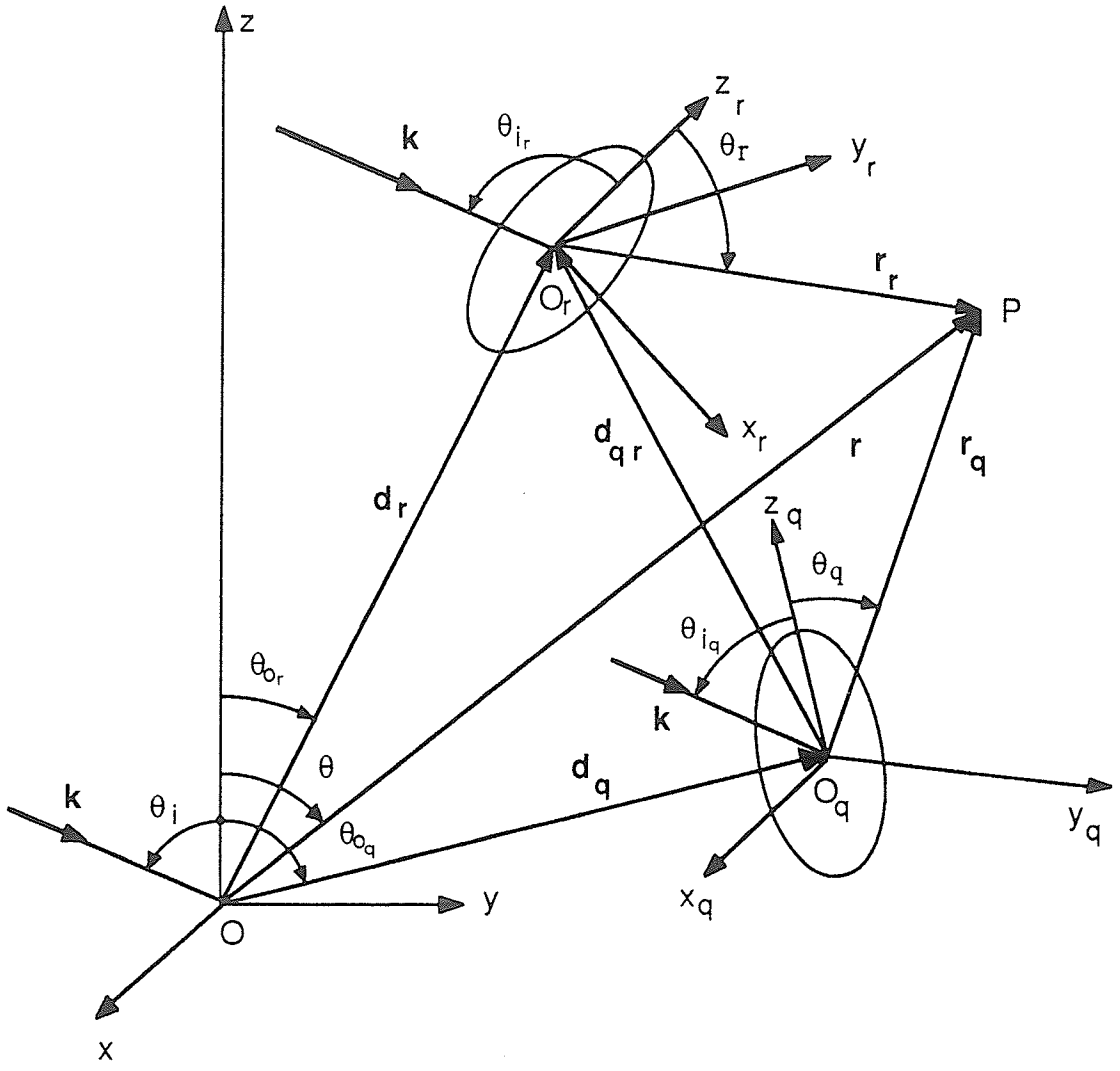

Fig. 3.1 The geometry of the qth and rth prolate spheroids and the associated Cartesian systems of arbitrary orientation.

is specified by the angular spherical coordinates θ_i and $\phi_i = 0$, we have

$$\mathbf{k} = -k\ (\sin\theta_i\,\hat{\mathbf{x}} + \cos\theta_i\,\hat{\mathbf{z}}) \tag{3.1}$$

If the direction of $\mathbf{k}$ with respect to the system $O_r x_r y_r z_r$ is specified by the angular spherical coordinates θ_{i_r}, ϕ_{i_r}, then

$$\mathbf{k} = -k\ (\sin\theta_{i_r}\cos\phi_{i_r}\,\hat{\mathbf{x}}_r + \sin\theta_{i_r}\sin\phi_{i_r}\,\hat{\mathbf{y}}_r + \cos\theta_{i_r}\,\hat{\mathbf{z}}_r) \tag{3.2}$$

The unit vectors $\hat{\mathbf{x}}$, $\hat{\mathbf{y}}$, $\hat{\mathbf{z}}$ in $Oxyz$ can be expressed in terms of $\hat{\mathbf{x}}_r$, $\hat{\mathbf{y}}_r$, $\hat{\mathbf{z}}_r$ in $O_r x_r y_r z_r$ as

$$\hat{\mathbf{a}} = {}^{r}c_{ax}\,\hat{\mathbf{x}}_r + {}^{r}c_{ay}\,\hat{\mathbf{y}}_r + {}^{r}c_{az}\,\hat{\mathbf{z}}_r \qquad \hat{\mathbf{a}} = \hat{\mathbf{x}}, \hat{\mathbf{y}}, \hat{\mathbf{z}} \tag{3.3}$$

where

$$\begin{aligned}
{}^{r}c_{xx} &= \cos\alpha_r\cos\beta_r\cos\gamma_r - \sin\alpha_r\sin\gamma_r \\
{}^{r}c_{xy} &= -(\cos\alpha_r\cos\beta_r\sin\gamma_r + \sin\alpha_r\cos\gamma_r) \\
{}^{r}c_{xz} &= \cos\alpha_r\sin\beta_r \\
{}^{r}c_{yx} &= \sin\alpha_r\cos\beta_r\cos\gamma_r + \cos\alpha_r\sin\gamma_r \\
{}^{r}c_{yy} &= \cos\alpha_r\cos\gamma_r - \sin\alpha_r\cos\beta_r\sin\gamma_r \\
{}^{r}c_{yz} &= \sin\alpha_r\sin\beta_r \\
{}^{r}c_{zx} &= -\sin\beta_r\cos\gamma_r \\
{}^{r}c_{zy} &= \sin\beta_r\sin\gamma_r \\
{}^{r}c_{zz} &= \cos\beta_r
\end{aligned} \tag{3.4}$$

with α_r, β_r, γ_r being the Euler angles as defined in [52]. Substituting $\hat{\mathbf{x}}$ and $\hat{\mathbf{z}}$ from (3.3) in (3.1) and identifying the corresponding coefficients of $\hat{\mathbf{x}}_r$, $\hat{\mathbf{y}}_r$, $\hat{\mathbf{z}}_r$ with those in (3.2) gives

$$\begin{aligned}
\sin\theta_{i_r}\cos\phi_{i_r} &= {}^{r}c_{xx}\sin\theta_i + {}^{r}c_{zx}\cos\theta_i \\
\sin\theta_{i_r}\sin\phi_{i_r} &= {}^{r}c_{xy}\sin\theta_i + {}^{r}c_{zy}\cos\theta_i \\
\cos\theta_{i_r} &= {}^{r}c_{xz}\sin\theta_i + {}^{r}c_{zz}\cos\theta_i
\end{aligned} \tag{3.5}$$

from which θ_{i_r} and ϕ_{i_r} can be evaluated.

The incident electric field intensity ${}^{(r)}\mathbf{E}_i$ in the system $O_r x_r y_r z_r$ can be written as

$$ {}^{(r)}\mathbf{E}_i = {}^{(r)}\mathbf{E}_i^{TE}\cos\gamma_k + {}^{(r)}\mathbf{E}_i^{TM}\sin\gamma_k \tag{3.6} $$

where

$$ {}^{(r)}\mathbf{E}_i^{TE} = \hat{\mathbf{y}} e^{-j\mathbf{k}\cdot\mathbf{r}} \tag{3.7} $$

$$ {}^{(r)}\mathbf{E}_i^{TM} = (-\cos\theta_i \hat{\mathbf{x}} + \sin\theta_i \hat{\mathbf{z}})\, e^{-j\mathbf{k}\cdot\mathbf{r}} \tag{3.8} $$

From the relationship between the vectors $\mathbf{r}$, $\mathbf{r}_r$, and $\mathbf{d}_r$ (see Fig. 3.1) we get

$$ e^{-j\mathbf{k}\cdot\mathbf{r}} = e^{-j\mathbf{k}\cdot\mathbf{d}_r} \cdot e^{-j\mathbf{k}\cdot\mathbf{r}_r} \tag{3.9} $$

Taking first the gradient on both sides of (3.9) and then the cross product with $\hat{\mathbf{x}}$ gives

$$ \hat{\mathbf{y}} e^{-j\mathbf{k}\cdot\mathbf{r}} = (jk\cos\theta_i)^{-1} e^{-j\mathbf{k}\cdot\mathbf{d}_r} \nabla(e^{-j\mathbf{k}\cdot\mathbf{r}_r}) \times \hat{\mathbf{x}} \tag{3.10} $$

Substituting $\hat{\mathbf{x}}$ from (3.3) and applying the expansion [28]

$$ e^{-j\mathbf{k}\cdot\mathbf{r}_r} = 2 \sum_{m=-\infty}^{\infty} \sum_{n=|m|}^{\infty} \frac{j^n}{N_{mn}(h_r)} S_{mn}(h_r, \cos\theta_{i_r}) e^{-jm\phi_{i_r}} \psi_{mn}^{(1)}(h_r; \xi_r, \eta_r, \phi_r) \tag{3.11} $$

gives

$$ {}^{(r)}\mathbf{E}_i^{TE} = 2\,(jk\cos\theta_i)^{-1} e^{-j\mathbf{k}\cdot\mathbf{d}_r} \sum_{m=-\infty}^{\infty} \sum_{n=|m|}^{\infty} \frac{j^n}{N_{mn}(h_r)} S_{mn}(h_r, \cos\theta_{i_r})\, e^{-jm\phi_{i_r}} $$

$$ \cdot \left[{}^{r}c_{xx}\, {}^{(r)}\mathbf{M}_{mn}^{x(1)}(h_r; \mathbf{r}_r) + {}^{r}c_{xy}\, {}^{(r)}\mathbf{M}_{mn}^{y(1)}(h_r; \mathbf{r}_r) + {}^{r}c_{xz}\, {}^{(r)}\mathbf{M}_{mn}^{z(1)}(h_r; \mathbf{r}_r) \right] \tag{3.12} $$

with $\mathbf{r}_r$ denoting the coordinate triad (ξ_r, η_r, ϕ_r), and the superscript (r) to the left of the vector wave functions denoting that they have been evaluated with respect to the rth spheroidal coordinate system centered at O_r. Using the vector wave functions [44]

$$ {}^{(r)}\mathbf{M}_{mn}^{\pm(i)}(h_r; \mathbf{r}_r) = \frac{1}{2} \left[{}^{(r)}\mathbf{M}_{mn}^{x(i)}(h_r; \mathbf{r}_r) \pm j\, {}^{(r)}\mathbf{M}_{mn}^{y(i)}(h_r; \mathbf{r}_r) \right], \qquad i = 1,2,3,4 \tag{3.13} $$

(3.12) can be rewritten as

$$ {}^{(r)}\mathbf{E}_i^{TE} = e^{-j\mathbf{k}\cdot\mathbf{d}_r} \sum_{m=-\infty}^{\infty} \sum_{n=|m|}^{\infty} q_{mn}^{TE} \left[({}^{r}c_{xx} - j\, {}^{r}c_{xy})\, {}^{(r)}\mathbf{M}_{mn}^{+(1)}(h_r; \mathbf{r}_r) \right. $$

$$ \left. + ({}^{r}c_{xx} + j\, {}^{r}c_{xy})\, {}^{(r)}\mathbf{M}_{mn}^{-(1)}(h_r; \mathbf{r}_r) + {}^{r}c_{xz}\, {}^{(r)}\mathbf{M}_{mn}^{z(1)}(h_r; \mathbf{r}_r) \right] \tag{3.14} $$

where

$$q_{mn}^{TE} = \frac{2j^{n-1}}{kN_{mn}(h_r)} S_{mn}(h_r, \cos\theta_{i_r}) \frac{e^{-jm\phi_{i_r}}}{\cos\theta_i} \tag{3.15}$$

This expansion can be used only when $\theta_i \neq \pi/2$. To obtain an expansion for the case $\theta_i = \pi/2$, we take the gradient on both sides of (3.9) and then the cross product with $\hat{\mathbf{z}}$, which yields

$${}^{(r)}\mathbf{E}_i^{TE} = -(jk\sin\theta_i)^{-1} e^{-j\mathbf{k}\cdot\mathbf{d}_r} \nabla(e^{-j\mathbf{k}\cdot\mathbf{r}_r}) \times \hat{\mathbf{z}} \tag{3.16}$$

Substituting $e^{-j\mathbf{k}\cdot\mathbf{r}_r}$ from (3.11) and $\hat{\mathbf{z}}$ from (3.3), and then using (3.13), we have

$$\begin{aligned} {}^{(r)}\mathbf{E}_i^{TE} = e^{-j\mathbf{k}\cdot\mathbf{d}_r} \sum_{m=-\infty}^{\infty} \sum_{n=|m|}^{\infty} {}^{*}q_{mn}^{TE} [({}^{r}c_{zx} - j\ {}^{r}c_{zy}) {}^{(r)}\mathbf{M}_{mn}^{+(1)}(h_r; \mathbf{r}_r) \\ + ({}^{r}c_{zx} + j\ {}^{r}c_{zy}) {}^{(r)}\mathbf{M}_{mn}^{-(1)}(h_r; \mathbf{r}_r) + {}^{r}c_{zz}\ {}^{(r)}\mathbf{M}_{mn}^{z(1)}(h_r; \mathbf{r}_r)] \end{aligned} \tag{3.17}$$

with

$${}^{*}q_{mn}^{TE} = -\frac{2j^{n-1}}{kN_{mn}(h_r)} S_{mn}(h_r, \cos\theta_{i_r}) \frac{e^{-jm\phi_{i_r}}}{\sin\theta_i} \tag{3.18}$$

which is valid for $\sin\theta_i \neq 0$. By taking now the gradient on both sides of (3.9) and then the cross product with $\hat{\mathbf{y}}$, we have

$$(-\cos\theta_i \hat{\mathbf{x}} + \sin\theta_i \hat{\mathbf{z}})\, e^{-j\mathbf{k}\cdot\mathbf{r}} = -jk^{-1} e^{-j\mathbf{k}\cdot\mathbf{d}_r} \nabla(e^{-j\mathbf{k}\cdot\mathbf{r}_r}) \times \hat{\mathbf{y}} \tag{3.19}$$

Substituting $e^{-j\mathbf{k}\cdot\mathbf{r}_r}$ from (3.11) and $\hat{\mathbf{y}}$ from (3.3), and then using (3.13), gives

$$\begin{aligned} {}^{(r)}\mathbf{E}_i^{TM} = e^{-j\mathbf{k}\cdot\mathbf{d}_r} \sum_{m=-\infty}^{\infty} \sum_{n=|m|}^{\infty} q_{mn}^{TM} [({}^{r}c_{yx} - j\ {}^{r}c_{yy}) {}^{(r)}\mathbf{M}_{mn}^{+(1)}(h_r; \mathbf{r}_r) \\ + ({}^{r}c_{yx} + j\ {}^{r}c_{yy}) {}^{(r)}\mathbf{M}_{mn}^{-(1)}(h_r; \mathbf{r}_r) + {}^{r}c_{yz}\ {}^{(r)}\mathbf{M}_{mn}^{z(1)}(h_r; \mathbf{r}_r)] \end{aligned} \tag{3.20}$$

where

$$q_{mn}^{TM} = \frac{2j^{n-1}}{kN_{mn}(h_r)} S_{mn}(h_r, \cos\theta_{i_r}) e^{-jm\phi_{i_r}} \tag{3.21}$$

From here onwards for the sake of convenience we will be denoting ${}^{(r)}\mathbf{M}(h_r; \mathbf{r}_r)$ by

$^{(r)}\mathbf{M}$ throughout. Thus the electric field intensity $^{(r)}\mathbf{E}_i$ given in (3.6) can be expanded in terms of spheroidal vector wave functions associated with the system $O_r x_r y_r z_r$ in the form

$$^{(r)}\mathbf{E}_i = e^{-j\mathbf{k}\cdot\mathbf{d}_r} \sum_{m=-\infty}^{\infty} \sum_{n=|m|}^{\infty} \left({}^{r}p_{mn}^{+} \, {}^{(r)}\mathbf{M}_{mn}^{+(1)} + {}^{r}p_{mn}^{-} \, {}^{(r)}\mathbf{M}_{mn}^{-(1)} + {}^{r}p_{mn}^{z} \, {}^{(r)}\mathbf{M}_{mn}^{z(1)} \right) \tag{3.22}$$

where

$$\begin{aligned} {}^{r}p_{mn}^{\pm} = \frac{2j^{n-1}}{kN_{mn}(h_r)} S_{mn}(h_r, \cos\theta_{i_r}) e^{-jm\phi_{i_r}} \Bigg[& ({}^{r}c_{yx} \mp j \, {}^{r}c_{yy}) \sin\gamma_k \\ & + \begin{cases} ({}^{r}c_{xx} \mp j \, {}^{r}c_{xy}) \dfrac{\cos\gamma_k}{\cos\theta_i} \Bigg] & \text{for} \quad \theta_i \neq \dfrac{\pi}{2} \\ -({}^{r}c_{zx} \mp j \, {}^{r}c_{zy}) \dfrac{\cos\gamma_k}{\sin\theta_i} \Bigg] & \text{for} \quad \theta_i \neq 0, \pi \end{cases} \end{aligned} \tag{3.23}$$

$$\begin{aligned} {}^{r}p_{mn}^{z} = \frac{2j^{n-1}}{kN_{mn}(h_r)} S_{mn}(h_r, \cos\theta_{i_r}) e^{-jm\phi_{i_r}} \Bigg[& {}^{r}c_{yz} \sin\gamma_k \\ & + \begin{cases} {}^{r}c_{xz} \dfrac{\cos\gamma_k}{\cos\theta_i} \Bigg] & \text{for} \quad \theta_i \neq \dfrac{\pi}{2} \\ -{}^{r}c_{zz} \dfrac{\cos\gamma_k}{\sin\theta_i} \Bigg] & \text{for} \quad \theta_i \neq 0, \pi \end{cases} \end{aligned} \tag{3.24}$$

If the terms in the series expansion of $^{(r)}\mathbf{E}_i$ are arranged in the ϕ_r sequence e^{j0}, $e^{\pm j\phi_r}$, $e^{\pm 2j\phi_r}$ . . . , then we can write this expansion in a matrix form as

$$^{(r)}\mathbf{E}_i = {}^{(r)}\overline{\mathbf{M}}_i^{(1)T} \, {}^{r}\overline{I} \tag{3.25}$$

where $^{(r)}\overline{\mathbf{M}}_i^{(1)}$ and $^{r}\overline{I}$ are column matrices whose elements are prolate spheroidal vector wave functions of the first kind, expressed in terms of the coordinates in the rth spheroidal system ξ_r, η_r, ϕ_r, and the corresponding known expansion coefficients, respectively,

$$ {}^{(r)}\overline{\mathbf{M}}_i^{(1)T} = [\,{}^{(r)}\overline{\mathbf{M}}_{i0}^{T}\ {}^{(r)}\overline{\mathbf{M}}_{i1}^{T}\ {}^{(r)}\overline{\mathbf{M}}_{i2}^{T}\ \ldots], \qquad {}^{r}\overline{I}^{T} = [\,{}^{r}\overline{p}_0^{T}\ {}^{r}\overline{p}_1^{T}\ {}^{r}\overline{p}_2^{T}\ \ldots]\, e^{-j\mathbf{k}\cdot\mathbf{d}_r} \tag{3.26} $$

in which

$$ \begin{aligned} {}^{(r)}\overline{\mathbf{M}}_{i0}^{T} &= [\,{}^{(r)}\overline{\mathbf{M}}_{-1}^{+(1)T}\ {}^{(r)}\overline{\mathbf{M}}_{1}^{-(1)}\ {}^{(r)}\overline{\mathbf{M}}_{0}^{z(1)T}\,] \\ {}^{(r)}\overline{\mathbf{M}}_{i\sigma}^{T} &= [\,{}^{(r)}\overline{\mathbf{M}}_{\sigma-1}^{+(1)T}\ {}^{(r)}\overline{\mathbf{M}}_{\sigma+1}^{-(1)T}\ {}^{(r)}\overline{\mathbf{M}}_{\sigma}^{z(1)T}\ {}^{(r)}\overline{\mathbf{M}}_{-(\sigma+1)}^{+(1)T}\ {}^{(r)}\overline{\mathbf{M}}_{-(\sigma-1)}^{-(1)T}\ {}^{(r)}\overline{\mathbf{M}}_{-\sigma}^{z(1)T}\,], \quad \sigma \geq 1 \end{aligned} \tag{3.27} $$

with

$$ \begin{aligned} {}^{(r)}\overline{\mathbf{M}}_{\tau}^{\pm(1)T} &= [\,{}^{(r)}\mathbf{M}_{\tau,|\tau|}^{\pm(1)}\ {}^{(r)}\mathbf{M}_{\tau,|\tau|+1}^{\pm(1)}\ {}^{(r)}\mathbf{M}_{\tau,|\tau|+2}^{\pm(1)}\ \ldots] \\ {}^{(r)}\overline{\mathbf{M}}_{\tau}^{z(1)T} &= [\,{}^{(r)}\mathbf{M}_{\tau,|\tau|}^{z(1)}\ {}^{(r)}\mathbf{M}_{\tau,|\tau|+1}^{z(1)}\ {}^{(r)}\mathbf{M}_{\tau,|\tau|+2}^{z(1)}\ \ldots] \end{aligned} \tag{3.28} $$

and

$$ \begin{aligned} {}^{r}\overline{p}_0^{T} &= [\,{}^{r}\overline{p}_{-1}^{+T}\ {}^{r}\overline{p}_{1}^{-T}\ {}^{r}\overline{p}_{0}^{zT}\,] \\ {}^{r}\overline{p}_{\sigma}^{T} &= [\,{}^{r}\overline{p}_{\sigma-1}^{+T}\ {}^{r}\overline{p}_{\sigma+1}^{-T}\ {}^{r}\overline{p}_{\sigma}^{zT}\ {}^{r}\overline{p}_{-(\sigma+1)}^{+T}\ {}^{r}\overline{p}_{-(\sigma-1)}^{-T}\ {}^{r}\overline{p}_{-\sigma}^{zT}\,], \qquad \sigma \geq 1 \end{aligned} \tag{3.29} $$

with

$$ \begin{aligned} {}^{r}\overline{p}_{\tau}^{\pm T} &= [\,{}^{r}p_{\tau,|\tau|}^{\pm}\ {}^{r}p_{\tau,|\tau|+1}^{\pm}\ {}^{r}p_{\tau,|\tau|+2}^{\pm}\ \ldots] \\ {}^{r}\overline{p}_{\tau}^{zT} &= [\,{}^{r}p_{\tau,|\tau|}^{z}\ {}^{r}p_{\tau,|\tau|+1}^{z}\ {}^{r}p_{\tau,|\tau|+2}^{z}\ \ldots] \end{aligned} \tag{3.30} $$

Similarly, the incident electric field intensity on any of the spheroids can be expanded in terms of the spheroidal coordinates attached to that particular spheroid. Now if we consider the electromagnetic field scattered by the rth spheroid which corresponds to a nonplane wave, then the scattered electric field intensity ${}^{(r)}\mathbf{E}_s$ can be expanded in terms of a set of vector spheroidal wave functions associated with the system $O_r x_r y_r z_r$ in the form [44]

$$ \begin{aligned} {}^{(r)}\mathbf{E}_s = &\sum_{m=0}^{\infty}\sum_{n=m}^{\infty}({}^{r}\beta_{mn}^{+}\,{}^{(r)}\mathbf{M}_{mn}^{+(4)} + {}^{r}\beta_{m+1,n+1}^{z}\,{}^{(r)}\mathbf{M}_{m+1,n+1}^{z(4)}) + \sum_{n=0}^{\infty}({}^{r}\beta_{-1,n+1}^{+}\,{}^{(r)}\mathbf{M}_{-1,n+1}^{+(4)} \\ &+ {}^{r}\beta_{0n}^{z}\,{}^{(r)}\mathbf{M}_{0n}^{z(4)}) + \sum_{m=0}^{\infty}\sum_{n=m}^{\infty}({}^{r}\beta_{-mn}^{-}\,{}^{(r)}\mathbf{M}_{-mn}^{-(4)} + {}^{r}\beta_{-(m+1),n+1}^{z}\,{}^{(r)}\mathbf{M}_{-(m+1),n+1}^{z(4)}) \end{aligned} \tag{3.31} $$

If the terms in the expansion of ${}^{(r)}\mathbf{E}_s$ are arranged in the same ϕ_r sequence as in the expansion of ${}^{(r)}\mathbf{E}_i$, then we can write

$$ {}^{(r)}\mathbf{E}_s = {}^{(r)}\overline{\mathbf{M}}_s^{(4)T}\, {}^{r}\bar{\beta} \tag{3.32} $$

where ${}^{(r)}\overline{\mathbf{M}}_s^{(4)}$ and ${}^{r}\bar{\beta}$ are column matrices whose elements are prolate spheroidal vector wave functions of the fourth kind, expressed in terms of the spheroidal coordinates associated with $O_r x_r y_r z_r$, and the corresponding unknown expansion coefficients, respectively,

$$ {}^{(r)}\overline{\mathbf{M}}_s^{(4)T} = [\,{}^{(r)}\overline{\mathbf{M}}_{s0}^{T}\ {}^{(r)}\overline{\mathbf{M}}_{s1}^{T}\ {}^{(r)}\overline{\mathbf{M}}_{s2}^{T}\ \ldots], \qquad {}^{r}\bar{\beta}^{T} = [\,{}^{r}\bar{\beta}_0^{T}\ {}^{r}\bar{\beta}_1^{T}\ {}^{r}\bar{\beta}_2^{T}\ \ldots] \tag{3.33} $$

in which

$$ \begin{aligned} {}^{(r)}\overline{\mathbf{M}}_{s0}^{T} &= [\,{}^{(r)}\overline{\mathbf{M}}_{-1}^{+(4)T}\ {}^{(r)}\overline{\mathbf{M}}_{0}^{z(4)T}\,] \\ {}^{(r)}\overline{\mathbf{M}}_{s\sigma}^{T} &= [\,{}^{(r)}\overline{\mathbf{M}}_{\sigma-1}^{+(4)T}\ {}^{(r)}\overline{\mathbf{M}}_{\sigma}^{z(4)T}\ \overline{\mathbf{M}}_{-(\sigma-1)}^{-(4)T}\ {}^{(r)}\overline{\mathbf{M}}_{-\sigma}^{z(4)T}\,], \qquad \sigma \geq 1 \end{aligned} \tag{3.34} $$

with

$$ \begin{aligned} {}^{(r)}\overline{\mathbf{M}}_{\tau}^{\pm(4)T} &= [\,{}^{(r)}\mathbf{M}_{\tau,|\tau|}^{\pm(4)}\ {}^{(r)}\mathbf{M}_{\tau,|\tau|+1}^{\pm(4)}\ {}^{(r)}\mathbf{M}_{\tau,|\tau|+2}^{\pm(4)}\ \ldots] \\ {}^{(r)}\overline{\mathbf{M}}_{\tau}^{z(4)T} &= [\,{}^{(r)}\mathbf{M}_{\tau,|\tau|}^{z(4)}\ {}^{(r)}\mathbf{M}_{\tau,|\tau|+1}^{z(4)}\ {}^{(r)}\mathbf{M}_{\tau,|\tau|+2}^{z(4)}\ \ldots] \end{aligned} \tag{3.35} $$

and

$$ \begin{aligned} {}^{r}\bar{\beta}_0^{T} &= [\,{}^{r}\bar{\beta}_{-1}^{+T}\ {}^{r}\bar{\beta}_0^{zT}\,] \\ {}^{r}\bar{\beta}_{\sigma}^{T} &= [\,{}^{r}\bar{\beta}_{\sigma-1}^{+T}\ {}^{r}\bar{\beta}_{\sigma}^{zT}\ {}^{r}\bar{\beta}_{-(\sigma-1)}^{-T}\ {}^{r}\bar{\beta}_{-\sigma}^{zT}\,], \qquad \sigma \geq 1 \end{aligned} \tag{3.36} $$

with

$$ \begin{aligned} {}^{r}\bar{\beta}_{\tau}^{\pm T} &= [\,{}^{r}\beta_{\tau,|\tau|}^{\pm}\ {}^{r}\beta_{\tau,|\tau|+1}^{\pm}\ {}^{r}\beta_{\tau,|\tau|+2}^{\pm}\ \ldots] \\ {}^{r}\bar{\beta}_{\tau}^{zT} &= [\,{}^{r}\beta_{\tau,|\tau|}^{z}\ {}^{r}\beta_{\tau,|\tau|+1}^{z}\ {}^{r}\beta_{\tau,|\tau|+2}^{z}\ \ldots] \end{aligned} \tag{3.37} $$

In order to impose the boundary conditions at the surface of the rth spheroid, the electromagnetic fields scattered by all the other $n-1$ spheroids should be expressed as incoming fields to the rth spheroid. This is done by using the rotational-translational addition theorems for vector spheroidal wave functions. Let us consider first the electric field scattered by the qth spheroid ${}^{(q)}\mathbf{E}_s$. Similar to ${}^{(r)}\mathbf{E}_s$, ${}^{(q)}\mathbf{E}_s$ can also be written as a series expansion in terms of vector spheroidal wave functions of the fourth

kind associated with the system $O_q x_q y_q z_q$ in the form

$$ {}^{(q)}\mathbf{E}_s = {}^{(q)}\overline{\mathbf{M}}_s^{(4)T}\, {}^{q}\bar{\beta} \tag{3.38} $$

where ${}^{(q)}\overline{\mathbf{M}}_s^{(4)}$ and ${}^{q}\bar{\beta}$ are column matrices whose elements are vector spheroidal wave functions of the fourth kind, and the corresponding unknown expansion coefficients, respectively, having the same structure as those of ${}^{(r)}\overline{\mathbf{M}}_s^{(4)}$ and ${}^{r}\bar{\beta}$, respectively. Thus, to express ${}^{(q)}\mathbf{E}_s$ as an incoming field to the rth spheroid, we have to express the vector spheroidal wave functions of the fourth kind associated with the system $O_q x_q y_q z_q$, in terms of vector spheroidal wave functions of the first kind associated with the system $O_r x_r y_r z_r$, using the appropriate rotational-translational addition theorems for vector spheroidal wave functions [55]:

$$ \begin{aligned} {}^{(q)}\mathbf{M}_{mn}^{+(4)}(h_q;\mathbf{r}_q) = \sum_{\nu=0}^{\infty}\sum_{\mu=-\nu}^{\nu} {}_{qr}^{(4)}Q_{\mu\nu}^{mn}(\alpha_{qr},\beta_{qr},\gamma_{qr};\mathbf{d}_{qr})\,[\,{}^{qr}C_1\,{}^{(r)}\mathbf{M}_{\mu\nu}^{+(1)}(h_r;\mathbf{r}_r) \\ + {}^{qr}C_2\,{}^{(r)}\mathbf{M}_{\mu\nu}^{-(1)}(h_r;\mathbf{r}_r) + {}^{qr}C_3\,{}^{(r)}\mathbf{M}_{\mu\nu}^{z(1)}(h_r;\mathbf{r}_r)\,], \qquad r_r \le d_{qr} \end{aligned} \tag{3.39} $$

$$ \begin{aligned} {}^{(q)}\mathbf{M}_{mn}^{-(4)}(h_q;\mathbf{r}_q) = \sum_{\nu=0}^{\infty}\sum_{\mu=-\nu}^{\nu} {}_{qr}^{(4)}Q_{\mu\nu}^{mn}(\alpha_{qr},\beta_{qr},\gamma_{qr};\mathbf{d}_{qr})\,[\,{}^{qr}C_2^{*}\,{}^{(r)}\mathbf{M}_{\mu\nu}^{+(1)}(h_r;\mathbf{r}_r) \\ + {}^{qr}C_1^{*}\,{}^{(r)}\mathbf{M}_{\mu\nu}^{-(1)}(h_r;\mathbf{r}_r) + {}^{qr}C_3^{*}\,{}^{(r)}\mathbf{M}_{\mu\nu}^{z(1)}(h_r;\mathbf{r}_r)], \qquad r_r \le d_{qr} \end{aligned} \tag{3.40} $$

$$ \begin{aligned} {}^{(q)}\mathbf{M}_{mn}^{z(4)}(h_q;\mathbf{r}_q) = \sum_{\nu=0}^{\infty}\sum_{\mu=-\nu}^{\nu} {}_{qr}^{(4)}Q_{\mu\nu}^{mn}(\alpha_{qr},\beta_{qr},\gamma_{qr};\mathbf{d}_{qr})\,[\,{}^{qr}C_4\,{}^{(r)}\mathbf{M}_{\mu\nu}^{+(1)}(h_r;\mathbf{r}_r) \\ + {}^{qr}C_4^{*}\,{}^{(r)}\mathbf{M}_{\mu\nu}^{-(1)}(h_r;\mathbf{r}_r) + {}^{qr}C_5\,{}^{(r)}\mathbf{M}_{\mu\nu}^{z(1)}(h_r;\mathbf{r}_r)], \qquad r_r \le d_{qr} \end{aligned} \tag{3.41} $$

where $\mathbf{r}_q$ and $\mathbf{r}_r$ represent the coordinate triads (ξ_q,η_q,ϕ_q) and (ξ_r,η_r,ϕ_r), respectively. $\mathbf{d}_{qr}$ is the vector drawn from O_q to O_r (see Fig. 3.1) and $\alpha_{qr},\beta_{qr},\gamma_{qr}$ are the Euler angles which describe the rotation of the system $O_r x_r y_r z_r$ relative to $O_q x_q y_q z_q$.

$$
\begin{aligned}
{}^{qr}C_1 &= \frac{1}{2}[({}^{qr}c_{xx} + {}^{qr}c_{yy}) + j({}^{qr}c_{xy} - {}^{qr}c_{yx})] \\
{}^{qr}C_2 &= \frac{1}{2}[({}^{qr}c_{xx} - {}^{qr}c_{yy}) + j({}^{qr}c_{xy} + {}^{qr}c_{yx})] \\
{}^{qr}C_3 &= \frac{1}{2}({}^{qr}c_{zx} + j\ {}^{qr}c_{zy}) \\
{}^{qr}C_4 &= {}^{qr}c_{xz} - j\ {}^{qr}c_{yz} \\
{}^{qr}C_5 &= {}^{qr}c_{zz}
\end{aligned}
\tag{3.42}
$$

with the asterisk denoting the complex conjugate. ${}^{qr}c_{xx}$, ${}^{qr}c_{xy}$, . . . are obtained from ${}^{r}c_{xx}$, ${}^{r}c_{xy}$, . . . (see eq. (3.4)), respectively, by replacing α_r, β_r, and γ_r, by α_{qr}, β_{qr}, and γ_{qr}, respectively. ${}^{(4)}_{qr}Q^{mn}_{\mu\nu}(\alpha_{qr},\beta_{qr},\gamma_{qr};\mathbf{d}_{qr})$ are the rotational-translational coefficients in the expansion of scalar spheroidal wave functions of the fourth kind associated with $O_q x_q y_q z_q$ in terms of the same functions of the first kind associated with $O_r x_r y_r z_r$, for $r_r \le d_{qr}$, and are defined in Appendix B. By arranging the terms in the series expansions (3.39)–(3.41), in the ϕ_r sequence e^{j0}, $e^{\pm j\phi_r}$, $e^{\pm 2j\phi_r}$, . . . , we can express the outgoing vector wave functions associated with $O_q x_q y_q z_q$, ${}^{(q)}\overline{\mathbf{M}}^{(4)}_s$, in terms of incoming vector wave functions associated with $O_r x_r y_r z_r$, ${}^{(qr)}\overline{\mathbf{M}}^{(1)}$, in the form [57], [58]

$$
{}^{(q)}\overline{\mathbf{M}}^{(4)}_s = [\Gamma_{qr}]\ {}^{(qr)}\overline{\mathbf{M}}^{(1)} \tag{3.43}
$$

in which the structure and elements of the matrix $[\Gamma_{qr}]$ are also defined in Appendix B. The transpose of ${}^{(qr)}\overline{\mathbf{M}}^{(1)}$ is

$$
{}^{(qr)}\overline{\mathbf{M}}^{(1)T} = \left[{}^{(qr)}\overline{\mathbf{M}}^{(1)T}_0\ {}^{(qr)}\overline{\mathbf{M}}^{(1)T}_1\ {}^{(qr)}\overline{\mathbf{M}}^{(1)T}_2\ \ldots . \right] \tag{3.44}
$$

where

$$
\begin{aligned}
{}^{(qr)}\overline{\mathbf{M}}^{(1)T}_0 &= \left[{}^{(r)}\overline{\mathbf{M}}^{+(1)T}_{-1}\ {}^{(r)}\overline{\mathbf{M}}^{-(1)T}_1\ {}^{(r)}\overline{\mathbf{M}}^{z(1)T}_0 \right] \\
{}^{(qr)}\overline{\mathbf{M}}^{(1)T}_\sigma &= \left[{}^{(r)}\overline{\mathbf{M}}^{+(1)T}_{\sigma-1}\ {}^{(r)}\overline{\mathbf{M}}^{-(1)T}_{\sigma+1}\ {}^{(r)}\overline{\mathbf{M}}^{z(1)T}_\sigma\ {}^{(r)}\overline{\mathbf{M}}^{+(1)T}_{-(\sigma+1)}\ {}^{(r)}\overline{\mathbf{M}}^{-(1)T}_{-(\sigma-1)}\ {}^{(r)}\overline{\mathbf{M}}^{z(1)T}_{-\sigma} \right]
\end{aligned}
\tag{3.45}
$$

for $\sigma \ge 1$.

Denoting the secondary incident field on the rth spheroid due to ${}^{(q)}\mathbf{E}_s$ by ${}^{(qr)}\mathbf{E}_s$, taking the transpose of both sides of (3.43) and then substituting ${}^{(q)}\overline{\mathbf{M}}_s^{(4)T}$ in (3.38) gives

$$ {}^{(qr)}\mathbf{E}_s = {}^{(qr)}\overline{\mathbf{M}}^{(1)T}\,[\Gamma_{qr}]^T\;{}^{q}\bar{\beta} \tag{3.46} $$

Thus for $q = 1, 2, \ldots, r-1, r+1, \ldots, n$, we get the secondary incident electric fields on the rth spheroid, due to the electric fields scattered by each of the spheroids $1, 2, \ldots, r-1, r+1, \ldots, n$.

The electromagnetic field transmitted inside the rth spheroid also corresponds to a nonplane wave whose electric field intensity ${}^{(r)}\mathbf{E}_t$ can be expanded in terms of a set of vector spheroidal wave functions as [46]

$$ {}^{(r)}\mathbf{E}_t = {}^{(r)}\overline{\mathbf{M}}_t^{(1)T}\,{}^{r}\overline{\alpha} \tag{3.47} $$

where ${}^{(r)}\overline{\mathbf{M}}_t^{(1)}$ and ${}^{r}\overline{\alpha}$ are column matrices whose elements are prolate spheroidal vector wave functions of the first kind, expressed in terms of spheroidal coordinates associated with $O_r x_r y_r z_r$, taking into account the permittivity of the material inside the rth spheroid, and the corresponding unknown coefficients in the series expansion, respectively. The structure of ${}^{r}\overline{\alpha}$ is similar to that of ${}^{r}\bar{\beta}$, with β replaced by α. The transpose of ${}^{(r)}\overline{\mathbf{M}}_t^{(1)}$ is

$$ {}^{(r)}\overline{\mathbf{M}}_t^{(1)T} = [\,{}^{(r)}\overline{\mathbf{M}}_{t0}^{T}\;\; {}^{(r)}\overline{\mathbf{M}}_{t1}^{T}\;\; {}^{(r)}\overline{\mathbf{M}}_{t2}^{T}\;\; \ldots\,] \tag{3.48} $$

where

$$ \begin{aligned} {}^{(r)}\overline{\mathbf{M}}_{t0}^{T} &= [\,{}^{(r)}\overline{\mathbf{M}}_{-1}^{+(1)T}(h_r';\mathbf{r}_r)\;\; {}^{(r)}\overline{\mathbf{M}}_{0}^{z(1)T}(h_r';\mathbf{r}_r)\,] \\ {}^{(r)}\overline{\mathbf{M}}_{t\sigma}^{T} &= [\,{}^{(r)}\overline{\mathbf{M}}_{\sigma-1}^{+(1)T}(h_r';\mathbf{r}_r)\;\; {}^{(r)}\overline{\mathbf{M}}_{\sigma}^{z(1)T}(h_r';\mathbf{r}_r)\;\; {}^{(r)}\overline{\mathbf{M}}_{-(\sigma-1)}^{-(1)T}(h_r';\mathbf{r}_r)\;\; {}^{(r)}\overline{\mathbf{M}}_{-\sigma}^{z(1)T}(h_r';\mathbf{r}_r)\,], \quad \sigma \geq 1 \end{aligned} \tag{3.49} $$

with

$$
\begin{aligned}
{}^{(r)}\overline{\mathbf{M}}_{\tau}^{\pm(1)T}(h_r';\mathbf{r}_r) &= [\,{}^{(r)}\mathbf{M}_{\tau,|\tau|}^{\pm(1)}(h_r';\mathbf{r}_r)\ \ {}^{(r)}\mathbf{M}_{\tau,|\tau|+1}^{\pm(1)}(h_r';\mathbf{r}_r)\ \ {}^{(r)}\mathbf{M}_{\tau,|\tau|+2}^{\pm(1)}(h_r';\mathbf{r}_r)\ \ldots] \\
{}^{(r)}\overline{\mathbf{M}}_{\tau}^{z(1)T}(h_r';\mathbf{r}_r) &= [\,{}^{(r)}\mathbf{M}_{\tau,|\tau|}^{z(1)}(h_r';\mathbf{r}_r)\ \ {}^{(r)}\mathbf{M}_{\tau,|\tau|+1}^{z(1)}(h_r';\mathbf{r}_r)\ \ {}^{(r)}\mathbf{M}_{\tau,|\tau|+2}^{z(1)}(h_r';\mathbf{r}_r)\ \ldots] \qquad (3.50)
\end{aligned}
$$

in which $h_r' = (\varepsilon_r/\varepsilon)^{1/2} h_r$. ε and ε_r are the permittivities of the media outside and inside the rth spheroid, respectively.

Using Maxwell's equation

$$\mathbf{H} = jk^{-1}(\varepsilon/\mu)^{1/2}\nabla\times\mathbf{E} \qquad (3.51)$$

where k, ε, and μ are the wavenumber, the permittivity, and the permeability, respectively, the expansions of the different magnetic ($\mathbf{H}$) fields in terms of appropriate vector spheroidal wave functions can be obtained from those of the corresponding electric ($\mathbf{E}$) fields by replacing $\mathbf{M}$ by $\mathbf{N}$ and multiplying each expansion by the appropriate value of $j(\varepsilon/\mu)^{1/2}$. Thus we have

$$ {}^{(r)}\mathbf{H}_i = j(\varepsilon/\mu_0)^{1/2}\ {}^{(r)}\overline{\mathbf{N}}_i^{(1)T}\ {}_r\overline{I} \qquad (3.52) $$

$$ {}^{(qr)}\mathbf{H}_s = j(\varepsilon/\mu_0)^{1/2}\ {}^{(qr)}\overline{\mathbf{N}}^{(1)T}\ [\Gamma_{qr}]^T\ {}_q\overline{\beta} \qquad (3.53) $$

$$ {}^{(r)}\mathbf{H}_s = j(\varepsilon/\mu_0)^{1/2}\ {}^{(r)}\overline{\mathbf{N}}_s^{(4)T}\ {}_r\overline{\beta} \qquad (3.54) $$

$$ {}^{(r)}\mathbf{H}_t = j(\varepsilon_r/\mu_0)^{1/2}\ {}^{(r)}\overline{\mathbf{N}}_t^{(1)T}\ {}_r\overline{\alpha} \qquad (3.55) $$

in which μ_0 is the permeability of free space. The elements of the matrices ${}^{(r)}\overline{\mathbf{N}}_i^{(1)T}$, ${}^{(qr)}\overline{\mathbf{N}}^{(1)T}$, ${}^{(r)}\overline{\mathbf{N}}_s^{(4)T}$, and ${}^{(r)}\overline{\mathbf{N}}_t^{(1)T}$ can be obtained from the corresponding elements of the matrices ${}^{(r)}\overline{\mathbf{M}}_i^{(1)T}$, ${}^{(qr)}\overline{\mathbf{M}}^{(1)T}$, ${}^{(r)}\overline{\mathbf{M}}_s^{(4)T}$, and ${}^{(r)}\overline{\mathbf{M}}_t^{(1)T}$, respectively, by replacing the vector wave functions $\mathbf{M}$ by $\mathbf{N}$, where $\mathbf{N} = k^{-1}(\nabla\times\mathbf{M})$.

3.2 Imposing the Boundary Conditions

The boundary conditions require that on the surface of each dielectric spheroid $\xi_r = \xi_{rs}$ $(r = 1, 2, \ldots, n)$, the tangential components of both $\mathbf{E}$ and $\mathbf{H}$ fields be continu-

ous across the boundary. Thus considering the r th spheroid we can write

$$({}^{(r)}\overline{\mathbf{M}}_i^{(1)T}\,{}^r\overline{I} + \sum_{q=1}^{n}[(1-\delta_{qr})\,{}^{(qr)}\overline{\mathbf{M}}^{(1)T}\,[\Gamma_{qr}]^T + \delta_{qr}\,{}^{(q)}\overline{\mathbf{M}}_s^{(4)T}]\,{}^q\overline{\beta})\times\hat{\xi}_r\,|_{\xi_r=\xi_{rs}}$$
$$=({}^{(r)}\overline{\mathbf{M}}_t^{(1)T}\,{}^r\overline{\alpha})\times\hat{\xi}_r\,|_{\xi_r=\xi_{rs}} \tag{3.56}$$

$$({}^{(r)}\overline{\mathbf{N}}_i^{(1)T}\,{}^r\overline{I} + \sum_{q=1}^{n}[(1-\delta_{qr})\,{}^{(qr)}\overline{\mathbf{N}}^{(1)T}\,[\Gamma_{qr}]^T + \delta_{qr}\,{}^{(q)}\overline{\mathbf{N}}_s^{(4)T}]\,{}^q\overline{\beta})\times\hat{\xi}_r\,|_{\xi_r=\xi_{rs}}$$
$$=(\frac{\varepsilon_r}{\varepsilon})^{1/2}\,({}^{(r)}\overline{\mathbf{N}}_t^{(1)T}\,{}^r\overline{\alpha})\times\hat{\xi}_r\,|_{\xi_r=\xi_{rs}} \tag{3.57}$$

where δ_{qr} is the Kronecker delta function. For $r=1,2,\ldots,n$, we obtain $2n$ such equations in total after imposing the boundary conditions on the surfaces of all the n spheroids. Taking the scalar product of both sides of (3.56) and (3.57) by $\begin{Bmatrix} {}^r l_\eta \hat{\eta}_r \\ {}^r l_\phi \hat{\phi} \end{Bmatrix}$. $S_{m,|m|+\kappa}(h_r,\eta_r)\,e^{\pm j(m\pm1)\phi_r}$ for $r=1,2,,\ldots,n$, $m=\ldots-2,-1,0,1,2,\ldots$, $\kappa=0,1,2,\ldots$, integrating correspondingly over the surfaces of the n spheroids, and using the orthogonality properties of the spheroidal angle functions, gives after rearranging [31], [44]

$$[G_d]\,\overline{S}_d = [R_d]\,\overline{I} \tag{3.58}$$

where

$$[G_d]=\begin{bmatrix}
[P_{M1}] & [0] & \ldots & [0] & [Q_{M1}] & [R_{M21}][\Gamma_{21}]^T & \ldots & [R_{Mn1}][\Gamma_{n1}]^T \\
[P_{N1}] & [0] & \ldots & [0] & [Q_{N1}] & [R_{N21}][\Gamma_{21}]^T & \ldots & [R_{Nn1}][\Gamma_{n1}]^T \\
[0] & [P_{M2}] & \ldots & [0] & [R_{M12}][\Gamma_{12}]^T & [Q_{M2}] & \ldots & [R_{Mn2}][\Gamma_{n2}]^T \\
[0] & [P_{N2}] & \ldots & [0] & [R_{N12}][\Gamma_{12}]^T & [Q_{N2}] & \ldots & [R_{Nn2}][\Gamma_{n2}]^T \\
. & . & . & . & . & . & . & . \\
. & . & . & . & . & . & . & . \\
. & . & . & . & . & . & . & . \\
[0] & [0] & \ldots & [P_{Mn}] & [R_{M1n}][\Gamma_{1n}]^T & [R_{M2n}][\Gamma_{2n}]^T & \ldots & [Q_{Mn}] \\
[0] & [0] & \ldots & [P_{Nn}] & [R_{N1n}][\Gamma_{1n}]^T & [R_{N2n}][\Gamma_{2n}]^T & \ldots & [Q_{Nn}]
\end{bmatrix} \tag{3.59}$$

$$\bar{S}_d = \begin{bmatrix} {}^1\bar{\alpha} \\ {}^2\bar{\alpha} \\ \cdot \\ \cdot \\ {}^n\bar{\alpha} \\ {}^1\bar{\beta} \\ {}^2\bar{\beta} \\ \cdot \\ \cdot \\ {}^n\bar{\beta} \end{bmatrix} \qquad [R_d] = \begin{bmatrix} [R_{M1}] & [0] & \dots & [0] \\ [R_{N1}] & [0] & \dots & [0] \\ [0] & [R_{M2}] & \dots & [0] \\ [0] & [R_{N2}] & \dots & [0] \\ \cdot & \cdot & \cdot & \cdot \\ \cdot & \cdot & \cdot & \cdot \\ \cdot & \cdot & \cdot & \cdot \\ [0] & [0] & \dots & [R_{Mn}] \\ [0] & [0] & \dots & [R_{Nn}] \end{bmatrix} \qquad \bar{I} = \begin{bmatrix} {}^1\bar{I} \\ {}^2\bar{I} \\ \cdot \\ \cdot \\ \cdot \\ {}^n\bar{I} \end{bmatrix} \tag{3.60}$$

The coefficients ${}^r l_\eta$ and ${}^r l_\phi$ used in the integrations of (3.56) are given by ${}^r l_\eta = j2F_r(\xi_{rs}^2 - \eta_r^2)^{1/2}$, ${}^r l_\phi = 2F_r(\xi_{rs}^2 - \eta_r^2)$ and those used in (3.57) by ${}^r l_\eta = 2F_r^2(\xi_{rs}^2 - \eta_r^2)^{5/2}/(\xi_{rs}^2 - 1)^{1/2}$, ${}^r l_\phi = j2F_r^2(\xi_{rs}^2 - \eta_r^2)/(\xi_{rs}^2 - 1)$. F_r is the semi-interfocal distance of the rth spheroid and ξ_{rs} is the value of ξ_r on the surface of the rth spheroid. Definitions of all the matrices are given in Appendix C.

Equation (3.58) can now be written in the form

$$\bar{S}_d = [G]\bar{I} \tag{3.61}$$

where

$$[G] = [G_d]^{-1}[R_d] \tag{3.62}$$

is the system matrix which is independent of the direction and polarization of the incident wave. The matrix form (3.61) gives the coefficients in the expansion of the electromagnetic fields scattered and transmitted by the n arbitrarily oriented spheroids.

3.3 Case of Perfectly Conducting Spheroids

The solution for the case of n perfectly conducting spheroids can be derived from the one for n dielectric spheroids, by letting the permittivity of each of the n dielectric spheroids become very high (theoretically infinite). In this case since the spheroids

cannot sustain any field inside them, the boundary conditions require that the tangential component of the resultant electric field be zero on the surface of each of the n spheroids. Hence if we consider the rth spheroid we can write

$$({}^{(r)}\overline{\mathbf{M}}_i^{(1)T}\,{}^{r}\overline{I} + \sum_{q=1}^{n}[(1-\delta_{qr})\,{}^{(qr)}\overline{\mathbf{M}}^{(1)T}\,[\Gamma_{qr}]^T + \delta_{qr}\,{}^{(r)}\overline{\mathbf{M}}_s^{(4)T}]\,{}^{q}\overline{\beta})\times\hat{\xi}_r|_{\xi=\xi_{rs}} = 0 \tag{3.63}$$

For $r = 1, 2, \ldots, n$, we obtain n such equations after imposing the boundary conditions on the surfaces of all the n spheroids. Following a procedure identical to that described in the previous section, we can finally obtain a system of algebraic equations which could be written in matrix form as

$$[G_c]\,\overline{S}_c = [R_c]\,\overline{I} \tag{3.64}$$

where

$$[G_c] = \begin{bmatrix} [Q_{M1}] & [R_{M21}][\Gamma_{21}]^T & \ldots & [R_{Mn1}][\Gamma_{n1}]^T \\ [R_{M12}][\Gamma_{12}]^T & [Q_{M2}] & \ldots & [R_{Mn2}][\Gamma_{n2}]^T \\ \cdot & \cdot & \cdot & \cdot \\ \cdot & \cdot & \cdot & \cdot \\ \cdot & \cdot & \cdot & \cdot \\ [R_{M1n}][\Gamma_{1n}]^T & [R_{M2n}][\Gamma_{2n}]^T & \ldots & [Q_{Mn}] \end{bmatrix} \tag{3.65}$$

$$\overline{S}_c = \begin{bmatrix} {}^{1}\overline{\beta} \\ {}^{2}\overline{\beta} \\ \cdot \\ \cdot \\ \cdot \\ {}^{n}\overline{\beta} \end{bmatrix} \qquad [R_c] = \begin{bmatrix} [R_{M1}] & [0] & \ldots & [0] \\ [0] & [R_{M2}] & \ldots & [0] \\ \cdot & \cdot & \cdot & \cdot \\ \cdot & \cdot & \cdot & \cdot \\ \cdot & \cdot & \cdot & \cdot \\ [0] & [0] & \ldots & [R_{Mn}] \end{bmatrix} \qquad \overline{I} = \begin{bmatrix} {}^{1}\overline{I} \\ {}^{2}\overline{I} \\ \cdot \\ \cdot \\ \cdot \\ {}^{n}\overline{I} \end{bmatrix} \tag{3.66}$$

Equation (3.64) can be rearranged and written as

$$\overline{S}_c = [G']\,\overline{I} \tag{3.67}$$

in which

$$[G'] = [G_c]^{-1}[R_c] \tag{3.68}$$

Similar to $[G]$, the system matrix $[G']$ in this case is also independent of the direction and polarization of the incident wave. However, the size of $[G']$ is half of that of $[G]$. The solution for the case of imperfectly conducting spheroids can be obtained by incorporating the surface impedance in the boundary conditions. For the case of a mixture of dielectric and perfectly conducting spheroids of arbitrary orientation, the solution can be obtained from that for the dielectric spheroids, by considering the permittivity of the perfectly conducting spheroids as being infinite.

3.4 Special Case of Two Spheroids of Arbitrary Orientation

We now consider the special form of solution for the case of two spheroids of arbitrary orientation. The system of algebraic equations we obtain in this case for dielectric spheroids can be derived from (3.58)–(3.60) as [59]

$$[G_d]\bar{S}_d = [R_d]\bar{I} \tag{3.69}$$

where

$$[G_d] = \begin{bmatrix} [P_{M1}] & [0] & [Q_{M1}] & [R_{M21}][\Gamma_{21}]^T \\ [P_{N1}] & [0] & [Q_{N1}] & [R_{N21}][\Gamma_{21}]^T \\ [0] & [P_{M2}] & [R_{M12}][\Gamma_{12}]^T & [Q_{M2}] \\ [0] & [P_{N2}] & [R_{N12}][\Gamma_{12}]^T & [Q_{N2}] \end{bmatrix} \tag{3.70}$$

$$\bar{S}_d = \begin{bmatrix} {}^1\bar{\alpha} \\ {}^2\bar{\alpha} \\ {}^1\bar{\beta} \\ {}^2\bar{\beta} \end{bmatrix} \qquad [R_d] = \begin{bmatrix} [R_{M1}] & [0] \\ [R_{N1}] & [0] \\ [0] & [R_{M2}] \\ [0] & [R_{N2}] \end{bmatrix} \qquad \bar{I} = \begin{bmatrix} {}^1\bar{I} \\ {}^2\bar{I} \end{bmatrix} \tag{3.71}$$

Similarly for the case of two perfectly conducting spheroids, from (3.64)–(3.66), we obtain [57], [58], [60]

$$[G_c]\,\bar{S}_c = [R_c]\,\bar{I} \tag{3.72}$$

where

$$[G_c] = \begin{bmatrix} [Q_{M1}] & [R_{M21}][\Gamma_{21}]^T \\ [R_{M12}][\Gamma_{12}]^T & [Q_{M2}] \end{bmatrix} \tag{3.73}$$

$$\bar{S}_c = \begin{bmatrix} {}^1\bar{\beta} \\ {}^2\bar{\beta} \end{bmatrix} \qquad [R_c] = \begin{bmatrix} [R_{M1}] & [0] \\ [0] & [R_{M2}] \end{bmatrix} \qquad \bar{I} = \begin{bmatrix} {}^1\bar{I} \\ {}^2\bar{I} \end{bmatrix} \tag{3.74}$$

CHAPTER 4

RADAR CROSS SECTIONS FOR SCATTERING BY TWO SPHEROIDS OF ARBITRARY ORIENTATION

The size of the system matrix in both dielectric and perfectly conducting cases increases with the number of spheroids. The computational times also increase correspondingly. In this chapter the scattering cross sections associated with the far field are computed for a system of two spheroids of arbitrary orientation, with the incident wave being a monochromatic uniform plane electromagnetic wave of arbitrary polarization and angle of incidence. In Section 4.1, we derive the asymptotic expressions of the different vector wave functions and the analytical expressions of the far field scattering cross sections. The criterion used for truncating all the series and matrices of infinite dimension that appear in Chapter 3, is given in Section 4.2, together with the numerical results in the form of normalized bistatic and backscattering cross sections for both perfectly conducting and dielectric spheroids having various axial ratios and orientations.

4.1 Normalized Scattering Cross Sections

Consider two spheroids A and B with the Cartesian system $Oxyz$ attached to the spheroid A, $O'x'y'z'$ attached to the spheroid B, and a point of observation having spherical coordinates r,θ,ϕ and r',θ',ϕ' with respect to the two systems $Oxyz$ and $O'x'y'z'$, respectively, as shown in Fig. 4.1. The spheroidal coordinates associated with the two systems are given by ξ,η,ϕ and ξ',η',ϕ', respectively. The scattering cross sections are calculated in the far zone ($r\rightarrow\infty, r'\rightarrow\infty$), where

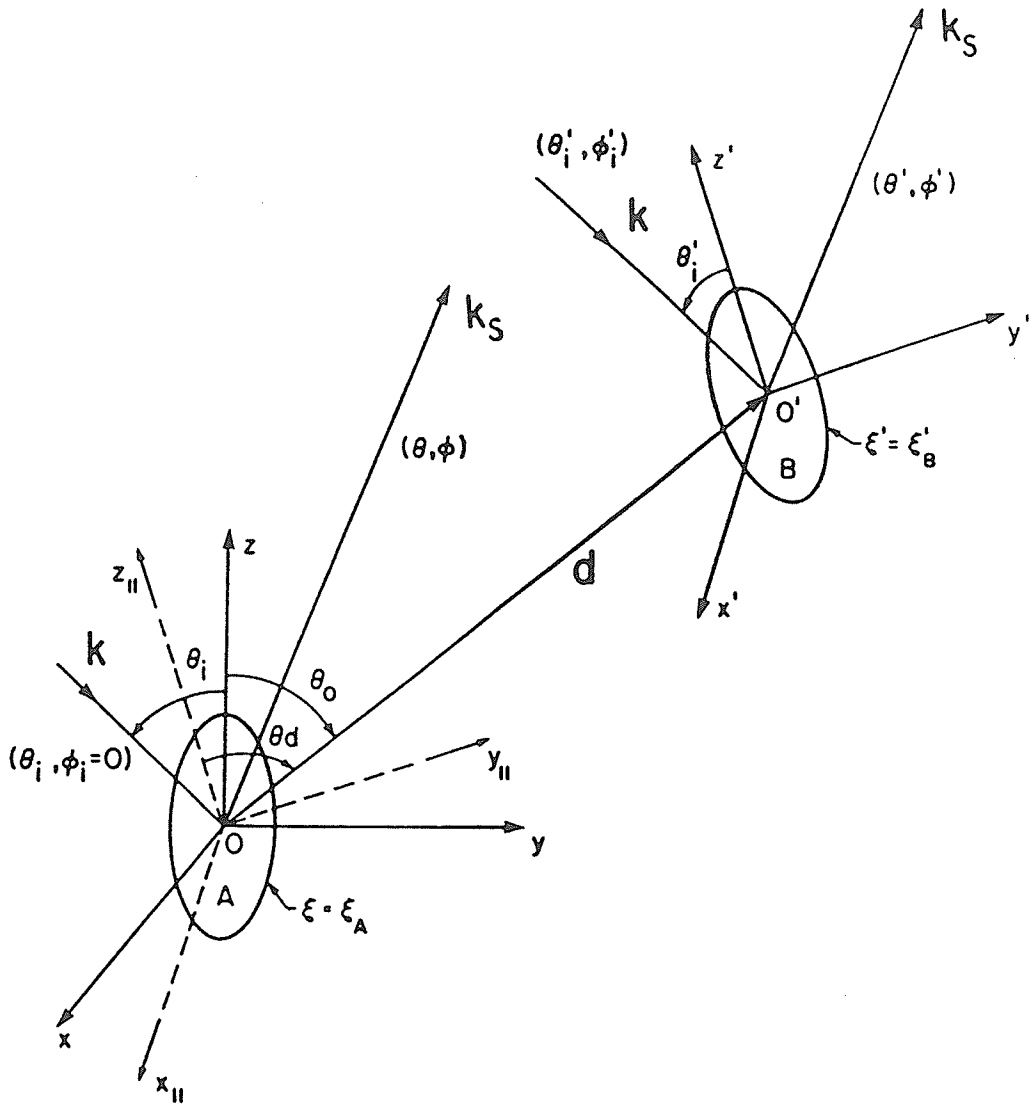

Fig. 4.1 Scattering system geometry

$$\lim_{r\to\infty} h\xi \to kr, \qquad \lim_{r\to\infty} \eta \to \cos\theta, \qquad \lim_{r\to\infty} \hat{\eta} \to -\hat{\theta}$$
$$\lim_{r'\to\infty} h'\xi' \to kr', \qquad \lim_{r'\to\infty} \eta' \to \cos\theta', \qquad \lim_{r'\to\infty} \hat{\eta}' \to -\hat{\theta}' \tag{4.1}$$

Using these asymptotic values, we can obtain the following asymptotic expressions of the radial functions $R_{mn}^{(4)}(h,\xi)$ and $R_{mn}^{(4)}(h',\xi')$:

$$\lim_{r\to\infty} R_{mn}^{(4)}(h,\xi) \to \frac{1}{h\xi} e^{-j[h\xi-(n+1)\pi/2]}, \qquad \lim_{r'\to\infty} R_{mn}^{(4)}(h',\xi') \to \frac{1}{h'\xi'} e^{-j[h'\xi'-(n+1)\pi/2]}$$
$$\to j^{n+1} e^{-jh\xi}/h\xi, \qquad \to j^{n+1} e^{-jh'\xi'}/h'\xi'$$
$$\to j^{n+1} e^{-jkr}/kr, \qquad \to j^{n+1} e^{-jkr}/kr\, e^{j\mathbf{k}_s\cdot\mathbf{d}} \tag{4.2}$$

and differentiating these expressions with respect to ξ and ξ', respectively, and neglecting the second and other higher inverse powers of ξ and ξ', the expressions of their derivatives $\frac{d}{d\xi}R_{mn}^{(4)}(h,\xi)$ and $\frac{d}{d\xi'}R_{mn}^{(4)}(h',\xi')$:

$$\lim_{r\to\infty} \frac{d}{d\xi} R_{mn}^{(4)}(h,\xi) \to j^{n+1}\frac{d}{d\xi}\left[\frac{e^{-jh\xi}}{h\xi}\right], \qquad \lim_{r'\to\infty} \frac{d}{d\xi'} R_{mn}^{(4)}(h',\xi') \to j^{n+1}\frac{d}{d\xi'}\left[\frac{e^{-jh'\xi'}}{h'\xi'}\right]$$
$$\to \frac{j^n}{\xi} e^{-jh\xi}, \qquad \to \frac{j^n}{\xi'} e^{-jh'\xi'}$$
$$\to j^n\, kF\, \frac{e^{-jkr}}{kr}, \qquad \to j^n\, kF'\, \frac{e^{-jkr}}{kr} e^{j\mathbf{k}_s\cdot\mathbf{d}} \tag{4.3}$$

in which F and F' are the semi-interfocal distances of the spheroids A and B, respectively, and

$$\mathbf{k}_s = k(\hat{\mathbf{x}}\sin\theta\cos\phi + \hat{\mathbf{y}}\sin\theta\sin\phi + \hat{\mathbf{z}}\cos\theta) \tag{4.4}$$

When $h\xi\to\infty$ and $h'\xi'\to\infty$, substituting the asymptotic expressions of $R_{mn}^{(4)}(h,\xi)$, $R_{mn}^{(4)}(h',\xi')$, $\frac{d}{d\xi}R_{mn}^{(4)}(h,\xi)$, and $\frac{d}{d\xi'}R_{mn}^{(4)}(h',\xi')$ in the explicit expressions of the $\xi-$, $\eta-$, and $\phi-$ components of the vector spheroidal wave functions $\mathbf{M}_{mn}^{\pm(4)}$, $\mathbf{M}_{mn}^{z(4)}$, and neglecting the second and other higher inverse powers of ξ and ξ', we obtain the asymptotic

forms of these components:

$$\lim_{h\xi\to\infty} {}_{\xi}\mathbf{M}_{mn}^{+(4)}(h;\xi,\eta,\phi) = \lim_{h\xi\to\infty} {}_{\xi}\mathbf{M}_{mn}^{-(4)}(h;\xi,\eta,\phi) = \lim_{h\xi\to\infty} {}_{\xi}\mathbf{M}_{mn}^{z(4)}(h;\xi,\eta,\phi) = 0 \tag{4.5}$$

$$\lim_{h\xi\to\infty} {}_{\eta}\mathbf{M}_{mn}^{+(4)}(h;\xi,\eta,\phi) = \frac{j^{n+1}}{2}\, k\, S_{mn}(h,\eta)\, \frac{e^{-jkr}}{kr}\, e^{j(m+1)\phi}$$

$$\lim_{h\xi\to\infty} {}_{\eta}\mathbf{M}_{mn}^{-(4)}(h;\xi,\eta,\phi) = -\frac{j^{n+1}}{2}\, k\, S_{mn}(h,\eta)\, \frac{e^{-jkr}}{kr}\, e^{j(m-1)\phi} \tag{4.6}$$

$$\lim_{h\xi\to\infty} {}_{\eta}\mathbf{M}_{mn}^{z(4)}(h;\xi,\eta,\phi) = 0$$

$$\lim_{h\xi\to\infty} {}_{\phi}\mathbf{M}_{mn}^{+(4)}(h;\xi,\eta,\phi) = \eta\, \frac{j^{n}}{2}\, k\, S_{mn}(h,\eta)\, \frac{e^{-jkr}}{kr}\, e^{j(m+1)\phi}$$

$$\lim_{h\xi\to\infty} {}_{\phi}\mathbf{M}_{mn}^{-(4)}(h;\xi,\eta,\phi) = \eta\, \frac{j^{n}}{2}\, k\, S_{mn}(h,\eta)\, \frac{e^{-jkr}}{kr}\, e^{j(m-1)\phi} \tag{4.7}$$

$$\lim_{h\xi\to\infty} {}_{\phi}\mathbf{M}_{mn}^{z(4)}(h;\xi,\eta,\phi) = -(1-\eta^2)^{1/2}\, j^{n}\, k\, S_{mn}(h,\eta)\, \frac{e^{-jkr}}{kr}\, e^{jm\phi}$$

The asymptotic expressions of ${}_{\eta}\mathbf{M}_{mn}(h';\xi',\eta',\phi')$ and ${}_{\phi}\mathbf{M}_{mn}(h';\xi',\eta',\phi')$ are obtained from those of ${}_{\eta}\mathbf{M}_{mn}(h;\xi,\eta,\phi)$ and ${}_{\phi}\mathbf{M}_{mn}(h;\xi,\eta,\phi)$, respectively, by replacing η, $S_{mn}(h,\eta)$ and ϕ by η', $S_{mn}(h',\eta')$, and ϕ', respectively, and multiplying each expression by the phase factor $e^{j\mathbf{k}_s\cdot\mathbf{d}}$. Substituting the above asymptotic expressions of the vector spheroidal wave function components in the series expansion of the scattered field due to each spheroid, the electric field intensity in the far zone can be written as [44], [59], [61]

$$\begin{aligned}
\mathbf{E}_s &= \mathbf{E}_{sA} + \mathbf{E}_{sB} \\
&= \frac{e^{-jkr}}{kr}\left[F_{\theta A}(\theta,\phi)\hat{\theta} + F_{\phi A}(\theta,\phi)\hat{\phi} + F_{\theta' B}(\theta',\phi')\hat{\theta}' + F_{\phi' B}(\theta',\phi')\hat{\phi}' \right] \\
&= \frac{e^{-jkr}}{kr}\left[F_{\theta A}(\theta,\phi)\hat{\theta} + F_{\phi A}(\theta,\phi)\hat{\phi} + F_{\theta' B}(\theta',\phi')\{g_1\hat{\theta}+g_2\hat{\phi}\} + F_{\phi' B}(\theta',\phi')\{g_3\hat{\theta}+g_4\hat{\phi}\} \right] \\
&= \frac{e^{-jkr}}{kr}\left[F_{\theta}(\theta,\phi)\hat{\theta} + F_{\phi}(\theta,\phi)\hat{\phi} \right]
\end{aligned} \tag{4.8}$$

where

$$F_\theta(\theta,\phi) = F_{\theta A}(\theta,\phi) + F'_{\theta B}(\theta,\phi)$$
$$F_\phi(\theta,\phi) = F_{\phi A}(\theta,\phi) + F'_{\phi B}(\theta,\phi) \tag{4.9}$$

$$[g_1 \;\; g_2]^T = [\Omega]\,[C]\,[\cos\theta'\cos\phi' \quad \cos\theta'\sin\phi' \quad -\sin\theta']^T \tag{4.10}$$

$$[g_3 \;\; g_4]^T = [\Omega]\,[C]\,[-\sin\phi' \quad \cos\phi' \quad 0]^T \tag{4.11}$$

with

$$F_{\theta A}(\theta,\phi) = -\sum_{m=0}^{\infty}\sum_{n=m}^{\infty} j^{n+1}\frac{S_{mn}}{2}\left\{(\alpha_{mn}^{+'} - \alpha_{-mn}^{-'})\cos(m+1)\phi + j\,(\alpha_{mn}^{+'} + \alpha_{-mn}^{-'})\sin(m+1)\phi\right\} - \sum_{n=1}^{\infty} j^{n+1}\frac{S_{1n}}{2}\alpha_{-1n}^{+'} \tag{4.12}$$

$$F_{\phi A}(\theta,\phi) = \sum_{m=0}^{\infty}\sum_{n=m}^{\infty} j^n\left[\cos\theta\,\frac{S_{mn}}{2}\left\{(\alpha_{mn}^{+'} + \alpha_{-mn}^{-'})\cos(m+1)\phi + j(\alpha_{mn}^{+'} - \alpha_{-mn}^{-'})\right.\right.$$
$$\left.\cdot\sin(m+1)\phi\right\} - j\,\sin\theta\,S_{m+1,n+1}\left\{(\alpha_{m+1,n+1}^{z'} + \alpha_{-(m+1),n+1}^{z'})\right.$$
$$\left.\cdot\cos(m+1)\phi + j(\alpha_{m+1,n+1}^{z'} - \alpha_{-(m+1),n+1}^{z'})\sin(m+1)\phi\right\}\Big]$$
$$+\cos\theta\sum_{n=1}^{\infty} j^n\frac{S_{1n}}{2}\alpha_{-1n}^{+'} - \sin\theta\sum_{n=0}^{\infty} j^n S_{0n}\alpha_{0n}^{z'} \tag{4.13}$$

and

$$[\Omega] = \begin{bmatrix} \cos\theta\cos\phi & \cos\theta\sin\phi & -\sin\theta \\ -\sin\phi & \cos\phi & 0 \end{bmatrix}, \qquad [C] = \begin{bmatrix} c_{xx'} & c_{xy'} & c_{xz'} \\ c_{yx'} & c_{yy'} & c_{yz'} \\ c_{zx'} & c_{zy'} & c_{zz'} \end{bmatrix} \tag{4.14}$$

in which

$$\alpha_{mn}^{\pm'} = k\,\alpha_{mn}^{\pm}, \qquad \alpha_{mn}^{z'} = k\,\alpha_{mn}^{z}, \qquad S_{mn} \equiv S_{mn}(h,\cos\theta) \tag{4.15}$$

$\alpha_{mn}^{\pm}$ and α_{mn}^{z} are the coefficients in the series expansion of the electric field scattered by spheroid A, in terms of vector spheroidal wave functions in the unprimed system, which are evaluated beforehand by solving the set of algebraic equations

$$\begin{bmatrix} [Q_{MA}] & [R_{MBA}][\Gamma_{BA}]^T \\ [R_{MAB}][\Gamma_{AB}]^T & [Q_{MB}] \end{bmatrix} \begin{bmatrix} \bar{\alpha} \\ \bar{\beta} \end{bmatrix} = \begin{bmatrix} [R_{MA}] & [0] \\ [0] & [R_{MB}] \end{bmatrix} \begin{bmatrix} \bar{I}_A \\ \bar{I}_B \end{bmatrix} \tag{4.16}$$

for the perfectly conducting case, which has the same form as (3.72), and

$$\begin{bmatrix} [P_{MA}] & [0] & [Q_{MA}] & [R_{MBA}][\Gamma_{BA}]^T \\ [P_{NA}] & [0] & [Q_{NA}] & [R_{NBA}][\Gamma_{BA}]^T \\ [0] & [P_{MB}] & [R_{MAB}][\Gamma_{AB}]^T & [Q_{MB}] \\ [0] & [P_{NB}] & [R_{NAB}][\Gamma_{AB}]^T & [Q_{NB}] \end{bmatrix} \begin{bmatrix} \bar{\gamma} \\ \bar{\delta} \\ \bar{\alpha} \\ \bar{\beta} \end{bmatrix} = \begin{bmatrix} [R_{MA}] & [0] \\ [R_{NA}] & [0] \\ [0] & [R_{MB}] \\ [0] & [R_{NB}] \end{bmatrix} \begin{bmatrix} \bar{I}_A \\ \bar{I}_B \end{bmatrix} \tag{4.17}$$

for the dielectric case, which has the same form as that of (3.69), and are obtained by imposing the boundary conditions at the surface of each of the spheroids, as described in Chapter 3. $c_{ax'}$, $c_{ay'}$, and $c_{az'}$ for $a = x, y, z$, are defined in (2.4). The explicit expressions of $F_{\theta' B}(\theta',\phi')$, and $F_{\phi' B}(\theta',\phi')$ in primed coordinates are obtained from those of $F_{\theta A}(\theta,\phi)$ and $F_{\phi A}(\theta,\phi)$, respectively, by replacing α by the corresponding β, which are the expansion coefficients in the expansion of the electric field scattered by spheroid B, in terms of vector wave functions in the primed system, and multiplying each expression by an overall phase factor $e^{j\mathbf{k}_s\cdot\mathbf{d}}$. The expressions of $F'_{\theta B}(\theta,\phi)$ and $F'_{\phi B}(\theta,\phi)$ are obtained from those of $[g_1 F_{\theta' B}(\theta',\phi') + g_3 F_{\phi' B}(\theta',\phi')]$ and $[g_2 F_{\theta' B}(\theta',\phi') + g_4 F_{\phi' B}(\theta',\phi')]$, respectively, by substituting all the functions in primed variables θ',ϕ' in terms of the unprimed variables θ,ϕ. Since the direction of the scattered wave vector $\mathbf{k}_s$ in the far field with respect to the primed system is specified by the angular spherical coordinates (θ',ϕ') (see Fig. 4.1), we have

$$\mathbf{k}_s = k(\hat{\mathbf{x}}'\sin\theta'\cos\phi' + \hat{\mathbf{y}}'\sin\theta'\sin\phi' + \hat{\mathbf{z}}'\cos\theta') \tag{4.18}$$

Substituting $\hat{\mathbf{x}}, \hat{\mathbf{y}}, \hat{\mathbf{z}}$ in (4.4) in terms of $\hat{\mathbf{x}}', \hat{\mathbf{y}}', \hat{\mathbf{z}}'$ (see 2.3), and identifying the corresponding coefficients of $\hat{\mathbf{x}}', \hat{\mathbf{y}}', \hat{\mathbf{z}}'$ with those in (4.18) gives

$$[\sin\theta'\cos\phi' \quad \sin\theta'\sin\phi' \quad \cos\theta']^T = [C]^T\,[\sin\theta\cos\phi \quad \sin\theta\sin\phi \quad \cos\theta]^T \tag{4.19}$$

which is the required relationship between the primed and unprimed angular coordinates.

The bistatic radar cross section is defined as

$$\sigma(\theta,\phi) = \lim_{r\to\infty} 4\pi r^2 \frac{|\mathbf{E}_s.\hat{\tau}|^2}{|\mathbf{E}_i|^2} \tag{4.20}$$

with the unit vector $\hat{\tau}$ denoting the direction of polarization of the receiver at the point of observation. When $\hat{\tau}$ has the same direction as $\mathbf{E}_s$, the normalized bistatic cross section is

$$\frac{\pi\sigma(\theta,\phi)}{\lambda^2} = |F_\theta(\theta,\phi)|^2 + |F_\phi(\theta,\phi)|^2 \tag{4.21}$$

The normalized bistatic cross sections in the $E-$ and $H-$ planes are obtained by substituting $\phi=\pi/2$ and $\phi=0$, respectively, in (4.21).

The normalized backscattering cross section is obtained from (4.21) for $\theta=\theta_i$ and $\phi=\phi_i=0$,

$$\frac{\pi\sigma(\theta_i)}{\lambda^2} = |F_\theta(\theta_i,0)|^2 + |F_\phi(\theta_i,0)|^2 \tag{4.22}$$

4.2 Numerical Results for Two Spheroids of Arbitrary Orientation

Results of numerical computation are presented in the form of plots of normalized bistatic and backscattering cross sections in the far field for scattering by two spheroids having various displacements of their centers and different relative orientations. As the formulation and the computation for the case of scattering by two perfectly conducting spheroids is much simpler than for the case of scattering by two dielectric spheroids, the plots for the perfectly conducting spheroids will be presented first, followed by

those for the dielectric spheroids.

4.2.1 Perfectly Conducting Spheroids

Since the series expansions of the different electromagnetic fields in terms of vector spheroidal wave functions are infinite in extent, all the matrices introduced in Chapter 3 are of infinite dimensions. Thus, in order to obtain numerical results it is necessary to truncate these matrices according to the required accuracy. As mentioned in Chapter 2, from the numerical experiments performed on the equations describing the rotational-translational addition theorems for vector spheroidal wave functions, it is clear that it is sufficient to consider $-2 \leq \mu \leq 2$ and $\nu = |\mu|, |\mu|+1, \ldots |\mu|+5$ on the right hand sides of these equations in order to obtain a two significant digit accuracy when compared with the values of the corresponding left hand sides, for different values of m and n. All the vector spheroidal wave functions and the rotational-translational coefficients have been calculated with a five significant digit accuracy. When using these functions and coefficients in our calculations, it has been found that to obtain a two significant digit accuracy in the computed bistatic and backscattering cross sections, it is sufficient to consider only the ϕ– harmonics e^{j0}, $e^{\pm j\phi}$, and $e^{\pm 2j\phi}$. All the results given in this section have thus been obtained with m corresponding to the above ϕ– harmonics, $n = |m|, \ldots |m|+3$, $\kappa = 0, 1, 2, 3$, in truncating the matrices $[Q_{MA}]$, $[Q_{MB}]$, $[R_{MA}]$, and $[R_{MB}]$ in (4.16), and with $n = |m|, \ldots |m|+5$, $\kappa = 0, 1, 2, 3$, in truncating the matrices $[\Gamma_{AB}]$, $[\Gamma_{BA}]$, $[R_{MAB}]$, and $[R_{MBA}]$ in (4.16).

The formulation presented in Chapter 3 is general. However, it is interesting to note that for a particular system of only two spheroidal objects, the relative position of one with respect to the other can always be obtained by choosing the x and y axes

appropriately, and then by performing only one rotation through the Euler angle β, i.e. with $\alpha=0^{\circ}$, $\gamma=0^{\circ}$, followed by the corresponding translation. Even though, to demonstrate the generality of the theory presented and the validity of the software being used, some of the results presented in this chapter have been obtained with α and γ different from zero. But the reduction in the total amount of computation time required when using $\alpha=0^{\circ}$, $\gamma=0^{\circ}$ is only about 5% with respect to the case when α and γ are different from zero.

Fig. 4.2 shows the normalized bistatic cross section as a function of the scattering angle, for two identical sets of prolate spheroids of axial ratios 2 and 10, semi-major axes $\lambda/4$, with the spheroid centers displaced along the z axis of spheroid A. The orientation of spheroid B with respect to A is specified by the Euler angles $\alpha=0^{\circ}$, $\beta=45^{\circ}$, $\gamma=0^{\circ}$. The incident field propagates along the negative z axis, as shown in the figure. In Fig. 4.2(a) the center-to-center distance is $\lambda/2$ and in Fig. 4.2(b), it is λ. When the axial ratio changes from 2 to 10, a significant decrease in the magnitude of the bistatic cross section is visible in both $E-$ and $H-$ plane patterns which is partly due to the reduction of the area available for scattering. When the distance between the centers of the spheroids is increased from $\lambda/2$ to λ we observe that the scattering cross sections are subject to more oscillations in general due to the interference pattern of the two spheroids.

Fig. 4.3 shows the plots of normalized backscattering cross section versus angle of incidence for TE and TM polarizations of the incident wave. The spheroids are identical to those in Fig. 4.2, and so are the orientation and center-to-center distances between the spheroids. Fig. 4.4 is for the same two spheroids and for the same separa-

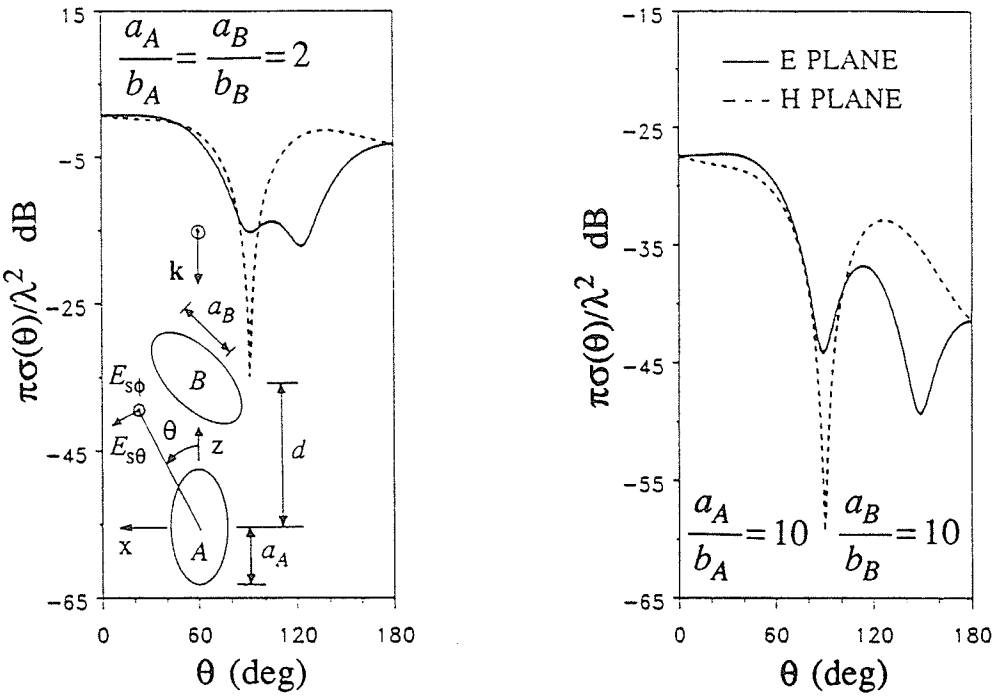

(*a*)

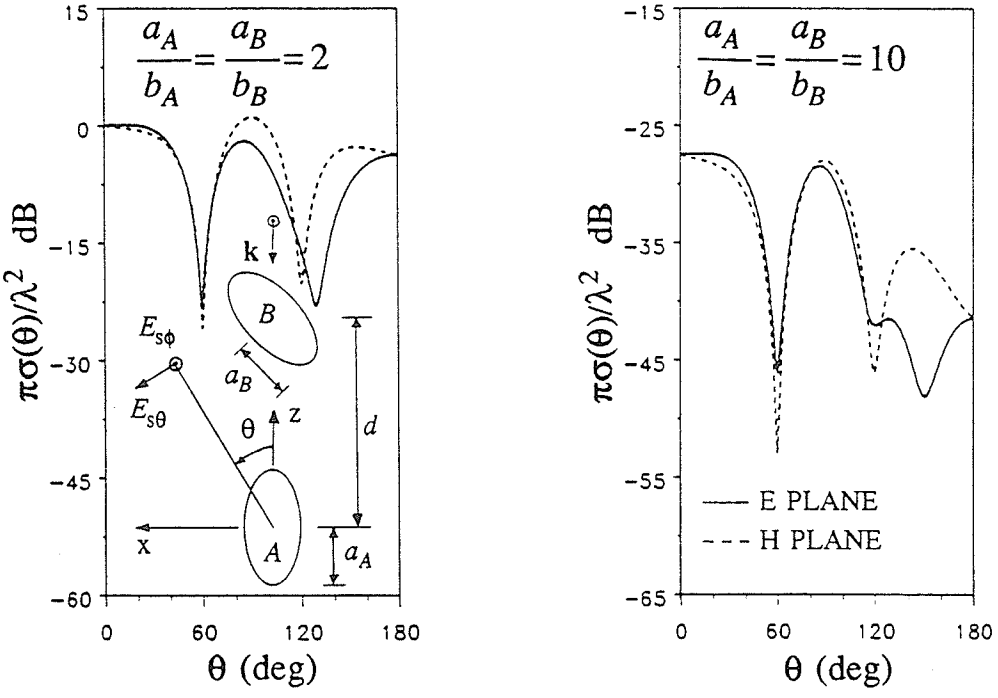

(*b*)

Fig. 4.2 Normalized bistatic cross section for TE polarization of the incident wave, as a function of the scattering angle for two identical prolate spheroids and for two axial ratios, with $a_A = a_B = \lambda/4$, Euler angles $\alpha = 0°, \beta = 45°, \gamma = 0°$ and displaced along the z axis: (a) $d = \lambda/2$ (b) $d = \lambda$.

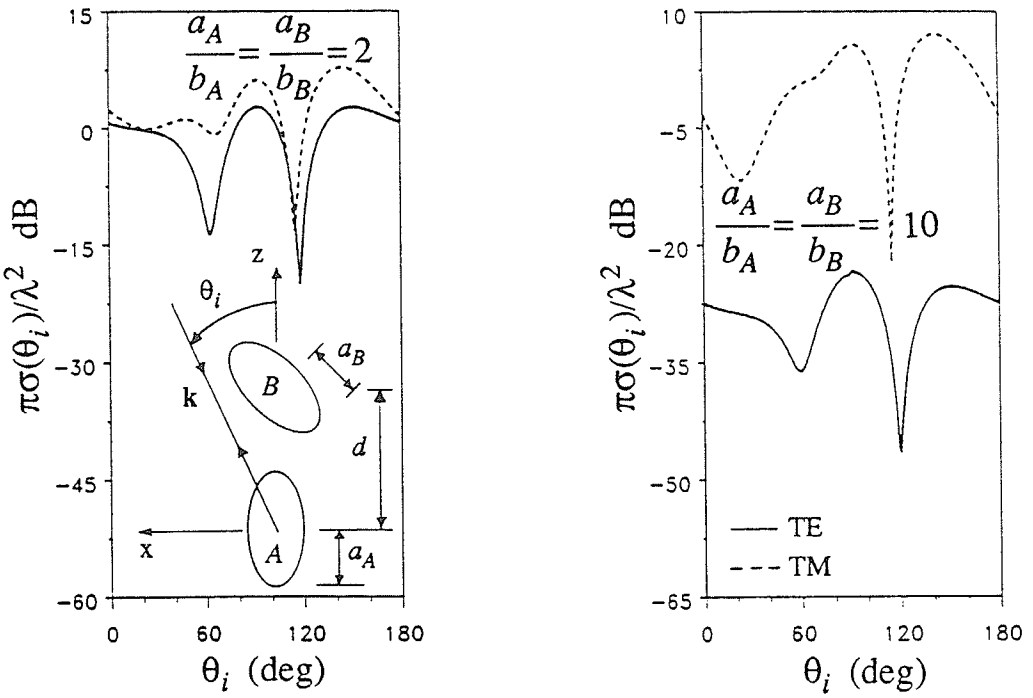

(*a*)

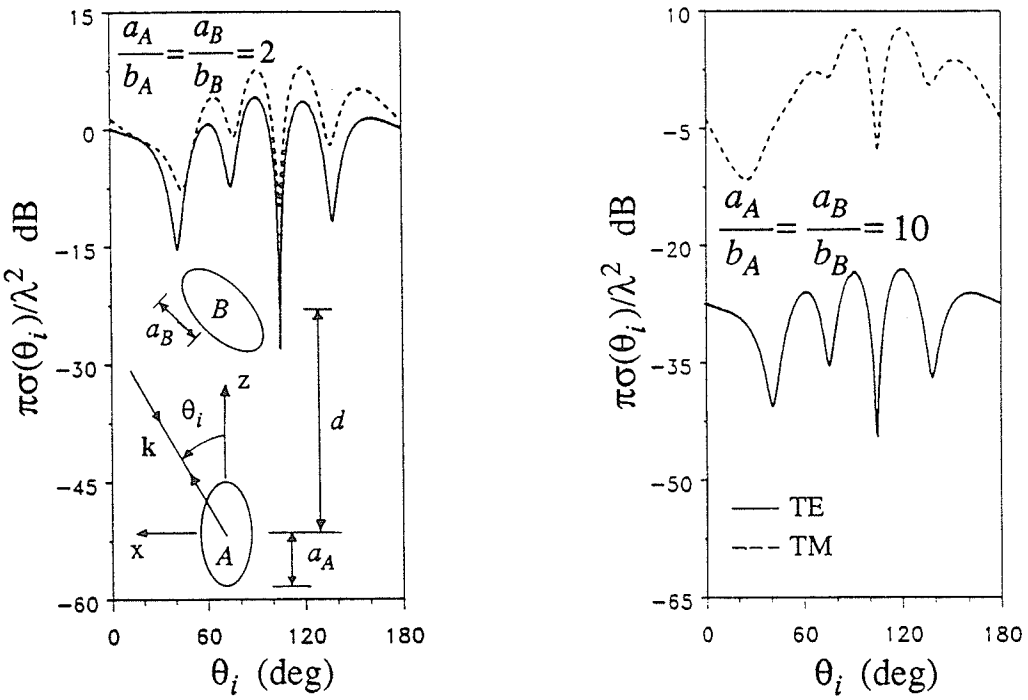

(*b*)

Fig. 4.3 Normalized backscattering cross section versus θ_i, for two identical prolate spheroids and for two axial ratios, with $a_A = a_B = \lambda/4$, Euler angles $\alpha = 0^o, \beta = 45^o, \gamma = 0^o$ and displaced along the z axis: (a) $d = \lambda/2$ (b) $d = \lambda$.

tion between the centers as in Fig. 4.3, but the orientation of spheroid B with respect to A changed to $\alpha=0°$, $\beta=90°$, $\gamma=0°$. It is interesting to note that for axial ratio 10, the cross sections in Fig. 4.4 are almost symmetrical about $\theta_i=90°$, and that for both axial ratios the behavior of the backscattering cross sections for TE and TM polarizations is almost the same.

In Fig. 4.5 we present the plots of normalized backscattering cross section as a function of θ_i for two spheroids of axial ratio 2, semi-major axes $\lambda/4$, with their centers displaced along the z axis of the spheroid A by distances $\lambda/2$ and λ, for both TE and TM polarizations of the incident wave. In Fig. 4.5(a) the orientation of spheroid B with respect to that of A is specified by the Euler angles $\alpha=45°$, $\beta=90°$, $\gamma=45°$, and in Fig. 4.5(b) by $\alpha=30°$, $\beta=45°$, $\gamma=60°$. As the distance between the centers of the two spheroids increases we observe an increase in the amount of oscillations in the curves for both polarizations. When comparing the corresponding plots in Figs. 4.5(a) and 4.5(b), we observe that the behavior of the curves for TE polarization remain the same, whereas the curves for TM polarization tend to oscillate more in Fig. 4.5(b).

If the centers of the two spheroids are displaced by $\lambda/2$ in a direction perpendicular to the z axis of spheroid A, the plots of the normalized backscattering cross section versus angle of incidence are shown in Fig. 4.6. In Figs. 4.6(a) and 4.6(b), the orientations of spheroid B with respect to that of A are identical to those in Figs. 4.5(a) and 4.5(b), respectively. When the axial ratio of the spheroids a/b is 2, in Fig. 4.6(a), the curve for TE polarization shows more oscillations than that for $a/b=10$. The minima for TM polarization occur near $\theta_i=30°$ and $\theta_i=150°$, the lower minimum being for

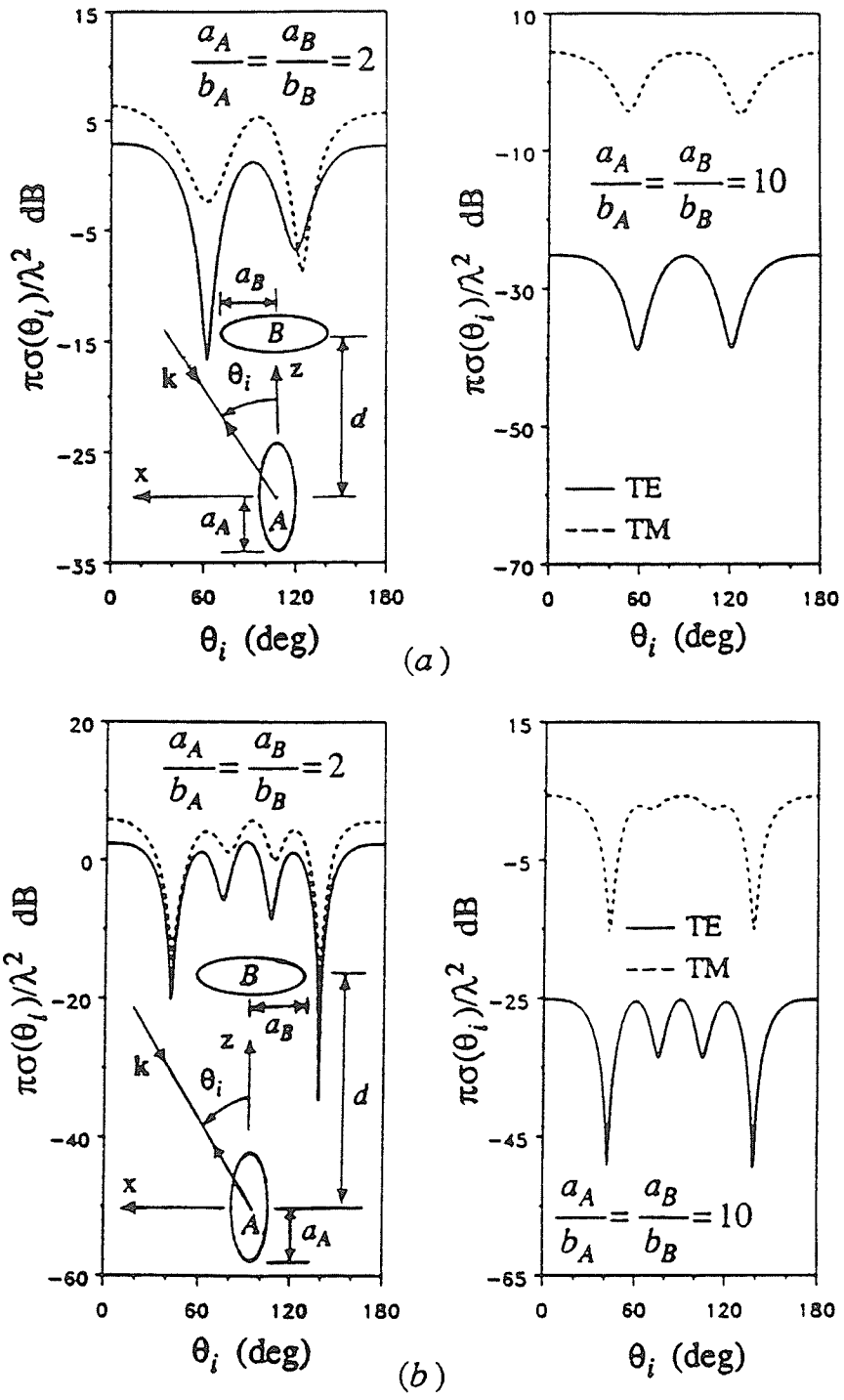

Fig. 4.4 Normalized backscattering cross section as a function of the angle of incidence, for the same two spheroids as in Fig. 4.3, but with the Euler angles $\alpha=0°, \beta=90°, \gamma=0°$ and displaced along the z axis: (a) $d=\lambda/2$ (b) $d=\lambda$.

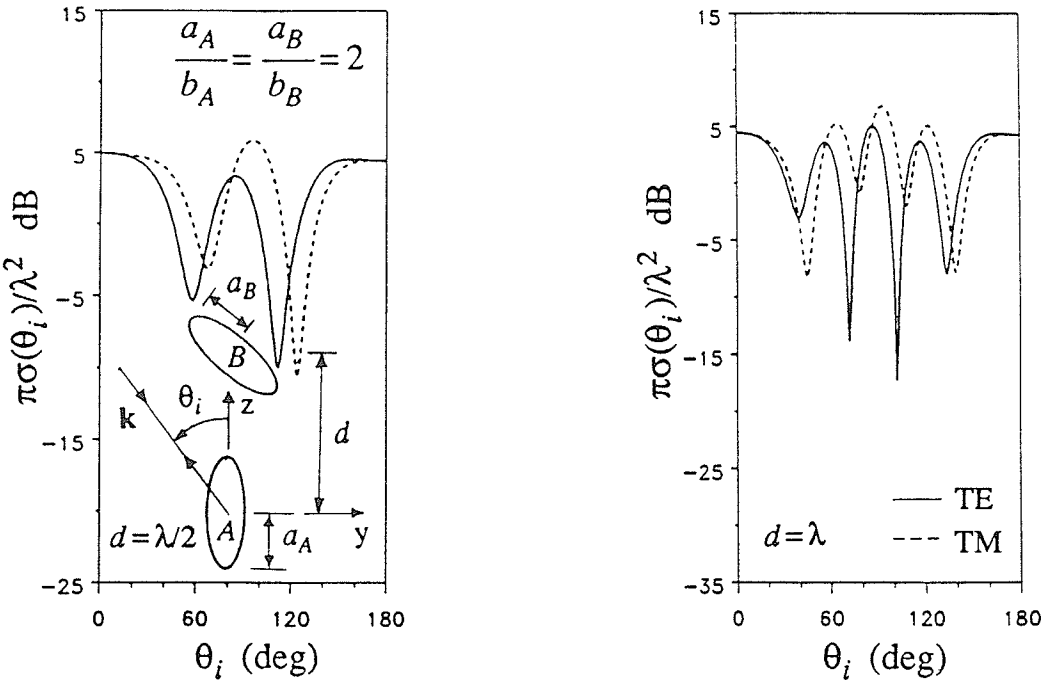

(*a*)

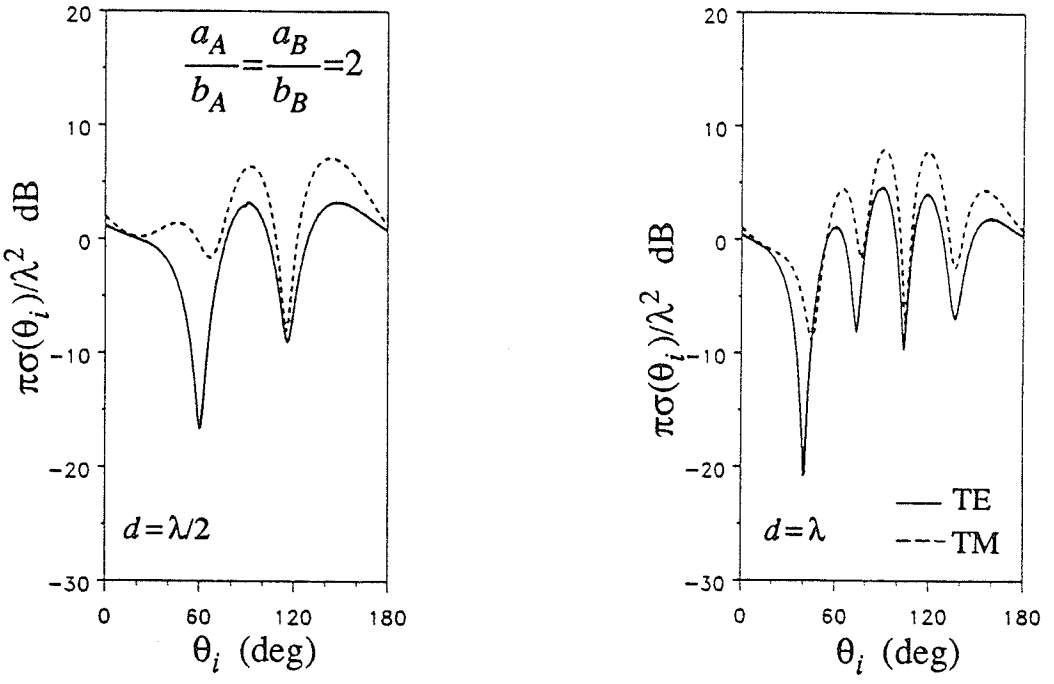

(*b*)

Fig. 4.5 Normalized backscattering cross section of two identical prolate spheroids each of semi-major axes λ/4, as a function of the angle of incidence for two center-to-center displacements along the z axis with Euler angles: (a) (45°, 90°, 45°) (b) (30°, 45°, 60°).

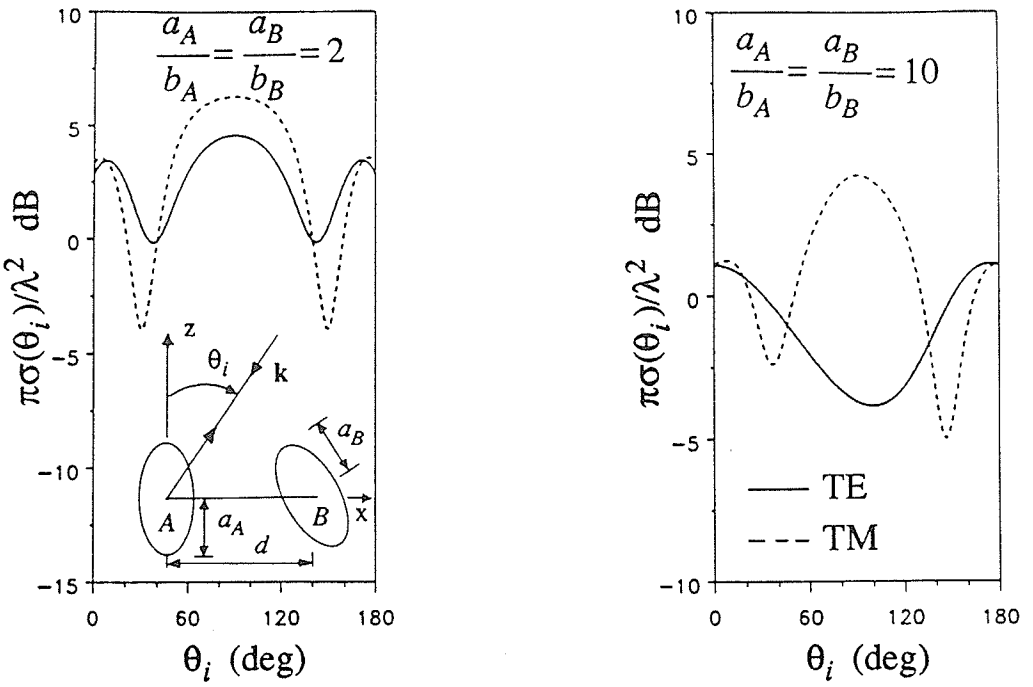

(*a*)

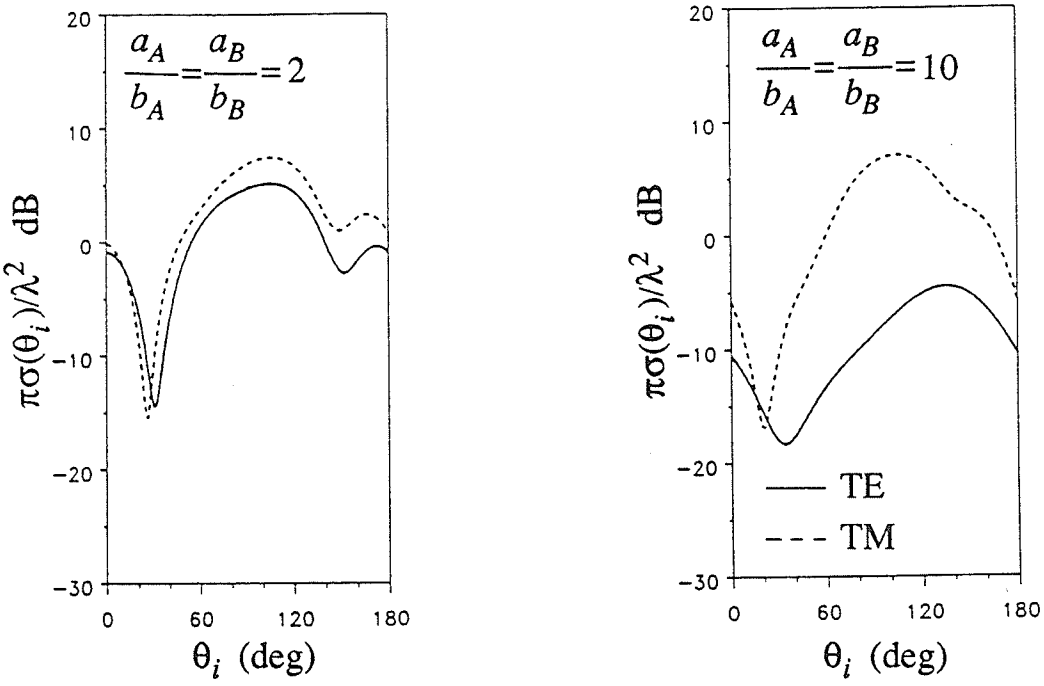

(*b*)

Fig. 4.6 Normalized backscattering cross section versus θ_i, for two identical prolate spheroids with semi-major axes $\lambda/4$ and for two axial ratios, with centers displaced along the x axis by $d = \lambda/2$ and Euler angles: (a) $(45°, 90°, 45°)$ (b) $(30°, 45°, 60°)$.

$a/b = 10$. For $a/b = 2$, the curve in Fig. 4.6(b) for TM polarization follows that of TE closely, but there is no such behavior for $a/b = 10$.

In Fig. 4.7, the variation of the normalized backscattering cross section with the angle of incidence is presented for two different spheroids of axial ratios 2 and 10, with the centers displaced along the direction specified by the spherical coordinates $\theta_0 = 60°$ and $\phi_0 = 20°$ by a distance $\lambda/2$. The Euler angles for the two spheroids in Fig. 4.7(a) are $\alpha = 45°$, $\beta = 90°$, $\gamma = 45°$, and for those in Fig. 4.7(b) are $\alpha = \beta = \gamma = 0.001°$. The plots obtained in Fig. 4.7(b) are compared with the corresponding ones obtained for the same two spheroids, but with parallel major axes [44]. As expected, the results are in agreement with the maximum relative difference being 3.2%, which validates the software that we use in our calculations in the case of two spheroids of arbitrary orientation.

4.2.2 Two Dielectric Spheroids

In this section we present the results for scattering by two dielectric spheroids of arbitrary orientation. When computing the numerical results for this case, again we have found that in order to obtain a two significant digit accuracy in the computed bistatic and backscattering cross sections, it is sufficient to consider only the $\phi-$ harmonics e^{j0}, $e^{\pm j\phi}$, and $e^{\pm 2j\phi}$. Thus the values of m being used in the truncation of the associated matrices in (4.17) remain the same as in the perfectly conducting case, but the values of n and κ are now given by $n = |m|, |m|+1, \ldots |m|+5$, and $\kappa = 0, 1, \ldots 5$.

Fig. 4.8 shows the normalized bistatic cross section for TE polarization of the incident wave versus the scattering angle for two identical sets of prolate spheroids of axial ratios 2 and 5, dielectric constant $\varepsilon_r = 3.0$, with the spheroid centers displaced

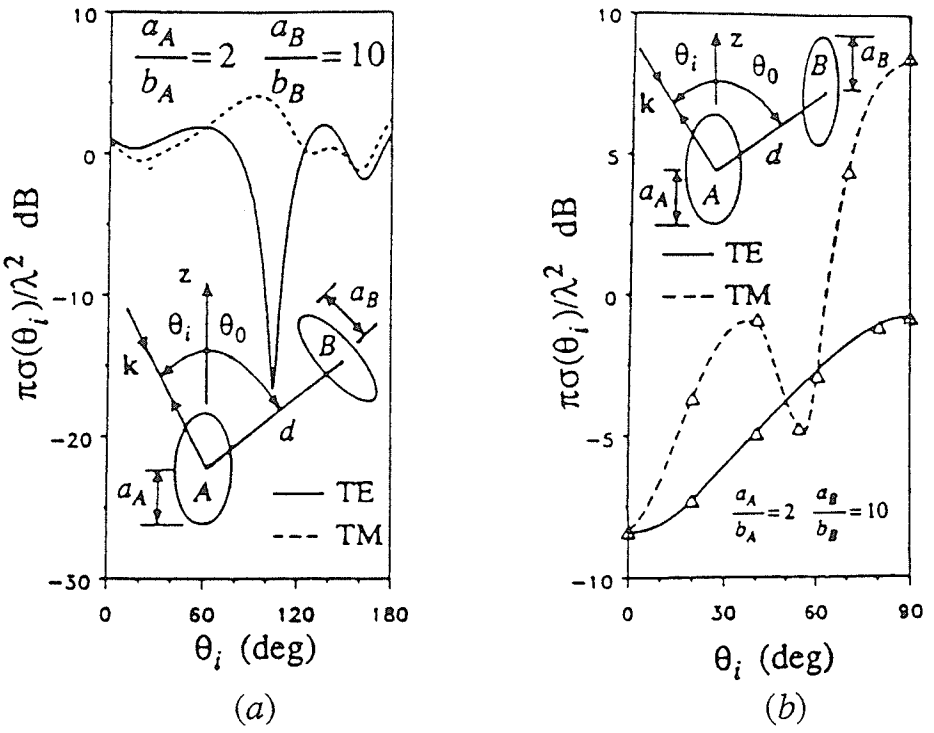

Fig. 4.7 Normalized backscattering cross section as a function of θ_i, for two prolate spheroids of different axial ratios, with $a_A = a_B = \lambda/4$, and centers displaced along the direction θ_0=60°, $\phi_0 = 20°$ by $d = \lambda/2$, with Euler angles: (a) (45°, 90°, 45°) (b) (0.001°, 0.001°, 0.001°). The triangles on Fig. (b) show the results obtained for parallel spheroids [44].

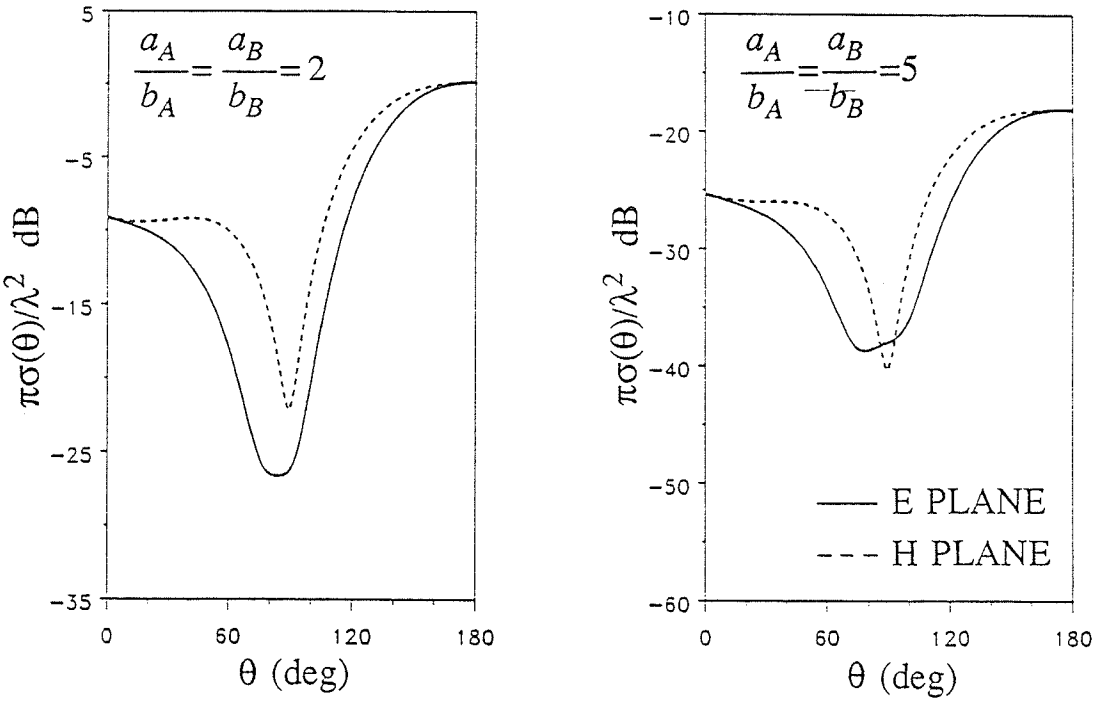

(*a*)

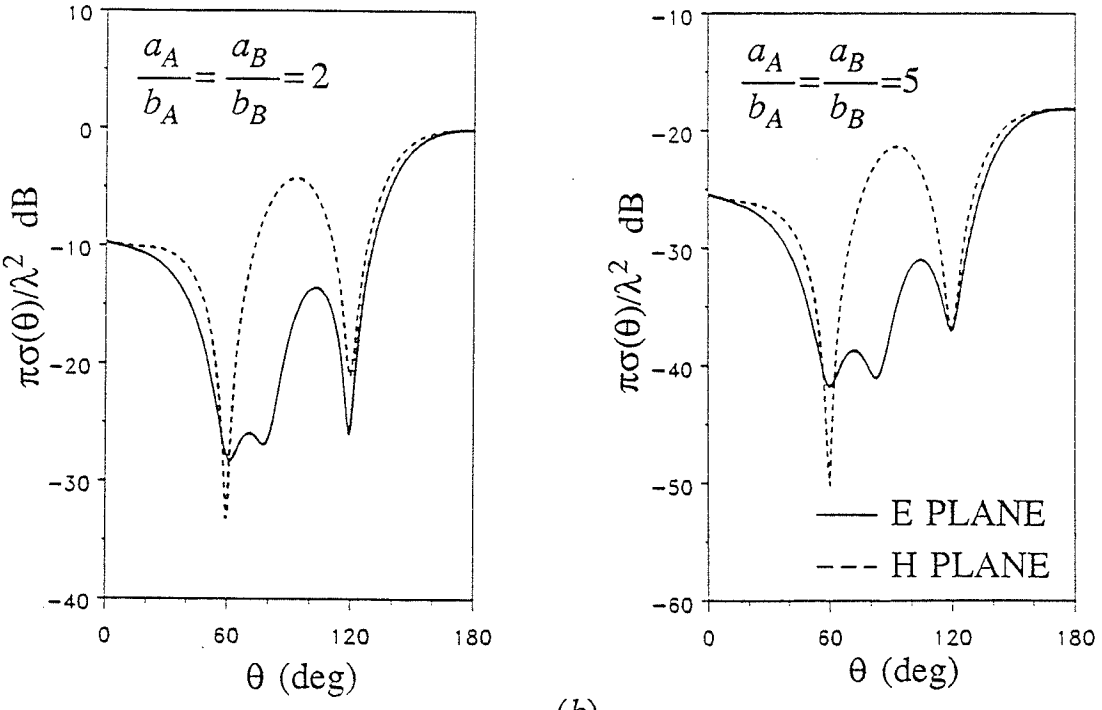

(*b*)

Fig. 4.8 Normalized bistatic cross section of two identical prolate spheroids for TE polarization of the incident wave, versus scattering angle, for two axial ratios with $a_A = a_B = \lambda/4$, Euler angles $\alpha = 30°, \beta = 45°, \gamma = 60°$, $\varepsilon_r = 3.0$, and displaced along the z axis: (a) $d = \lambda/2$ (b) $d = \lambda$.

along the z axis of the spheroid A. The orientation of spheroid B with respect to A is specified by the Euler angles $\alpha=30°$, $\beta=45°$, $\gamma=60°$. The incident field propagates along the negative z axis. It should be noted that the geometries of the systems of spheroids considered in all the cases are similar to those shown for the perfectly conducting case, and therefore are not shown again with the figures. In Fig. 4.8(a) the center-to-center distance is $\lambda/2$ and in Fig. 4.8(b), it is λ. Here we observe that in all the figures, the magnitude of the forward scattering cross section ($\theta=\pi$) is higher than that of the backscattering cross section ($\theta=0$). This is partly due to the contribution to the forward scattered field from the field transmitted inside the spheroid. A reduction in the magnitude of the scattering cross section is also observed due to the reduction in the area available for scattering.

In Fig. 4.9 we present the plots of normalized backscattering cross section as a function of the angle of incidence, for two spheroids of axial ratio 2, semi-major axes $\lambda/4$, $\varepsilon_r=3.0$, with their centers displaced along the z axis of the spheroid A by distances $\lambda/2$ and λ, for both TE and TM polarizations of the incident wave. In Fig. 4.9(a) the orientation of the spheroid B with respect to that of A is specified by the Euler angles $\alpha=30°$, $\beta=45°$, $\gamma=60°$, and in Fig. 4.5(b) by $\alpha=15°$, $\beta=90°$, $\gamma=45°$. When the curves in Fig. 4.9(a) are compared with the corresponding curves in Fig. 4.5(b) for the perfectly conducting case, we observe that the magnitudes of the backscattering cross section are now less, for both polarizations. This is due to the fact that a part of the incident field is now being transmitted inside the spheroid, without being scattered. In Fig. 4.9(b) it is interesting to note that the curves are almost symmetrical about $\theta_i=90°$, for both TE and TM polarizations.

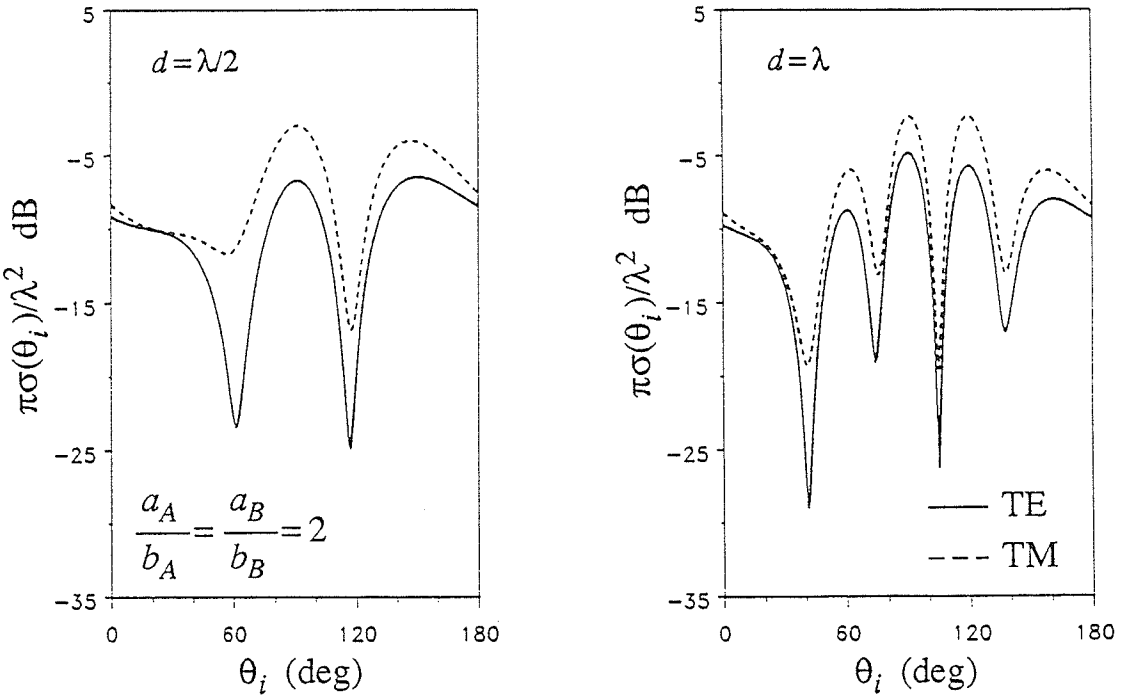

(a)

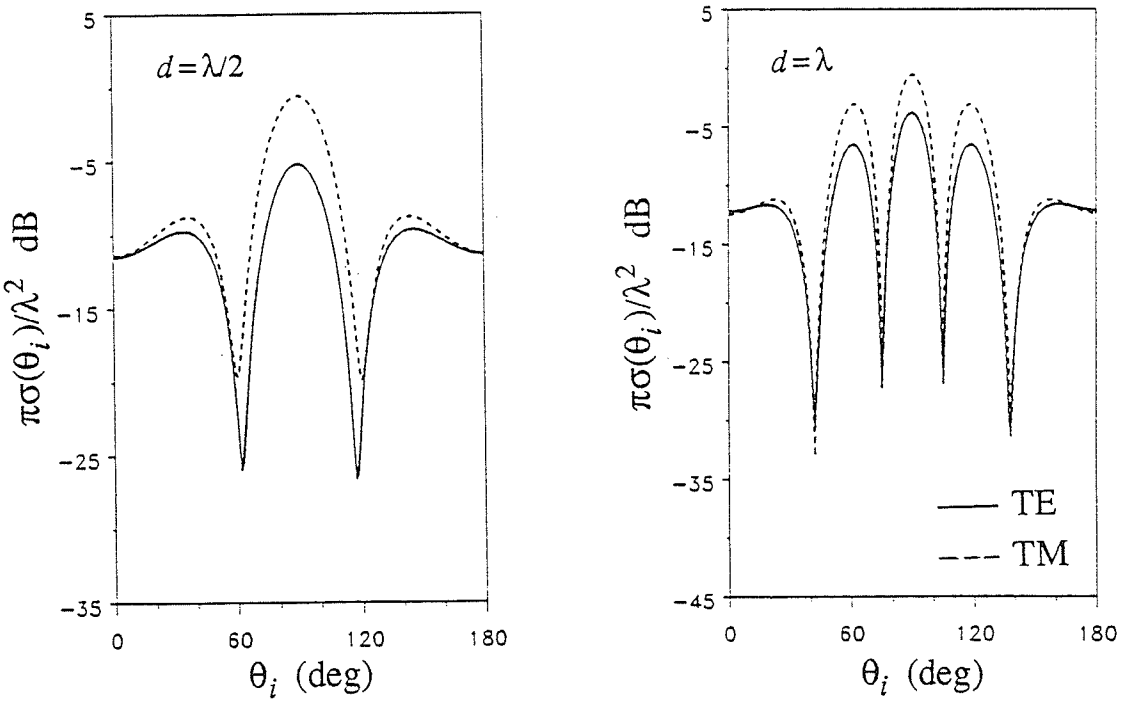

(b)

Fig. 4.9 Normalized backscattering cross section of two identical prolate spheroids each of semi-major axes λ/4, as a function of θ_i for two center-to-center displacements along the z axis with $\varepsilon_r = 3.0$, Euler angles: (a) $(30°, 45°, 60°)$ (b) $(15°, 90°, 45°)$.

The variation of the normalized backscattering cross section with the angle of incidence is shown in Fig. 4.10, for the general case of two non identical spheroids, one having an axial ratio 2, the other 5, and separated center-to- center by a distance $\lambda/2$ in the direction specified by the spherical coordinates $\theta_0 = 60°$, $\phi_0 = 20°$. The orientation of the spheroid B with respect to A is given by the Euler angles $\alpha = 30°$, $\beta = 45°$, $\gamma = 60°$. Spheroids of two different dielectric constants are being considered to observe the effect of the change in dielectric constant on the backscattering cross section. In Fig. 4.10(a), both spheroids A and B have dielectric constants ε_{rA} and ε_{rB} equal to 3.0. In Fig. 4.10(b), $\varepsilon_{rA} = 3.0$, $\varepsilon_{rB} = 4.0$, and in Fig. 4.10 (c), $\varepsilon_{rA} = 4.0$, $\varepsilon_{rB} = 3.0$. The behavior of the curves for both TE and TM polarizations is almost the same in each figure. However, the positions of the minima are slightly different in each figure, and the minima in Fig. 4.10 (b) are deeper than in the other two figures.

Fig. 4.11 shows the plots of normalized backscattering cross section versus θ_i, for two sets of identical spheroids of axial ratios 2 and 5, and dielectric constant 3.0, with their centers displaced along a direction perpendicular to the z axis of spheroid A. The orientation of spheroid B with respect to A is given by $\alpha = 30°$, $\beta = 45°$, $\gamma = 60°$. When the curves for axial ratio 2, are compared with the corresponding curves in Fig. 4.6(b), for the perfectly conducting case, we observe a reduction in the magnitude of the scattering cross section. Also we observe that for axial ratio 2, the lower minima in Fig. 4.11 for both TE and TM polarizations occur at the same position, whereas in Fig. 4.6(b) they are not. Other than this the general behavior of the curves is almost the same. In Fig. 4.11, when the axial ratio changes from 2 to 5, we observe a significant

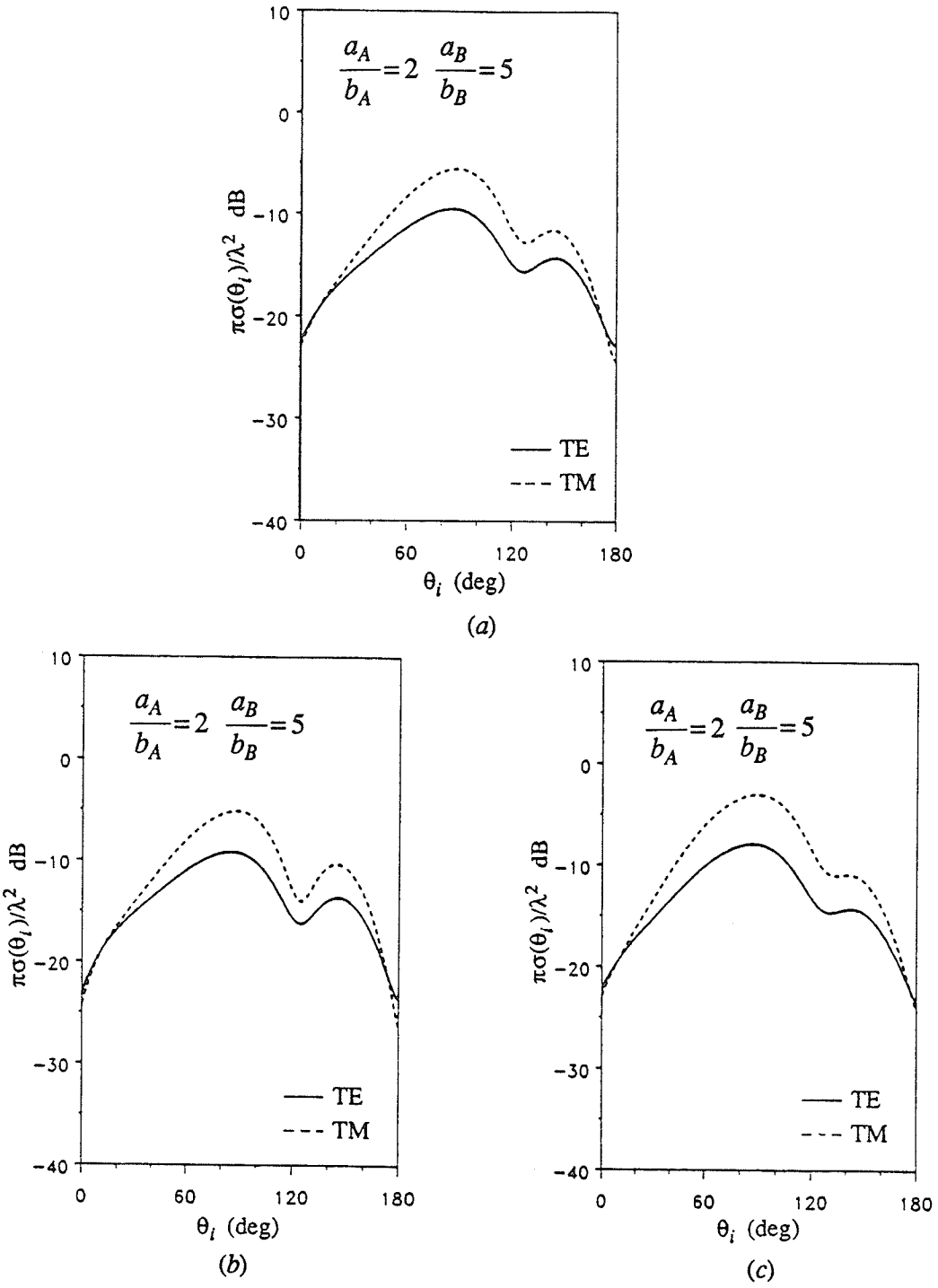

Fig. 4.10 Normalized backscattering cross section as a function of the angle of incidence, for two prolate spheroids of different axial ratios, with $a_A = a_B = \lambda/4$, Euler angles $\alpha = 30°, \beta = 45°, \gamma = 60°$, and centers displaced along the direction $\theta_0 = 60°$, $\phi_0 = 20°$ by $d = \lambda/2$, having dielectric constants (a) $\varepsilon_{rA} = \varepsilon_{rB} = 3.0$ (b) $\varepsilon_{rA} = 3.0$, $\varepsilon_{rB} = 4.0$ (c) $\varepsilon_{rA} = 4.0$, $\varepsilon_{rB} = 3.0$

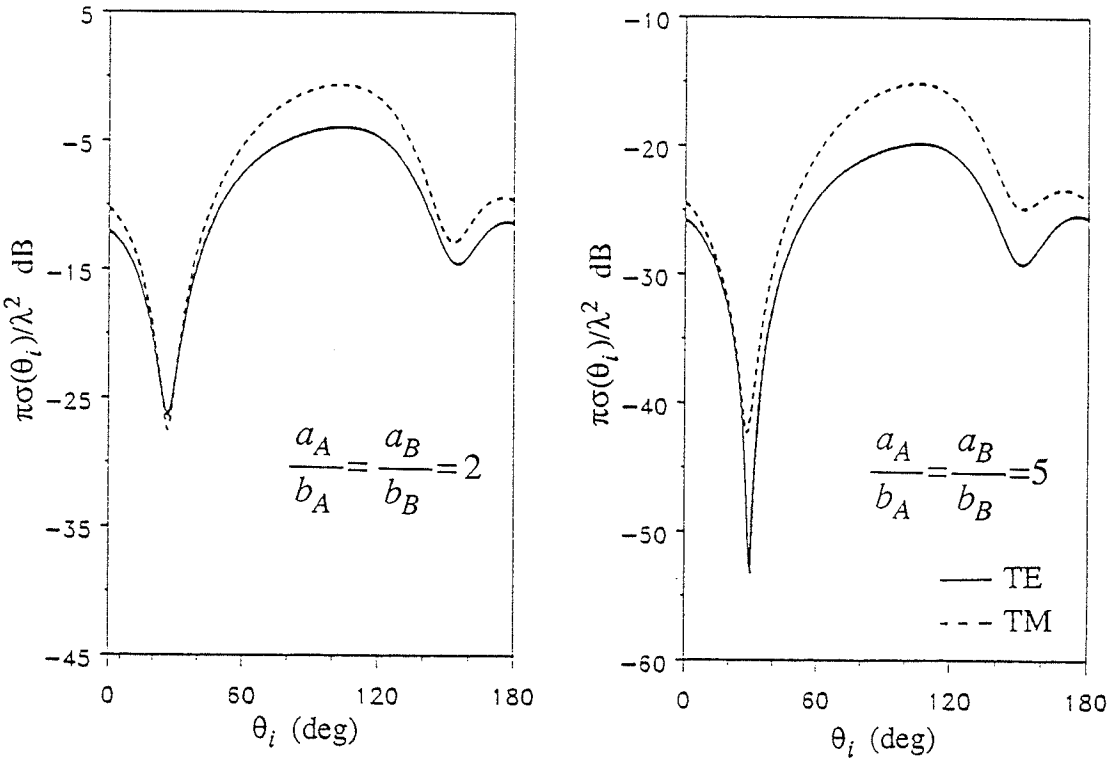

Fig. 4.11 Normalized backscattering cross section versus θ_i, for two identical prolate spheroids of semi-major axes $\lambda/4$, $\varepsilon_r = 3.0$, with Euler angles $(30°, 45°, 60°)$, and centers displaced along the x axis by $d = \lambda/2$.

reduction in the magnitude of the backscattering cross section due to the fact that the semi-minor axes are now 2.5 times smaller. The lower minima for both axial ratios occur around $\theta_i = 30°$. However, when the axial ratio is 5, the lower minimum in the curve for TE polarization is much deeper and sharper than the corresponding one for axial ratio 2.

It should be noted that the results for a system of perfectly conducting spheroids can be obtained as a special case from the corresponding results for a system of dielectric spheroids for $\varepsilon_r \to \infty$. In Fig. 4.12 we present results for such a case. In this figure, the normalized backscattering cross section calculated for two spheroids A and B each of an axial ratio 2, semi-major axis $\lambda/4$, with the spheroid B rotated with respect to A by the Euler angles $\alpha = 0°$, $\beta = 90°$, $\gamma = 0°$, the spheroid centers displaced along the z axis of the spheroid A, and a relative permittivity ε_r taken to be 10^6, is compared with the corresponding results for an identical set of perfectly conducting spheroids. As seen from the figure, the results are in good agreement with the maximum relative difference being 1.4%, which validates the software being used in the calculations. From the above result we can also verify that the accuracy obtained in the case of scattering by two dielectric spheroids with more terms in the series expansion, is still the same as that for scattering by two conducting spheroids.

To show further the applicability of the general software to limiting cases of eccentricity, the backscattering cross section has been calculated for two spheroids of axial ratio 1.001 with arbitrary Euler angles and a given separation between the centers. The results have been compared with those obtained for two spheres having the same center-to-center distance, and are in good agreement, with the maximum rela-

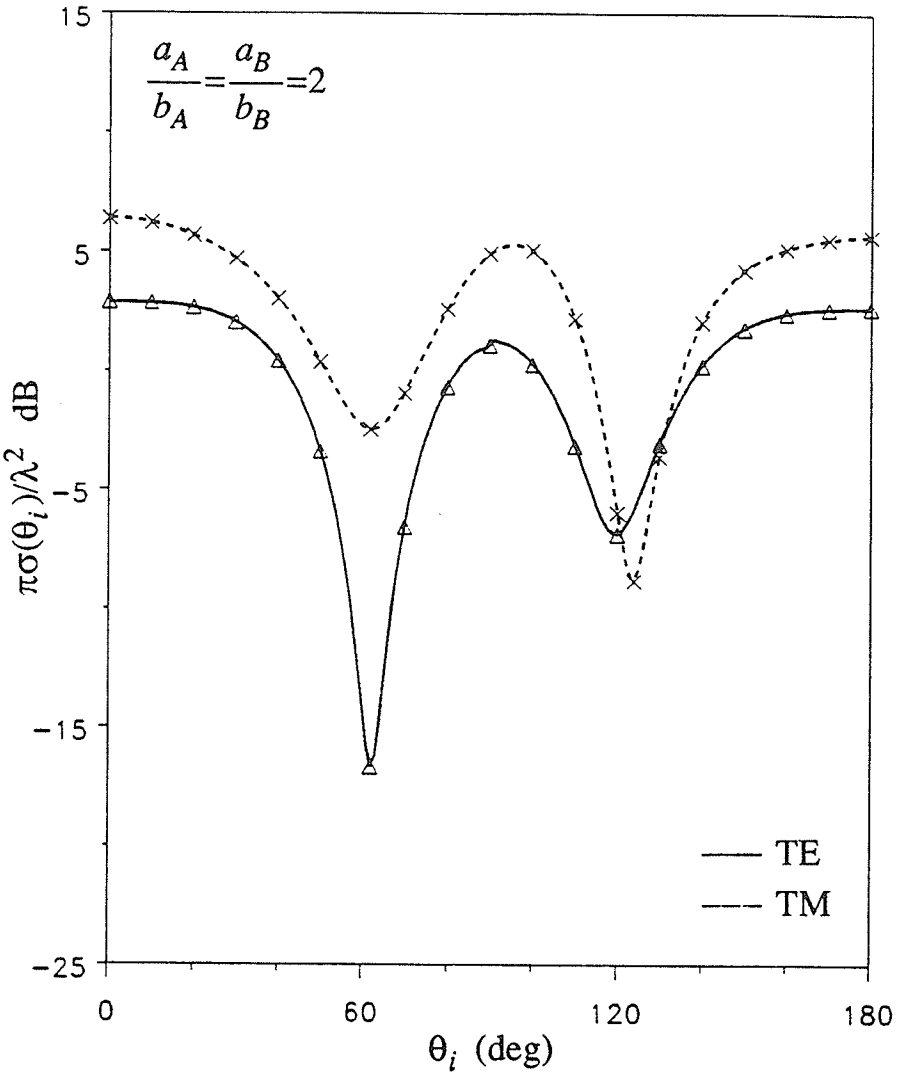

Fig. 4.12 Normalized backscattering cross section as a function of θ_i, for two identical prolate spheroids with $a_A = a_B = \lambda/4$, Euler angles $\alpha = 0°, \beta = 90°, \gamma = 0°$, dielectric constant $\varepsilon_r = 10^6$, and displaced along the z axis by $d = \lambda/2$. The triangles and the crosses show the results obtained for the corresponding case with perfectly conducting spheroids.

tive difference being 3.9%. Also the backscattering cross sections calculated for the same two spheroids with two different sets of Euler angles and a given separation are found to be almost the same.

CHAPTER 5

AN APPROXIMATE METHOD FOR THE PROBLEM OF SCATTERING BY TWO COAXIAL SPHEROIDS

In this chapter we present an approximate method for solving the problem of scattering of electromagnetic waves by two coaxial prolate spheroids, with their major axes along the common axis, the excitation being a uniform plane wave at oblique incidence, having an electric field of unit amplitude. The method is based on the exact solution to scattering of a plane wave by a single spheroid. To account for the multiple interactions between the spheroids, the total field seen by each spheroid is written as the sum of the corresponding fields of the incident plane wave and another plane wave of unknown magnitude propagating along the common axis from the other spheroid. Thus the total far field scattered by each spheroid can be written as the sum of the field scattered due to the incident plane wave and the field scattered due to the plane wave of unknown magnitude, propagating axially. The total far field scattered by one spheroid can also be written as the sum of the field scattered by that spheroid due to the incident plane wave and the field scattered due to the total far field scattered by the other spheroid, acting as an incident plane wave on the first spheroid. Equating the two different expressions of the total far field scattered by each of the spheroids corresponding to TE and TM polarizations separately, yields a set of simultaneous linear equations, whose solution gives finally the total far scattered field at any given point in space. Similar conditions for the scattered fields have been used in [62] for a linear array of perfectly conducting spheres in the special case of an axially incident field. For the case of two dimensional electromagnetic fields, equivalent sources from point of view of scattered far fields were first proposed in [63], and were recently used

by other researchers [64]–[65].

5.1 Scattering by a Single Spheroid

When the incident wave has an electric field of unit amplitude, for axial incidence and TE polarization, the far field scattered by a single spheroid at any given point (r,θ,ϕ) can be written as

$$\mathbf{E}_s^{TE}(r,\theta,\phi)=\frac{e^{-jkr}}{kr}\left[F_\theta^{TE}(\theta,\phi)\,\hat{\theta}+F_\phi^{TE}(\theta,\phi)\,\hat{\phi}\right] \tag{5.1}$$

Explicit expressions of $F_\theta^{TE}(\theta,\phi)$ and $F_\phi^{TE}(\theta,\phi)$ are similar to those given in (4.12) and (4.13), respectively, but with the corresponding expansion coefficients for axial incidence. Substituting for $\hat{\theta}$ and $\hat{\phi}$ in terms of $\hat{\mathbf{x}}$ and $\hat{\mathbf{y}}$ appropriately, we obtain the backscattered $(\theta=0)$ and forward scattered $(\theta=\pi)$ far fields respectively as

$$\mathbf{E}_s^{TE}(r,0,\phi)=\frac{e^{-jkr}}{kr}A(0)\,\hat{\mathbf{y}} \tag{5.2}$$

and

$$\mathbf{E}_s^{TE}(r,\pi,\phi)=-\frac{e^{-jkr}}{kr}A(\pi)\,\hat{\mathbf{y}} \tag{5.3}$$

in which

$$A(0)=\sum_{n=0}^{\infty}j^n S_{0n}(h,1)\,\alpha_{0n}^{+\,TE} \qquad A(\pi)=\sum_{n=0}^{\infty}j^n S_{0n}(h,-1)\,\alpha_{0n}^{+\,TE} \tag{5.4}$$

where $\alpha_{0n}^{+\,TE}$ are the coefficients in the expansion of $\mathbf{E}_s^{TE}$ in terms of vector spheroidal wave functions for axial incidence of the TE polarized incident wave. If only the polarization of this incident wave changes from TE to TM, then the far field at the point (r,θ,ϕ) can be written as

$$\mathbf{E}_s^{TM}(r,\theta,\phi)=\frac{e^{-jkr}}{kr}\left[F_\theta^{TM}(\theta,\phi)\,\hat{\theta}+F_\phi^{TM}(\theta,\phi)\,\hat{\phi}\right] \tag{5.5}$$

The explicit expressions of $F_\theta^{TM}(\theta,\phi)$ and $F_\phi^{TM}(\theta,\phi)$ are the same as those of $F_\theta^{TE}(\theta,\phi)$

and $F_{\phi}^{TE}(\theta,\phi)$, respectively, with the expansion coefficients correspondingly defined. The backscattered and forward scattered far fields in this case can be written as

$$\mathbf{E}_s^{TM}(r,0,\phi) = \frac{e^{-jkr}}{kr} B(0)\,\hat{\mathbf{x}} \tag{5.6}$$

and

$$\mathbf{E}_s^{TM}(r,\pi,\phi) = -\frac{e^{-jkr}}{kr} B(\pi)\,\hat{\mathbf{x}} \tag{5.7}$$

in which

$$B(0) = -\sum_{n=0}^{\infty} j^{n+1} S_{0n}(h,1)\,\alpha_{0n}^{+\,TM} \qquad B(\pi) = -\sum_{n=0}^{\infty} j^{n+1} S_{0n}(h,-1)\,\alpha_{0n}^{+\,TM} \tag{5.8}$$

where $\alpha_{0n}^{+\,TM}$ are the coefficients in the expansion of $\mathbf{E}_s^{TM}$ in terms of vector spheroidal wave functions for axial incidence of the TM polarized incident wave. From (5.2), (5.3), (5.6), and (5.7), it is obvious that in the case of axial incidence, both the backscattered and forward scattered far fields have the same polarization as that of the incident field. This property of the far scattered field allows the implementation of the proposed approximate method.

5.2 Formulation

Consider the two coaxial prolate spheroids 1 and 2 with the Cartesian system $O_1x_1y_1z_1$ attached to the spheroid 1 and the system $O_2x_2y_2z_2$ attached to the spheroid 2, as shown in Fig. 5.1. The major axes of the two spheroids lie along the common z axis, with the distance between the centers denoted by d. The system $O_1x_1y_1z_1$ is taken as the global system. Assume a linearly polarized plane wave, having an electric field of unit amplitude being incident on the system of two spheroids, the plane of incidence being chosen as the x_1–z_1 plane ($\phi_i = 0$) so that the angle of incidence θ_i, is

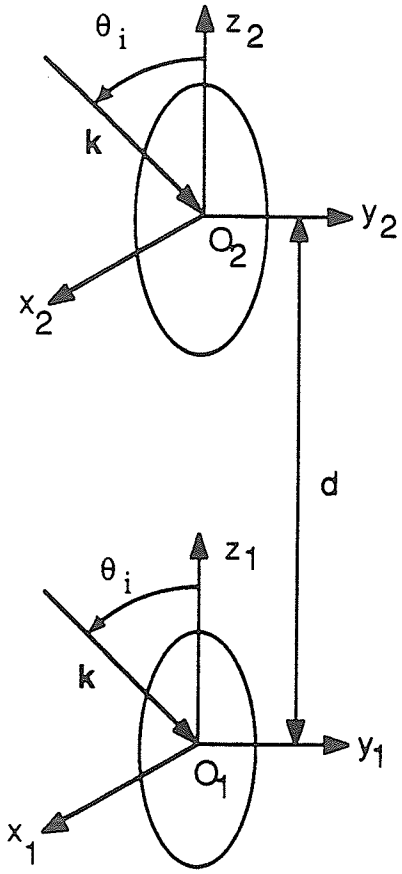

Fig. 5.1 System of two coaxial prolate spheroids and the associated Cartesian systems.

the angle the incident propagation vector makes with the z_1 axis.

The far field scattered by the spheroid 1 at any point (r,θ,ϕ) due to the plane wave propagating along the negative z axis can be written as

$$\mathbf{E}_{s1}^{C_1} = \frac{e^{-jkr}}{kr}\left\{[F_\theta^{TE}(\theta,\phi)\,\hat{\theta} + F_\phi^{TE}(\theta,\phi)\,\hat{\phi}]\,C_1^{TE} + [F_\theta^{TM}(\theta,\phi)\,\hat{\theta} + F_\phi^{TM}(\theta,\phi)\,\hat{\phi}]\,C_1^{TM}\right\} \quad (5.9)$$

in which C_1^{TE} and C_1^{TM} are the unknown amplitudes corresponding to TE and TM polarizations of the wave. The far field scattered by the spheroid 2 at the same point due to the incident plane wave with an electric field of unit amplitude, propagating along the direction $(\theta_i,\phi_i = 0)$ is given by

$$\mathbf{E}_{s2}^{i} = \frac{e^{-jkr}}{kr}[F_\theta(\theta,\phi)\,\hat{\theta} + F_\phi(\theta,\phi)\,\hat{\phi}]\,e^{jkd\cos\theta_i}\,e^{jkd\cos\theta} \quad (5.10)$$

The expressions of $F_\theta(\theta,\phi)$ and $F_\phi(\theta,\phi)$ have the same form as those defined in (4.12) and (4.13), respectively, but with the expansion coefficients corresponding to the particular angle of incidence θ_i. The far field scattered by the spheroid 2 due to the plane wave of unknown amplitude propagating along the positive z axis can be written as

$$\begin{aligned}\mathbf{E}_{s2}^{C_2} = \frac{e^{-jkr}}{kr}\Big\{&[-F_\theta^{TE}(\pi-\theta,\phi)\,\hat{\theta} + F_\phi^{TE}(\pi-\theta,\phi)\,\hat{\phi}]\,C_2^{TE} \\ &+ [F_\theta^{TM}(\pi-\theta,\phi)\,\hat{\theta} - F_\phi^{TM}(\pi-\theta,\phi)\,\hat{\phi}]\,C_2^{TM}\Big\}\,e^{jkd\cos\theta}\end{aligned} \quad (5.11)$$

in which C_2^{TE} and C_2^{TM} are also unknown amplitudes. Evaluating $\mathbf{E}_{s2}^{i}$ at O_1 yields

$$\mathbf{E}_{s2}^{i}\big|_{O_1} = -\frac{e^{-jkd}}{kd}[\bar{A}''(\pi)\,\hat{\mathbf{y}} + \bar{B}''(\pi)\,\hat{\mathbf{x}}]\,e^{jkd\cos\theta_i}\,e^{-jkd} \quad (5.12)$$

where

$$\bar{A}''(\theta) = \sum_{n=0}^{\infty}\frac{j^n}{2}S_{0n}(h,\cos\theta)\,(\alpha_{0n}^{+} + \alpha_{0n}^{-}) \quad (5.13)$$

$$\bar{B}''(\theta) = -\sum_{n=0}^{\infty} \frac{j^{n+1}}{2} S_{0n}(h, \cos\theta)\,(\alpha_{0n}^{+} - \alpha_{0n}^{-}) \tag{5.14}$$

with $\alpha_{0n}^{\pm}$ correspond to the expansion coefficients in the expansion of $\mathbf{E}_{s2}^{i}$ in terms of vector spheroidal wave functions. Evaluating $\mathbf{E}_{s2}^{C_2}$ at O_1 gives

$$\mathbf{E}_{s2}^{C_2}|_{O_1} = \frac{e^{-2jkd}}{kd}\,[A''(0)\,C_2^{TE}\,\hat{\mathbf{y}} - B''(0)\,C_2^{TM}\,\hat{\mathbf{x}}] \tag{5.15}$$

with $A''(0)$ and $B''(0)$ given in (5.4) and (5.8) corresponding to spheroid 2. The far field scattered by the spheroid 1 due to the incidence of $\mathbf{E}_{s2}^{i}|_{O_1}$ and $\mathbf{E}_{s2}^{C_2}|_{O_1}$ is

$$\begin{aligned}\mathbf{E}_{s1}' = \frac{e^{-jkr}}{kr}\,\{&[F_\theta^{TE}(\theta,\phi)\,\hat{\theta} + F_\phi^{TE}(\theta,\phi)\,\hat{\phi}]\,[A''(0)\,C_2^{TE} - \bar{A}''(\pi)\,e^{jkd\cos\theta_i}] \\ &+ [F_\theta^{TM}(\theta,\phi)\,\hat{\theta} + F_\phi^{TM}(\theta,\phi)\,\hat{\phi}]\,[B''(0)\,C_2^{TM} + \bar{B}''(\pi)\,e^{jkd\cos\theta_i}]\}\,\frac{e^{-2jkd}}{kd}\end{aligned} \tag{5.16}$$

From (5.9) and (5.16) we now obtain

$$C_1^{TE} = \frac{e^{-2jkd}}{kd}\,[A''(0)\,C_2^{TE} - \bar{A}''(\pi)\,e^{jkd\cos\theta_i}] \tag{5.17}$$

$$C_1^{TM} = \frac{e^{-2jkd}}{kd}\,[B''(0)\,C_2^{TM} + \bar{B}''(\pi)\,e^{jkd\cos\theta_i}] \tag{5.18}$$

The far field scattered by the spheroid 1 due to the incident plane wave with an electric field of unit amplitude, propagating along the direction $(\theta_i, \phi_i = 0)$ can be written as

$$\mathbf{E}_{s1}^{i} = \frac{e^{-jkr}}{kr}[F_\theta(\theta,\phi)\,\hat{\theta} + F_\phi(\theta,\phi)\,\hat{\phi}] \tag{5.19}$$

Evaluating $\mathbf{E}_{s1}^{i}$ and $\mathbf{E}_{s1}^{C_1}$ at O_2 gives

$$\mathbf{E}_{s1}^{i}|_{O_2} = \frac{e^{-jkd}}{kd}[\bar{A}'(0)\hat{\mathbf{y}} + \bar{B}'(0)\hat{\mathbf{x}}] \tag{5.20}$$

where $\bar{A}'(0)$ and $\bar{B}'(0)$ have the form in (5.13) and (5.14) corresponding to spheroid 1, and

$$\mathbf{E}_{s1}^{C_1}|_{O_2} = \frac{e^{-jkd}}{kd}\,[A'(0)\,C_1^{TE}\,\hat{\mathbf{y}} + B'(0)\,C_1^{TM}\,\hat{\mathbf{x}}] \tag{5.21}$$

with $A'(0)$ and $B'(0)$ given in (5.4) and (5.8) corresponding to spheroid 1. The far field scattered by the spheroid 2 due to the incidence of $\mathbf{E}_{s1}^{i}|_{O_2}$ and $\mathbf{E}_{s1}^{C_1}|_{O_2}$ is

$$\begin{aligned}\mathbf{E}'_{s2} = \frac{e^{-jkr}}{kr}\,\{&[-F_\theta^{TE}(\pi-\theta,\phi)\,\hat{\theta} + F_\phi^{TE}(\pi-\theta,\phi)\,\hat{\phi}]\,[A'(0)\,C_1^{TE} + \bar{A}'(0)] \\ &-[F_\theta^{TM}(\pi-\theta,\phi)\,\hat{\theta} - F_\phi^{TM}(\pi-\theta,\phi)\,\hat{\phi}]\,[B'(0)C_1^{TM} + \bar{B}'(0)]\}\,\frac{e^{-jkd}}{kd}\,e^{jkd\cos\theta}\end{aligned} \tag{5.22}$$

From equations (5.11) and (5.22) now we get

$$C_2^{TE} = \frac{e^{-jkd}}{kd}\,[A'(0)\,C_1^{TE} + \bar{A}'(0)] \tag{5.23}$$

$$C_2^{TM} = -\frac{e^{-jkd}}{kd}\,[B'(0)\,C_1^{TM} + \bar{B}'(0)] \tag{5.24}$$

Solving the four algebraic equations (5.17), (5.23) and (5.18), (5.24), simultaneously, yields the four unknown constants. Once these are known, the total far scattered field at any given point (r,θ,ϕ) is calculated as

$$\begin{aligned}\mathbf{E}_s = \frac{e^{-jkr}}{kr}\,\{&[F_\theta(\theta,\phi)\,\hat{\theta} + F_\phi(\theta,\phi)\,\hat{\phi}]\,(1 + e^{jkd\cos\theta_i}\,e^{jkd\cos\theta}) \\ &+[F_\theta^{TE}(\theta,\phi)\,\hat{\theta} + F_\phi^{TE}(\theta,\phi)\,\hat{\phi}]\,C_1^{TE} + [F_\theta^{TM}(\theta,\phi)\,\hat{\theta} + F_\phi^{TM}(\theta,\phi)\,\hat{\phi}]\,C_1^{TM} \\ &+[-F_\theta^{TE}(\pi-\theta,\phi)\,\hat{\theta} + F_\phi^{TE}(\pi-\theta,\phi)\,\hat{\phi}]\,C_2^{TE}\,e^{jkd\cos\theta} \\ &+[F_\theta^{TM}(\pi-\theta,\phi)\,\hat{\theta} - F_\phi^{TM}(\pi-\theta,\phi)\,\hat{\phi}]\,C_2^{TM}\,e^{jkd\cos\theta}\}\end{aligned} \tag{5.25}$$

This equation can be written in a condensed form as

$$\mathbf{E}_s = \frac{e^{-jkr}}{kr}\,[F_\theta^T(\theta,\phi)\,\hat{\theta} + F_\phi^T(\theta,\phi)\,\hat{\phi}] \tag{5.26}$$

The normalized bistatic cross section is then calculated from

$$\frac{\pi\sigma(\theta,\phi)}{\lambda^2} = |F_\theta^T(\theta,\phi)|^2 + |F_\phi^T(\theta,\phi)|^2 \tag{5.27}$$

with the $E-$ and $H-$ plane patterns corresponding to $\phi=\pi/2$ and $\phi=0$, respectively.

In the special case of axial incidence and TE polarization, $C_1^{TM}=C_2^{TM}=0$. Thus in this case the expression of the far scattered field at (r,θ,ϕ) simplifies to

$$\begin{aligned}\mathbf{E}_s = \frac{e^{-jkr}}{kr}\{&[F_\theta^{TE}(\theta,\phi)\,\hat{\theta}+F_\phi^{TE}(\theta,\phi)\,\hat{\phi}](1+e^{jkd\cos\theta_i}\,e^{jkd\cos\theta}+C_1^{TE})\\&+[-F_\theta^{TE}(\pi-\theta,\phi)\,\hat{\theta}+F_\phi^{TE}(\pi-\theta,\phi)\,\hat{\phi}]\,C_2^{TE}\,e^{jkd\cos\theta}\}\end{aligned} \tag{5.28}$$

5.3 Computed Results

Numerical results obtained for scattering by two coaxial perfectly conducting spheroids at oblique incidence, are presented in this section in the form of normalized bistatic scattering cross sections in the $E-$ and $H-$ planes. The corresponding results obtained for the same problem by using the exact method, and also by neglecting the interaction between the two spheroids, are also included for the purpose of comparison. The cases of $\theta_i=0°$, 45°, and 90°, where θ_i is the angle of incidence, are considered separately, for TE polarization of the incident wave.

Fig. 5.2 shows the plots of normalized bistatic cross section in the $E-$ plane as a function of the scattering angle, for two coaxial perfectly conducting spheroids of axial ratio 2, semi-major axes $a_A=a_B=\lambda/4$, having a center-to-center distance $d=0.6\lambda$. When compared with the other two plots in the same figure, we observe that the result obtained by the approximate method is better than that obtained by neglecting the interaction between the spheroids for all the range of the scattering angle, in particular for this small separation of 0.1λ between the tips of the spheroids. It is in good agreement with the result obtained by the exact method, the maximum relative difference

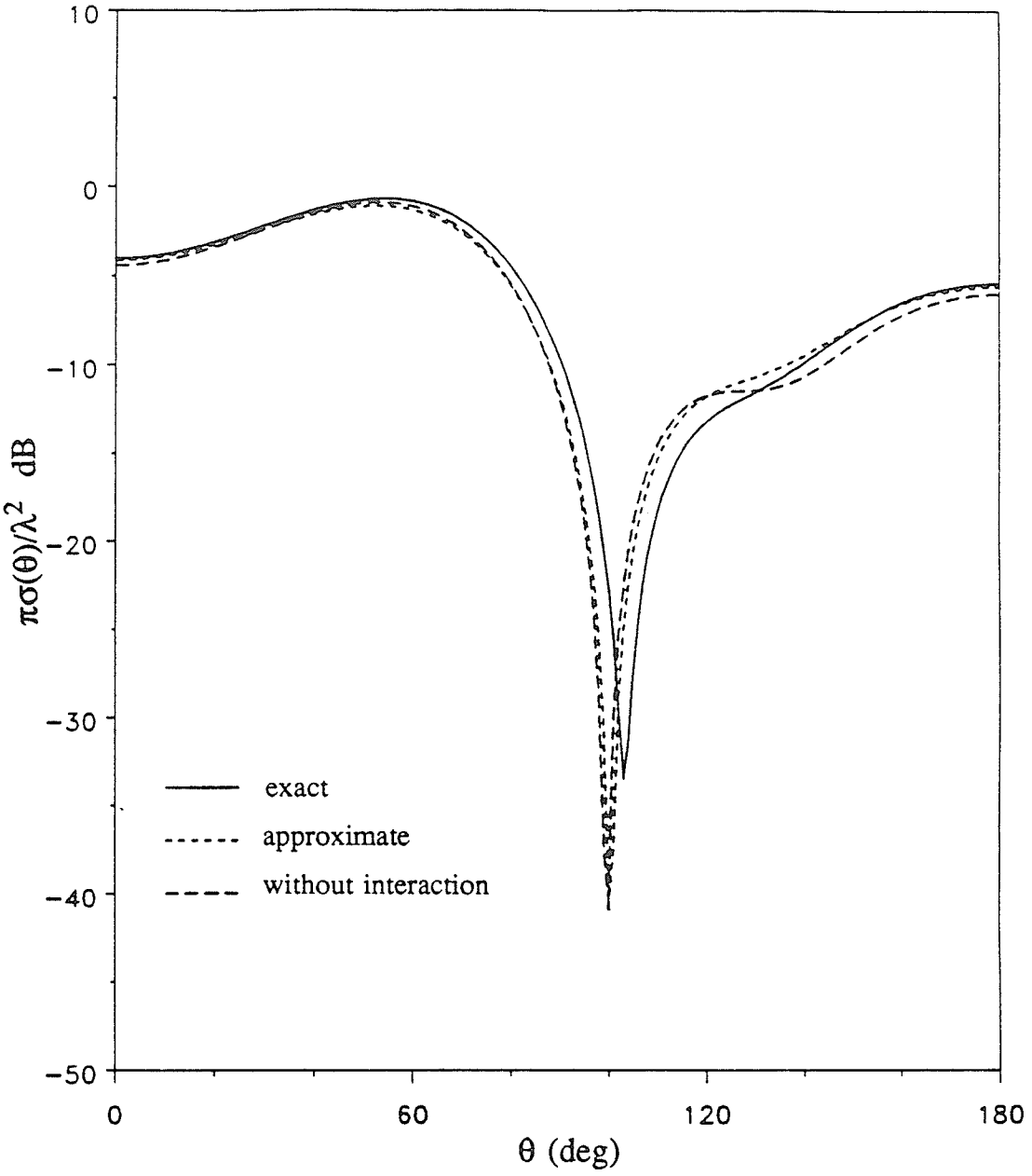

Fig. 5.2 Normalized bistatic cross section in the $E-$ plane for axial incidence of the incident wave, as a function of the scattering angle for two identical coaxial prolate spheroids of axial ratio 2 with $a_A = a_B = \lambda/4$, and displaced along the z axis by $d = 0.6\lambda$.

being 2.6%, in the range $\theta = 0°–30°$ and $\theta = 150°–180°$. The result calculated near $\theta = 100°$ with the interaction neglected is drastically low, but the result obtained using the approximate method has a reasonable value.

The normalized bistatic cross section versus scattering angle in the $E-$ and $H-$ planes are given in Figs. 5.3 and 5.4, respectively, for two spheroids which are the same as in Fig. 5.2, but with the distance between the centers now being λ. When we compare the results of Figs. 5.2, and 5.3, we find that the one in Fig. 5.3 is in much better agreement with the result obtained by the exact method, except around the minima. However, since the effect of the interaction becomes less influential as the distance between the centers increases, the result obtained by neglecting the interaction also doesn't deviate too much from the other two except in the region $\theta = 120°–150°$. For the $H-$ plane pattern given in Fig. 5.4 we observe a similar type of variation in the curves. It should be noted that the values of the minima in the results obtained by neglecting the interaction are minus infinity in dB theoretically and therefore are not represented on the plot. These values are due to the superposition of the individual interference patterns of the two spheroids. It should be remarked that the positions of the minima are given reasonably accurately for all the cases considered.

Figs. 5.5 and 5.6 show plots similar to those in Figs 5.3 and 5.4, respectively, for the same configuration of the two spheroids as in these latter figures, but with the angle of incidence now being 45°. Figs. 5.7 and 5.8 also show the $E-$ and $H-$ plane patterns for the same two spheroids as in the two previous figures, but the angle of incidence now being 90°. In all these figures we observe that in general the results obtained by the approximate method are closer to the exact result than the one

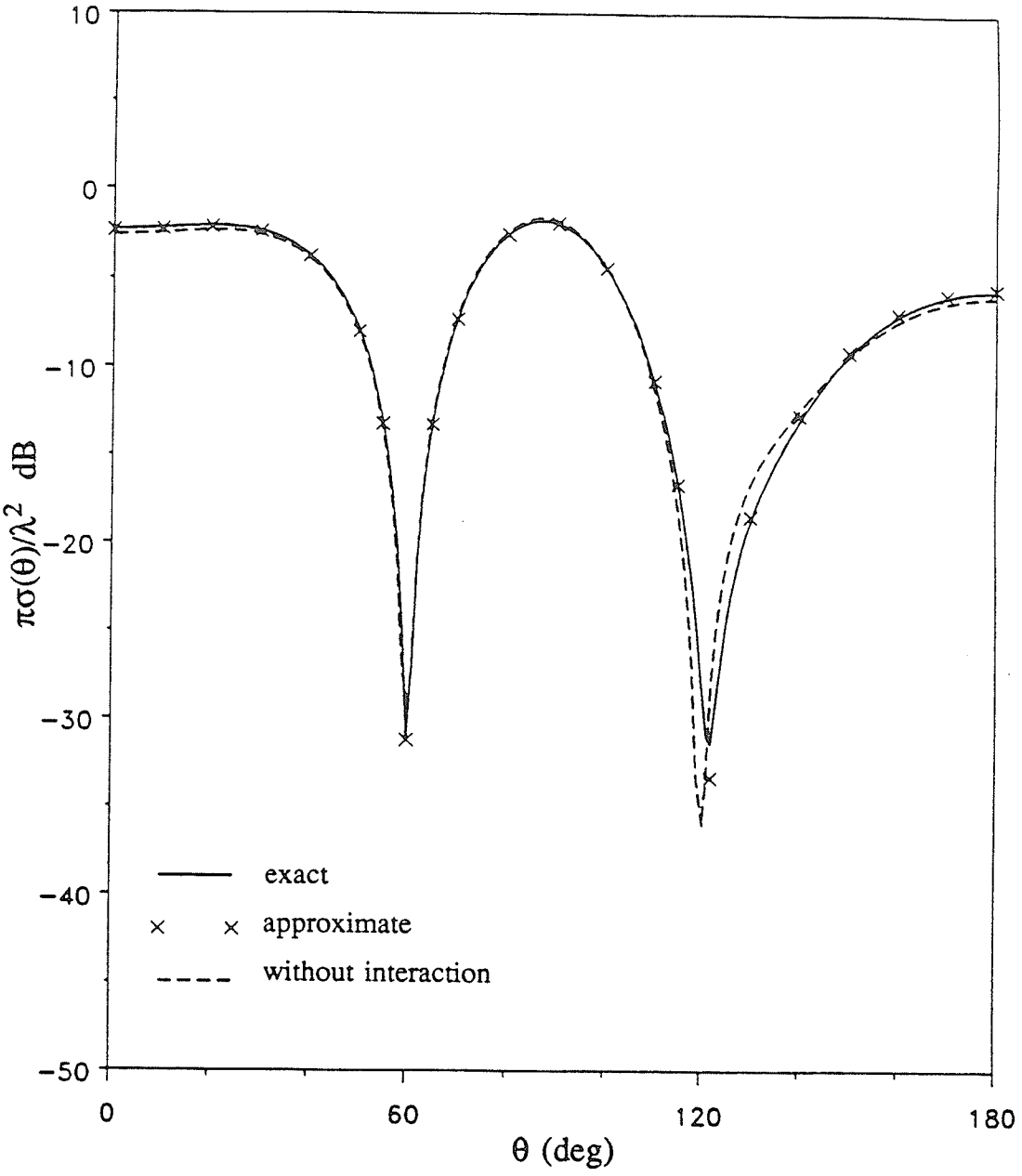

Fig. 5.3 Normalized bistatic cross section in the $E-$ plane for axial incidence of the incident wave, as a function of the scattering angle for two identical coaxial prolate spheroids of axial ratio 2 with $a_A = a_B = \lambda/4$, and displaced along the z axis by $d = \lambda$.

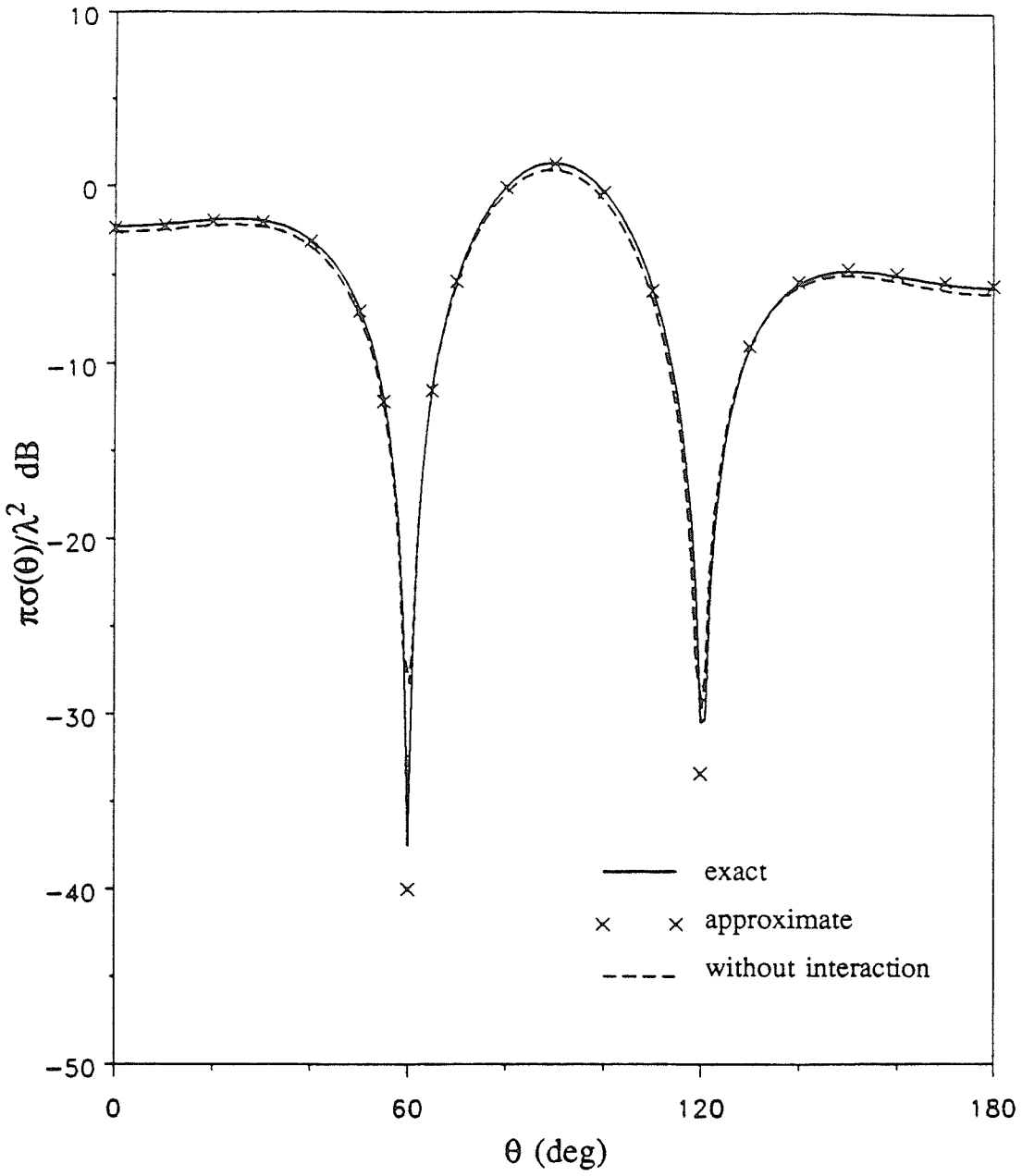

Fig. 5.4 Normalized bistatic cross section in the $H-$ plane for axial incidence of the incident wave, as a function of the scattering angle for two identical coaxial prolate spheroids of axial ratio 2 with $a_A = a_B = \lambda/4$, and displaced along the z axis by $d = \lambda$.

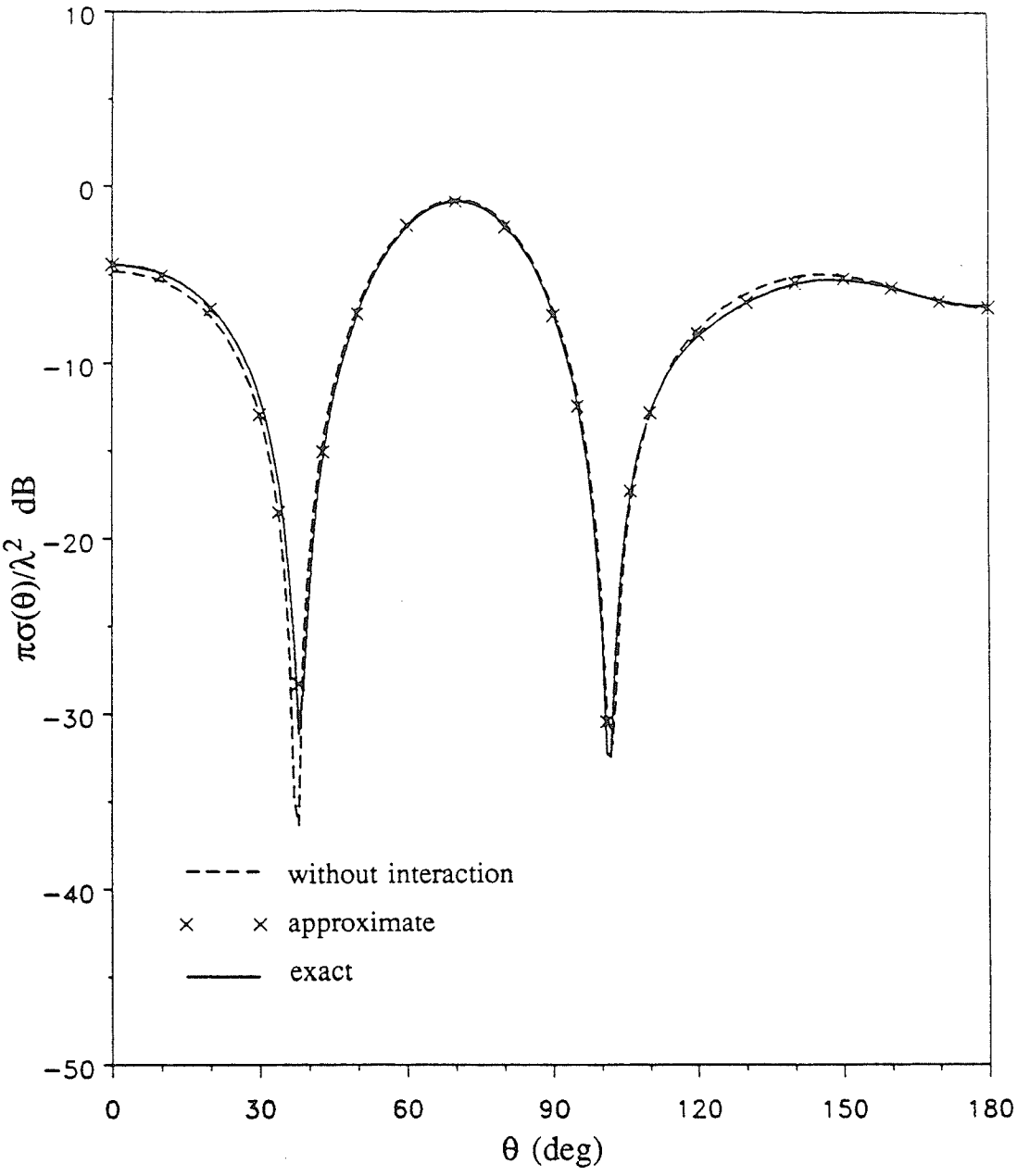

Fig. 5.5 Normalized bistatic cross section in the $E-$ plane for $\theta_i = 45°$, versus scattering angle for the same configuration of the two spheroids as in Fig. 5.3.

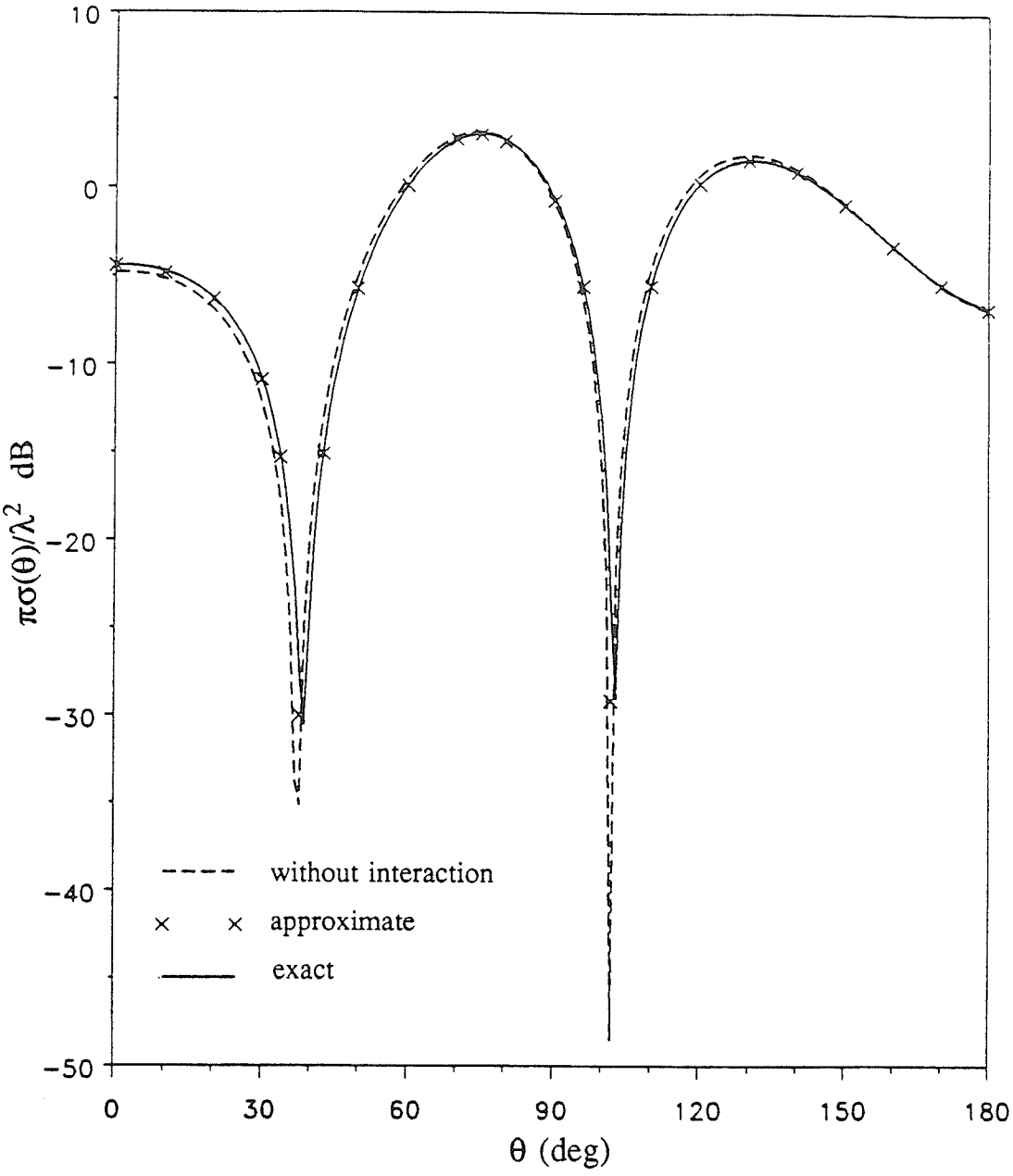

Fig. 5.6 Normalized bistatic cross section in the $H-$ plane for $\theta_i = 45°$, versus scattering angle for the same configuration of the two spheroids as in Fig. 5.4.

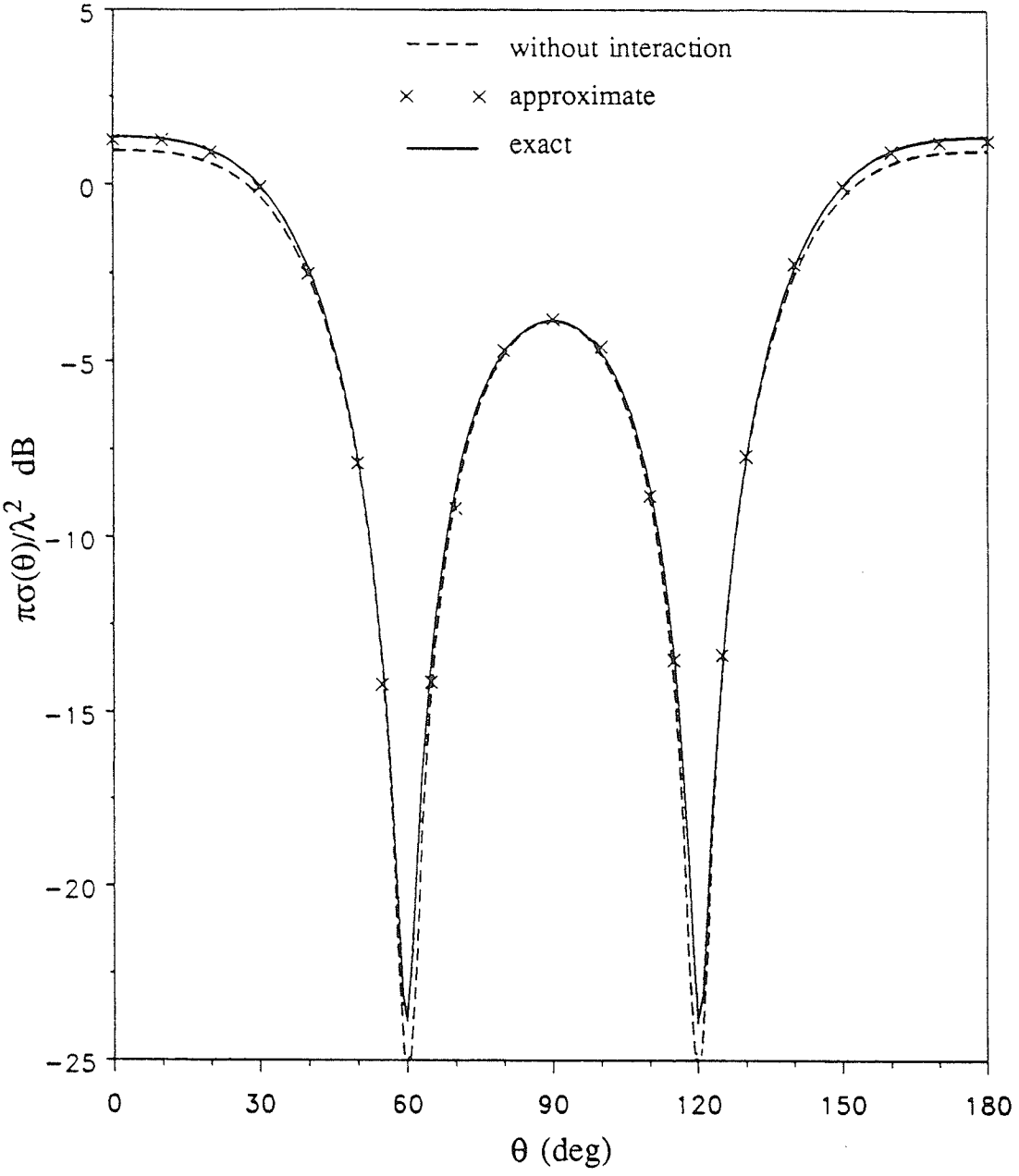

Fig. 5.7 Normalized bistatic cross section in the $E-$ plane for $\theta_i = 90°$, as a function of θ for the same configuration of the two spheroids as in Fig. 5.3.

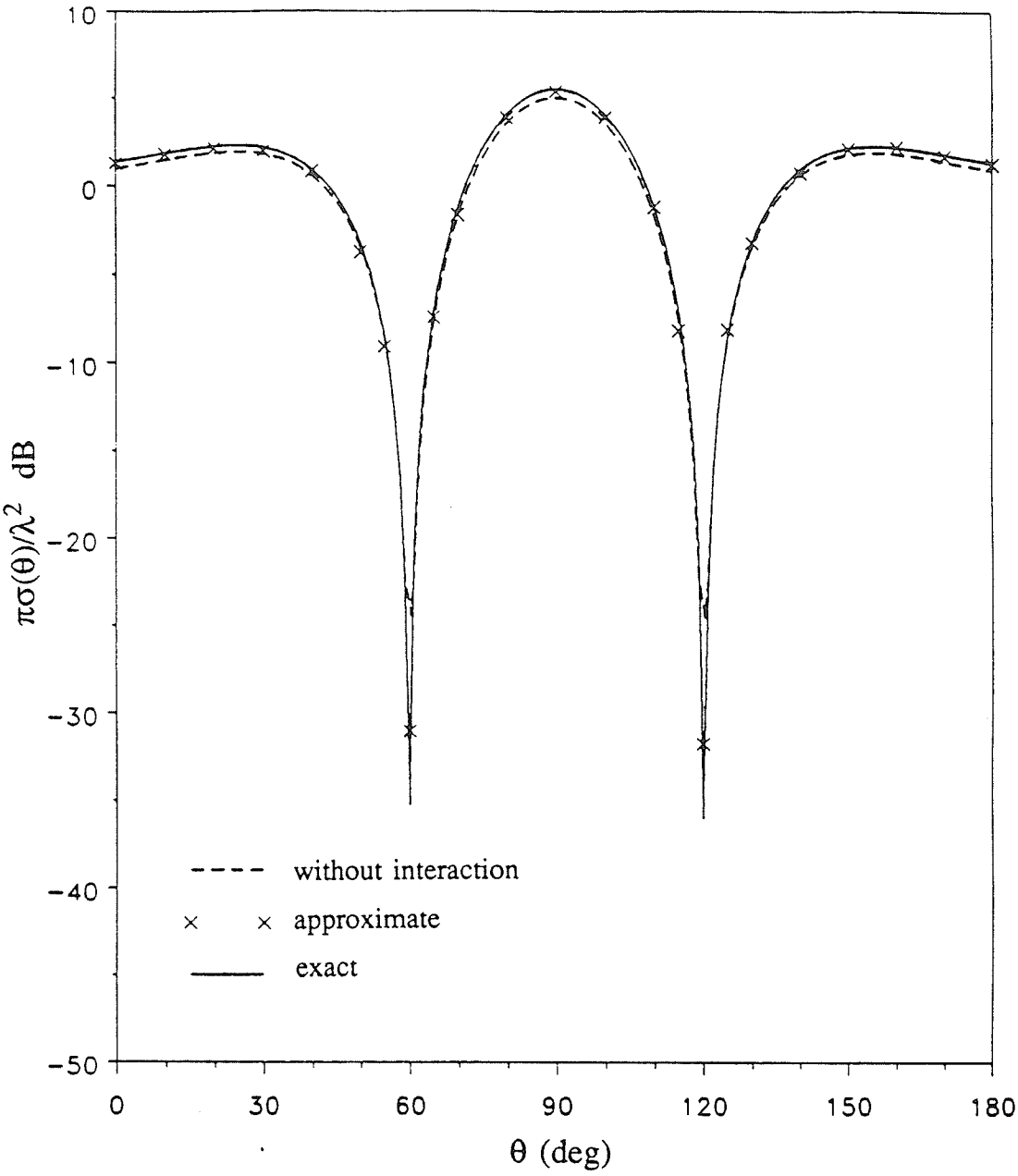

Fig. 5.8 Normalized bistatic cross section in the $H-$ plane for $\theta_i = 90°$, as a function of θ for the same configuration of the two spheroids as in Fig. 5.4.

obtained by neglecting the interaction, except around the peak region, with the maximum relative difference on an average being 4.3%, and the agreement being better close to $\theta = 0^{\circ}$ and $\theta = 180^{\circ}$.

Finally in Fig. 5.9 we present the variation of the normalized bistatic cross section in the $E-$ plane as a function of θ, for two prolate spheroids of axial ratio 2, semi-major axes $\lambda/2$, having a center-to-center distance of 1.5λ. Here we observe that from about $\theta = 30^{\circ}$ to $\theta = 150^{\circ}$, the results obtained by the approximate method as well as by neglecting interaction, are very close to that obtained by the exact method except near minima. At and near minima they both deviate from the exact value, but still the one calculated by using the approximate method being closer to the exact. Outside this range of θ the agreement is not very good. However, with the curve for the approximate method it is still possible to find out approximately the location of the minima which are close to 10° and 170°. This is not the case when neglecting the interaction for θ less than about 10° or greater than about 170°, as seen from Fig. 5.9.

From the numerical analysis performed on the basis of this approximate method, it is possible to conclude that it gives acceptable results for spheroids of semi-major axes lengths up to $\lambda/2$, and for separations between the tips of the spheroids that are greater than $\lambda/2$. Much more accurate results are obtained for larger separations between the tips of the spheroids compared to their sizes, and also for larger axial ratios of the spheroids. The reduction in computation time as compared to that of the exact method, calculated on an average for the cases considered is about 30%.

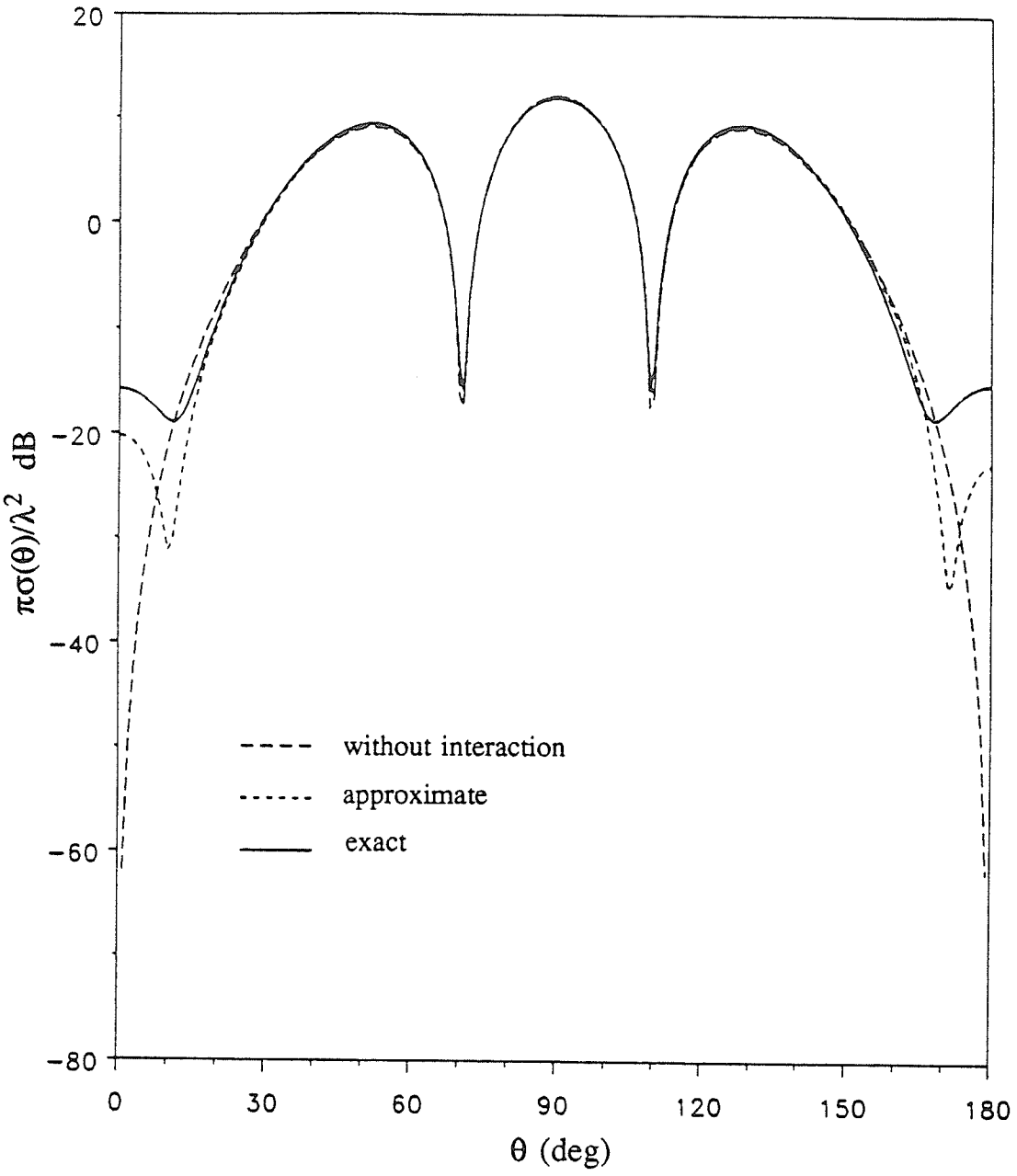

Fig. 5.9 Normalized bistatic cross section in the $E-$ plane for $\theta_i = 90^\circ$ as a function of the scattering angle for two identical coaxial prolate spheroids of axial ratio 2 with $a_A = a_B = \lambda/2$, and displaced along the z axis by $d = 1.5\lambda$.

CHAPTER 6

ADMITTANCE CHARACTERISTICS AND FAR FIELD PATTERNS FOR COUPLED SPHEROIDAL DIPOLE ANTENNAS IN ARBITRARY CONFIGURATION

Practical dipole antennas modeled by using spheroids of large axial ratios, fed by a central gap voltage, have been under investigation for a long period of time [4], [28], [66]–[69]. Admittance characteristics of a system of two such antennas in parallel configuration have already been studied [45] by applying the translational addition theorems for vector spheroidal wave functions [43]. In this chapter we present an analytic solution to the electromagnetic coupling between two spheroidal dipole antennas in an arbitrary configuration, which enables one to study the admittance characteristics of a system of two such antennas. Each antenna is modeled by a very thin prolate spheroid which is centrally fed by a gap voltage. By using the equivalence principle, each spheroidal dipole is replaced by a solid spheroidal conductor of the same size without gap, encircled by a corresponding filamentary ring carrying magnetic current of proper magnitude. The associated electric and magnetic fields are expanded in terms of appropriate vector spheroidal eigenfunctions, and the boundary conditions at the surface of each spheroid are imposed by using the rotational-translational addition theorems for vector spheroidal wave functions derived in Chapter 2. The solution of the resulting set of algebraic equations gives the unknown scattered field expansion coefficients.

The formulation of the problem and the expansion of the electric fields associated with the two antennas in terms of appropriate vector spheroidal wave functions are given in Section 6.1. Section 6.2 deals with imposing of the boundary conditions at the surface of each spheroidal dipole antenna, from which a set of linear algebraic

equations is obtained for the unknown scattered field expansion coefficients. The calculation of the mutual and self admittances, as well as of the electric field in the far zone, is discussed in Section 6.3. Finally in Section 6.4, numerical results are presented for the variation of the real and imaginary parts of the mutual admittance with the distance between two spheroidal dipole antennas of arbitrary orientation, having unequal major axis lengths. Also given in this section are the $E-$ and $H-$ plane patterns for the same two antennas in different configurations, with one antenna now being parasitic.

6.1 Electromagnetic Field Modeling

Consider two arbitrarily oriented prolate spheroidal antennas A and B, as shown in Fig. 6.1. The unprimed coordinate system is attached to antenna A, which is fed by a central gap voltage V_A, and the primed coordinate system to antenna B, which is fed by a central gap voltage V_B. Major axes of A and B are along the z and z' axes of the Cartesian systems $Oxyz$ and $O'x'y'z'$, respectively. The system $Ox_{\|}y_{\|}z_{\|}$ is parallel to $O'x'y'z'$ and is rotated with respect to $Oxyz$ through the Euler angles α, β, γ. The center O' of B has spherical coordinates d, θ_0, ϕ_0 relative to $Oxyz$ and d, θ_d, ϕ_d, relative to $Ox_{\|}y_{\|}z_{\|}$. The prolate spheroidal coordinates associated with the unprimed and primed systems are denoted by ξ,η,ϕ and ξ',η',ϕ', respectively. The surfaces of the two antennas A and B coincide with the coordinate surfaces $\xi=\xi_A$ and $\xi'=\xi'_B$, respectively.

Using the equivalence principle, the pair of centrally fed spheroidal antennas A and B is modeled by two solid spheroidal conductors, without gaps, of the same size as the respective antennas, encircled at their middle ($\eta=0, \eta'=0$) by filamentary rings of

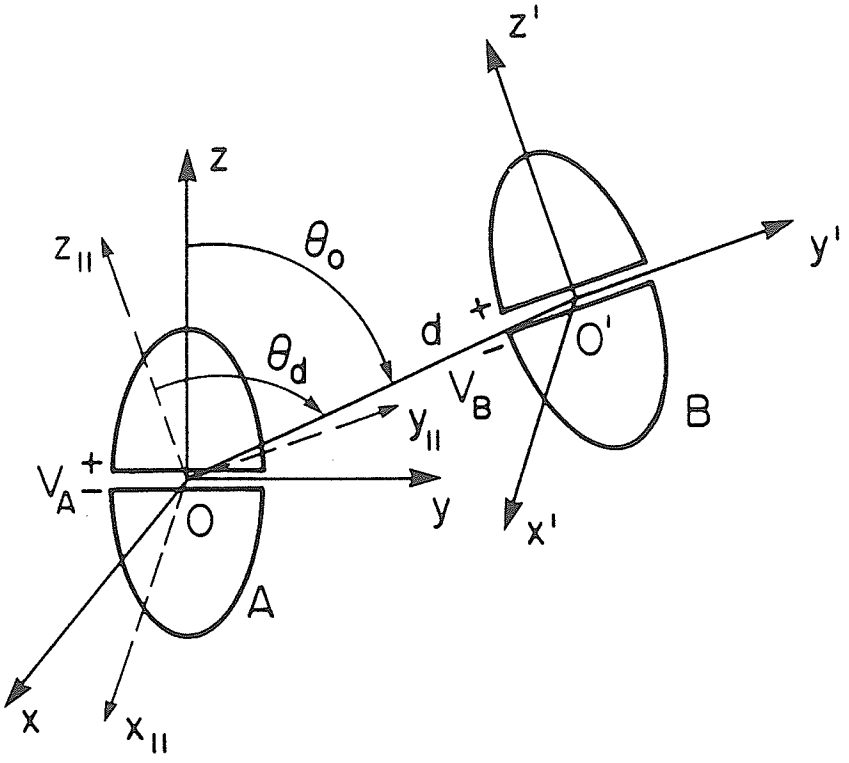

Fig. 6.1 System of two spheroidal dipole antennas of arbitrary orientation.

magnetic currents V_A and V_B, respectively. The resultant electromagnetic field can be determined by the superposition of the fields produced by the filamentary magnetic currents and the fields scattered by the solid spheroids assumed to be perfect conductors. The electric field intensities due to these filamentary magnetic currents considered to be alone in an unbounded free space can be expressed in a matrix form as [45]:

$$ {}_S\mathbf{E}_A(\xi,\eta) = \begin{cases} \overline{\mathbf{M}}^{(4)T}(\xi,\eta)\,[R]\,\overline{A}, & \xi > \xi_A^+ \\ \overline{\mathbf{M}}^{(1)T}(\xi,\eta)\,\overline{A}, & \xi < \xi_A^+ \end{cases} \tag{6.1} $$

$$ {}_S\mathbf{E}_B(\xi',\eta') = \begin{cases} \overline{\mathbf{M}}^{(4)T}(\xi',\eta')\,[R']\,\overline{B}, & \xi' > \xi_B'^+ \\ \overline{\mathbf{M}}^{(1)T}(\xi',\eta')\,\overline{B}, & \xi' < \xi_B'^+ \end{cases} \tag{6.2} $$

where ξ_A^+ and $\xi_B'^+$ are the values of ξ and ξ' just outside the surfaces of the spheroids A and B, respectively, the overbar denotes a column matrix, and T the transpose of a matrix. The matrices $\overline{\mathbf{M}}^{(1)T}$, $\overline{\mathbf{M}}^{(4)T}$, $\overline{A}$, and $\overline{B}$ are all defined in Appendix E. $[R]$ and $[R']$ are diagonal matrices, with the respective n th diagonal elements given by

$$ R_{nn} = \frac{R_{1n}^{(1)}(h,\xi_A)}{R_{1n}^{(4)}(h,\xi_A)}, \qquad R'_{nn} = \frac{R_{1n}^{(1)}(h',\xi'_B)}{R_{1n}^{(4)}(h',\xi'_B)} \tag{6.3} $$

where $R_{1n}^{(1)}(h,\xi)$ and $R_{1n}^{(4)}(h,\xi)$ are the spheroidal radial functions of the first kind and the fourth kind, respectively, given in Appendix A.

The electric field scattered by the spheroid B can be expanded in the form

$$ \mathbf{E}_{sB} = \overline{\mathbf{M}}_{sB}^{(4)T}\,\bar{\beta} \tag{6.4} $$

as given in (3.32), where $\overline{\mathbf{M}}_{sB}^{(4)}$ and $\bar{\beta}$ are column matrices whose elements are prolate spheroidal vector wave functions of the fourth kind, expressed in terms of the primed spheroidal coordinates, and the corresponding unknown expansion coefficients,

respectively. In order to impose the boundary conditions at the surface of antenna A, it is necessary to express the scattered field $\mathbf{E}_{sB}$ and the source field ${}_S\mathbf{E}_B$ for $\xi' > \xi_B'^{+}$, which are seen from A as incoming fields, in terms of vector wave functions of the first kind in unprimed coordinates. This is achieved by using the appropriate rotational-translational addition theorem for vector spheroidal wave functions (see Chapter 2) to express the outgoing vector wave functions in primed coordinates $\overline{\mathbf{M}}_{sB}^{(4)}$ and $\overline{\mathbf{M}}^{(4)}$ in terms of incoming vector wave functions in unprimed coordinates $\overline{\mathbf{M}}_{BA}^{(1)}$ as in (3.43)

$$\overline{\mathbf{M}}_{sB}^{(4)} = [\Gamma]\, \overline{\mathbf{M}}_{BA}^{(1)} \tag{6.5}$$

$$\overline{\mathbf{M}}^{(4)} = [\Delta]\, \overline{\mathbf{M}}_{BA}^{(1)} \tag{6.6}$$

in which $[\Gamma]$ and $[\Delta]$ are defined in Appendix E. The structure of $\overline{\mathbf{M}}_{BA}^{(1)T}$ is similar to that of ${}^{(qr)}\overline{\mathbf{M}}^{(1)T}$ given in (3.44) with the vector wave functions evaluated with respect to the unprimed coordinate system. Denoting the incoming fields corresponding to $\mathbf{E}_{sB}$ and ${}_S\mathbf{E}_B$ by $\mathbf{E}_{sBA}$ and ${}_S\mathbf{E}_{BA}$, respectively, taking the transpose of both sides of (6.5) and (6.6), and then substituting $\overline{\mathbf{M}}_{sB}^{(4)T}$ in (6.4) and $\overline{\mathbf{M}}^{(4)T}$ in (6.2) gives

$$\mathbf{E}_{sBA} = \overline{\mathbf{M}}_{BA}^{(1)T} [\Gamma]^T\, \bar{\beta} \tag{6.7}$$

$${}_S\mathbf{E}_{BA} = \overline{\mathbf{M}}_{BA}^{(1)T} [\Delta]^T\, [R']\, \overline{B} \tag{6.8}$$

In the presence of fields ${}_S\mathbf{E}_{BA}$, $\mathbf{E}_{sBA}$, and ${}_S\mathbf{E}_A$, antenna A scatters an electric field which can also be expanded in a series of prolate spheroidal vector wave functions and expressed in a matrix form similar to $\mathbf{E}_{sB}$ as

$$\mathbf{E}_{sA} = \overline{\mathbf{M}}_{sA}^{(4)T}\, \overline{\alpha} \tag{6.9}$$

where $\overline{\mathbf{M}}_{sA}^{(4)}$ and $\overline{\alpha}$ are column matrices whose elements are prolate spheroidal vector wave functions of the fourth kind, expressed in terms of unprimed spheroidal

coordinates, and the corresponding unknown expansion coefficients, respectively. Thus, the total electric field seen from the antenna A is given by

$$\begin{aligned}\mathbf{E}_A &= {}_S\mathbf{E}_A + {}_S\mathbf{E}_{BA} + \mathbf{E}_{sBA} + \mathbf{E}_{sA} \\ &= \overline{\mathbf{M}}^{(1)T}\,\overline{A} + \overline{\mathbf{M}}_{BA}^{(1)T}\,[\Delta]^T\,[R']\,\overline{B} + \overline{\mathbf{M}}_{BA}^{(1)T}\,[\Gamma]^T\,\overline{\beta} + \overline{\mathbf{M}}_{sA}^{(4)T}\,\overline{\alpha} \qquad (6.10)\end{aligned}$$

Similarly, the total electric field seen from the antenna B can be expressed in terms of appropriate prolate spheroidal vector wave functions in the primed coordinate system as

$$\begin{aligned}\mathbf{E}_B &= {}_S\mathbf{E}_B + {}_S\mathbf{E}_{AB} + \mathbf{E}_{sAB} + \mathbf{E}_{sB} \\ &= \overline{\mathbf{M}}^{(1)T}\,\overline{B} + \overline{\mathbf{M}}_{AB}^{(1)T}\,[\Delta']^T\,[R]\,\overline{A} + \overline{\mathbf{M}}_{AB}^{(1)T}\,[\Gamma']^T\,\overline{\alpha} + \overline{\mathbf{M}}_{sB}^{(4)T}\,\overline{\beta} \qquad (6.11)\end{aligned}$$

with $[\Gamma']$ and $[\Delta']$ defined in Appendix E. The elements of the matrix $\overline{\mathbf{M}}_{AB}^{(1)T}$ are obtained from the corresponding elements of $\overline{\mathbf{M}}_{BA}^{(1)T}$ by evaluating the vector wave functions with respect to the primed coordinate system.

6.2 Boundary Conditions and Field Solution

On the surface of each perfectly conducting spheroid $\xi=\xi_A$ and $\xi'=\xi'_B$, the tangential components (η and ϕ) of the total electric field intensity must be equal to zero. Thus from (6.10) and (6.11) we get

$$(\overline{\mathbf{M}}^{(1)T}\,\overline{A} + \overline{\mathbf{M}}_{BA}^{(1)T}\,[\Delta]^T\,[R']\,\overline{B} + \overline{\mathbf{M}}_{BA}^{(1)T}\,[\Gamma]^T\,\overline{\beta} + \overline{\mathbf{M}}_{sA}^{(4)T}\,\overline{\alpha})\times\hat{\xi}\,|_{\xi=\xi_A} = 0 \qquad (6.12)$$

$$(\overline{\mathbf{M}}^{(1)T}\,\overline{B} + \overline{\mathbf{M}}_{AB}^{(1)T}\,[\Delta']^T\,[R]\,\overline{A} + \overline{\mathbf{M}}_{AB}^{(1)T}\,[\Gamma']^T\,\overline{\alpha} + \overline{\mathbf{M}}_{sB}^{(4)T}\,\overline{\beta})\times\hat{\xi}'\,|_{\xi'=\xi'_B} = 0 \qquad (6.13)$$

Taking the scalar product of both sides of (6.12) and (6.13) by $\begin{Bmatrix}\hat{\eta}\,l_\eta \\ \hat{\phi}\,l_\phi\end{Bmatrix} S_{m,|m|+\kappa}(h,\eta)\,e^{\pm j(m\pm1)\phi}$ and $\begin{Bmatrix}\hat{\eta}'\,l_{\eta'} \\ \hat{\phi}'\,l_{\phi'}\end{Bmatrix} S_{m,|m|+\kappa}(h',\eta')\,e^{\pm j(m\pm1)\phi'}$, respectively, for $m = \ldots -2, -1, 0, 1, 2, \ldots,$ $\kappa = 0, 1, 2, \ldots,$ with $l_\eta = 2jF\,(\xi_A^2-\eta^2)^{1/2}$, $l_{\eta'} = 2jF'(\xi_B'^2-\eta'^2)^{1/2}$, $l_\phi = 2F\,(\xi_A^2-\eta^2)$, and $l_{\phi'} = 2F'(\xi_B'^2-\eta'^2)$, integrating over ϕ and ϕ'

from 0 to 2π, and in η and η' from -1 to 1, and using the orthogonality properties of trigonometric functions and spheroidal angle functions, yields [31], [44], [57]

$$\begin{bmatrix} [Q_A] & [R_{BA}][\Gamma]^T \\ [R_{AB}][\Gamma']^T & [Q_B] \end{bmatrix} \begin{bmatrix} \bar{\alpha} \\ \bar{\beta} \end{bmatrix} = \begin{bmatrix} [R_A] & [R_{BA}][\Delta]^T [R'] \\ [R_{AB}][\Delta']^T [R] & [R_B] \end{bmatrix} \begin{bmatrix} \bar{A} \\ \bar{B} \end{bmatrix} \tag{6.14}$$

with $[R_A]$ and $[R_B]$ defined in Appendix E. The structure of the matrices $[Q_A]$ and $[R_{BA}]$ are the same as those of $[Q_{M1}]$ and $[R_{M21}]$, respectively, given in (3.73), but with the elements evaluated with respect to the unprimed coordinate system. The elements of $[Q_B]$ and $[R_{AB}]$ are obtained from the corresponding elements of $[Q_A]$ and $[R_{BA}]$, respectively, by evaluating them with respect to the primed coordinate system. Equation (6.14) can be rewritten in the form [45], [70]

$$\bar{S} = [G]\bar{I} \tag{6.15}$$

where

$$\bar{S} = \begin{bmatrix} \bar{\alpha} \\ \bar{\beta} \end{bmatrix}, \qquad \bar{I} = \begin{bmatrix} \bar{A} \\ \bar{B} \end{bmatrix} \tag{6.16}$$

$$[G] = \begin{bmatrix} [Q_A] & [R_{BA}][\Gamma]^T \\ [R_{AB}][\Gamma']^T & [Q_B] \end{bmatrix}^{-1} \begin{bmatrix} [R_A] & [R_{BA}][\Delta]^T [R'] \\ [R_{AB}][\Delta']^T [R] & [R_B] \end{bmatrix} \tag{6.17}$$

$[G]$ is the system matrix, which depends only on the geometry of the scattering system and frequency, being independent of the position of the voltage gaps along the antenna axes.

6.3 System Admittances and Far Field Patterns

For the two spheroidal dipole antennas A and B, the gap electric currents I_A and I_B corresponding to the gap voltages V_A and V_B, respectively, can be defined in terms

of an admittance matrix:

$$\begin{bmatrix} I_A \\ I_B \end{bmatrix} = \begin{bmatrix} Y_{AA} & Y_{AB} \\ Y_{BA} & Y_{BB} \end{bmatrix} \begin{bmatrix} V_A \\ V_B \end{bmatrix} \tag{6.18}$$

where

$$Y_{AA} = \left.\frac{I_A}{V_A}\right|_{V_B=0}, \qquad Y_{BB} = \left.\frac{I_B}{V_B}\right|_{V_A=0} \tag{6.19}$$

are the self admittances and

$$Y_{AB} = \left.\frac{I_A}{V_B}\right|_{V_A=0}, \qquad Y_{BA} = \left.\frac{I_B}{V_A}\right|_{V_B=0} \tag{6.20}$$

are the mutual admittances associated with A and B.

6.3.1 Calculation of the Mutual and Self Admittances

In order to calculate Y_{AB} and Y_{BB}, for instance, we let $V_A = 0$, such that all the elements of $\bar{A}$ are zero, which makes ${}_S\mathbf{E}_A = 0$. In this case the total electric field intensities seen from antennas A and B can be written from (6.10) and (6.11), respectively, as

$$\mathbf{E}_A = \overline{\mathbf{M}}_{BA}^{(1)T}\,[\Delta]^T\,[R']\,\bar{B} + \overline{\mathbf{M}}_{BA}^{(1)T}\,[\Gamma]^T\,\bar{\beta} + \overline{\mathbf{M}}_{sA}^{(4)T}\,\bar{\alpha} \tag{6.21}$$

$$\mathbf{E}_B = \overline{\mathbf{M}}^{(1)T}\,\bar{B} + \overline{\mathbf{M}}_{AB}^{(1)T}\,[\Gamma']^T\,\bar{\alpha} + \overline{\mathbf{M}}_{sB}^{(4)T}\,\bar{\beta} \tag{6.22}$$

Using Maxwell's equation

$$\mathbf{H} = j\,(\varepsilon/\mu)^{1/2}\,\frac{1}{k}\,(\nabla\times\mathbf{E}) \tag{6.23}$$

in which ε and μ are the permittivity and permeability, respectively, gives the total magnetic field intensities seen from antennas A and B,

$$\mathbf{H}_A = j\,(\varepsilon/\mu)^{1/2}\,(\overline{\mathbf{N}}_{BA}^{(1)T}\,[\Delta]^T\,[R']\,\bar{B} + \overline{\mathbf{N}}_{BA}^{(1)T}\,[\Gamma]^T\,\bar{\beta} + \overline{\mathbf{N}}_{sA}^{(4)T}\,\bar{\alpha}) \tag{6.24}$$

$$\mathbf{H}_B = j\,(\varepsilon/\mu)^{1/2}\,(\overline{\mathbf{N}}^{(1)T}\,\bar{B} + \overline{\mathbf{N}}_{AB}^{(1)T}\,[\Gamma']^T\,\bar{\alpha} + \overline{\mathbf{N}}_{sB}^{(4)T}\,\bar{\beta}) \tag{6.25}$$

The electric current I_A at the feed point of the antenna A is

$$\begin{aligned} I_A &= \int \mathbf{H}\cdot\mathbf{dl}\,\Big|_{\eta=0,\,\xi=\xi_A} \\ &= \int (\,{}_{\xi}H_A\,\hat{\xi} + {}_{\eta}H_A\,\hat{\eta} + {}_{\phi}H_A\,\hat{\phi})\cdot(h_\phi\, d\phi\,\hat{\phi})\,\Big|_{\eta=0,\,\xi=\xi_A} \\ &= F\,(\xi_A^2-1)^{1/2}\int_0^{2\pi} {}_{\phi}H_A\,(\xi_A,0,\phi)\,d\phi \end{aligned} \tag{6.26}$$

where h_ϕ is the scale factor and F the semi-interfocal distance of the spheroid A. Similarly, for the electric current I_B we can write

$$I_B = F'(\xi_B'^2-1)^{1/2}\int_0^{2\pi} {}_{\phi}H_B\,(\xi_B',0,\phi')\,d\phi' \tag{6.27}$$

where F' is the semi-interfocal distance of the spheroid B. Substituting ${}_{\phi}H_A$ from (6.24) in (6.26) and using

$${}_{\phi}N_{-1n}^{+(i)}(\xi_A,0,\phi) = -\,{}_{\phi}N_{1n}^{-(i)}(\xi_A,0,\phi) = 0.5jkR_{1n}^{(i)}S_{1n}, \qquad i=1,2,3,4 \tag{6.28}$$

where ${}_{\phi}N_{mn}$ denotes the ϕ–component of the vector wave functions $\mathbf{N}_{mn}$ defined in Appendix A, finally yields [71]

$$\begin{aligned} Y_{AB} = -(\varepsilon/\mu)^{1/2}(\pi h/V_B)(\xi_A^2-1)^{1/2}\Bigg[& \sum_{n=1}^{\infty} B_n^{>} \sum_{\nu=1}^{\infty} (C_1' Q'^{-1n}_{-1\nu} - C_2' Q'^{-1n}_{1\nu} + C_1'^{*} Q'^{1n}_{1\nu} - C_2'^{*} Q'^{1n}_{-1\nu}) \\ & . R_{1\nu}^{(1)} S_{1\nu} + \sum_{n=0}^{\infty} \beta_{-1,n+1}^{+} \sum_{\nu=1}^{\infty} (C_1' Q'^{-1,n+1}_{-1\nu} - C_2' Q'^{-1,n+1}_{1\nu}) R_{1\nu}^{(1)} S_{1\nu} \\ & + \beta_{0n}^{z} \sum_{\nu=1}^{\infty} (C_4' Q'^{0n}_{-1\nu} - C_4'^{*} Q'^{0n}_{1\nu}) R_{1\nu}^{(1)} S_{1\nu} + \sum_{m=0}^{\infty}\sum_{n=m}^{\infty} \Big\{ \beta_{mn}^{+} \sum_{\nu=1}^{\infty} (C_1' Q'^{mn}_{-1\nu} - C_2' Q'^{mn}_{1\nu}) R_{1\nu}^{(1)} S_{1\nu} \\ & + \beta_{m+1,n+1}^{z} \sum_{\nu=1}^{\infty} (C_4' Q'^{m+1,n+1}_{-1\nu} - C_4'^{*} Q'^{m+1,n+1}_{1\nu}) R_{1\nu}^{(1)} S_{1\nu} \Big\} \\ & + \sum_{m=0}^{\infty}\sum_{n=m}^{\infty} \Big\{ \beta_{-mn}^{-} \sum_{\nu=1}^{\infty} (C_2'^{*} Q'^{-mn}_{-1\nu} - C_1'^{*} Q'^{-mn}_{1\nu}) R_{1\nu}^{(1)} S_{1\nu} + \beta_{-(m+1),n+1}^{z} \\ & \sum_{\nu=1}^{\infty} (C_4' Q'^{-(m+1),n+1}_{-1\nu} - C_4'^{*} Q'^{-(m+1),n+1}_{1\nu}) R_{1\nu}^{(1)} S_{1\nu} \Big\} + \sum_{n=1}^{\infty} \alpha_{-1n}^{+} R_{1n}^{(4)} S_{1n} \Bigg] \end{aligned} \tag{6.29}$$

with the asterisk denoting the complex conjugate and

$$S_{1\nu} \equiv S_{1\nu}(h,0), \qquad R_{1\nu}^{(i)} \equiv R_{1\nu}^{(i)}(h,\xi_A), \qquad i=1,2,3,4 \tag{6.30}$$

C_i', $(i=1,2,3,4,5)$ and $B_n^>$ are defined in Appendix E and the rotational-translational coefficients $Q'^{mn}_{\mu\nu}$ are given in Appendix B. The coefficients α and β in (6.29) are the elements of the column matrices $\bar{\alpha}$ and $\bar{\beta}$, respectively. Substituting ${}_{\phi}H_B$ from (6.25) in (6.27), integrating and using (6.28) yields

$$\begin{aligned}
Y_{BB} = &-(\varepsilon/\mu)^{1/2}(\pi h'/V_B)(\xi_B'^2-1)^{1/2}\Bigg[\sum_{n=1}^{\infty} 2B_n R_{1n}^{(1)} S_{1n} + \sum_{n=1}^{\infty} \beta_{-1n}^{+} R_{1n}^{(4)} S_{1n} \\
&+ \sum_{n=0}^{\infty} \alpha_{-1,n+1}^{+} \sum_{\nu=1}^{\infty} (C_1 Q_{-1\nu}^{-1,n+1} - C_2 Q_{1\nu}^{-1,n+1}) R_{1\nu}^{(1)} S_{1\nu} \\
&+ \alpha_{0n}^{z} \sum_{\nu=1}^{\infty} (C_4 Q_{-1\nu}^{0n} - C_4^* Q_{1\nu}^{0n}) R_{1\nu}^{(1)} S_{1\nu} + \sum_{m=0}^{\infty} \sum_{n=m}^{\infty} \Big\{ \alpha_{mn}^{+} \sum_{\nu=1}^{\infty} (C_1 Q_{-1\nu}^{mn} - C_2 Q_{1\nu}^{mn}) R_{1\nu}^{(1)} S_{1\nu} \\
&+ \alpha_{m+1,n+1}^{z} \sum_{\nu=1}^{\infty} (C_4 Q_{-1\nu}^{m+1,n+1} - C_4^* Q_{1\nu}^{m+1,n+1}) R_{1\nu}^{(1)} S_{1\nu} \Big\} \\
&+ \sum_{m=0}^{\infty} \sum_{n=m}^{\infty} \Big\{ \alpha_{-mn}^{-} \sum_{\nu=1}^{\infty} (C_2^* Q_{-1\nu}^{-mn} - C_1^* Q_{1\nu}^{-mn}) R_{1\nu}^{(1)} S_{1\nu} \\
&+ \alpha_{-(m+1),n+1}^{z} \sum_{\nu=1}^{\infty} (C_4 Q_{-1\nu}^{-(m+1),n+1} - C_4^* Q_{1\nu}^{-(m+1),n+1}) R_{1\nu}^{(1)} S_{1\nu} \Big\} \Bigg]
\end{aligned} \tag{6.31}$$

where now

$$S_{1\nu} \equiv S_{1\nu}(h',0), \qquad R_{1\nu}^{(i)} \equiv R_{1\nu}^{(i)}(h',\xi_B'), \qquad i=1,2,3,4 \tag{6.32}$$

C_i, $(i=1,2,3,4,5)$ are defined in (2.16) and $Q_{\mu\nu}^{mn}$ and B_n are given in Appendixes B and E, respectively. Y_{BA} can be obtained from Y_{BB} by replacing the first summation in the expression of Y_{BB} by the summation

$$\sum_{n=1}^{\infty} A_n^> \sum_{\nu=1}^{\infty} (C_1 Q_{-1\nu}^{-1n} - C_2 Q_{1\nu}^{-1n} + C_1^* Q_{1\nu}^{1n} - C_2^* Q_{-1\nu}^{1n}) R_{1\nu}^{(1)} S_{1\nu}$$

and Y_{AA}, from Y_{AB} by replacing the first summation in the expression of Y_{AB} by the summation $\sum_{n=1}^{\infty} 2A_n R_{1n}^{(1)} S_{1n}$, with A_n and $A_n^>$ both given in Appendix E.

6.3.2 Far Field Patterns

If the spheroidal dipole antenna B is assumed to be parasitic, we have $V_B = 0$, and the expansion coefficients B_n are zero for all n. The total electric field at any given point in space is therefore given by

$$\mathbf{E}_A = {}_S\mathbf{E}_A + \mathbf{E}_{sA} + \mathbf{E}_{sB} \tag{6.33}$$

If all the field components are expanded in terms of appropriate vector spheroidal eigenfunctions, then by using their asymptotic expressions as $r \to \infty$, $r' \to \infty$, the electric field intensity in the far zone can be written in terms of spherical coordinates attached to the two antennas in the form [44], [57]

$$\mathbf{E} = \frac{e^{-jkr}}{r}\left[F_{\theta A}(\theta,\phi)\hat{\theta} + F_{\phi A}(\theta,\phi)\hat{\phi} + F_{\theta' B}(\theta',\phi')\hat{\theta}' + F_{\phi' B}(\theta',\phi')\hat{\phi}' \right] \tag{6.34}$$

where

$$F_{\theta A}(\theta,\phi) = -\sum_{m=0}^{\infty}\sum_{n=m}^{\infty}\frac{j^{n+1}}{2}S_{mn}(h,\cos\theta)\left\{(\alpha_{mn}^{+} - \alpha_{-mn}^{-})\cos(m+1)\phi \right.$$
$$\left. + j\,(\alpha_{mn}^{+} + \alpha_{-mn}^{-})\sin(m+1)\phi\right\} - \sum_{n=1}^{\infty}\frac{j^{n+1}}{2}S_{1n}(h,\cos\theta)\,(\alpha_{-1n}^{+} + 2A_n^{>}) \tag{6.35}$$

$$F_{\phi A}(\theta,\phi) = \sum_{m=0}^{\infty}\sum_{n=m}^{\infty} j^n \left[\frac{\cos\theta}{2} S_{mn}(h,\cos\theta)\left\{(\alpha_{mn}^{+} + \alpha_{-mn}^{-})\cos(m+1)\phi + j(\alpha_{mn}^{+} - \alpha_{-mn}^{-}) \right.\right.$$
$$\left. \cdot \sin(m+1)\phi\right\} - j\,\sin\theta\, S_{m+1,n+1}(h,\cos\theta)\left\{(\alpha_{m+1,n+1}^{z} + \alpha_{-(m+1),n+1}^{z})\right.$$
$$\left. \cdot \cos(m+1)\phi + j(\alpha_{m+1,n+1}^{z} - \alpha_{-(m+1),n+1}^{z})\sin(m+1)\phi\right\}\left.\right]$$
$$+\cos\theta\sum_{n=1}^{\infty}\frac{j^n}{2}S_{1n}(h,\cos\theta)\,\alpha_{-1n}^{+} - \sin\theta\sum_{n=0}^{\infty} j^n S_{0n}(h,\cos\theta)\,\alpha_{0n}^{z} \tag{6.36}$$

$F_{\theta' B}(\theta',\phi')$ and $F_{\phi' B}(\theta',\phi')$ in primed coordinates can be obtained from the expressions for $F_{\theta A}(\theta,\phi)$ and $F_{\phi A}(\theta,\phi)$, respectively. This is done by replacing α by β, $A_n^{>}$ by 0, and multiplying each expression by the phase factor $\exp(j\mathbf{k}_s\cdot\mathbf{d})$, with $\mathbf{k}_s$ being the

scattered wave vector in the far field. Expressing $\hat{\theta}'$ and $\hat{\phi}'$ in terms of $\hat{\theta}$ and $\hat{\phi}$, and using the relation between the primed and unprimed spherical coordinates, $\mathbf{E}$ can be written in terms of unprimed coordinates only as [45]

$$\mathbf{E} = \frac{e^{-jkr}}{r}\left[F_\theta(\theta,\phi)\hat{\theta} + F_\phi(\theta,\phi)\hat{\phi}\right] \tag{6.37}$$

The magnitude of this far field is

$$E = F(\theta,\phi)/r \tag{6.38}$$

where

$$F(\theta,\phi) = [\,|F_\theta(\theta,\phi)|^2 + |F_\phi(\theta,\phi)|^2]^{1/2} \tag{6.39}$$

The $E-$ plane pattern is obtained from (6.39) by plotting $F(\theta,\phi)$ versus θ. Numerical results are presented in the following section for $\phi = 0,\pi$ when the centers of the two spheroids are displaced along the x axis, and for $\phi = \pm\pi/2$ when they are displaced along the y axis. The $H-$ plane pattern is obtained by plotting $F(\theta,\phi)$ versus ϕ when $\theta = \pi/2$.

6.4 Numerical results

Computed results are presented for the real and imaginary parts of the mutual admittance of two spheroidal dipole antennas of arbitrary orientation and also for the $E-$ and $H-$ plane patterns of the same antennas when one of them is parasitic. Since all the matrices defined in Sections 6.2 and 6.3 are infinite in extent, it is necessary to truncate these series and matrices according to the required accuracy. All the computed results have been obtained with a two significant digit accuracy by considering the ϕ–harmonics e^{j0}, $e^{\pm j\phi}$, and $e^{\pm 2j\phi}$ only [57]. We take $n = |m|, |m|+1 \ldots |m|+3$ in truncating the matrices $[Q_A]$ and $[Q_B]$, and $n = |m|, |m|+1, \ldots |m|+5$ in truncating matrices $[\Gamma]$, $[\Gamma']$, $[\Delta]$, $[\Delta']$, $[R_{BA}]$, and $[R_{AB}]$, with m corresponding to the above

ϕ–harmonics. The truncation of matrices $[R_A]$ and $[R_B]$ is performed by retaining $n = 1, 2, 3, 4$. For truncating all the matrices we consider $\kappa = 0, 1, 2, 3$.

Fig. 6.2 shows the variation of the real part G_{AB} and the imaginary part B_{AB} of the mutual admittance $Y_{AB} = Y_{BA}$ for two spheroidal dipole antennas A and B, each of axial ratio 100, for an arbitrary orientation, as a function of the center to center distance d. The location of the center of B with respect to that of A is specified by the spherical coordinates $\theta_0 = 90°$, $\phi_0 = 0°$. As d varies from 0.5λ to 2.0λ, we observe an oscillatory behavior in the variation of both the real and imaginary parts of Y_{AB}, with the minima and maxima for the imaginary part being higher in magnitude than the corresponding ones for the real part. The accuracy of the numerical algorithm has also been checked by computing the real and imaginary parts of Y_{BA}. Detailed numerical experiments yield plots of G_{AB} for axial ratios between 10 and 100 which are practically the same and so are those of B_{AB}. For instance, in the case of an orientation specified by $\alpha = 60°$, $\beta = 45°$, and $\gamma = 60°$, the maximum relative difference for both G_{AB} and B_{AB} is 10%.

The mutual admittance for the special case of two parallel spheroidal antennas is calculated in [45] using the approximate one mode solution corresponding to the ϕ–harmonic e^{j0}. The numerical values are in agreement with those of the mutual admittance calculated for the same two dipole antennas with very small values of the three Euler angles, on the basis of the general analytical formulation presented in this chapter.

$E-$ and $H-$ plane patterns are presented in Figs. 6.3 and 6.4 for various orientations of the two spheroidal antennas A and B, with antenna A being excited and B

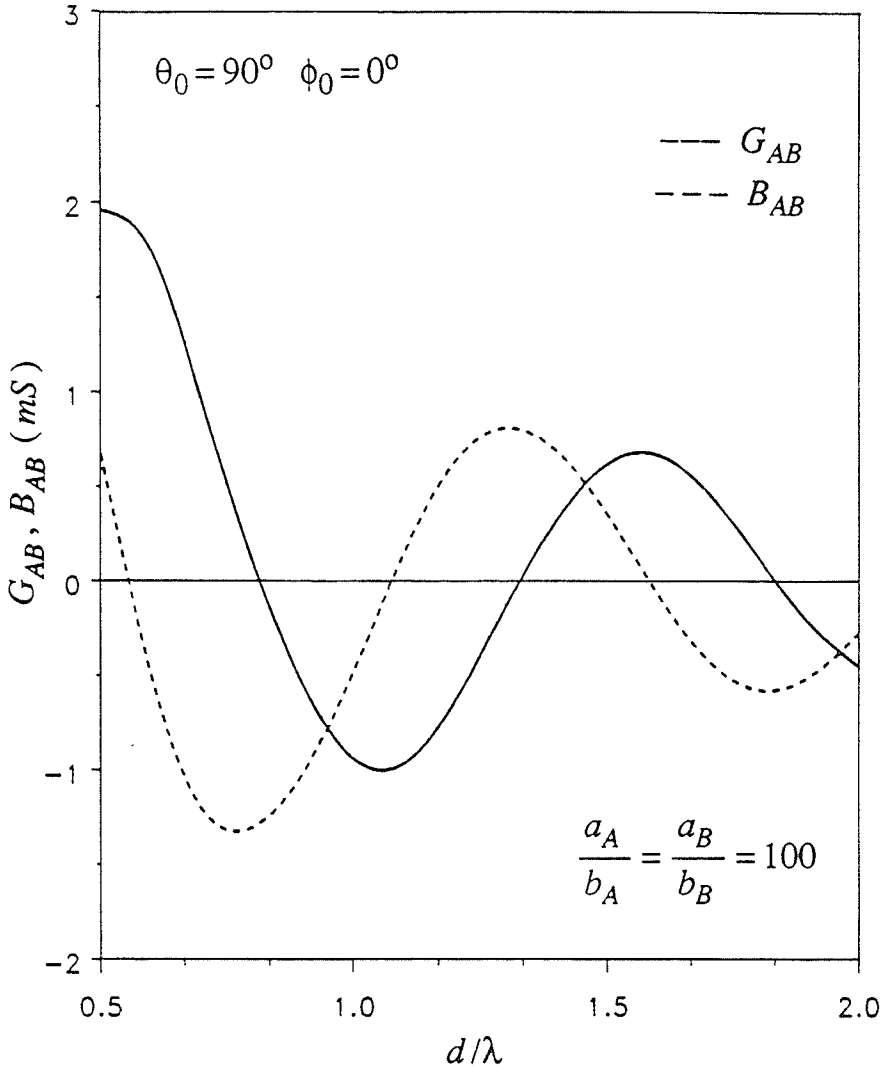

Fig. 6.2 Real and imaginary parts of the mutual admittance versus center to center distance for two antennas of semi-major axes $a_A = \lambda/4$, $a_B = 5\lambda/16$ and Euler angles $\alpha = 30^\circ$, $\beta = 45^\circ$, $\gamma = 90^\circ$.

parasitic, and the distance between the centers of the two fixed at 0.6λ. In Fig. 6.3 the centers of the two antennas are displaced along the y axis and in Fig. 6.4 along the x axis. Different $E-$ and $H-$ plane patterns are obtained by changing the Euler angle β, with the angles α and γ held fixed at 90° and 0°, respectively. The axes shown in Figs. 6.3 and 6.4 are those of the unprimed system of coordinates, attached to spheroid A. The pattern for any given orientation is drawn by normalizing the magnitude of F in (6.39) with respect to the maximum value of F out of the two plane patterns when the two antennas are parallel ($\beta = 0^\circ$).

As β increases from 0° to 90°, we observe an increase in the size of the back lobe compared to that of the front lobe, for both $E-$ plane patterns. When $\phi = 0^\circ$, the variation of the $E-$ plane patterns in Fig. 6.4 is somewhat regular with changing β, for $\theta \geq 40^\circ$, but curves start again intersecting each other around $\theta = 140^\circ$. All the $E-$ plane patterns shown in Fig. 6.4 are symmetrical about the x axis, but the same patterns in Fig. 6.3, when the axes of the elements A and B are in the same plane, do not present such symmetry. However the $H-$ plane patterns in Fig. 6.3 are symmetrical about the y axis and those in Fig. 6.4 are symmetrical about the x axis. For the $H-$ plane patterns we again observe an increase in the size of the back lobe compared to that of the front lobe for increasing β.

When $\beta = 0^\circ$, the $E-$ and $H-$ plane patterns in Fig. 6.3 are identical with the corresponding ones in Fig. 6.4, as expected. The front to back ratio for the patterns increases with decreasing β, the maximum being obtained for $\beta = 0^\circ$, in which case the two dipole antennas are parallel to each other. As expected, the worst coupling is when they are perpendicular to each other. It should be noted that in this case the minimum

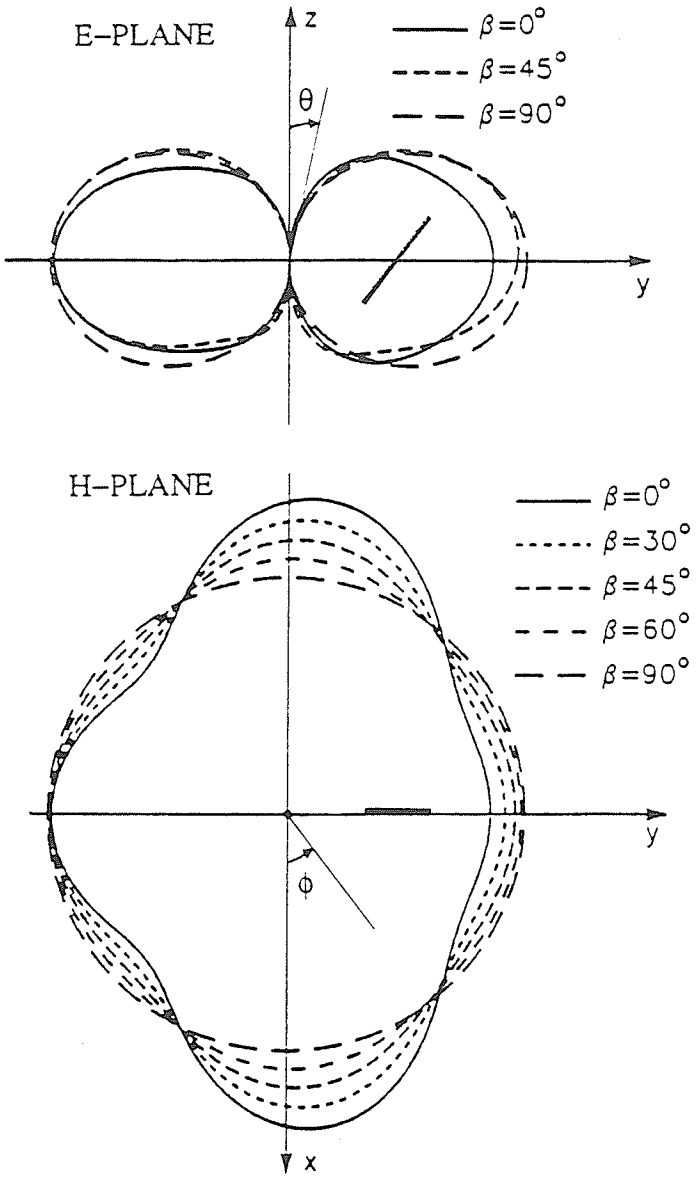

Fig. 6.3 Normalized $E-$ and $H-$ plane patterns for two spheroidal dipoles of axial ratio 100, with the semi-major axis lengths of the excited and parasitic dipoles of $\lambda/4$ and $5\lambda/16$, respectively, Euler angles $\alpha=90°$, $\gamma=0°$, and the centers displaced along the y axis by $d=0.6\lambda$.

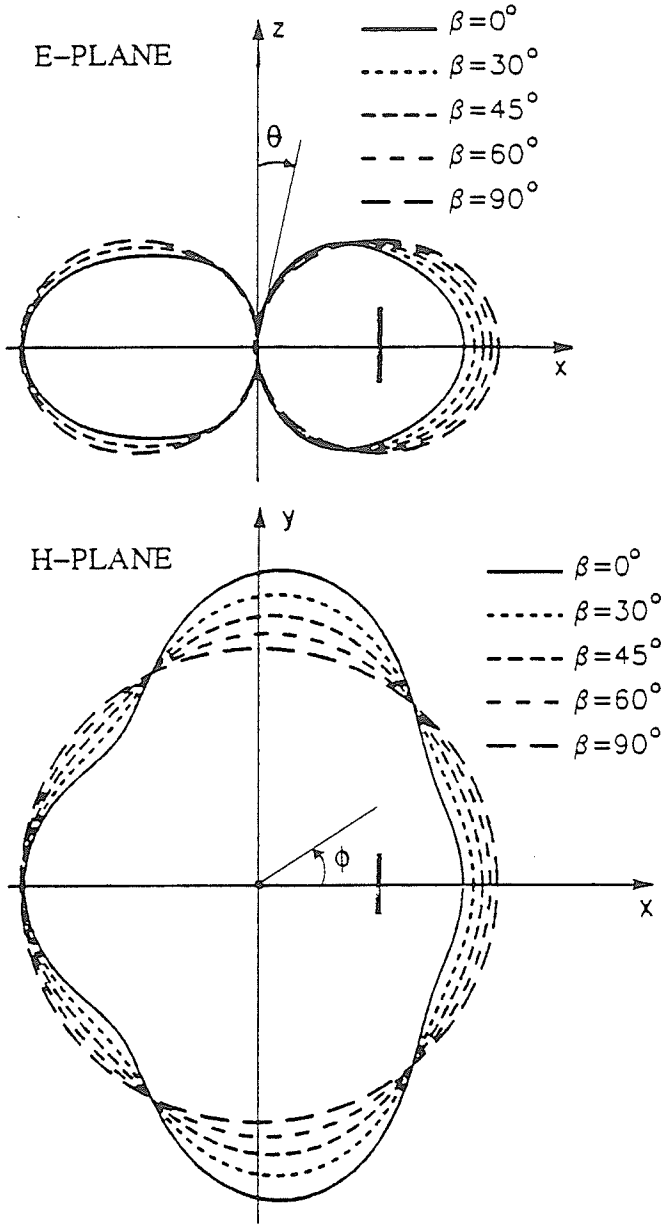

Fig. 6.4 Normalized $E-$ and $H-$ plane patterns for the two spheroidal dipoles in Fig. 6.3, with the centers displaced along the x axis by $d = 0.6\lambda$.

d for which the rotational-translational addition theorems are valid is equal to the greater of the two semi-major axes, i.e. $5\lambda/16$. The practical relevance of the work presented here consists in the fact that the reduction in the coupling between the two antennas for various relative orientations has been evaluated quantitatively.

CHAPTER 7

GENERAL CONCLUSIONS AND SUGGESTIONS FOR FUTURE RESEARCH

7.1 Discussion

The main objective of the thesis has been to provide analytical solutions to various problems involving electromagnetic scattering by spheroids of arbitrary orientation. These solutions are useful in analyzing models which have similar configurations for important engineering problems such as scattering of radar signals from hydrometeors, visible light absorption by heterogeneous particles, and also in biomedical engineering. Results obtained by the exact method developed here with a controllable accuracy are also important for evaluating the accuracy of other approximate methods and validating numerical codes which can be used for the analysis of electromagnetic scattering by similar configuration systems.

The formulation and analysis of all the problems are based on the rotational-translational addition theorems for vector spheroidal wave functions which are derived in this thesis. Rotational-translational addition theorems for the vector spheroidal wave functions $\mathbf{M}_{mn}^{a(i)}$, $\mathbf{N}_{mn}^{a(i)}$, $\mathbf{M}_{mn}^{\pm(i)}$, $\mathbf{N}_{mn}^{\pm(i)}$ $(a=x,y,z,\ i=1,2,3,4)$ as well as for $\mathbf{M}_{e,omn}^{r(i)}$ and $\mathbf{N}_{e,omn}^{r(i)}$ $(i=1,2,3,4)$ have been derived in Chapter 2. Translational addition theorems for vector spheroidal wave functions $\mathbf{M}_{mn}^{a(i)}$ and $\mathbf{N}_{mn}^{a(i)}$ $(a=x,y,z)$ have been deduced as special cases. Even though translational addition theorems and rotational addition theorems for vector spherical wave functions already exist in the literature [41], [42], they cannot be simply combined to obtain rotational-translational addition theorems for vector spherical wave functions. Thus new rotational-translational addition theorems

for vector spherical wave functions $\mathbf{m}_{mn}^{(i)}$ and $\mathbf{n}_{mn}^{(i)}$ have also been deduced as a special case. These theorems are useful in solving problems associated with spheres which do not have homogeneous material properties, such as spheres with different kinds of coatings on the surfaces, for instance, spheres whose material properties change with the spherical coordinate θ.

On the basis of the rotational-translational addition theorems for vector spheroidal wave functions $\mathbf{M}_{mn}^{\pm(i)}$, $\mathbf{N}_{mn}^{\pm(i)}$ $\mathbf{M}_{mn}^{z(i)}$, and $\mathbf{N}_{mn}^{z(i)}$ derived in Chapter 2, an exact solution of the problem of scattering of electromagnetic waves by a system of n lossless dielectric prolate spheroids of arbitrary orientation has been obtained in Chapter 3 for the first time. The exact boundary conditions are imposed by expanding the resultant field seen from a system of coordinates attached to each spheroid in terms of appropriate vector spheroidal eigenfunctions. The unknown coefficients in the series expansion of the scattered and transmitted electromagnetic fields are obtained by using a matrix formulation, in which the column matrix of the total transmitted and scattered field expansion coefficients is equal to the product of a matrix, which is generally known as the system matrix, and the column matrix of the known incident field expansion coefficients. As in the case of scattering by two spheroids with parallel major axes [44], [46], the system matrix has the special feature of being independent of the direction and polarization of the incident wave. This makes it possible to evaluate the unknown transmitted and scattered field expansion coefficients for various angles of incidence and for both TE and TM polarizations of the incident wave, using the same system matrix, which is a great advantage in numerical computations. Results of a prescribed accuracy, corresponding to a whole range of angles of incidence, are there-

fore calculated with a better computational efficiency as compared to those obtained by various numerical techniques, for instance, moment methods where the problem has to be solved for each angle of incidence separately.

The solution for the case of n perfectly conducting spheroids of arbitrary orientation is derived from that for n dielectric spheroids, by letting the dielectric constant (or the refractive index) of the material of each dielectric spheroid become very high (theoretically infinite). In this case, since the spheroids cannot sustain any electromagnetic fields inside them, there is no transmitted field present inside, and as a result the size of the system matrix reduces to half of that of the corresponding dielectric case. However, the system matrix still retains the special feature it possessed in the dielectric case. The solutions for the special case of scattering by two dielectric spheroids and by two perfectly conducting spheroids of arbitrary orientation are obtained directly from the general formulation for scattering by n spheroids of arbitrary orientation.

Numerical results are given in Chapter 4 in the form of plots of normalized bistatic cross sections in the $E-$ and $H-$ planes, and plots of normalized backscattering cross sections corresponding to scattering by two spheroids of arbitrary orientation. Spheroids of axial ratios 2 and 10 are considered in the perfectly conducting case, and spheroids of axial ratios 2 and 5 in the dielectric case, rotated with respect to each other in various configurations. In Chapter 5 we present an approximate method for solving the problem of scattering of a plane electromagnetic wave by two coaxial spheroids, with their centers displaced along the common axis, for oblique incidence. The formulation of the problem is based on the exact solution to scattering by a single spheroid. The greatest advantage of the method is to be able to reduce the amount of

computational time involved as compared to that of the exact method, and still obtain results of an acceptable accuracy. Numerical results are presented in the form of far field scattering cross sections. It is seen that this method gives acceptable results compared to those obtained by the exact solution, for spheroids of semi-major axes lengths up to $\lambda/2$ and for distances between the tips of the spheroids greater than 0.5λ. The agreement with the exact solution becomes better as the axial ratios of the spheroids become higher and/or the distance between their centers becomes larger.

Using the rotational-translational addition theorems for vector spheroidal wave functions, an analytic solution is obtained in Chapter 6, to the problem of electromagnetic coupling between two spheroidal dipole antennas in arbitrary configuration. Explicit expressions for the self and mutual admittances of a system of two such antennas are derived, and plots of real and imaginary parts of the mutual admittances have been presented to show their dependence on the distance between the two antennas. As well, the $E-$ and $H-$ plane patterns for two dipole antennas of different orientations and configurations having a fixed separation, with one antenna being parasitic, have been computed. It is seen from the $E-$ and $H-$ plane patterns that the coupling between the antennas is worst when they are perpendicular to each other, and that it is best when they are parallel to each other.

7.2 Recommendations for Future Research

The solution presented in this thesis for non-lossy dielectric spheroids can be extended to lossy dielectric spheroids. The major change in this case is due to the dielectric constant of the material of the spheroid becoming complex. As a result, in expanding the electromagnetic field transmitted inside the spheroid it becomes

necessary to use vector spheroidal wave functions with complex arguments. The rest of the formulation is similar to that in the case of scattering by non-lossy dielectric spheroids. It is also be possible to obtain the solution for a mixture of perfectly conducting and dielectric spheroids by imposing the proper boundary conditions, and the solution for imperfectly conducting spheroids or for spheroids with very thin coatings, by incorporating the surface impedance in the boundary conditions.

Another extension would be to consider scattering by two spheroids of arbitrary orientation, when the excitation is different from that of a plane wave, e.g. as that due to the field of an electric dipole. To formulate the problem for such a case it is necessary to know the expansion of the incident field in terms of spheroidal wave functions. Once this is known, the rest of the formulation is similar to the case of plane wave incidence.

It would also be important from a computational point of view to extend the approximate method we have proposed in Chapter 5 for solving the problem of scattering by two coaxial spheroids, to the more general case of two spheroids of arbitrary orientation.

LIST OF REFERENCES

[1] C. Niven, "On the conduction of heat in ellipsoids of revolution," *Phil. Roy. Soc. London, Ser. A*, vol. 171, part I, pp. 117–151, 1880.

[2] R. C. Maclaurin, "On the solution of the equation $(V^2+k^2)\phi=0$ in elliptic coordinates and their physical applications," *Trans. Camb. Phil. Soc.*, vol. 17, pp. 41–108, 1898.

[3] M. Abraham, "Die electrischen Schwingungen um einen stabförmigen Leiter, behandelt nach der Maxwell'schen Theorie," *Ann. Phys.*, vol. 66, pp. 435–472, 1898.

[4] L. J. Chu and J. A. Stratton, "Steady state solutions of electromagnetic field problems part III. Forced oscillations of a prolate spheroid," *J. Appl. Phys.*, vol. 12, pp. 241–248, 1941.

[5] R. M. Ryder, "The electrical oscillations of a perfectly conducting prolate spheroid," *J. Appl. Phys.*, vol. 13, pp. 327–343, 1942.

[6] L. Page and N. I. Adams Jr., "Electrical oscillations of a prolate spheroid," *Phys. Rev.*, vol. 53, pp. 819–831, 1938.

[7] C. Flammer, "The prolate spheroidal monopole antenna," *Tech. Rep. No. 22*, Stanford Research Institute, Stanford, Calif., 1954.

[8] E. C. Hatcher Jr. and A. Leitner, "Radiation from a point dipole located at the tip of a prolate spheroid," *J. Appl. Phys.*, vol. 25, no. 10, pp. 1250–1253, 1954.

[9] A. Leitner and R. D. Spence, "Effect of a circular ground plane on antenna radiation," *J. Appl. Phys.*, vol. 21, pp. 1001–1006, 1950.

[10] W. Kloepfer, *Theorie der Kreisscheibenantennen.* Diss. Aachen, 1952.

[11] C. Flammer, "The vector wave function solution of the diffraction of electromagnetic waves by circular disks and apertures, parts I and II," *J. Appl. Phys.*, vol. 24, no. 9, pp. 1218–1231, 1953.

[12] J. R. Wait, "Theories of prolate spheroidal antennas," *Radio Sci.*, vol. 1, no. 4, pp. 475–512, 1966.

[13] T. Oguchi, "Attenuation and phase rotation of radio waves due to rain: calculations at 19.3 and 34.8 GHz," *Radio Sci.*, vol. 8, no. 1, pp. 31–38, 1973.

[14] J. A. Morrison and M. J. Cross, "Scattering of a plane electromagnetic wave by axisymmetric raindrops," *Bell Syst. Tech. J.*, vol. 53, pp. 955–1019, 1974.

[15] R. Ruppin, "Calculation of electromagnetic energy absorption in prolate spheroids by the point matching method," *IEEE Microwave Theory and Tech.*, vol. MTT-26, no. 2, pp. 87–90, 1978.

[16] P. C. Waterman, "Matrix formulation of electromagnetic scattering," *Proc. IEEE*, vol. 53, no. 8, pp. 805–812, 1965.

[17] C. Warner and A. Hizal, "Scattering and depolarization of microwaves by spheroidal raindrops," *Radio Sci.*, vol. 11, no. 11, pp. 921–930, 1976.

[18] P. W. Barber and C. Yeh, "Scattering of electromagnetic waves by arbitrarily shaped dielectric bodies," *Appl. Opt.*, vol. 14, no. 12, pp. 2864–2872, 1975.

[19] P. W. Barber, "Resonance electromagnetic absorption by nonspherical dielectric objects," *IEEE Microwave Theory and Tech.*, Vol. MTT-25, no. 5, pp. 373–381, 1977.

[20] B. Peterson and S. Strom, "T matrix for electromagnetic scattering from an arbitrary number of scatterers and representation of E(3)," *Phys. Rev. D*, vol. 8, pp. 3661–3678, 1973.

[21] B. Peterson and S. Strom, "T matrix formulation of electromagnetic scattering from multilayered scatterers," *Phys. Rev. D*, vol. 10, pp. 2670–2684, 1974.

[22] K. K. Mei, "Unimoment method for solving antenna and scattering problems," *IEEE Trans. Antennas Propagat.*, vol. AP-22, pp. 760–766, 1974.

[23] K. K. Mei, J. F. Hunka, and S. K. Chang, "Recent developments at the unimoment method," in *Acoustic, Electromagnetic, and Elastic Wave Scattering - Focus on T-matrix Approach*, V. K. Varadan, V. V. Varadan, Eds. New York: Pergamon, 1980, pp. 485–505.

[24] V. Twersky, "Coherent electromagnetic waves in pair-correlated random distributions of aligned scatterers," *J. Math. Phys.*, vol. 19, pp. 215–230, 1978.

[25] V. K. Varadan, V. N. Bringi, and V. V. Varadan, "Coherent electromagnetic wave propagation through randomly distributed dielectric scatterers," *Phys. Rev. D*, vol. 19, pp. 2480–2489, 1979.

[26] V. V. Varadan and V. K. Varadan, "Multiple scattering of electromagnetic waves by randomly distributed and oriented dielectric scatterers," *Phys. Rev. D*, vol. 21, pp. 388–394, 1980.

[27] V. Twersky, "Lattice sums and scattering coefficients for rectangular planar arrays," *J. Math. Phys.*, vol. 16, pp. 644–657, 1975.

[28] C. Flammer, *Spheroidal Wave Functions*. Stanford Univ. Press, Stanford, Calif., 1957.

[29] J. A. Stratton, P. M. Morse, L. J. Chu, and F. J. Corbarto, *Spheroidal Wave Functions*. John Wiley & Sons, Inc., New York, 1956.

[30] F. V. Schultz, "Scattering by a prolate spheroid," *Rep. VMM-42*, Willow Run Research Center (Univ. of Michigan), Ann Arbor, Michigan, 1950.

[31] K. M. Siegel, F. V. Schultz, B. H. Gere, and F. B. Sleator, "The theoretical and numerical determination of the radar cross section of a prolate spheroid," *IRE Trans. Antennas Propagat.*, vol. AP-4, no. 3, pp. 266–275, 1956.

[32] T. B. A. Senior, "Axial backscattering by a prolate spheroid," *IEEE Trans. Antennas Propagat.*, vol. AP-15, no. 4, pp. 587–588, 1967.

[33] C. D. Taylor, "On the exact theory of a prolate spheroidal receiving and scattering antenna," *Radio Sci.*, vol. 2, no. 3, pp. 351–360, 1967.

[34] N. Reitilinger, "Scattering of a plane wave incident on a prolate spheroid at an arbitrary angle," *Memo No.* 2868–506–*M*, Radiation Laboratory, Univ. of Michigan, Ann Arbor, Michigan, 1957.

[35] B. P. Sinha and R. H. MacPhie, "Electromagnetic scattering by prolate spheroids for plane waves with arbitrary polarization and angle of incidence," *Radio Sci.*, vol. 12, no. 2, pp. 171–184, 1977.

[36] J. Dalmas, "Diffusion d'une onde électromagnétique par un ellipsoïde de révolution allongé de conduction," *Optica Acta*, vol. 28, no. 7, pp. 933–948, 1981.

[37] J. Dalmas, "Indicatrices de diffusion d'un ellipsoïde revolution allongé, de conduction infinie, en incidence oblique," *Optica Acta*, vol. 28, no. 9, pp. 1277–1287, 1981.

[38] S. Asano and G. Yamamoto, "Light scattering by a spheroidal particle," *Appl. Opt.*, vol. 14, no. 1, pp. 29–49, 1975.

[39] A. Sebak and L. Shafai, "Electromagnetic scattering by spheroidal objects with impedance boundary conditions at axial incidence," *Radio Sci.*, vol. 23, no. 6, pp. 1048–1060, 1988.

[40] B. Friedman and J. Russek, "Addition theorems for spherical waves," *Quart. Appl. Math.*, vol. 12, no. 1, pp. 13–23, 1954.

[41] S. Stein, "Addition theorems for spherical wave functions," *Quart. Appl. Math.*, vol. 19, no. 1, pp. 15–24, 1961.

[42] O. R. Cruzan, "Translational addition theorems for spherical vector wave functions," *Quart. Appl. Math.*, vol. 20, no. 1, pp. 33–40, 1962.

[43] B. P. Sinha and R. H. MacPhie, "Translational addition theorems for spheroidal scalar and vector wave functions," *Quart. Appl. Math.*, vol. 38, no. 2, pp. 143–158, 1980.

[44] B. P. Sinha and R. H. MacPhie, "Electromagnetic plane wave scattering by a system of two parallel conducting prolate spheroids," *IEEE Trans. Antennas Propagat.*, vol. AP-31, no. 2, pp. 294–304, 1983.

[45] B. P. Sinha and R. H. MacPhie, "Mutual admittance characteristics for two-element parallel prolate spheroidal antenna systems," *IEEE Trans. Antennas Propagat.*, vol. AP-33, no. 11, pp. 1255–1263, 1985.

[46] M. F. R. Cooray, I. R. Ciric, and B. P. Sinha, "Electromagnetic scattering by a system of two parallel dielectric prolate spheroids," *Can. J. Phys.*, vol. 68, 1990, (in press).

[47] J. Dalmas and R. Deleuil, "Translational addition theorems for prolate spheroidal vector wave functions $\mathbf{M}^r$ and $\mathbf{N}^r$," *Quart. Appl. Math.*, vol. 44, no. 2, pp. 213–222, 1986.

[48] J. Dalmas and R. Deleuil, "Diffusion multiple des ondes électromagnétiques par des ellipsoïdes de révolution allongés," *Optica Acta*, vol. 29, no. 8, pp. 1117–1131, 1982.

[49] J. Dalmas and R. Deleuil, "Multiple scattering of electromagnetic waves from two infinitely conducting prolate spheroids which are centered in a plane perpendicular to their axes of revolution," *Radio Sci.*, vol. 20, no. 3, pp. 575–581, 1985.

[50] J. Dalmas and R. Deleuil, "Diffusion d'une onde électromagnétique par un ellipsoïde de révolution allongé et par un demi-ellipsoïde posé sur un plan en incidence axiale," *Optica Acta*, vol. 27, no. 5, pp. 637–649, 1980.

[51] R. H. MacPhie, J. Dalmas, and R. Deleuil, "Rotational-translational addition theorems for scalar spheroidal wave functions," *Quart. Appl. Math.*, vol. 44, no. 4, pp. 737–749, 1987.

[52] A. R. Edmonds, *Angular Momentum in Quantum Mechanics*. 3rd printing. Princeton Univ. Press, Princeton, NJ, 1974.

[53] J. A. Stratton, *Electromagnetic Theory*. McGraw-Hill, NY, 1941.

[54] M. F. R. Cooray and I. R. Ciric, "Addition theorems for electromagnetic wave scattering by spheroids of arbitrary orientation," in *Digest 1988 IEEE AP-S Symp.*, Syracuse, NY, 1988.

[55] M. F. R. Cooray and I. R. Ciric, "Rotational-translational addition theorems for vector spheroidal wave functions," *Compel*, vol. 8, no. 3, pp. 151–166, 1989.

[56] J. Dalmas, R. Deleuil, and R. H. MacPhie, "Rotational-translational addition theorems for spheroidal vector wave functions," *Quart. Appl. Math.*, vol. 47, pp. 351–364, 1989.

[57] M. F. R. Cooray and I. R. Ciric, "Electromagnetic wave scattering by a system of two spheroids of arbitrary orientation," *IEEE Trans. Antennas Propagat.*, vol. 37, no. 5, pp. 608–618, 1989.

[58] M. F. R. Cooray and I. R. Ciric, "Scattering of electromagnetic waves by a system of two conducting spheroids of arbitrary orientation," in *Radar Cross Sections of Complex Objects*, W. Ross Stone, Ed. pp. 342–355, IEEE Book Press, New York, NY, 1989

[59] M. F. R. Cooray and I. R. Ciric, "Radar cross sections for two dielectric spheroids in arbitrary configuration," in *Digest 1989 IEEE AP-S Symp.*, San Jose, CA, 1989.

[60] M. F. R. Cooray and I. R. Ciric, "Analytic solution for electromagnetic scattering by spheroids with non-parallel axes," in *Proc. ANTEM Symp.*, Winnipeg, Manitoba, 1988.

[61] M. F. R. Cooray and I. R. Ciric, "Radar cross sections for two conducting spheroids of arbitrary orientation," in *Proc. ANTEM Symp.*, Winnipeg, Manitoba, 1988.

[62] A. K. Hamid, I. R. Ciric, and M. Hamid, "Multiple scattering by a linear array of conducting spheres," *Can. J. Phys.*, (accepted).

[63] S. N. Karp and A. Russek, "Diffraction by a wide slit," *J. Appl. Phys.*, vol. 27, pp. 886-894, 1956.

[64] A. Z. Elsherbeni, *Diffraction by Two Conducting Wedges*, Ph.D. Thesis, Department of Electrical Engineering, University of Manitoba, Winnipeg, Manitoba, Canada, 1986.

[65] H. A. Ragheb, *Simulation of Cylindrical Reflector Antennas*, Ph.D. Thesis, Department of Electrical Engineering, University of Manitoba, Winnipeg, Manitoba, Canada, 1987.

[66] L. Infeld, "The influence of the width of the gap upon the theory of antennas," *Quart. Appl. Math.*, vol. 5, pp. 113-132, 1947.

[67] S. A. Schelkunoff, *Advanced Antenna Theory*. Wiley, NY, 1952.

[68] W. L. Weeks, *Electromagnetic Theory for Engineering Applications*. Wiley, NY, 1964.

[69] R. E. Collin and F. Zucker, *Antenna Theory Part I*. McGraw-Hill, NY, 1969.

[70] M. F. R. Cooray and I. R. Ciric, "Interaction between two prolate spheroidal antennas in arbitrary configuration," in *Proc. URSI Symp. EM Theory*, Stockholm, Sweden, 1988.

[71] I. R. Ciric and M. F. R. Cooray, "Admittance characteristics and far field patterns for coupled spheroidal dipole antennas in arbitrary configuration," *Proc. Inst. Elect. Eng. Part H*, (accepted).

[72] P. M. Morse and H. Feshbach, *Methods of Mathematical Physics*. Mc-Graw Hill, NY, 1953.

APPENDIX A

PROLATE SPHEROIDAL WAVE FUNCTIONS

In this Appendix we give explicit expressions of the spheroidal scalar wave function, the spheroidal angle function and the spheroidal radial functions. Also defined here are the different types of vector spheroidal wave functions.

A.1 Spheroidal Scalar Wave Function

The relation between the Cartesian coordinates x,y,z and spheroidal coordinates ξ,η,ϕ is as follows:

$$\begin{aligned} x &= F(1-\eta^2)^{1/2}(\xi^2-1)^{1/2}\cos\phi \\ y &= F(1-\eta^2)^{1/2}(\xi^2-1)^{1/2}\sin\phi \\ z &= F\xi\eta \end{aligned} \tag{A.1}$$

where F is the semi-interfocal distance, and $-1\le\eta\le 1$, $1\le\xi<\infty$, $0\le\phi\le 2\pi$. The differential equation

$$\nabla^2\psi + k^2\psi = 0 \tag{A.2}$$

known as the scalar wave equation, is separable in eleven orthogonal coordinate systems out of which the prolate spheroidal system is one. By using the method of separation of variables, the solution of (A.2) can be written as [28]

$$\psi_{\substack{e\\o}mn}(h;\xi,\eta,\phi) = R_{mn}(h,\xi)\,S_{mn}(h,\eta)\begin{matrix}\cos\\ \sin\end{matrix} m\phi \tag{A.3}$$

The functions $R_{mn}(h,\xi)$ and $S_{mn}(h,\eta)$ are known as spheroidal radial functions and spheroidal angle functions, respectively, and they satisfy the ordinary differential equations

$$\frac{d}{d\xi}\left[(\xi^2-1)\frac{d}{d\xi}R_{mn}(h,\xi)\right]-\left[\lambda_{mn}-h^2\xi^2+\frac{m^2}{\xi^2-1}\right]R_{mn}(h,\xi)=0 \qquad (A.4)$$

and

$$\frac{d}{d\eta}\left[(1-\eta^2)\frac{d}{d\eta}S_{mn}(h,\eta)\right]+\left[\lambda_{mn}-h^2\eta^2-\frac{m^2}{1-\eta^2}\right]S_{mn}(h,\eta)=0 \qquad (A.5)$$

In these equations λ_{mn} and m are separation constants; λ_{mn} being a function of $h\ (=kF)$. The discrete values of λ_{mn} $(n=m,m+1,m+2,\ldots)$, for which the differential equation (A.5) gives solutions that are finite at $\eta=\pm1$ are the desired eigenvalues, the value of m being an integer which includes zero, and $n\geq m$ [28].

A.2 Spheroidal Angle Functions

The spheroidal angle functions are the associated eigenfunctions $S_{mn}(h,\eta)$ corresponding to the eigenvalues $\lambda_{mn}(h)$ of (A.5). There are two kinds of angle functions, $S_{mn}^{(1)}(h,\eta)$, which is known as the angle function of the first kind and $S_{mn}^{(2)}(h,\eta)$, which is known as the angle function of the second kind. Out of these it is $S_{mn}^{(1)}(h,\eta)$ that is used frequently in physical problems, since it is regular throughout the interval $-1\leq\eta\leq1$. Hence we simplify the notation by writing $S_{mn}(h,\eta)$ to mean the angle function of the first kind.

$S_{mn}(h,\eta)$ can be expressed in the form of an infinite series of associated Legendre functions of the first kind as [28], [72]

$$S_{mn}(h,\eta)=\sum_{r=0,1}^{\infty}{}'\,d_r^{mn}(h)\,P_{m+r}^{m}(\eta) \qquad (A.6)$$

in which the prime over the Σ indicates that the summation is over only even values of r, when $(n-m)$ is even and over only odd values of r, when $(n-m)$ is odd. $d_r^{mn}(h)$ are the spheroidal expansion coefficients.

An important property of angle functions is the orthogonality in the interval $-1 \le \eta \le 1$, which results from the theory of Sturm – Liouville differential equations. Thus

$$\int_{-1}^{1} S_{mn}(\eta)\, S_{mn'}(\eta)\, d\eta = \delta_{nn'} N_{mn} \tag{A.7}$$

where $\delta_{nn'}$ is the Kronecker delta function, and

$$N_{mn} = 2 \sum_{r=0,1}^{\infty}{}' \frac{(r+2m)!\,(d_r^{mn})^2}{(2r+2m+1)\,r!} \tag{A.8}$$

is the normalization constant.

A.3 Spheroidal Radial Functions

The spheroidal radial functions are the solutions of the differential equation (A.4). The range of the coordinate ξ is $1 \le \xi < \infty$ and the eigenvalues λ_{mn} which occur in (A.4) are those to which the angle functions $S_{mn}(h,\eta)$ belong.

In physical problems one usually requires both spheroidal radial functions of the first kind $R_{mn}^{(1)}(h,\xi)$ and the second kind $R_{mn}^{(2)}(h,\xi)$, which are independent solutions of (A.4). The third and fourth kind of functions $R_{mn}^{(3)}(h,\xi)$ and $R_{mn}^{(4)}(h,\xi)$ however are a linear combination of $R_{mn}^{(1)}(h,\xi)$ and $R_{mn}^{(2)}(h,\xi)$.

Similar to the spheroidal angle functions, the spheroidal radial functions $R_{mn}^{(1)}(h,\xi)$ and $R_{mn}^{(2)}(h,\xi)$ can also be expanded as the sum of an infinite series given by [29], [72]

$$R_{mn}^{(1)}(h,\xi) = \left[\frac{\xi^2-1}{\xi^2}\right]^{m/2} \sum_{r=0,1}^{\infty}{}' a_r^{mn}(h)\, j_{m+r}(h\xi) \tag{A.9}$$

and

$$R_{mn}^{(2)}(h,\xi) = \left[\frac{\xi^2-1}{\xi^2}\right]^{m/2} \sum_{r=0,1}^{\infty}{}' a_r^{mn}(h)\, n_{m+r}(h\xi) \tag{A.10}$$

where j_{m+r} and n_{m+r} are spherical Bessel and spherical Neumann functions, respectively, and $a_r^{mn}(h)$ are the expansion coefficients.

The spheroidal radial functions of the third and fourth kind are given by

$$R_{mn}^{(3)}(h,\xi) = R_{mn}^{(1)}(h,\xi) + j\, R_{mn}^{(2)}(h,\xi) \tag{A.11}$$

and

$$R_{mn}^{(4)}(h,\xi) = R_{mn}^{(1)}(h,\xi) - j\, R_{mn}^{(2)}(h,\xi) \tag{A.12}$$

respectively. The asymptotic behavior of $R_{mn}^{(1)}(h,\xi)$, $R_{mn}^{(2)}(h,\xi)$, $R_{mn}^{(3)}(h,\xi)$, and $R_{mn}^{(4)}(h,\xi)$ is readily obtained by the asymptotic behavior of the spherical Bessel and Neumann functions as $h\xi \to \infty$, and is given by

$$R_{mn}^{(1)}(h,\xi) \to \frac{1}{h\xi}\cos\left[h\xi - (n+1)\pi/2\right] \tag{A.13}$$

$$R_{mn}^{(2)}(h,\xi) \to \frac{1}{h\xi}\sin\left[h\xi - (n+1)\pi/2\right] \tag{A.14}$$

$$R_{mn}^{(3)}(h,\xi) \to \frac{1}{h\xi}\, e^{j[h\xi - (n+1)\pi/2]} \tag{A.15}$$

$$R_{mn}^{(4)}(h,\xi) \to \frac{1}{h\xi}\, e^{-j[h\xi - (n+1)\pi/2]} \tag{A.16}$$

From the above expressions of $R_{mn}^{(3)}(h,\xi)$ and $R_{mn}^{(4)}(h,\xi)$ it is evident that they have the properties of diverging spherical waves at large distances from the spheroid.

A.4 Spheroidal Vector Wave Functions

By the application of vector differential operators to the scalar spheroidal wave function given in (A.3), it is possible to obtain the vector spheroidal wave functions **M**

and $\mathbf{N}$ as [28]

$$\mathbf{M}_{mn} = \nabla\psi_{mn} \times \boldsymbol{a} \tag{A.17}$$

$$\mathbf{N}_{mn} = k^{-1}(\nabla \times \mathbf{M}_{mn}) \tag{A.18}$$

in which $\boldsymbol{a}$ is either an arbitrary constant unit vector or the position vector $\mathbf{r}$. None of the coordinate unit vectors $\hat{\xi}, \hat{\eta}$, or $\hat{\phi}$ in the spheroidal coordinate system, has the properties required for $\boldsymbol{a}$. Hence the Cartesian system is used, as it has the properties required for $\boldsymbol{a}$ and also since the transformation from Cartesian to spheroidal system is known.

The three Cartesian unit vectors $\hat{\mathbf{x}}$, $\hat{\mathbf{y}}$, and $\hat{\mathbf{z}}$ generate three distinct classes of spheroidal vector wave functions $\mathbf{M}$ and $\mathbf{N}$, viz.,

$$\mathbf{M}_{\substack{e\\o}mn}^{p(i)}(h;\xi,\eta,\phi) = \nabla\psi_{\substack{e\\o}mn}^{(i)}(h;\xi,\eta,\phi) \times \hat{\mathbf{p}}, \quad p = x, y, z \tag{A.19}$$

and

$$\mathbf{N}_{\substack{e\\o}mn}^{p(i)}(h;\xi,\eta,\phi) = k^{-1}\left[\nabla \times \mathbf{M}_{\substack{e\\o}mn}^{p(i)}(h;\xi,\eta,\phi)\right], \quad p = x, y, z \tag{A.20}$$

in which e and o refer to the even and odd functions respectively. Explicit expressions of these spheroidal vector wave functions are available in [28]. In the functions $\mathbf{M}_{\substack{e\\o}mn}^{x(i)}$, $\mathbf{M}_{\substack{e\\o}mn}^{y(i)}$ $\mathbf{N}_{\substack{e\\o}mn}^{x(i)}$, and $\mathbf{N}_{\substack{e\\o}mn}^{y(i)}$ the ϕ–dependence of various components is equal to the product of $\cos\phi$ or $\sin\phi$ with either $\cos m\phi$ or $\sin m\phi$. It is convenient therefore to define the following additional vector wave functions where the components labeled with the index $m+1$ have either a $\cos(m+1)\phi$ or $\sin(m+1)\phi$ ϕ–dependence, while the components of those labeled with $m-1$ have either a $\cos(m-1)\phi$ or $\sin(m-1)\phi$, ϕ–dependence [28].

$$\mathbf{M}^{+(i)}_{\substack{e\\o}m+1,n}(h;\xi,\eta,\phi)=\frac{1}{2}\left[\mathbf{M}^{x(i)}_{\substack{e\\o}mn}(h;\xi,\eta,\phi)\mp\mathbf{M}^{y(i)}_{\substack{o\\e}mn}(h;\xi,\eta,\phi)\right] \tag{A.21}$$

$$\mathbf{M}^{-(i)}_{\substack{e\\o}m-1,n}(h;\xi,\eta,\phi)=\frac{1}{2}\left[\mathbf{M}^{x(i)}_{\substack{e\\o}mn}(h;\xi,\eta,\phi)\pm\mathbf{M}^{y(i)}_{\substack{o\\e}mn}(h;\xi,\eta,\phi)\right] \tag{A.22}$$

$$\mathbf{N}^{+(i)}_{\substack{e\\o}m+1,n}(h;\xi,\eta,\phi)=\frac{1}{2}\left[\mathbf{N}^{x(i)}_{\substack{e\\o}mn}(h;\xi,\eta,\phi)\mp\mathbf{N}^{y(i)}_{\substack{o\\e}mn}(h;\xi,\eta,\phi)\right] \tag{A.23}$$

$$\mathbf{N}^{-(i)}_{\substack{e\\o}m-1,n}(h;\xi,\eta,\phi)=\frac{1}{2}\left[\mathbf{N}^{x(i)}_{\substack{e\\o}mn}(h;\xi,\eta,\phi)\pm\mathbf{N}^{y(i)}_{\substack{o\\e}mn}(h;\xi,\eta,\phi)\right] \tag{A.24}$$

Explicit expressions for $\mathbf{M}^{+(i)}_{\substack{e\\o}m+1,n}$, $\mathbf{M}^{-(i)}_{\substack{e\\o}m-1,n}$, $\mathbf{N}^{+(i)}_{\substack{e\\o}m+1,n}$, and $\mathbf{N}^{-(i)}_{\substack{e\\o}m-1,n}$ are also given in [28]. As shown in [44], it is possible to express the sinusoidal variation of ϕ present in the above vector spheroidal wave functions $\mathbf{M}$ and $\mathbf{N}$ as an exponential variation, but with $\mathbf{M}^{+(i)}_{m+1,n}$, $\mathbf{M}^{-(i)}_{m-1,n}$, $\mathbf{N}^{+(i)}_{m+1,n}$, and $\mathbf{N}^{-(i)}_{m-1,n}$ in [28] being denoted by $\mathbf{M}^{+(i)}_{mn}$, $\mathbf{M}^{-(i)}_{mn}$, $\mathbf{N}^{+(i)}_{mn}$, and $\mathbf{N}^{-(i)}_{mn}$, respectively, so that $\mathbf{M}^{\pm(i)}_{mn}$ and $\mathbf{N}^{\pm(i)}_{mn}$ have $\exp[j(m\pm1)\phi]$ $\phi-$ dependence. It is these vector wave functions that we have used throughout this thesis. All the spheroidal wave functions described above are for a prolate spheroidal system. The corresponding functions for the oblate spheroidal system can be obtained from those for the prolate spheroidal system by the transformation $\xi\rightarrow j\xi$ and $h\rightarrow -jh$ (or $F\rightarrow -jF$).

APPENDIX B

THE ROTATIONAL-TRANSLATIONAL COEFFICIENTS AND THE ASSOCIATED MATRICES

The rotational-translational coefficients ${}^{(i)}Q_{\mu\nu}^{mn}(\alpha,\beta,\gamma;\mathbf{d})$ and $P_{\mu\nu}^{mn}(\alpha,\beta,\gamma;\mathbf{d})$ given in eqs. (2.1) and (2.2) are those obtained in [51]:

$$
{}^{(i)}Q_{\mu\nu}^{mn}(\alpha,\beta,\gamma;\mathbf{d}) = \sum_{s=|m|,|m|+1}^{\infty}{}' d_{s-|m|}^{mn}(h) \sum_{\bar{\mu}=-s}^{s} R_{\bar{\mu}s}^{ms}(\alpha,\beta,\gamma)
$$

$$
\cdot \sum_{l=|\mu|,|\mu|+1}^{\infty}{}' {}^{(i)}a_{\mu l}^{\bar{\mu}s}(\mathbf{d})\, j^{s-n+\nu-l} \frac{\cdot N_{\mu l}}{N_{\mu\nu}(h')} d_{l-|\mu|}^{\mu\nu}(h') \qquad \text{(B.1)}
$$

$$
P_{\mu\nu}^{mn}(\alpha,\beta,\gamma;\mathbf{d}) = \sum_{s=|m|,|m|+1}^{\infty}{}' d_{s-|m|}^{mn}(h) \sum_{\bar{\mu}=-s}^{s} R_{\bar{\mu}s}^{ms}(\alpha,\beta,\gamma)
$$

$$
\cdot \sum_{p=|\mu|,|\mu|+1}^{\infty}{}' b_{\mu p}^{\bar{\mu}s}(\mathbf{d})\, j^{s-n+\nu-p} \frac{\cdot N_{\mu p}}{N_{\mu\nu}(h')} d_{p-|\mu|}^{\mu\nu}(h') \qquad \text{(B.2)}
$$

in which $d_q^{mn}(h)$, $d_q^{\mu\nu}(h')$ are the spheroidal expansion coefficients, and $N_{\mu\nu}(h')$ is the normalization constant [28]. In these expressions the following notation is used:

$$
\cdot N_{ml} = \frac{2}{(2l+1)} \frac{(l+m)!}{(l-m)!} \qquad \text{(B.3)}
$$

$$
R_{m'l}^{ml}(\alpha,\beta,\gamma) = (-1)^{m'-m} \left[\frac{\cdot N_{ml}}{\cdot N_{m'l}} \right]^{1/2} e^{jm'\gamma} d_{m'm}^{(l)}(\beta)\, e^{jm\alpha} \qquad \text{(B.4)}
$$

$$
d_{m'm}^{(l)}(\beta) = \left[\frac{(l+m')!\,(l-m')!}{(l+m)!\,(l-m)!} \right]^{1/2} \left(\cos\frac{\beta}{2}\right)^{m'+m} \left(\sin\frac{\beta}{2}\right)^{m'-m}
$$

$$
\cdot P_{l-m'}^{(m'-m,\,m'+m)}(\cos\beta) \qquad \text{(B.5)}
$$

with $P_{l-m'}^{(m'-m,\,m'+m)}(\cos\beta)$ being the Jacobi polynomial of argument $\cos\beta$;

$$ {}^{(i)}a_{\mu l}^{\bar{\mu}s}(\mathbf{d}) = (-1)^{\mu} \sum_{p=p_0,p_0+1}^{l+s}{}' j^{l+p-s}\,(2l+1)\,a(\bar{\mu},s|-\mu,l|p)\cdot\psi_{\bar{\mu}-\mu,p}^{(i)}(\mathbf{d}) \tag{B.6} $$

in which $a(\bar{\mu},s|-\mu,l|p)$ are the linearization expansion coefficients [40]–[43], the first term in the series being $p_0=\max(|l-s|,|\bar{\mu}-\mu|)$ or p_0+1 so that its last term is $l+s$, and

$$ \psi_{\bar{\mu}-\mu,p}^{(i)}(\mathbf{d}) = z_p^{(i)}(kd)\,P_p^{\bar{\mu}-\mu}(\cos\theta_d)\,e^{j(\bar{\mu}-\mu)\phi_d} \tag{B.7} $$

where $z_p^{(i)}$, $i=1,2,3,4$, are the spherical Bessel functions j_p, n_p, $h_p^{(1)}$, and $h_p^{(2)}$, respectively, and $P_p^{\bar{\mu}-\mu}$ is the Legendre function of the first kind;

$$ b_{\mu p}^{\bar{\mu}s}(\mathbf{d}) = \sum_{l=l_0,l_0+1}^{p+s}{}' b_{\bar{\mu}-\mu,l,p}^{\bar{\mu}s}(\mathbf{d}) \tag{B.8} $$

$$ b_{\bar{\mu}-\mu,l,p}^{\bar{\mu}s}(\mathbf{d}) = (-1)^{\bar{\mu}-\mu}\,j^{l+p-s}\,(2l+1)\,a(\bar{\mu},s|\mu-\bar{\mu},l|p)\cdot\psi_{\bar{\mu}-\mu,l}^{(1)}(\mathbf{d}) \tag{B.9} $$

with $l_0=\max(|p-s|,|\bar{\mu}-\mu|)$

Considering the translation from the system $O'x'y'z'$ to $Ox_{\|}y_{\|}z_{\|}$ and then the rotation of the system $Ox_{\|}y_{\|}z_{\|}$ about O through the Euler angles $-\gamma,-\beta,-\alpha$, we derive the rotational-translational coefficients ${}^{(i)}Q'^{mn}_{\mu\nu}$ for the expansion of spheroidal wave functions in primed coordinates in terms of functions in unprimed coordinates, for $r \le d$ and $i=1,2,3,4$, as

$$ {}^{(i)}Q'^{mn}_{\mu\nu}(\alpha,\beta,\gamma;\mathbf{d}) = \sum_{s=|m|,|m|+1}^{\infty}{}' d_{s-|m|}^{mn}(h') \sum_{l=|\mu|,|\mu|+1}^{\infty}{}' j^{s-n+\nu-l}\,\frac{N_{\mu l}}{N_{\mu\nu}(h)}\,d_{l-|\mu|}^{\mu\nu}(h) \cdot \sum_{c=-l}^{l} R_{\mu l}^{cl}(-\gamma,-\beta,-\alpha)\,{}^{(i)}b_{cl}^{ms}(\mathbf{d}) \tag{B.10} $$

with

$$ {}^{(i)}b_{cl}^{ms}(\mathbf{d}) = (-1)^{c} \sum_{p=p_0,p_0+1}^{l+s}{}' (-1)^{p}\,j^{l+p-s}\,(2l+1)\,a(m,s|-c,l|p)\cdot\psi_{m-c,p}^{(i)}(\mathbf{d}) \tag{B.11} $$

Substituting $s = |m|+q$, $l = |\mu|+r$ in (B.1) and (B.10) we get, respectively,

$$
{}^{(i)}Q^{mn}_{\mu\nu}(\alpha,\beta,\gamma;\mathbf{d}) = \sum_{q=0,1}^{\infty}{}' d_q^{mn}(h) \sum_{\bar{\mu}=-(|m|+q)}^{|m|+q} R^{m,|m|+q}_{\bar{\mu},|m|+q}(\alpha,\beta,\gamma)
$$
$$
\cdot \sum_{r=0,1}^{\infty}{}' {}^{(i)}a^{\bar{\mu},|m|+q}_{\mu,|\mu|+r}(\mathbf{d})\, j^{|m|+q-n+\nu-|\mu|-r} \frac{N_{\mu,|\mu|+r}}{N_{\mu\nu}(h')} d_r^{\mu\nu}(h') \qquad \text{(B.12)}
$$

and

$$
{}^{(i)}Q'^{mn}_{\mu\nu}(\alpha,\beta,\gamma;\mathbf{d}) = \sum_{q=0,1}^{\infty}{}' d_q^{mn}(h') \sum_{r=0,1}^{\infty}{}' j^{|m|+q-n+\nu-|\mu|-r} \frac{N_{\mu,|\mu|+r}}{N_{\mu\nu}(h)} d_r^{\mu\nu}(h)
$$
$$
\cdot \sum_{c=-(|\mu|+r)}^{|\mu|+r} R^{c,|\mu|+r}_{\mu,|\mu|+r}(-\gamma,-\beta,-\alpha)\, {}^{(i)}b^{m,|m|+q}_{c,|\mu|+r}(\mathbf{d}) \qquad \text{(B.13)}
$$

The rotational-translational coefficients ${}^{(i)}_{qr}Q^{mn}_{\mu\nu}(\alpha_{qr},\beta_{qr},\gamma_{qr};\mathbf{d}_{qr})$, $i = 1, 2, 3, 4$, that are used in Chapter 3, for expressing vector spheroidal wave functions associated with the system $O_q x_q y_q z_q$ in terms of those associated with the system $O_r x_r y_r z_r$, can be derived from (B.12) as

$$
{}^{(i)}_{qr}Q^{mn}_{\mu\nu}(\alpha_{qr},\beta_{qr},\gamma_{qr};\mathbf{d}_{qr}) = \sum_{u=0,1}^{\infty}{}' d_u^{mn}(h_q) \sum_{\bar{\mu}=-(|m|+u)}^{|m|+u} R^{m,|m|+u}_{\bar{\mu},|m|+u}(\alpha_{qr},\beta_{qr},\gamma_{qr})
$$
$$
\cdot \sum_{w=0,1}^{\infty}{}' {}^{(i)}a^{\bar{\mu},|m|+u}_{\mu,|\mu|+w}(\mathbf{d}_{qr})\, j^{|m|+u-n+\nu-|\mu|-w} \frac{N_{\mu,|\mu|+w}}{N_{\mu\nu}(h_r)} d_w^{\mu\nu}(h_r) \qquad \text{(B.14)}
$$

The matrix $[\Gamma_{qr}]$ introduced in (3.43) can be written as

$$
[\Gamma_{qr}] = \begin{bmatrix} [\Gamma_{qr}]_{00} & [\Gamma_{qr}]_{01} & [\Gamma_{qr}]_{02} & - & - & - \\ [\Gamma_{qr}]_{10} & [\Gamma_{qr}]_{11} & [\Gamma_{qr}]_{12} & - & - & - \\ [\Gamma_{qr}]_{20} & [\Gamma_{qr}]_{21} & [\Gamma_{qr}]_{22} & - & - & - \\ - & - & - & - & - & - \end{bmatrix} \qquad \text{(B.15)}
$$

with

$$[\Gamma_{qr}]_{00} = \begin{bmatrix} [\Gamma_1]_{-1}^{-1} & [\Gamma_2]_{1}^{-1} & [\Gamma_3]_{0}^{-1} \\ [\Gamma_4]_{-1}^{0} & [^*\Gamma_4]_{1}^{0} & [\Gamma_5]_{0}^{0} \end{bmatrix} \tag{B.16}$$

$$[\Gamma_{qr}]_{0\sigma} = \begin{bmatrix} [\Gamma_1]_{\sigma-1}^{-1} & [\Gamma_2]_{\sigma+1}^{-1} & [\Gamma_3]_{\sigma}^{-1} & [\Gamma_1]_{-(\sigma+1)}^{-1} & [\Gamma_2]_{-(\sigma-1)}^{-1} & [\Gamma_3]_{-\sigma}^{-1} \\ [\Gamma_4]_{\sigma-1}^{0} & [^*\Gamma_4]_{\sigma+1}^{0} & [\Gamma_5]_{\sigma}^{0} & [\Gamma_4]_{-(\sigma+1)}^{0} & [^*\Gamma_4]_{-(\sigma-1)}^{0} & [\Gamma_5]_{-\sigma}^{0} \end{bmatrix}, \quad \sigma \geq 1 \tag{B.17}$$

$$[\Gamma_{qr}]_{\tau 0} = \begin{bmatrix} [\Gamma_1]_{-1}^{\tau-1} & [\Gamma_2]_{1}^{\tau-1} & [\Gamma_3]_{0}^{\tau-1} \\ [\Gamma_4]_{-1}^{\tau} & [^*\Gamma_4]_{1}^{\tau} & [\Gamma_5]_{0}^{\tau} \\ [^*\Gamma_2]_{-1}^{-(\tau-1)} & [^*\Gamma_1]_{1}^{-(\tau-1)} & [^*\Gamma_3]_{0}^{-(\tau-1)} \\ [\Gamma_4]_{-1}^{-\tau} & [^*\Gamma_4]_{1}^{-\tau} & [\Gamma_5]_{0}^{-\tau} \end{bmatrix}, \quad \tau \geq 1 \tag{B.18}$$

$$[\Gamma_{qr}]_{\tau\sigma} = \begin{bmatrix} [\Gamma_1]_{\sigma-1}^{\tau-1} & [\Gamma_2]_{\sigma+1}^{\tau-1} & [\Gamma_3]_{\sigma}^{\tau-1} & [\Gamma_1]_{-(\sigma+1)}^{\tau-1} & [\Gamma_2]_{-(\sigma-1)}^{\tau-1} & [\Gamma_3]_{-\sigma}^{\tau-1} \\ [\Gamma_4]_{\sigma-1}^{\tau} & [^*\Gamma_4]_{\sigma+1}^{\tau} & [\Gamma_5]_{\sigma}^{\tau} & [\Gamma_4]_{-(\sigma+1)}^{\tau} & [^*\Gamma_4]_{-(\sigma-1)}^{\tau} & [\Gamma_5]_{-\sigma}^{\tau} \\ [^*\Gamma_2]_{\sigma-1}^{-(\tau-1)} & [^*\Gamma_1]_{\sigma+1}^{-(\tau-1)} & [^*\Gamma_3]_{\sigma}^{-(\tau-1)} & [^*\Gamma_2]_{-(\sigma+1)}^{-(\tau-1)} & [^*\Gamma_1]_{-(\sigma-1)}^{-(\tau-1)} & [^*\Gamma_3]_{-\sigma}^{-(\tau-1)} \\ [\Gamma_4]_{\sigma-1}^{-\tau} & [^*\Gamma_4]_{\sigma+1}^{-\tau} & [\Gamma_5]_{\sigma}^{-\tau} & [\Gamma_4]_{-(\sigma+1)}^{-\tau} & [^*\Gamma_4]_{-(\sigma-1)}^{-\tau} & [\Gamma_5]_{-\sigma}^{-\tau} \end{bmatrix},$$

$$\tau \geq 1, \sigma \geq 1 \tag{B.19}$$

The submatrices $[\Gamma_i]_{\sigma}^{\tau}$ and $[^*\Gamma_i]_{\sigma}^{\tau}$ for $\tau, \sigma = \ldots -2, -1, 0, 1, 2, \ldots$ and $i = 1, 2, 3, 4, 5$, are ${}^{qr}C_i\,[\Gamma_{qr}]_{\sigma}^{\tau}$ and ${}^{qr}C_i^*\,[\Gamma_{qr}]_{\sigma}^{\tau}$, respectively, where ${}^{qr}C_i$ are defined in (3.42), the asterisk denotes the complex conjugate, and

$$[\Gamma_{qr}]_{\sigma}^{\tau} = \begin{bmatrix} {}^{(4)}_{qr}Q^{\tau,|\tau|}_{\sigma,|\sigma|} & {}^{(4)}_{qr}Q^{\tau,|\tau|}_{\sigma,|\sigma|+1} & {}^{(4)}_{qr}Q^{\tau,|\tau|}_{\sigma,|\sigma|+2} & {}^{(4)}_{qr}Q^{\tau,|\tau|}_{\sigma,|\sigma|+3} & - \\ {}^{(4)}_{qr}Q^{\tau,|\tau|+1}_{\sigma,|\sigma|} & {}^{(4)}_{qr}Q^{\tau,|\tau|+1}_{\sigma,|\sigma|+1} & {}^{(4)}_{qr}Q^{\tau,|\tau|+1}_{\sigma,|\sigma|+2} & {}^{(4)}_{qr}Q^{\tau,|\tau|+1}_{\sigma,|\sigma|+3} & - \\ {}^{(4)}_{qr}Q^{\tau,|\tau|+2}_{\sigma,|\sigma|} & {}^{(4)}_{qr}Q^{\tau,|\tau|+2}_{\sigma,|\sigma|+1} & {}^{(4)}_{qr}Q^{\tau,|\tau|+2}_{\sigma,|\sigma|+2} & {}^{(4)}_{qr}Q^{\tau,|\tau|+2}_{\sigma,|\sigma|+3} & - \\ - & - & - & - & - \end{bmatrix} \tag{B.20}$$

APPENDIX C

MATRICES [P], [Q], AND [R] RESULTING FROM IMPOSING THE BOUNDARY CONDITIONS

The elements of the matrices $[P_{Jr}]$, $[Q_{Jr}]$, $[R_{Jr}]$, and $[R_{Jqr}]$, for $q = 1, 2, \ldots n$ and $r = 1, 2, \ldots n$, can be grouped in submatrices, such that all these matrices are quasi-diagonal in the sense that only the diagonal submatrices are different from zero. All null off-diagonal submatrices have the same size as the corresponding diagonal submatrices. The diagonal submatrices of $[P_{Jr}]$, $[Q_{Jr}]$, $[R_{Jr}]$, and $[R_{Jqr}]$ can be written as [44], [46], [57], [58]

$$[P_{Jr}]_0 = \begin{bmatrix} [\,{}^{(r)}_{\eta}Y^{+(4)}_{-1}\,] & [\,{}^{(r)}_{\eta}Y^{z\,(4)}_{0}\,] \\ [\,{}^{(r)}_{\phi}Y^{+(4)}_{-1}\,] & [\,{}^{(r)}_{\phi}Y^{z\,(4)}_{0}\,] \end{bmatrix}, \tag{C.1}$$

$$[P_{Jr}]_m = \begin{bmatrix} [\,{}^{(r)}_{\eta}Y^{+(4)}_{m-1}\,] & [\,{}^{(r)}_{\eta}Y^{z\,(4)}_{m}\,] & & \\ [\,{}^{(r)}_{\phi}Y^{+(4)}_{m-1}\,] & [\,{}^{(r)}_{\phi}Y^{z\,(4)}_{m}\,] & [0] & \\ & & [\,{}^{(r)}_{\eta}Y^{-(4)}_{-(m-1)}\,] & [\,{}^{(r)}_{\eta}Y^{z\,(4)}_{-m}\,] \\ [0] & & [\,{}^{(r)}_{\phi}Y^{-(4)}_{-(m-1)}\,] & [\,{}^{(r)}_{\phi}Y^{z\,(4)}_{-m}\,] \end{bmatrix}, \quad m \geq 1 \tag{C.2}$$

$$[Q_{Jr}]_0 = -\begin{bmatrix} [\,{}^{(r)}_{\eta}X^{+(4)}_{-1}\,] & [\,{}^{(r)}_{\eta}X^{z\,(4)}_{0}\,] \\ [\,{}^{(r)}_{\phi}X^{+(4)}_{-1}\,] & [\,{}^{(r)}_{\phi}X^{z\,(4)}_{0}\,] \end{bmatrix}, \tag{C.3}$$

$$[Q_{Jr}]_m = -\begin{bmatrix} [\,{}^{(r)}_{\eta}X^{+(4)}_{m-1}\,] & [\,{}^{(r)}_{\eta}X^{z\,(4)}_{m}\,] & & \\ [\,{}^{(r)}_{\phi}X^{+(4)}_{m-1}\,] & [\,{}^{(r)}_{\phi}X^{z\,(4)}_{m}\,] & [0] & \\ & & [\,{}^{(r)}_{\eta}X^{-(4)}_{-(m-1)}\,] & [\,{}^{(r)}_{\eta}X^{z\,(4)}_{-m}\,] \\ [0] & & [\,{}^{(r)}_{\phi}X^{-(4)}_{-(m-1)}\,] & [\,{}^{(r)}_{\phi}X^{z\,(4)}_{-m}\,] \end{bmatrix}, \quad m \geq 1 \tag{C.4}$$

$$[R_{Jr}]_0 = \begin{bmatrix} [\,{}^{(r)}_{\eta}X^{+(1)}_{-1}\,] & [\,{}^{(r)}_{\eta}X^{-(1)}_{1}\,] \\ [\,{}^{(r)}_{\phi}X^{+(1)}_{-1}\,] & [\,{}^{(r)}_{\phi}X^{-(1)}_{1}\,] \end{bmatrix}, \tag{C.5}$$

$$[R_{Jr}]_m = \begin{bmatrix} [\,{}^{(r)}_{\eta}X^{+(1)}_{m-1}\,] & [\,{}^{(r)}_{\eta}X^{-(1)}_{m+1}\,] & & [0] & \\ [\,{}^{(r)}_{\phi}X^{+(1)}_{m-1}\,] & [\,{}^{(r)}_{\phi}X^{-(1)}_{m+1}\,] & & & \\ & & [\,{}^{(r)}_{\eta}X^{+(1)}_{-(m+1)}\,] & [\,{}^{(r)}_{\eta}X^{-(1)}_{-(m-1)}\,] \\ & [0] & [\,{}^{(r)}_{\phi}X^{+(1)}_{-(m+1)}\,] & [\,{}^{(r)}_{\phi}X^{-(1)}_{-(m-1)}\,] \end{bmatrix}, \quad m \geq 1 \tag{C.6}$$

$$[R_{Jqr}]_0 = -\begin{bmatrix} [\,{}^{(r)}_{\eta}X^{+(1)}_{-1}\,] & [\,{}^{(r)}_{\eta}X^{-(1)}_{1}\,] & [\,{}^{(r)}_{\eta}X^{z(1)}_{0}\,] \\ [\,{}^{(r)}_{\phi}X^{+(1)}_{-1}\,] & [\,{}^{(r)}_{\phi}X^{-(1)}_{1}\,] & [\,{}^{(r)}_{\phi}X^{z(1)}_{0}\,] \end{bmatrix}, \tag{C.7}$$

$$[R_{Jqr}]_m = -\begin{bmatrix} [\,{}^{(r)}_{\eta}X^{+(1)}_{m-1}\,] & [\,{}^{(r)}_{\eta}X^{-(1)}_{m+1}\,] & [\,{}^{(r)}_{\eta}X^{z(1)}_{m}\,] & & [0] & \\ [\,{}^{(r)}_{\phi}X^{+(1)}_{m-1}\,] & [\,{}^{(r)}_{\phi}X^{-(1)}_{m+1}\,] & [\,{}^{(r)}_{\phi}X^{z(1)}_{m}\,] & & & \\ & & & [\,{}^{(r)}_{\eta}X^{+(1)}_{-(m+1)}\,] & [\,{}^{(r)}_{\eta}X^{-(1)}_{-(m-1)}\,] & [\,{}^{(r)}_{\eta}X^{z(1)}_{-m}\,] \\ & [0] & & [\,{}^{(r)}_{\phi}X^{+(1)}_{-(m+1)}\,] & [\,{}^{(r)}_{\phi}X^{-(1)}_{-(m-1)}\,] & [\,{}^{(r)}_{\phi}X^{z(1)}_{-m}\,] \end{bmatrix}, \tag{C.8}$$

$m \geq 1.$

The submatrices $[X_m]$ have the form

$$[X_m] = \begin{bmatrix} X_{m,0,|m|} & X_{m,0,|m|+1} & X_{m,0,|m|+2} & - & - & - \\ X_{m,1,|m|} & X_{m,1,|m|+1} & X_{m,1,|m|+2} & - & - & - \\ X_{m,2,|m|} & X_{m,2,|m|+1} & X_{m,2,|m|+2} & - & - & - \\ - & - & - & - & - & - \\ - & - & - & - & - & - \end{bmatrix} \tag{C.9}$$

where the elements are given by

$$\underset{(\phi)}{\eta}{}^{(r)}X^{\pm(i)}_{m+\upsilon,\kappa,n} = \frac{1}{2\pi}\int_0^{2\pi}\int_{-1}^{1}\binom{r}{r}l_{\eta}\,\underset{(\phi)}{\eta}{}^{(r)}J^{\pm(i)}_{m+\upsilon,n}(h_r;\mathbf{r}_r)\,S_{m,|m|+\kappa}(h_r,\eta_r)\,e^{-j(m+\upsilon\pm1)\phi_r}\,d\eta_r\,d\phi_r \tag{C.10}$$

$$ {}^{\eta}_{(\phi)}{}^{(r)}X^{z(i)}_{m+1,\kappa,n} = \frac{1}{2\pi}\int_0^{2\pi}\int_{-1}^{1} ({}^{r}_{r}l^{\eta}_{\phi})\, {}^{\eta}_{(\phi)}{}^{(r)}J^{z(i)}_{m+1,n}(h_r;\mathbf{r}_r)\, S_{m,|m|+\kappa}(h_r,\eta_r)\, e^{-j(m+1)\phi_r}\, d\eta_r\, d\phi_r \tag{C.11} $$

with J being either M or N, i.e. the respective component of $\mathbf{M}$ or $\mathbf{N}$. The submatrices $[Y_m]$ have the same form as those of $[X_m]$, with the elements given by

$$ {}^{\eta}_{(\phi)}{}^{(r)}Y^{\pm(i)}_{m+\upsilon,\kappa,n} = \frac{1}{2\pi}\int_0^{2\pi}\int_{-1}^{1} ({}^{r}_{r}l^{\eta}_{\phi})\, {}^{\eta}_{(\phi)}{}^{(r)}J^{\pm(i)}_{m+\upsilon,n}(h_r';\mathbf{r}_r)\, S_{m,|m|+\kappa}(h_r,\eta_r)\, e^{-j(m+\upsilon\pm1)\phi_r}\, d\eta_r\, d\phi_r \tag{C.12} $$

$$ {}^{\eta}_{(\phi)}{}^{(r)}Y^{z(i)}_{m+1,\kappa,n} = \frac{1}{2\pi}\int_0^{2\pi}\int_{-1}^{1} ({}^{r}_{r}l^{\eta}_{\phi})\, {}^{\eta}_{(\phi)}{}^{(r)}J^{z(i)}_{m+1,n}(h_r';\mathbf{r}_r)\, S_{m,|m|+\kappa}(h_r,\eta_r)\, e^{-j(m+1)\phi_r}\, d\eta_r\, d\phi_r \tag{C.13} $$

in which J is either M or N. The explicit expressions of X for $J=M$ are given in [35]. The explicit expressions of ${}^{(r)}X^{\pm(i)}_{m,\kappa,n}$ $(\upsilon=0)$, ${}^{(r)}X^{\pm(i)}_{m+2,\kappa,n}$ $(\upsilon=2)$, and ${}^{(r)}X^{z(i)}_{m+1,\kappa,n}$ for $J=N$ are given below.

$$ \begin{aligned} {}^{(r)}_{\eta}X^{\pm(i)}_{m,\kappa,n} = {} & \left[(\xi_s^2-1)\frac{d^2}{d\xi_r^2}R^{(i)}_{mn}(h_r,\xi_r)\Big|_{\xi_r=\xi_s} + \xi_s\frac{d}{d\xi_r}R^{(i)}_{mn}(h_r,\xi_r)\Big|_{\xi_r=\xi_s}\right]\cdot[(\xi_s^2-1)I_{3m\kappa n} + I_{14m\kappa n}] \\ & + \xi_s\frac{d}{d\xi_r}R^{(i)}_{mn}(h_r,\xi_r)\Big|_{\xi_r=\xi_s}\left[(\xi_s^2-1)I_{4m\kappa n} + I_{15m\kappa n} + 2I_{14m\kappa n}\right] \\ & - R^{(i)}_{mn}(h_r,\xi_s)\left[I_{16m\kappa n} - \frac{\xi_s^2}{(\xi_s^2-1)}I_{15m\kappa n}\right] \\ & \mp (m\pm1)R^{(i)}_{mn}(h_r,\xi_s)\left[(\xi_s^2-1)I_{18m\kappa n} + 2I_{4m\kappa n}\right] \\ & - m(m\pm1)R^{(i)}_{mn}(h_r,\xi_s)\left[(\xi_s^2-1)I_{17m\kappa n} + 2I_{3m\kappa n}\right] \\ & - \frac{(m\pm1)}{(\xi_s^2-1)}R^{(i)}_{mn}(h_r,\xi_s)(m\,I_{14m\kappa n} \pm I_{15m\kappa n}) \end{aligned} \tag{C.14} $$

$$
{}^{(r)}_{\eta}X^{\pm(i)}_{m+2,\kappa,n} = \left[(\xi_s^2-1)\frac{d^2}{d\xi_r^2}R^{(i)}_{m+2,n}(h_r,\xi_r)\Big|_{\xi_r=\xi_s} + \xi_s\frac{d}{d\xi_r}R^{(i)}_{m+2,n}(h_r,\xi_r)\Big|_{\xi_r=\xi_s}\right].[(\xi_s^2-1)I_{8m\kappa n}
$$

$$
+I_{19m\kappa n}] + \xi_s\frac{d}{d\xi_r}R^{(i)}_{mn}(h_r,\xi_r)\Big|_{\xi_r=\xi_s}\left[(\xi_s^2-1)I_{9m\kappa n} + I_{20m\kappa n} + 2I_{19m\kappa n}\right]
$$

$$
-R^{(i)}_{m+2,n}(h_r,\xi_s)\left[I_{21m\kappa n} - \frac{\xi_s^2}{(\xi_s^2-1)}I_{20m\kappa n}\right]
$$

$$
\mp(m+2\pm1)R^{(i)}_{m+2,n}(h_r,\xi_s)\left[(\xi_s^2-1)I_{23m\kappa n} + 2I_{9m\kappa n}\right]
$$

$$
-(m+2)(m+2\pm1)R^{(i)}_{m+2,n}(h_r,\xi_s)\left[(\xi_s^2-1)I_{22m\kappa n} + 2I_{8m\kappa n}\right]
$$

$$
-\frac{(m+2\pm1)}{(\xi_s^2-1)}R^{(i)}_{m+2,n}(h_r,\xi_s)\left[(m+2)I_{19m\kappa n} \pm I_{20m\kappa n}\right] \qquad \text{(C.15)}
$$

$$
{}^{(r)}_{\eta}X^{z(i)}_{m+1,\kappa,n} = 2\left[(\xi_s^2-1)^{3/2}\frac{d}{d\xi_r}R^{(i)}_{m+1,n}(h_r,\xi_r)\Big|_{\xi_r=\xi_s}(I_{6m\kappa n} - I_{5m\kappa n})\right.
$$

$$
+(\xi_s^2-1)^{1/2}\frac{d}{d\xi_r}R^{(i)}_{m+1,n}(h_r,\xi_r)\Big|_{\xi_r=\xi_s}(I_{24m\kappa n} - I_{25m\kappa n})
$$

$$
-\xi_s(\xi_s^2-1)^{1/2}\frac{d^2}{d\xi_r^2}R^{(i)}_{m+1,n}(h_r,\xi_r)\Big|_{\xi_r=\xi_s}((\xi_s^2-1)I_{5m\kappa n} + I_{25m\kappa n})
$$

$$
+\frac{(m+1)^2\xi_s}{(\xi_s^2-1)^{3/2}}\frac{d}{d\xi_r}R^{(i)}_{m+1,n}(h_r,\xi_r)\Big|_{\xi_r=\xi_s}\left\{(\xi_s^2-1)^2 I_{26m\kappa n}\right.
$$

$$
\left.+2(\xi_s^2-1)I_{5m\kappa n} + I_{25m\kappa n}\right\} + \frac{2\xi_s}{(\xi_s^2-1)}R^{(i)}_{m+1,n}(h_r,\xi_s)I_{24m\kappa n}
$$

$$
\left.-\frac{2\xi_s^2}{(\xi_s^2-1)^{1/2}}\frac{d}{d\xi_r}R^{(i)}_{m+1,n}(h_r,\xi_r)\Big|_{\xi_r=\xi_s}I_{25m\kappa n}\right] \qquad \text{(C.16)}
$$

$$
{}^{(r)}_{\phi}X^{\pm(i)}_{m,\kappa,n} = (\xi_s^2-1)R^{(i)}_{mn}(h_r,\xi_s)(m\,I_{28m\kappa n} \pm I_{27m\kappa n}) \pm \left[(\xi_s^2-1)^2\frac{d^2}{d\xi_r^2}R^{(i)}_{mn}(h_r,\xi_r)\Big|_{\xi_r=\xi_s}\right.
$$

$$
\left.-\xi_s(\xi_s^2-1)\frac{d}{d\xi_r}R^{(i)}_{mn}(h_r,\xi_r)\Big|_{\xi_r=\xi_s}.(-1\pm m)(\pm m)R^{(i)}_{mn}(h_r,\xi_s)\right]I_{1m\kappa n} \qquad \text{(C.17)}
$$

$$
{}^{(r)}_{\phi}X^{\pm(i)}_{m+2,\kappa,n} = (\xi_s^2-1)\,R^{(i)}_{m+2,n}(h_r,\xi_s)\,((m+2)\,(I_{31m\kappa n}+I_{32m\kappa n})\pm(I_{33m\kappa n}-I_{31m\kappa n}))
$$

$$
\pm\left[(\xi_s^2-1)^2\,\frac{d^2}{d\xi_r^2}R^{(i)}_{m+2,n}(h_r,\xi_r)\Big|_{\xi_r=\xi_s}-\xi_s\,(\xi_s^2-1)\,\{-1\pm(m+2)\}\right.
$$

$$
\left.\cdot\,\frac{d}{d\xi_r}R^{(i)}_{m+2,n}(h_r,\xi_r)\Big|_{\xi_r=\xi_s}\pm(m+2)\,R^{(i)}_{m+2,n}(h_r,\xi_s)\right]\cdot I_{7m\kappa n} \qquad \text{(C.18)}
$$

$$
{}^{(r)}_{\phi}X^{z(i)}_{m+1,\kappa,n} = -2\,(m+1)\,(\xi_s^2-1)^{1/2}\left[\xi_s\,R^{(i)}_{m+1,n}(h_r,\xi_s)\,I_{29m\kappa n}\right.
$$

$$
\left.+(\xi_s^2-1)\,\frac{d}{d\xi_r}R^{(i)}_{m+1,n}(h_r,\xi_r)\Big|_{\xi_r=\xi_s}I_{2m\kappa n}\right] \qquad \text{(C.19)}
$$

$$
{}^{(r)}_{\eta}X^{z(i)}_{0,\kappa,n} = -2\left[(\xi_s^2-1)^{1/2}\,\frac{d}{d\xi_r}R^{(i)}_{0n}(h_r,\xi_r)\Big|_{\xi_r=\xi_s}\left\{(\xi_s^2-1)\,I_{11,\kappa n}+I_{12,\kappa n}\right\}\right.
$$

$$
-\xi_s\,(\xi_s^2-1)^{1/2}\,\frac{d^2}{d\xi_r^2}R^{(i)}_{0n}(h_r,\xi_r)\Big|_{\xi_r=\xi_s}\left\{(\xi_s^2-1)\,I_{10,\kappa n}+I_{13,\kappa n}\right\}
$$

$$
-(\xi_s^2-1)^{1/2}\,\frac{d}{d\xi_r}R^{(i)}_{0n}(h_r,\xi_r)\Big|_{\xi_r=\xi_s}\left\{(\xi_s^2-1)\,I_{10,\kappa n}+I_{13,\kappa n}\right\}
$$

$$
\left.+\frac{2\xi_s}{(\xi_s^2-1)}\,R^{(i)}_{0n}(h_r,\xi_s)\left\{I_{12,\kappa n}-\xi_s\,(\xi_s^2-1)^{1/2}I_{13,\kappa n}\right\}\right] \qquad \text{(C.20)}
$$

$$
{}^{(r)}_{\phi}X^{z(i)}_{0,\kappa,n} = 0 \qquad \text{(C.21)}
$$

Explicit expressions of ${}^{(r)}Y^{\pm(i)}_{m,\kappa,n}$ ($\upsilon=0$), ${}^{(r)}Y^{\pm(i)}_{m+2,\kappa,n}$ ($\upsilon=2$), and ${}^{(r)}Y^{z(i)}_{m+1,\kappa,n}$, for $J=M$ and $J=N$ have the same structure as those of the corresponding X, but with the functions J evaluated with respect to h_r', which is the value of h inside the rth spheroid. ξ_s is the value of ξ on the surface of the spheroid considered. $I_{1m\kappa n}-I_{11,\kappa n}$ are given in [35] and $I_{12,\kappa n}-I_{33m\kappa n}$ in Appendix D.

It should be noted that for computational purposes, the following relations are used [28],[44]:

$$
\begin{aligned}
S_{mn}(h,\eta) &= K_{mn}\, S_{|m|n}(h,\eta) \\
R_{mn}^{(i)}(h_r,\xi_r) &= R_{|m|n}^{(i)}(h_r,\xi_r), \qquad i=1,2,3,4 \\
d_q^{mn}(h) &= (-1)^{\frac{m-|m|}{2}} \frac{(|m|-m+q)!}{q!} K_{mn}\, d_q^{|m|n}(h) \\
N_{mn}(h) &= K_{mn}^2\, N_{|m|n}(h)
\end{aligned}
\tag{C.22}
$$

where

$$
K_{mn} = (-1)^{\frac{|m|-m}{2}} \frac{(n+m)!}{(n+|m|)!} \tag{C.23}
$$

APPENDIX D

EVALUATION OF THE INTEGRALS IN APPENDIX C

The integrals $I_{1mNn} - I_{33mNn}$ that result when applying the orthogonality properties of the spheroidal angle functions in equations $(C.10) - (C.13)$ are evaluated using the recurrence relations for the associated Legendre functions and the integrals [34], [35], [53]

$$\int_{-1}^{1} P_\mu^m(\eta) P_\nu^m(\eta)\, d\eta = \frac{2}{(2\mu+1)} \frac{(\mu+m)!}{(\mu-m)!} \delta_{\mu\nu} \tag{D.1}$$

$$\int_{-1}^{1} P_\mu^{m+2}(\eta) P_\nu^m(\eta)\, d\eta = \begin{cases} 0, & \nu>\mu \\ \dfrac{-2}{(2\nu+1)} \dfrac{(\nu+m)!}{(\nu-m-2)!}, & \nu=\mu \\ 2(m+1) \dfrac{(\nu+m)!}{(\nu-m)!} [1+(-1)^{\nu+\mu}], & \nu<\mu \end{cases} \tag{D.2}$$

where $\delta_{\mu\nu}$ is the Kronecker delta function. The integrals $I_{1mNn} - I_{9mNn}$, $I_{10,Nn}$, and $I_{11,Nn}$ are evaluated in [35]. We derived expressions for $I_{12,Nn}$, $I_{13,Nn}$, and $I_{14mNn} - I_{33mNn}$ in the form:

$$\begin{aligned} I_{12,Nn} &= \int_{-1}^{1} \eta (1-\eta^2)^{3/2} \frac{d}{d\eta} S_{0n} S_{1,1+N}\, d\eta \\ &= 2 \sum_{q=0,1}^{\infty}{}' \frac{(q+1)(q+2)}{(2q+3)} \left[- \frac{(q-2)(q-1)q d_{q-2}^{0n}}{(2q-3)(2q-1)(2q+1)} + \frac{q(q+1)^2 d_q^{0n}}{(2q-1)(2q+1)(2q+5)} \right. \\ &\quad \left. + \frac{(q+2)^2(q+3) d_{q+2}^{0n}}{(2q+1)(2q+5)(2q+7)} - \frac{(q+3)(q+4)(q+5) d_{q+4}^{0n}}{(2q+5)(2q+7)(2q+9)} \right] d_q^{1,1+N}, \quad (n+N) \text{ even} \\ &= 0, \quad (n+N) \text{ odd} \end{aligned} \tag{D.3}$$

$$I_{13,Nn} = \int_{-1}^{1} (1-\eta^2)^{3/2} S_{0n}\, S_{1,1+N}\, d\eta$$

$$= 2 \sum_{q=0,1}^{\infty}{}' \frac{(q+1)(q+2)}{(2q+3)} \left[- \frac{(q-1)q d_{q-2}^{0n}}{(2q-3)(2q-1)(2q+1)} + \frac{(3q^2+5q-4) d_q^{0n}}{(2q-1)(2q+1)(2q+5)} \right.$$

$$\left. - \frac{(3q^2+13q+8) d_{q+2}^{0n}}{(2q+1)(2q+5)(2q+7)} - \frac{(q+3)(q+4) d_{q+4}^{0n}}{(2q+5)(2q+7)(2q+9)} \right] d_q^{1,1+N}, \quad (n+N) \text{ even}$$

$$= 0, \quad (n+N) \text{ odd} \tag{D.4}$$

$$I_{14mNn} = \int_{-1}^{1} (1-\eta^2)\, \eta\, S_{mn}\, S_{m,m+N}\, d\eta$$

$$= 2 \sum_{q=0,1}^{\infty}{}' \left\{ - \frac{(q-2)(q-1)q}{(2m+2q-3)(2m+2q-1)} \left[\frac{d_{q-3}^{m,m+N}}{(2m+2q-5)} - \frac{d_{q-1}^{m,m+N}}{(2m+2q-1)} \right] \right.$$

$$+ \frac{(2m+1)(2m+q+1)q}{(2m+2q-1)(2m+2q+3)} \left[\frac{d_{q-1}^{m,m+N}}{(2m+2q-1)} - \frac{d_{q+1}^{m,m+N}}{(2m+2q+3)} \right]$$

$$\left. + \frac{(2m+q+1)(2m+q+2)(2m+q+3)}{(2m+2q+3)(2m+2q+5)} \left[\frac{d_{q+1}^{m,m+N}}{(2m+2q+3)} - \frac{d_{q+3}^{m,m+N}}{(2m+2q+7)} \right] \right\}$$

$$\cdot \frac{(2m+q)!}{(2m+2q+1)q!} d_q^{mn}, \quad (n+N) \text{ odd}$$

$$= 0, \quad (n+N) \text{ even} \tag{D.5}$$

$$I_{15mNn} = \int_{-1}^{1} (1-\eta^2)^2 \frac{d}{d\eta} S_{mn}\, S_{m,m+N}\, d\eta$$

$$= 2 \sum_{q=0,1}^{\infty}{}' \frac{(2m+q)! d_q^{mn}}{(2m+2q+1)q!} \left\{ \frac{(m+q+1)(q-2)(q-1)q}{(2m+2q-3)(2m+2q-1)} \left[\frac{d_{q-3}^{m,m+N}}{(2m+2q-5)} - \frac{d_{q-1}^{m,m+N}}{(2m+2q-1)} \right] \right.$$

$$\left. + \frac{[2(m+q)^2+5m+2q](2m+q+1)q}{(2m+2q-1)(2m+2q+3)} \left[\frac{d_{q-1}^{m,m+N}}{(2m+2q-1)} - \frac{d_{q+1}^{m,m+N}}{(2m+2q+3)} \right] \right.$$

$$- \frac{(m+q)(2m+q+1)(2m+q+2)(2m+q+3)}{(2m+2q+3)(2m+2q+5)} \left[\frac{d_{q+1}^{m,m+N}}{(2m+2q+3)} - \frac{d_{q+3}^{m,m+N}}{(2m+2q+7)} \right] \Bigg\},$$

$(n+N)$ odd

$$= 0, \quad (n+N) \text{ even} \tag{D.6}$$

$$I_{16mNn} = \int_{-1}^{1} (1-\eta^2)\,\eta^2 \frac{d}{d\eta} S_{mn}\, S_{m,m+N}\, d\eta$$

$$= I_{4mNn} - I_{15mNn} \tag{D.7}$$

$$I_{17mNn} = \int_{-1}^{1} \frac{m\eta}{(1-\eta^2)} S_{mn}\, S_{m,m+N}\, d\eta$$

$$= \sum_{q=0,1}^{\infty}{}' \frac{(2m+q)!}{q!} d_q^{mn} \sum_{r=q+1}^{\infty}{}' d_r^{m,m+N}$$

$$+ \sum_{q=1,0}^{\infty}{}' \frac{(2m+q)!}{q!} d_q^{m,m+N} \sum_{r=q+1}^{\infty}{}' d_r^{mn}, \quad (n+N) \text{ odd}$$

$$= 0, \quad (n+N) \text{ even} \tag{D.8}$$

$$I_{18mNn} = \int_{-1}^{1} \frac{d}{d\eta} S_{mn}\, S_{m,m+N}\, d\eta$$

$$= \sum_{q=1,0}^{\infty}{}' \frac{(2m+q)!}{q!} d_q^{m,m+N} \sum_{r=q+1}^{\infty}{}' d_r^{mn}$$

$$- \sum_{q=0,1}^{\infty}{}' \frac{(2m+q)!}{q!} d_q^{mn} \sum_{r=q+1}^{\infty}{}' d_r^{m,m+N}, \quad (n+N) \text{ odd}, \quad m \neq 0$$

$$= 0, \quad (n+N) \text{ even}, \quad m \neq 0 \tag{D.9}$$

$$I_{19mNn} = \int_{-1}^{1} (1-\eta^2)\,\eta\, S_{m+2,n}\, S_{m,m+N}\, d\eta$$

$$= 2 \sum_{q=0,1}^{\infty}{}' \left\{ \frac{(2m+q+5)}{(2m+2q+5)(2m+q+7)} \left[\frac{d_{q+1}^{m,m+N}}{(2m+2q+3)} - \frac{2\, d_{q+3}^{m,m+N}}{(2m+2q+9)} \right] \right.$$

$$+ \frac{1}{(2m+2q+7)} \left[\frac{q\; d_{q+3}^{m,m+N}}{(2m+2q+3)(2m+2q+5)} + \frac{(2m+q+5)\, d_{q+5}^{m,m+N}}{(2m+2q+9)(2m+2q+11)} \right]$$

$$\left. + \frac{q}{(2m+2q+1)} \left[\frac{d_{q-1}^{m,m+N}}{(2m+2q-1)(2m+2q+3)} - \frac{2\, d_{q+1}^{m,m+N}}{(2m+2q+3)(2m+2q+5)} \right] \right\}$$

$$\cdot \frac{(2m+q+4)!}{(2m+2q+5)q!}\, d_q^{m+2,n}, \quad (n+N) \text{ odd}$$

$$= 0, \quad (n+N) \text{ even} \tag{D.10}$$

$$I_{20mNn} = \int_{-1}^{1} (1-\eta^2)^2 \frac{d}{d\eta}\, S_{m+2,n}\, S_{m,m+N}\, d\eta$$

$$= 2 \sum_{q=0,1}^{\infty}{}' \left\{ \frac{(m+q+3)q}{(2m+2q+1)(2m+2q+3)} \left[\frac{d_{q-1}^{m,m+N}}{(2m+2q-1)} - \frac{2\, d_{q+1}^{m,m+N}}{(2m+2q+5)} \right] \right.$$

$$- \frac{(m+q+2)(2m+q+5)}{(2m+2q+5)(2m+2q+7)} \left[\frac{d_{q+1}^{m,m+N}}{(2m+2q+3)} - \frac{2\, d_{q+3}^{m,m+N}}{(2m+2q+9)} \right]$$

$$\left. + \left[\frac{(m+q+3)q\; d_{q+3}^{m,m+N}}{(2m+2q+3)(2m+2q+5)} - \frac{(m+q+2)(2m+q+5)\, d_{q+5}^{m,m+N}}{(2m+2q+9)(2m+2q+11)} \right] \frac{1}{(2m+2q+7)} \right\}$$

$$\cdot \frac{(2m+q+4)!}{(2m+2q+5)q!}\, d_q^{m+2,n}, \quad (n+N) \text{ odd}$$

$$= 0, \quad (n+N) \text{ even} \tag{D.11}$$

$$I_{21mNn} = \int_{-1}^{1} (1-\eta^2)\,\eta^2 \frac{d}{d\eta}\, S_{m+2,n}\, S_{m,m+N}\, d\eta$$

$$= I_{9mNn} - I_{20mNn} \tag{D.12}$$

$$I_{22mNn} = \int_{-1}^{1} \frac{\eta}{(1-\eta^2)} S_{m+2,n}\, S_{m,m+N}\, d\eta$$

$$= 2 \sum_{r=0,1}^{\infty}{}' \frac{(2m+r)!}{r!} d_r^{m,m+N} \sum_{q=r}^{\infty}{}' [q d_{q-1}^{m+2,n} + (2m+2q+3) \sum_{\nu=q+1}^{\infty}{}' d_\nu^{m+2,n}], \quad (n+N) \text{ odd}$$

$$= 0, \quad (n+N) \text{ even} \tag{D.13}$$

$$I_{23mNn} = \int_{-1}^{1} \frac{d}{d\eta} S_{m+2,n}\, S_{m,m+N}\, d\eta$$

$$= 2 \sum_{r=0,1}^{\infty}{}' \frac{(2m+r)!}{r!} d_r^{m,m+N} \sum_{q=r}^{\infty}{}' [-q(m+q+1) d_{q-1}^{m+2,n}$$

$$+ (m+2)(2m+2q+3) \sum_{\nu=q+1}^{\infty}{}' d_\nu^{m+2,n}], \quad (n+N) \text{ odd}$$

$$= 0 \quad (n+N) \text{ even} \tag{D.14}$$

$$I_{24mNn} = \int_{-1}^{1} \eta (1-\eta^2)^{3/2} \frac{d}{d\eta} S_{m+1,n}\, S_{m,m+N}\, d\eta$$

$$= 2 \sum_{q=0,1}^{\infty}{}' \frac{(2m+q+2)!\, d_q^{m+1,n}}{(2m+2q+3) q!} \left\{ \frac{(m+q+2)q}{(2m+2q+1)} \left[\frac{(q-1)\, d_{q-2}^{m,m+N}}{(2m+2q-3)(2m+2q-1)} \right.\right.$$

$$\left. + \frac{(2m+1)\, d_q^{m,m+N}}{(2m+2q-1)(2m+2q+3)} - \frac{(2m+q+2)\, d_{q+2}^{m,m+N}}{(2m+2q+3)(2m+2q+5)} \right]$$

$$- \frac{(m+q+1)(2m+q+3)}{(2m+2q+5)} \left[\frac{(q+1)\, d_q^{m,m+N}}{(2m+2q+1)(2m+2q+3)} \right.$$

$$\left.\left. + \frac{(2m+1)\, d_{q+2}^{m,m+N}}{(2m+2q+3)(2m+2q+7)} - \frac{(2m+q+4)\, d_{q+4}^{m,m+N}}{(2m+2q+7)(2m+2q+9)} \right] \right\}, \quad (n+N) \text{ even}$$

$$= 0, \quad (n+N) \text{ odd} \tag{D.15}$$

$$I_{25mNn} = \int_{-1}^{1} (1-\eta^2)^{3/2} S_{m+1,n}\, S_{m,m+N}\, d\eta$$

$$= 2 \sum_{q=0,1}^{\infty}{}' \frac{(2m+q+2)!\, d_q^{m+1,n}}{(2m+2q+3)q!} \left\{ \frac{(2m+q+3)(2m+q+4)}{(2m+2q+5)} \right.$$

$$\cdot \left[\frac{d_q^{m,m+N}}{(2m+2q+1)(2m+2q+3)} - \frac{2\, d_{q+2}^{m,m+N}}{(2m+2q+3)(2m+2q+7)} \right.$$

$$\left. + \frac{d_{q+4}^{m,m+N}}{(2m+2q+7)(2m+2q+9)} \right] - \frac{(q-1)q}{(2m+2q+1)} \left[\frac{d_{q-2}^{m,m+N}}{(2m+2q-3)(2m+2q-1)} \right.$$

$$\left. \left. - \frac{2\, d_q^{m,m+N}}{(2m+2q-1)(2m+2q+3)} + \frac{d_{q+2}^{m,m+N}}{(2m+2q+3)(2m+2q+5)} \right] \right\}, \quad (n+N) \text{ even}$$

$$= 0, \quad (n+N) \text{ odd} \tag{D.16}$$

$$I_{26mNn} = \int_{-1}^{1} \frac{1}{(1-\eta^2)^{1/2}} S_{m+1,n}\, S_{m,m+N}\, d\eta$$

$$= 2 \sum_{r=0,1}^{\infty}{}' \frac{(2m+r)!}{r!} d_r^{m,m+N} \sum_{q=r}^{\infty}{}' d_q^{m+1,n}, \quad (n+N) \text{ even}$$

$$= 0, \quad (n+N) \text{ odd} \tag{D.17}$$

$$I_{27mNn} = \int_{-1}^{1} (1-\eta^2)^{1/2} \frac{d}{d\eta} \left[(1-\eta^2)^{1/2} \frac{d}{d\eta} S_{mn} \right] S_{m,m+N}\, d\eta$$

$$= -2 \sum_{q=1,0}^{\infty}{}' \frac{(q+1)^2}{(2q+3)} d_{q+1}^{0n}\, d_{q+1}^{0N} + 2 \sum_{r=0,1}^{\infty}{}' d_r^{0N} \sum_{t=r+1}^{\infty}{}' d_{t+1}^{0n}, \quad (n+N) \text{ even}, \quad m=0$$

$$= - \sum_{q=0,1}^{\infty}{}' \frac{(2m+q)!}{q!} \left[q \frac{(m+q)+(q+1)(m+q+1)}{(2m+2q+1)} d_q^{mn} d_q^{m,m+N} - (m+1) \right.$$

$$\left. \cdot d_q^{m,m+N} \sum_{r=q+2}^{\infty}{}' d_r^{mn} - (m-1)\, d_q^{mn} \sum_{r=q+2}^{\infty}{}' d_r^{m,m+N} \right], \quad (n+N) \text{ even}, \quad m \neq 0$$

$$= 0, \quad (n+N) \text{ odd} \tag{D.18}$$

$$I_{28mNn} = \int_{-1}^{1} m(1-\eta^2)^{1/2} \frac{d}{d\eta} \left[\frac{\eta}{(1-\eta^2)^{1/2}} S_{mn} \right] S_{m,m+N}\, d\eta$$

$$= \sum_{q=0,1}^{\infty}{}' \frac{(2m+q)!}{q!} \left[\frac{(m+2q+1)}{(2m+2q+1)} d_q^{mn} d_q^{m,m+N} + (m+1) d_q^{m,m+N} \right.$$

$$\left. \cdot \sum_{r=q+2}^{\infty}{}' d_r^{mn} - (m-1) d_q^{mn} \sum_{r=q+2}^{\infty}{}' d_r^{m,m+N} \right], \quad (n+N) \text{ even}$$

$$= 0, \quad (n+N) \text{ odd} \tag{D.19}$$

$$I_{29mNn} = \int_{-1}^{1} (1-\eta^2)^{1/2} \frac{d}{d\eta} S_{m+1,n}\, S_{m,m+N}\, d\eta$$

$$= -2 \sum_{q=0,1}^{\infty}{}' \frac{(m+q+1)(2m+q+1)!}{(2m+2q+3)q!} d_q^{m+1,n} d_{q+1}^{m,m+N}$$

$$+ 2(m+1) \sum_{q=1,0}^{\infty}{}' \frac{(2m+q)!}{q!} d_q^{m,m+N} \sum_{r=q+1}^{\infty}{}' d_r^{m+1,n}, \quad (n+N) \text{ odd}$$

$$= 0, \quad (n+N) \text{ even} \tag{D.20}$$

$$I_{30mNn} = \int_{-1}^{1} \eta^2 S_{m+2,n}\, S_{m,m+N}\, d\eta$$

$$= 2 \sum_{r=0,1}^{\infty}{}' \frac{(2m+r)!\, d_r^{m,m+N}}{(2m+2r+1)r!} \left\{ \frac{(2m+r+1)(2m+r+2)(2m+r+3)}{(2m+2r+3)(2m+2r+5)} \left[(r+1) d_r^{m+2,n} \right.\right.$$

$$\left. + (2m+2r+5) \sum_{q=r+2}^{\infty}{}' d_q^{m+2,n} \right] + \frac{(2m+1)(2m+r+1)r}{(2m+2r-1)(2m+2r+3)} \left[(r-1) d_{r-2}^{m+2,n} \right.$$

$$\left. + (2m+2r+1) \sum_{q=r}^{\infty}{}' d_q^{m+2,n} \right] - \frac{(r-2)(r-1)r}{(2m+2r-3)(2m+2r-1)} \left[(r-3) d_{r-4}^{m+2,n} \right.$$

$$\left.\left. + (2m+2r-3) \sum_{q=r-2}^{\infty}{}' d_q^{m+2,n} \right] \right\}, \quad (n+N) \text{ even}$$

$$= 0, \quad (n+N) \text{ odd} \tag{D.21}$$

$$I_{31mNn} = \int_{-1}^{1} \eta \frac{d}{d\eta} S_{m+2,n} S_{m,m+N} \, d\eta$$

$$= 2 \sum_{r=0,1}^{\infty}{}' \frac{(2m+r)! d_r^{m,m+N}}{r!} \left\{ \frac{r}{(2m+2r+1)} \left[-(r-1)(r+m) d_{r-2}^{m+2,n} \right.\right.$$

$$\left. + (m+2)(2m+2r+1) \sum_{\nu=r}^{\infty}{}' d_\nu^{m+2,n} \right] + \sum_{q=r+1}^{\infty}{}' \left[-q(m+q+1) d_{q-1}^{m+2,n} \right.$$

$$\left.\left. + (m+2)(2m+2q+3) \sum_{\nu=q+1}^{\infty}{}' d_\nu^{m+2,n} \right] \right\}, \quad (n+N) \text{ even}$$

$$= 0, \quad (n+N) \text{ odd} \tag{D.22}$$

$$I_{32mNn} = \int_{-1}^{1} \frac{1}{(1-\eta^2)} S_{m+2,n} S_{m,m+N} \, d\eta$$

$$= -2 \sum_{q=0,1}^{\infty}{}' \frac{(2m+q-2)!}{q!} \left\{ (2m+q-1)(2m+q)(2m+2q+3) \cdot \sum_{r=q}^{\infty}{}' d_r^{m+2,n} \right.$$

$$\cdot \sum_{r=q+2}^{\infty}{}' d_r^{m,m+N} - 2m(2m+2q-1) \cdot \sum_{r=q}^{\infty}{}' d_r^{m,m+N}$$

$$\left. \cdot \left[\sum_{t=q}^{\infty}{}' (2m+2t+3) \sum_{r=t}^{\infty}{}' d_r^{m+2,n} \right] \right\}, \quad (n+N) \text{ even}$$

$$= 0, \quad (n+N) \text{ odd} \tag{D.23}$$

$$I_{33mNn} = \int_{-1}^{1} (1-\eta^2) \frac{d^2}{d\eta^2} S_{m+2,n} S_{m,m+N} \, d\eta$$

$$= 2 I_{31mNn} + (m+2)^2 I_{32mNn} - \lambda_{m+2,n} I_{7mNn} + h^2 I_{30mNn} \tag{D.24}$$

For $m = 0$, $\qquad I_{18mNn} = 2 d_r^{0N} \sum_{\nu=r}^{\infty}{}' d_{\nu+1}^{0n}$

APPENDIX E

DEFINITIONS OF THE VARIOUS MATRICES INTRODUCED IN CHAPTER 6

The matrices $\overline{\mathbf{M}}^{(i)T}(\xi,\eta)$, $\overline{\mathbf{M}}^{(i)T}(\xi',\eta')$ for $i=1,4$, and the transpose of the matrices $\overline{A}$, $\overline{B}$ in (6.1) and (6.2) are [45]

$$\overline{\mathbf{M}}^{(i)T}(\xi,\eta)=[\mathbf{M}_1^{(i)}(\xi,\eta)\quad \mathbf{M}_2^{(i)}(\xi,\eta)\ \ldots\ ],$$

$$\overline{\mathbf{M}}^{(i)T}(\xi',\eta')=[\mathbf{M}_1^{(i)}(\xi',\eta')\quad \mathbf{M}_2^{(i)}(\xi',\eta')\ \ldots\ ],\qquad i=1,4 \tag{E.1}$$

$$\overline{A}^T=[A_1\ A_2\ldots],\qquad \overline{B}^T=[B_1\ B_2\ldots] \tag{E.2}$$

in which

$$\mathbf{M}_n^{(i)}(\xi,\eta)=\mathbf{M}_{-1n}^{+(i)}(\xi,\eta,\phi)-\mathbf{M}_{1n}^{-(i)}(\xi,\eta,\phi)\qquad i=1,2,3,4 \tag{E.3}$$

$$A_n=V_A\,h\,\frac{(\xi_A^2-1)^{1/2}}{N_{1n}(h)}\,R_{1n}^{(4)}(h,\xi_A)\,S_{1n}(h,0) \tag{E.4}$$

and

$$B_n=V_B\,h'\,\frac{(\xi_B'^2-1)^{1/2}}{N_{1n}(h')}\,R_{1n}^{(4)}(h',\xi_B')\,S_{1n}(h',0) \tag{E.5}$$

$R_{1n}^{(4)}$, S_{1n}, and N_{1n} are the spheroidal radial function of the fourth kind, the spheroidal angle function, and the normalization constant, respectively which are given in Appendix A.

The structure of the matrix $[\Gamma]$ in (6.5) is similar to that of $[\Gamma_{qr}]$ defined in Appendix B, but with its elements being submatrices of the form $[\Gamma_i]_\sigma^\tau$ and $[{}^*\Gamma_i]_\sigma^\tau$ for $\tau,\sigma=\ldots-2,-1,0,1,2,\ldots$ and $i=1,2,3,4,5$, defined by $C_i'[\Gamma]_\sigma^\tau$ and $C_i'^*[\Gamma]_\sigma^\tau$, respectively, with the asterisk denoting the complex conjugate, and

$$
\begin{aligned}
C_1' &= \frac{1}{2}[(c_{xx'} + c_{yy'}) + j(c_{xy'} - c_{yx'})] \\
C_2' &= \frac{1}{2}[(c_{xx'} - c_{yy'}) + j(c_{xy'} + c_{yx'})] \\
C_3' &= \frac{1}{2}(c_{zx'} + jc_{zy'}) \\
C_4' &= c_{xz'} - jc_{yz'} \\
C_5' &= c_{zz'}
\end{aligned}
\tag{E.6}
$$

$$
[\Gamma]_\sigma^\tau = \begin{bmatrix}
{}^{(4)}Q'^{\tau,|\tau|}_{\sigma,|\sigma|} & {}^{(4)}Q'^{\tau,|\tau|}_{\sigma,|\sigma|+1} & {}^{(4)}Q'^{\tau,|\tau|}_{\sigma,|\sigma|+2} & {}^{(4)}Q'^{\tau,|\tau|}_{\sigma,|\sigma|+3} & - \\
{}^{(4)}Q'^{\tau,|\tau|+1}_{\sigma,|\sigma|} & {}^{(4)}Q'^{\tau,|\tau|+1}_{\sigma,|\sigma|+1} & {}^{(4)}Q'^{\tau,|\tau|+1}_{\sigma,|\sigma|+2} & {}^{(4)}Q'^{\tau,|\tau|+1}_{\sigma,|\sigma|+3} & - \\
{}^{(4)}Q'^{\tau,|\tau|+2}_{\sigma,|\sigma|} & {}^{(4)}Q'^{\tau,|\tau|+2}_{\sigma,|\sigma|+1} & {}^{(4)}Q'^{\tau,|\tau|+2}_{\sigma,|\sigma|+2} & {}^{(4)}Q'^{\tau,|\tau|+2}_{\sigma,|\sigma|+3} & - \\
- & - & - & - & -
\end{bmatrix}
\tag{E.7}
$$

The coefficients $c_{ax'}, c_{ay'}, c_{az'}$, for $a = x, y, z$, are given in (2.4), and the rotational-translational coefficients ${}^{(4)}Q'^{mn}_{\mu\nu}$ are given in Appendix B. The structure of the matrix $[\Gamma']$ in (6.11) is similar to that of $[\Gamma]$, with its elements consisting of the submatrices $[\Gamma_i']_\sigma^\tau$, $[{}^*\Gamma_i']_\sigma^\tau$. The elements of the submatrices $[\Gamma_i']_\sigma^\tau$ are obtained from the corresponding ones of $[\Gamma_i]_\sigma^\tau$ by replacing ${}^{(4)}Q'^{mn}_{\mu\nu}$ by ${}^{(4)}Q^{mn}_{\mu\nu}$, given in Appendix B, and C_i' by C_i, given in (2.16).

The matrix $[\Delta]$ introduced in (6.6) is given by

$$
[\Delta] = [[\Delta_0] \;\; [\Delta_1] \;\; [\Delta_2] \ldots] \tag{E.8}
$$

where

$$
[\Delta_0] = [[\Gamma_1]_{-1}^{-1} - [{}^*\Gamma_2]_{-1}^{1} \quad [\Gamma_2]_1^{-1} - [{}^*\Gamma_1]_1^{1} \quad [\Gamma_3]_0^{-1} - [{}^*\Gamma_3]_0^{1}] \tag{E.9}
$$

$$
\begin{aligned}
[\Delta_\sigma] = [\; & [\Gamma_1]_{\sigma-1}^{-1} - [{}^*\Gamma_2]_{\sigma-1}^{1} \quad [\Gamma_2]_{\sigma+1}^{-1} - [{}^*\Gamma_1]_{\sigma+1}^{1} \quad [\Gamma_3]_\sigma^{-1} - [{}^*\Gamma_3]_\sigma^{1} \\
& [\Gamma_1]_{-(\sigma+1)}^{-1} - [{}^*\Gamma_2]_{-(\sigma+1)}^{1} \quad [\Gamma_2]_{-(\sigma-1)}^{-1} - [{}^*\Gamma_1]_{-(\sigma-1)}^{1} \quad [\Gamma_3]_{-\sigma}^{-1} - [{}^*\Gamma_3]_{-\sigma}^{1}]
\end{aligned}
\tag{E.10}
$$

for $\sigma \geq 1$. The submatrices $[\Gamma_i]_\sigma^{\pm 1}$, and $[{}^*\Gamma_i]_\sigma^{\pm 1}$ for $\sigma = \ldots -2, -1, 0, 1, 2, \ldots$ and $i = 1, 2, 3, 4, 5$, are $C_i'[\Gamma]_\sigma^{\pm 1}$ and $C_i'^*[\Gamma]_\sigma^{\pm 1}$, respectively, with C_i' and $[\Gamma]_\sigma^{\pm 1}$ as defined

above. The elements of the matrix $[\Delta']$ introduced in (6.11) are obtained from the corresponding elements of $[\Delta]$ by replacing C_i' by C_i and Γ by Γ'.

The transpose of the matrix $[R_A]$ in (6.14) is defined as

$$[R_A]^T = [\,[\,{}_{\eta}X_{-1}^{+(1)}\,] - [\,{}_{\eta}X_{1}^{-(1)}\,] \quad [\,{}_{\phi}X_{-1}^{+(1)}\,] - [\,{}_{\phi}X_{1}^{-(1)}\,] \quad [0] \quad [0] \quad . \quad . \quad .] \tag{E.11}$$

$[R_B]$ has the same structure as that of $[R_A]$, but with the corresponding elements evaluated with respect to the primed system. $[\,{}_{\eta}X_{\pm 1}^{\pm(1)}\,]$ and $[\,{}_{\phi}X_{\pm 1}^{\pm(1)}\,]$ are given in Appendix C.

The coefficients $A_n^{>}$ and $B_n^{>}$ introduced in Chapter 6 are given by

$$A_n^{>} = V_A\, h\, \frac{(\xi_A^2 - 1)^{1/2}}{N_{1n}(h)}\, R_{1n}^{(1)}(h, \xi_A)\, S_{1n}(h, 0) \tag{E.12}$$

$$B_n^{>} = V_B\, h'\, \frac{(\xi_B'^2 - 1)^{1/2}}{N_{1n}(h')}\, R_{1n}^{(1)}(h', \xi_B')\, S_{1n}(h', 0) \tag{E.13}$$